University of Kentucky
UKnowledge

Theses and Dissertations--Nutritional Sciences | Nutritional Sciences

2013

POLYCHLORINATED BIPHENYL LIGANDS OF THE ARYL HYDROCARBON RECEPTOR PROMOTE ADIPOCYTE-MEDIATED DIABETES

Nicki A. Baker
University of Kentucky, nicki.baker.uk@gmail.com

Right click to open a feedback form in a new tab to let us know how this document benefits you.

Recommended Citation

Baker, Nicki A., "POLYCHLORINATED BIPHENYL LIGANDS OF THE ARYL HYDROCARBON RECEPTOR PROMOTE ADIPOCYTE-MEDIATED DIABETES" (2013). *Theses and Dissertations--Nutritional Sciences*. 7.
https://uknowledge.uky.edu/nutrisci_etds/7

This Doctoral Dissertation is brought to you for free and open access by the Nutritional Sciences at UKnowledge. It has been accepted for inclusion in Theses and Dissertations--Nutritional Sciences by an authorized administrator of UKnowledge. For more information, please contact UKnowledge@lsv.uky.edu.

STUDENT AGREEMENT:

I represent that my thesis or dissertation and abstract are my original work. Proper attribution has been given to all outside sources. I understand that I am solely responsible for obtaining any needed copyright permissions. I have obtained and attached hereto needed written permission statements(s) from the owner(s) of each third-party copyrighted matter to be included in my work, allowing electronic distribution (if such use is not permitted by the fair use doctrine).

I hereby grant to The University of Kentucky and its agents the non-exclusive license to archive and make accessible my work in whole or in part in all forms of media, now or hereafter known. I agree that the document mentioned above may be made available immediately for worldwide access unless a preapproved embargo applies.

I retain all other ownership rights to the copyright of my work. I also retain the right to use in future works (such as articles or books) all or part of my work. I understand that I am free to register the copyright to my work.

REVIEW, APPROVAL AND ACCEPTANCE

The document mentioned above has been reviewed and accepted by the student's advisor, on behalf of the advisory committee, and by the Director of Graduate Studies (DGS), on behalf of the program; we verify that this is the final, approved version of the student's dissertation including all changes required by the advisory committee. The undersigned agree to abide by the statements above.

Nicki A. Baker, Student

Dr. Lisa A. Cassis, Major Professor

Dr. Howard Glauert, Director of Graduate Studies

POLYCHLORINATED BIPHENYL LIGANDS OF THE ARYL HYDROCARBON RECEPTOR PROMOTE ADIPOCYTE-MEDIATED DIABETES

DISSERTATION

A dissertation submitted in partial fulfillment of the
requirements for the degree of Doctor of Philosophy in the Graduate School,
Center for Nutritional Sciences,
at the University of Kentucky

By

Nicki Alyssa Baker

Lexington, Kentucky

Chair: Dr. Shuxia Wang, Professor of Nutritional Sciences

Lexington, Kentucky

2013

Copyright © Nicki Alyssa Baker 2013

ABSTRACT OF DISSERTATION

POLYCHLORINATED BIPHENYL LIGANDS OF THE ARYL HYDROCARBON RECEPTOR PROMOTE ADIPOCYTE-MEDIATED DIABETES

Numerous epidemiology studies suggest a correlation between exposures to polychlorinated biphenyls (PCBs) and the development and severity of type 2 diabetes (T2D); however, mechanisms remain largely unknown. Previous studies demonstrated that PCBs that are ligands of the aryl hydrocarbon receptor (AhR) promote the expression of proinflammatory cytokines, including tumor necrosis factor-α (TNF-α), that are linked to insulin resistance in adipocytes. To explore potential mechanisms linking PCB exposures to diabetes, we developed a mouse model of glucose and insulin intolerance induced by acute and chronic exposures to PCB-77. We hypothesized that PCB ligands of AhR result in adipocyte-specific elevations in TNF-α and dysregulated glucose homeostasis. Results demonstrated that PCB77 resulted in rapid and sustained glucose and insulin intolerance in low fat (LF)-fed mice, and that these effects were associated with adipose-specific elevations in TNF-α. When mice were made obese from consumption of a high fat (HF) diet, effects of PCB77 were lost presumably due to concentration of the toxin in adipose lipids. However, upon weight loss, mice exposed to PCB77 exhibit impaired glucose homeostasis. These results suggest that lipophilic PCBs redistribute from adipose lipids with weight loss and mitigate beneficial effects to improve glucose homeostasis. To define the role of adipocyte AhR in PCB-induced diabetes, we created a mouse model of adipocyte AhR deficiency using the Cre/LoxP system. Adipocyte-AhR deficiency conferred protection from the development of PCB-77-induced impairments in glucose and insulin tolerance in obese mice undergoing weight loss. Unexpectedly, adipocyte-AhR deficient mice fed the HF diet exhibited adipocyte hypertrophy, increased adipose mass and elevated body weight. These results suggest that (1) adipocyte AhRs are responsible for effects of PCB77 to impair glucose homeostasis during weight loss and (2) adipocyte AhRs respond to the HF diet to regulate adipose mass and body weight. We used resveratrol as a putative AhR antagonist to determine if the polyphenol confers protection against PCB-77-induced diabetes. Resveratrol abolished acute effects of PCB77 to impair glucose and insulin tolerance in LF-fed mice. Notably, PCB77 administration abolished insulin-induced phosphorylation of Akt in adipose tissue and these effects were abolished by resveratrol. Resveratrol also abolished marked suppressions in glucose uptake in adipocytes exposed to PCB77. These studies suggest the adipocyte AhR plays a potentially significant role in the development of diabetes and obesity, and that resveratrol may represent a novel therapeutic for PCB exposed populations.

Keywords: Polychlorinated biphenyls, adipocytes, diabetes, resveratrol, aryl hydrocarbon receptor

Nicki Alyssa Baker

6-6-2013

POLYCHLORINATED BIPHENYL LIGANDS OF THE ARYL HYDROCARBON RECEPTOR PROMOTE ADIPOCYTE-MEDIATED DIABETES

By

Nicki Alyssa Baker

_____Dr. Lisa Cassis_____
Director of Dissertation

_____Dr. Howard Glauert_____
Director of Graduate Studies

_____6-6-2013_____

ACKNOWLEDGMENTS

Many individuals have supported me throughout graduate school, and I am incredibly grateful for their assistance in obtaining my PhD. in Nutritional Sciences. Above all, I would like to thank my mentor, Dr. Lisa Cassis, who accepted me into her lab despite my background in engineering, and was consistently generous with her time and guidance in my graduate school career. Dr. Cassis is an exceptional scientist, a dedicated colleague and mentor, and a mother. In short, she is an amazing role model for female scientists and academics and I consider myself lucky to have worked with her. None of this would have been possible without her peerless mentorship.

I also thank fellow graduate students in the Cassis lab, Dr. Kelly Downing and Robin Shoemaker, who provided much appreciated moral support and deep friendship that will last well beyond our graduate school tenure. Drs. Frederique Yiannikouris and Sean Thatcher have not only patiently taught me nearly ever laboratory technique utilized in my dissertation, but I also count them as cherished friends. I must also thank lab manager Vicki English for her support and assistance. I thank the other Cassis lab members who have been delightful to work with over the years and will be missed.

I would like to thank the members of my Dissertation Committee, Drs. Kevin Pearson, Hollie Swanson, and Shuxia Wang. Dr. Pearson's boundless scientific enthusiasm and general kindness were key motivators during challenging periods of graduate school, and his glowing reference letters supported my future academic endeavors. I admire Dr. Swanson's unrivaled

expertise in her field of study, and her insights and challenges have shaped my growth as a scientist. Dr. Wang has been consistently supportive of myself and my project and assisted me with methods used in my dissertation. I appreciate all of your contributions and it has been a privilege to work with you all. I would also thank Dr. Debski for agreeing to be the outside examiner for my final examination.

In addition to my esteemed colleagues, I also need to thank my family for their support and encouragement. A special thanks to my husband, Rory, who has been incredibly positive and supportive of my career, is a wonderful father to my little sweet-pea Ava, and is my devoted best friend. We have loved our time in Lexington, and I hope to maintain the professional and personal relationships that we have built here. Thank you all for your substantial part in my success.

TABLE OF CONTENTS

ACKNOWLEDGMENTS iii
LIST OF TABLES xi
LIST OF FIGURES xii
LIST OF ABBREVIATIONS xv
Section I. BACKGROUND 1
1.1 Polychlorinated biphenyls 1
1.1.1 Polychlorinated biphenyls 1
1.1.1.1 PCB chemistry 1
1.1.1.2 PCB lipophilicity 3
1.1.1.3 General health effects of PCBs 4
1.1.2 Aryl-hydrocarbon receptor (AhR) 5
1.1.2.1 Protein functional domains 6
1.1.2.2 Aryl-hydrocarbon receptor ligands 7
1.1.2.3 Aryl-hydrocarbon receptor signaling pathways 7
1.1.2.4 Functional role of AhR in physiology and toxicology 8
1.1.2.5 AhR in glucose homeostasis and metabolic studies 10
1.1.3 PCBs and type 2 diabetes 12
1.1.3.1 The pathophysiology of type 2 diabetes 12
1.1.3.2 General characteristics of adipose tissue 14
1.1.3.3 Mechanisms of IR in adipose tissue 16
1.1.3.4 Emerging evidence of a positive correlation between xenobiotic AhR ligand exposure and the development of T2D: Agent Orange and U.S. Vietnam veterans 19
1.1.3.5 Evidence of a positive correlation between PCB exposure and the development of T2D: Anniston, AL Community 21
1.1.3.6 The role of PCBs in oxidative stress and inflammation 23
1.1.4 PCBs and obesity 24
1.1.4.1 The pathophysiology of obesity 24

1.1.4.2 Polychlorinated biphenyl-77 induces adipocyte differentiation and proinflammatory adipokines and promotes obesity 25
1.2 Resveratrol 26
1.2.2 General mechanism of action of resveratrol 27
1.2.3 Resveratrol dosing in rodent and human studies 28
1.2.4 Effects of resveratrol on glucose and insulin tolerance 30
Statement of the problem 41
Section II. SPECIFIC AIM 1 44
2.1 Summary 44
2.2 Introduction 46
2.3 Materials and Methods 49
2.3.1 Chemicals 49
2.3.2 Animal treatments and sample collection 49
2.3.3 Glucose tolerance tests (GTT) and insulin tolerance tests (ITT) 51
2.3.4 Quantification of PCBs 51
2.3.5 Quantification of plasma components 52
2.3.6 Extraction of RNA and quantification of mRNA abundance using real-time polymerase chain reaction (PCR) 52
2.3.7 Western blotting 53
2.3.8 Cell culture 54
2.3.9 Statistical analysis 55
2.4 Results 56
2.4.1 Coplanar PCBs dose-dependently impair glucose and insulin tolerance in LF-fed mice in an AhR-dependent manner 56
2.4.2 PCB-77 treatment results in sustained impairment of glucose and insulin tolerance in LF-fed mice 57
2.4.3 Effects of PCB-77 to promote glucose and insulin intolerance are lost in mice with diet-induced obesity, but manifest when obese mice lose weight 59

2.4.4 PCB-77 results in an AhR-dependent increase in expression of TNF-α in 3T3-L1 adipocytes 60
2.5 Discussion 61
Section III. SPECIFIC AIM 2.....88
3.1 Summary 88
3.2 Introduction.....90
3.3 Materials and Methods 93
3.3.1 Materials.....93
3.3.2 Quantification of PCB-77, RSV, and metabolites in serum and tissues 93
3.3.3 Cell culture 94
3.3.4 Measurement of insulin-stimulated uptake of 2DG.....95
3.3.5 Measurement of oxidative stress.....95
3.3.6 Animals and experimental diets 96
3.3.7 Glucose tolerance test (GTT) and insulin tolerance test (ITT)....97
3.3.8 Quantification of adipose tissue Akt and P-Akt.....97
3.3.9 RNA isolation and gene expression analysis using real-time polymerase chain reaction (PCR) 97
3.3.10 Statistical analysis 98
3.4 Results.....100
3.4.1 RSV promotes Nrf2 signaling, suppresses oxidative stress, and restores insulin-stimulated glucose uptake in PCB-77 treated adipocytes 100
3.4.2 RSV has no effect on tissue levels of PCB-77 or PCB-77 metabolites 101
3.4.3 RSV improves glucose tolerance and insulin signaling in adipose tissue of mice administered PCB-77 101
3.5 Discussion 103
Section IV. SPECIFIC AIM 3 117
4.1 Summary 117
4.2 Introduction.....119

4.3 Materials and Methods 122
4.3.1 Chemical procurement 122
4.3.2 Quantification of PCB-77 and hydroxylated metabolites in serum and tissues 122
4.3.3 Animals and experimental diets 124
4.3.4 Measurement of body composition 125
4.3.5 Measurement of glucose and insulin tolerance 125
4.3.6 Quantification of mRNA abundance 126
4.3.7 Determination of adipocyte size and cell number 127
4.3.8 Differentiation of preadipocytes from SVC 127
4.3.9 Statistical analysis 128
4.4 Results.....129
4.4.1 Generation of mice with adipocyte AhR deficiency 129
4.4.2 Adipocyte AhR deficiency improves glucose and insulin tolerance in lean mice acutely exposed to PCB-77 130
4.4.3 Adipocyte AhR deficiency promotes the development of obesity during HF-feeding and alters body fat distribution 131
4.4.4 Adipocyte AhR deficiency resulted in adipose depot-specific changes in adipocyte cell number in HF-fed mice 132
4.4.5 Adipocyte AhR deficiency protects against PCB-77 induced disruptions in glucose homeostasis and adipose tissue inflammation during weight loss 132
4.5 Discussion 135
Section V. GENERAL DISCUSSION 159
5.1 Summary 159
5.2 The interplay between adipose tissue and persistent organic pollutants: Insights from mouse models of PCB-77 induced diabetes 160
5.2.1 PCB distribution in the body 160
5.2.2 Potential target organs of coplanar PCB induced diabetes 162
5.2.2.1 Adipose tissue 162

5.2.2.2 Liver 163
5.2.2.3 Skeletal muscle 165
5.2.2.4 Pancreas 166
5.2.3 The progression of adipose inflammation in LF time course studies 167
5.2.3.1 ROS as the initiating event for adipose inflammation 167
5.2.3.2 Potential role of PCB-77 metabolites 168
5.3 The potential therapeutic benefits of resveratrol supplementation in PCB exposed populations: Insights from resveratrol supplementation mouse model of PCB-77 induced diabetes 169
5.3.1 Resveratrol intervention in populations with known PCB exposures 169
5.3.2 General use of resveratrol supplements for weight loss 170
5.3.3. Pharmaceutical resveratrol analogues and resveratrol use in tandem with other nutritional supplements 171
5.4 Adipose AhR: Role in mediating PCB-77 induced diabetes, and a potentially novel role in regulating body weight, body composition, and fat deposition 172
5.4.1 Limitations of the model of adipocyte-AhR deficiency 172
5.4.1.1 Non-specific reductions in AhR mRNA abundance 172
5.4.1.2 Model validation 173
5.4.2 HF diet induced phenotype in adipose AhR deficient mice 173
5.4.2.1 Differential expression of AhR in LF versus HF feeding 173
5.4.2.2 Arachidonic acid or ecosanoid metabolites as a potential endogenous AhR ligand 174
5.5 Further exploration of the adipose AhR: Dietary manipulations 174
5.6 Additional future directions 176
5.6.1 The role of noncoplanar PCBs in the development of diabetes..... 176
5.6.2 The role of mixtures of persistent organic pollutants in the development of diabetes 177

5.6.3 Potential gender differences in development of PCB or POP associated diabetes 178
5.7 Clinical implications 179
5.8 Concluding remarks 180
REFERENCES 191
VITA 244

LIST OF TABLES

Table 1.1 World Health Organization TEF values of TCDD and selected PCBs 37

Table 1.2 Synthetic and naturally occuring AhR ligands.....37

Table 1.3 Summary of studies investigating the correlation between Agent Orange/TCDD exposure in Vietnam veterans and the development of type 2 diabetes 38

Table 1.4 Summary of studies investigating the correlation between dioxin exposure and the development of type 2 diabetes 39

Table 1.5 Summary of studies investigating the correlation between PCB exposure and the development of type 2 diabetes 40

Table 3.1 Primer sequences for real-time PCR 108

Table 3.2 Levels of PCB-77, RSV, and their metabolites in serum, liver, and retroperitoneal fat of mice 109

LIST OF FIGURES

Figure 1.1 Chemical Structure of PCBs 36

Figure 1.2 AhR Signaling Pathway 36

Figure 1.3 Protein functional domains of AhR 37

Figure 2.1 PCB-77 (A) and PCB-126 (B) impair glucose tolerance in LF-fed mice 66

Figure 2.2 Insulin tolerance tests in mice administered vehicle (VEH), PCB-77 (2.5, 50 or 248 mg/kg, A) or PCB-126 (0.3, 1.6 or 3.3 mg/kg, B) 68

Figure 2.3 Glucose (A) and insulin (B) tolerance tests in mice administered vehicle (VEH), CH-223191 (10 mg/kg/day), or PCB-77 (50 mg/kg) 70

Figure 2.4 PCB-77 results in sustained impairment of glucose (A) and insulin (B) tolerance in LF-fed mice 72

Figure 2.5 PCB-77 increases mRNA abundance of CYP1A1 in adipose (A) and liver (B) of LF-fed mice 74

Figure 2.6 TNF-α (A) and F4/80 (B) mRNA abundance in adipose from mice administered vehicle (VEH) or PCB-77 76

Figure 2.7 PCB-77 results in elevated TNF-α expression in adipose, but not in liver or soleus muscle of LF-fed mice 78

Figure 2.8 Plasma concentrations of TNF-α (A) and IL-6 (B) following administration of vehicle (VEH) or PCB-77.....80

Figure 2.9 Body weight in LF and HF-fed mice administered vehicle (VEH) or PCB-77 (50 mg/kg, doses in weeks 1, 2, 9, and 10) during the weight gain phase of HF feeding (A), and after mice are switched to a LF diet at week 12 – 16 to induce weight loss (B).....82

Figure 2.10 PCB-77 has no effect on glucose (A) or insulin (B) tolerance in HF-fed mice during weight gain, but impairs glucose homeostasis during weight loss 83

Figure 2.11 TNF-α mRNA abundance in adipose from mice during weight gain (week 12 of HF feeding), and after mice are switched to a LF diet to induce weight loss (week 16) 85
Figure 2.12 CYP1A1 (A) and TNF-α mRNA abundance in 3T3-L1 adipocytes incubated with vehicle, α-NF, PCB-77, or PCB-77 + α-NF 86
Figure 3.1 Resveratrol protects 3T3-L1 adipocytes against PCB-77-induced oxidative stress and impaired glucose uptake 110
Figure 3.2 PCB-77 increases CYP1A1 mRNA abundance in adipose tissue 112
Figure 3.3 RSV prevents PCB-77-induced impairment of glucose or insulin tolerance.....113
Figure 3.4 RSV promotes the anti-oxidant NRF2 target, NQO1, and reverses PCB-77-induced impairment of insulin signaling in adipose tissue 115
Figure 4.1 Development of mice with adipocyte deficiency of AhR 140
Figure 4.2 Body weight and composition of adipocyte AhR deficient mice... 142
Figure 4.3 Adipocyte AhR deficiency abolishes PCB-77-induced impairment of glucose and insulin tolerance in lean mice 144
Figure 4.4 Adipocyte AhR deficiency promotes the development of obesity 146
Figure 4.5 Adipocyte AhR deficiency modestly impairs glucose tolerance... 148
Figure 4.6 Adipocyte AhR deficiency promotes adipocyte hypertrophy and increases adipose F4/80 gene expression 150
Figure 4.7 Following weight loss body weight is similar between genotypes and treatments 152
Figure 4.8 Adipocyte AhR deficiency prevents PCB7-77-induced impairment of glucose and insulin tolerance following weight loss.....153
Figure 4.9 Adipose levels of PCB-77 and hydroxy PCB-77 metabolite in obese mice (week 12 of HF feeding) and after 4 weeks of weight loss 155

Figure 4.10 PCB-77-induced increases in mRNA abundance of CYP1A1 and TNF-α are abolished in mice with adipocyte AhR deficiency 157
Figure 5.1 Summary of findings: Proposed mechanism of PCB-77 induced adipocyte mediated T2D and inhibition with resveratrol 182
Figure 5.2 PCB-77 treatment decreases hepatic mRNA abundance of gluconeogenic enzymes 183
Figure 5.3 PCB-77 treatment decreases fasted plasma insulin in LF fed mice 184
Figure 5.4 Adipocyte AhR deficiency does not affect heart weight 185
Figure 5.5 Differential expression of AhR in adipose tissue during LF vs. HF feeding.....186
Figure 5.6 PCB-153 has no effect on insulin-stimulated glucose uptake in 3T3-L1 adipocytes 187
Figure 5.7 PCB-77 impairs glucose tolerance (A) in female C57BL/6 mice, but has no effect on insulin tolerance (B) 188
Figure 5.8 PCB-77 increases adipose depot weight of female C57BL/6 mice 190

LIST OF ABBREVIATIONS

2DG, 2-deoxy-glucose; α-NF, alpha napthtoflavone; ADAM17, ADAM metallopeptidase domain 17; adjOR, adjusted odds ratio; AdQ, adiponectin; AhR, aryl hydrocarbon receptor; AhR^{AdQ}, adipocyte AhR deficient mice; $AhR^{fl/fl}$, AhR floxed mice; AHRE, aryl hydrocarbon receptor response element; AIP, aryl hydrocarbon receptor-interacting protein; Akt, protein kinase B; ALDH3A1, aldehyde dehydrogenase 3 family, member A1; AMPK, AMP-activated protein kinase; ANOVA, analysis of variance; ARA9, aryl hydrocarbon receptor activated 9; ARE, antioxidant response element; ARNT, aryl hydrocarbon receptor nuclear translocator; ARNTL, aryl hydrocarbon receptor nuclear translocator-like; ATP, adenosine triphosphate; AUC, area under the curve; BaP, benzo(a)pyrene; BAT, brown adipose tissue; BMI, body mass index; cAMP, cyclic adenosine monophosphate; CAR, constitutive androstane receptor; CYP1A1, cytochrome P450 1A1; CYP1A2, cytochrome P450 1A2; CYP1B1, cytochrome P450 1B1; DCF, dichlorofluorescein; DMEM, Dubecco's modified Eagles medium; DMSO, dimethyl sulfoxide; DRE, dioxin response element; EF, epididymal fat; EPA, Environmental Protection Agency; ERα, estrogen receptor alpha; ERß, estrogen receptor beta; FBS, fetal bovine serum; FFA, free fatty acids; G6P, glucose-6-phosphatase; GAPDH, glyceraldehyde 3-phosphate dehydrogenase; GC, gas chromatography; GLUT4, glucose transporter type 4; GSTA1, glutathione S-transferase-A1; GTT, glucose tolerance test; HbA1c, glycated hemoglobin; HIF1-α, hypoxia-inducible factor 1 alpha; HF, high fat; Hsp90, heat shock protein 90; IARC, International Agency for Research on Cancer; IBMX, 3-isobutyl-1-

methylxanthine; IL-1ß, interleukin 1 beta; IL-6, interleukin 6; i.p., intra-peritoneal; IR, insulin resistance; IRS-1, insulin receptor substrate 1; ITT, insulin tolerance test; KO, knock out; LF, low fat; M-PER, mammalian protein extraction reagent; MRI, magnetic resonance imaging; MS, mass spectrometry; NAFLD, non-alcoholic fatty liver disease; N.D., not detected; NF-κB, nuclear factor kappa-light-chain-enhancer of activated B cells; NHANES, National Health and Nutrition Examination Survey; NIEHS, National Institute of Environmental Health Sciences; NLS, nuclear localization sequence; NQO1, NAD(P)H dehydrogenase quinone 1; Nrf2, nuclear factor (erythroid-derived 2)-like 2; NTP, National Toxicology Program; PAI-1, plasminogen activator inhibitor 1; pAkt, phosphorylated protein kinase B; PBS, phosphate buffered saline; PC, pyruvate carboxylase; PCB, polychlorinated biphenyl; PCDD, polychlorinated dibenzodioxin; PCR, polymerase chain reaction; PEPCK, phosphoenolpyruvate carboxykinase; PGC1-α, peroxisome proliferator-activated receptor gamma coactivator 1-alpha; POF, periovarian fat; POP, persistent organic pollutant; PPAR-α, peroxisome proliferator-activated receptor alpha; PPAR-γ, peroxisome proliferator-activated receptor gamma; Ptges3, prostaglandin E synthase 3; PXR, pregnane X receptor; ROS, reactive oxygen species; RPF, retroperitoneal fat; RR, relative risk; RSV, resveratrol; SE, standard error; SIRT1, sirtuin 1; SMR, standardized mortality ratio; STZ, streptozotocin; SUBQ, subcutaneous; SVC, stromal vascular cells; SVF, stromal vascular fraction; T2D, type 2 diabetes; TACE, tumor necrosis factor-α-converting enzyme; TCDD, 2,3,7,8-tetrachlorodibenzo-*p*-dioxin; TEF, toxic equivalency factor; TNF-α, tumor necrosis

factor-alpha; UGT1A2, UDP glucuronosyltransferase 1 family, polypeptide 2; VCAM-1, vascular cell adhesion protein 1; VEH, vehicle; WAT, white adipose tissue; WHO, World Health Organization; WT, wild type; XAP2, immunophilin-like protein hepatitis B virus X-associated protein 2; XRE, xenobiotic response element

SECTION I. BACKGROUND

1.1 Polychlorinated biphenyls

1.1.1 Polychlorinated biphenyls

Polychlorinated biphenyls (PCBs) are the general name describing any of the 209 arrangements of organochlorides with 1 to 10 chlorine atoms attached to a biphenyl structure (a molecule with two benzene rings) (Figure 1.1). They are synthetic compounds that were primarily used as dielectric and coolant fluids in transformers, capacitors, and electric motors. In light of emerging environmental concerns and health impacts in humans and wildlife, PCB manufacturing was banned by the United States Congress in 1979 and by the Stockholm Convention on Persistent Organic Pollutants (POPs) in 2001 (1). According to the U.S. Environmental Protection Agency (EPA), PCBs can cause cancer in animals, and there is causal evidence for a link to cancer in humans (2-3).

The toxicity of PCBs became a topic of global concern when it was discovered that compounds within this group can share a structural resemblance and toxicity pathways with 3,4,7,8-tetrachlorodibenzo-p-dixon (TCDD). PCB compounds within this group have positive associations with toxic effects of TCDD; namely endocrine disruption, neurotoxicity, immune system suppression, and reproductive effects (4).

1.1.1.1 PCB chemistry

PCB congeners are odorless, tasteless, viscous liquids with the chemical formula $C_{12}H_{10-x}Cl_x$ (Figure 1.1). They are formed via electrophilic chlorination

of a biphenyl with chlorine gas. PCBs have low water solubility and low vapor pressure at room temperature, but they are highly soluble in most organic solvents, oils, and fats (5). PCBs have high dielectric constants, high thermal conductivity, high flash points and are fairly inert chemically; all qualities which made the compounds ideal for use as coolants in electrical systems (5). They are highly resistant to chemical degradation such as oxidation, reduction, addition, elimination, and electrophilic substitution, making PCB removal from the environment extremely problematic (5).

PCBs can be divided into two distinct categories with regards to their structural relationship to toxicity; (1) coplanar or non-*ortho*-substituted arene substitution patterns and (2) noncoplanar or *ortho*-substituted congeners. The coplanar group members have 2 phenyl rings which occupy the same plane, giving the molecule structural similarities to polychlorinated dibenzo-p-dioxins (PCDDs) and dibenzofurans, and allowing coplanar PCBs to elicit similar toxic effects via agonist activity at the aryl hydrocarbon receptor (AhR) in humans and animals (5). Noncoplanar PCBs have chlorine atoms at the *ortho* position on one or both of the biphenyl rings; this chlorine position causes steric hindrance and forces the molecule to twist out of plane. Members of the noncoplanar group have not been found to interact with AhR, but rather have been shown to bind both the constitutive androstane receptor (CAR) and the pregnane x receptor (PXR) (5).

1.1.1.2 PCB lipophilicity

Part of the persistence of PCBs in the environment stems from their high lipophilicity; the octanol:water partition coefficient of $\geq 10^4$ for most congeners dictates that their accumulation in nonlipid substances will be minimal (6). We have previously reported that mice orally gavaged with two doses of PCB-77 overwhelming accumulate the contaminant in adipose tissue, with secondary tissue accumulation in liver and trace amounts in serum (7). These findings are consistent with studies by Kodavanti et.al., in which rats were gavaged five times per week for 4 weeks with Aroclor 1254 and the reported mean ratio of total PCB in blood:liver:adipose tissue was 1:22:359 (8). Most likely as a result of their lipophilicity, obese subjects store approximately two to three times the quantity of total PCBs in adipose tissue, which would indicate that hydrophobic PCBs were highly attracted to the large lipid pools present during obesity. Conversely, in obese subjects experiencing drastic weight loss from bariatric surgery, serum levels of PCBs increased and were suggested to decrease the beneficial effects of weight loss with respect to liver toxicity markers and serum lipid parameters (9).

These studies suggest that adipose tissue can store lipophilic PCBs and that adipose tissue might be a target for the adverse health effects associated with these chemicals. Furthermore, adipose tissue would represent a low-grade internal source of stored PCBs which could then act systemically upon release from adipose lipids.

1.1.1.3 General health effects of PCBs

The toxicity of PCBs varies among congeners. The coplanar PCBs, due to dioxin-like properties, are among the most toxic congeners. Since PCBs are frequently found in complex mixtures due to their industrial use, the concept of toxic equivalency factors (TEFs) has been developed to aid in risk assessment and regulatory control. In the TEF system, more toxic PCB congeners are assigned higher TEF values on a scale from 0 to 1, and the highest TEF value of 1 is assigned to TCDD (10) (Table 1.1).

Humans may be exposed to PCBs by breathing in contaminated air, eating contaminated food, and through accidental skin contact with contaminated materials. PCBs in foods tend to be most prevalent in meat (particularly beef) and dairy products which are high in fat and conversely less prevalent in grain, fruit, and vegetable food stuffs (11). Furthermore, PCB levels have been found to be greater in farm raised salmon compared to wild caught fish, apparently due to PCB contamination in commercial fish meal (12). PCBs can be excreted in feces or stored in adipose tissue (13). Due to high lipophilicity, PCBs also tend to collect in milk fat and can be transmitted to infants through breast-feeding (14-15).

A frequently observed health effect in populations with very high levels of PCB exposure are skin conditions (chloracne and rashes). In the Japanese Yusho poisoning incident (1968), more than 14,000 people suffered mass poisoning when 280 kg of PCB-contaminated rice bran oil was used as chicken

feed (16). Reported symptoms included dermal and ocular lesions, including unusual skin sores, fatigue, and lowered immune responses (17).

A growing body of evidence suggests that PCB exposure may have a positive association with the development of non-Hodgkin lymphoma, a cancer of the immune system (18-19), and they may also mimic the action of estrogen in breast cancer cells and increase breast carcinogenesis (20). The U.S. EPA and the International Agency for Research on Cancer (IARC) have concluded that PCBs are probable carcinogens (2, 21). PCBs are also considered as probably carcinogenic to humans by the World Health Organization (22).

Finally, TCDD and PCB exposure are positively correlated with the development of T2D in numerous epidemiology studies (Tables 1.3, 1.4, and 1.5). These findings are consistent with the published opinion of the National Institutes of Environmental Health Sciences (NIEHS) Division of the National Toxicology Program (NTP), which reviewed many of the epidemiology studies examining the correlation between PCBs and diabetes and concluded that there is a positive association between these two factors and that more research is needed to understand underlying mechanisms (23).

1.1.2 Aryl-hydrocarbon receptor (AhR)

The aryl-hydrocarbon receptor (AhR) is a member of the family of basic helix-loop-helix transcription factors. The endogenous ligands of this receptor remain unknown, although it binds numerous exogenous ligands including natural plant flavonoids, polyphenolics, and indoles, and additionally synthetic polycyclic aromatic hydrocarbons and dioxin-like compounds such as coplanar PCBs

(Table 1.2). AhR is a cytosolic transcription factor which is inactive when bound to several co-chaperones. Subsequent to ligand binding to chemicals such as 2,3,7,8-tetrachlorodibenzo-*p*-dioxin (TCDD), the chaperones dissociate and allow for AhR translocation to the nucleus and dimerization with aryl-hydrocarbon receptor nuclear translocator (ARNT), initiating changes in gene transcription (Figure 1.2).

1.1.2.1 Protein functional domains

The AhR protein contains a number of domains critical for function and is classified as a member of the basic helix-loop-helix/Per-Arnt-Sim (bHLH/PAS) family of transcription factors (24-25) (Figure 1.3). The bHLH motif is located in the N-terminal of the protein (26). Transcription factors of the bHLH superfamily have two highly conserved and functionally distinctive domains; the basic-region (b), which is necessary for the binding of the transcription factor to DNA, and the helix-loop-helix (HLH) region, which promotes protein-protein interactions. In addition, the AhR contains two PAS domains, PAS-A and PAS-B; sequences of 200 to 350 amino acids that display a high sequence homology to the protein domains that were originally discovered in the Drosophila genes period (Per), single-minded (Sim), and ARNT (27). The PAS domains facilitate particular secondary interactions with other PAS domain-containing proteins, specifically between AhR and ARNT, allowing the protein complex to form. The ligand binding site of AhR is located within the PAS-B domain (28) and contains conserved residues necessary for ligand binding (29). A Q-rich domain is

contained in the C-terminal region of AhR and is needed for co-activator recruitment and transactivation (30).

1.1.2.2 Aryl-hydrocarbon receptor ligands

AhR ligands can be broadly classified into synthetic or naturally occurring categories (Table 1.2). The first recognized AhR ligands were synthetic halogenated aromatic hydrocarbons (polychlorinated dibenzodioxins, dibenzofurans, and biphenyls) and polycyclic aromatic hydrocarbons (3-methylcholanthrene, benzo(a)pyrene, and benzoflavones) (31-32). More recently, several studies have examined naturally occurring ligands, hinting toward the identity of an endogenous ligand.

Potential endogenous ligands of AhR include the following: derivatives of tryptophan such as indigo dye and indirubin (33), bilirubin (34), arachidonic acid and ecosanoid metabolites lipoxin A4 and prostaglandin G (35), modified low-density lipoprotein (36), and numerous dietary carotinoids (32).

1.1.2.3 Aryl-hydrocarbon receptor signaling pathways

AhR in the absence of ligand binding is located in the cytoplasm as an inactive protein complex consisting of a dimer of Hsp90 (37-38), prostaglandin E synthase 3 (Ptges3, p23) (39-42), the immunophilin-like protein hepatitis B virus X-associated protein 2 (XAP2) (43) (previously known as AhR interacting protein, AIP (44)), and AhR-activated 9 (ARA9) (45). The dimer of Hsp90 with p23 has several functions in the protection of AhR from proteolysis, holding the receptor in a conformation to facilitate ligand binding, and blocking the inappropriate binding of ARNT (28, 40, 42, 45-47). XAP2 interacts with the carboxyl-terminal of

Hsp90 and binds to the AhR nuclear localization sequence (NLS), which prevents the premature trafficking of the receptor into the nucleus (48-50).

After ligand binding to AhR, XAP2 is released resulting in exposure of the NLS and translocation into the nucleus (51). It is hypothesized that Hsp90 dissociates from AhR in the nucleus, exposing the two PAS domains to facilitate the binding of ARNT (52-55). The activated AhR/ARNT heterodimer complex interacts with DNA by binding to recognition sequences located in the 5'-regulatory region of dioxin-responsive genes (52, 54, 56).

The conventional recognition motif of the AhR/ARNT heterodimer complex, known as either the AhR-, dioxin- or xenobiotic- responsive element (AHRE, DRE or XRE), includes the core sequence 5'-GCGTG-3' (57) within the consensus sequence 5'-T/GNGCGTGA/CG/CA-3' (58-59) in the promoter region of AhR responsive genes. The AhR/ARNT complex directly binds the AHRE/DRE/XRE core sequence in a manner such that ARNT binds to 5'-GTG-3' and AhR binds 5'-TC/TGC-3' (60-61). Current publications postulate that the element termed AHRE-II, 5'-CATG(N6)C[T/A]TG-3', is capable of indirectly acting with the AhR/ARNT complex (62-63). The culmination of these steps results in an array of differential changes in gene expression.

1.1.2.4 Functional role of AhR in physiology and toxicology

Evolutionarily, the most primitive physiological role of AhR is in development. AhR is believed to have evolved from invertebrates where the receptor functioned in a ligand-independent manner in normal development processes (64). The AhR homolog in *Drosophila, spineless* (ss) is required for development

of the antenna and legs (65-66). In developing vertebrates, AhR appears to play a role in cellular proliferation and differentiation (6, 67). AhR has been shown to be involved in differentiation of several developmental pathways, including hematopoiesis (68), lymphoid systems (69-70), T-cells (71), neurons (72), hepatocytes (73), and adipocytes (6).

The adaptive response is evidenced by the induction of xenobiotic metabolizing enzymes. Proof of the adaptive response was first detected from the AhR-dependent induction of cytochrome P450, family 1, subfamily A, polypeptide 1 (CYP1A1) due to TCDD exposure (74-76). The hunt for the presence of DREs in the promoter region of genes has led to the identification of an AhR gene battery of Phase I and Phase II metabolizing enzymes consisting of CYP1A1, cytochrome P450, family 1, subfamily A, polypeptide 2 (CYP1A2), cytochrome P450, family 1, subfamily B, polypeptide 1 (CYP1B1), NADPH dehydrogenase quinine 1 (NQO1), aldehyde dehydrogenase family 3, member A1 (ALDH3A1), UDP-glucuronosyltransferase family 1, polypeptide A2 (UGT1A2), and glutathione S-transferase A1 (GSTA1) (77). Through activation of the classical AhR gene battery, vertebrates can detect a wide range of chemicals at the cellular level which AhR is capable of binding to facilitate their biotransformation and elimination. Intriguingly, a recent study by Lensu et.al. implies that the AhR might signal the presence of toxins in food and cause aversion to those foodstuffs (78).

The toxic response is an expansion of the adaptive response induced by AhR activation. Toxicity may stem from two different arms of AhR signaling. In

the first arm, the induction of metabolizing enzymes can result in the generation of toxic metabolites. For instance, the AhR ligand benzo(a)pyrene (BaP), is converted to a toxic metabolite via the induction of CYP1A1 and CYP1B1 in a variety of tissues (79). The second arm of toxicity occurs through irregular changes in global gene transcription beyond those seen in the classical AhR gene battery, leading to global changes in gene expression and adverse modifications in cellular processes and function (67, 80-85). Interestingly, recent microarray analysis implies that different synthetic AhR ligands regulate distinct genetic networks (86).

1.1.2.5 AhR in glucose homeostasis and metabolic studies

While the toxicological functions of the AhR have been vigorously studied, the role of the AhR in glucose homeostasis and metabolism remains largely unexplored. Wang et.al. examined glucose tolerance, insulin resistance, expression of peroxisome proliferator–activated receptor-α (PPAR-α), and genes affecting glucose metabolism and fatty acid oxidation rhythms in wild-type (WT) versus AhR-deficient [knockout (KO)] mice (87). In this study, KO mice displayed enhanced insulin sensitivity and improved glucose tolerance, accompanied by decreased PPAR-α and key gluconeogenic and fatty acid oxidation enzymes, indicating a link between AhR signaling and glucose metabolism. The authors further conclude that hepatic activation of the PPAR-α pathway might be a mechanism underlying AhR-mediated insulin resistance.

Further clues to the role of AhR in glucose metabolism can be found by examining gene microarray studies utilizing high-affinity receptor ligands. Nault

et.al. utilized livers from chow-fed C57BL/6 mice for gene microarray, 1, 3 and 7 days after a single oral gavage of 30 μg/kg TCDD (85). Administration of TCDD resulted in robust activation of not only genes involved in the xenobiotic response, but also genes associated with steroid, phospholipid, fatty acid, and carbohydrate metabolism. Arzuaga et.al. performed gene DNA analysis on livers from C57BL/6 mice fed diets enriched with high-linoleic acid oils (20% and 40% as calories), with half of each group exposed to PCB77 (84). This study demonstrated a significant interaction between dietary fat and PCB exposure, such that deregulated genes were organized into patterns describing the interaction of diet and PCB exposure. Control animals demonstrated a significant high-fat mediated induction of genes associated with fatty acid metabolism, triacylglycerol synthesis and cholesterol catabolism, but this effect was down-regulated in animals exposed to PCB77. Several of these genes are regulated by PPAR-α and as predicted, changes in PPAR-α gene expression followed the same pattern as described above, demonstrating that dietary fat can interact with environmental pollutants to compromise lipid metabolism. Taken together, the results of these gene microarray studies would suggest not only that there is a distinctive role for the AhR in metabolism, but that overall nutritional status and the presence of lipids can modulate the interaction between AhR and exogenous ligands.

Recent studies demonstrated that consumption of farmed salmon containing persistent organic pollutants, including increased levels of seven different PCBs, promoted glucose intolerance associated with elevations in

adipose tissue expression of tumor necrosis factor-α (TNF-α) in high fat (HF) fed C57BL/6 mice (88).Interestingly, when levels of pollutants were decreased by feeding salmon purified fish oil, glucose tolerance improved and adipose expression of TNF-α decreased. This study suggested that the adipocyte AhR may be of importance in mediating some of the observed effects.

Another recent study tested the role of the AhR in obesity and fat metabolism in the absence of exogenous ligands (89). Utilizing two congenic mouse strains that differed at the AhR gene and encode AhRs with a 10-fold difference in signaling activity, the mouse strains were fed low-fat (LF) diet or HF diets. The HF diet differentially increased body weight and body fat to body mass ratios in the mouse strain expressing the higher affinity and higher response AhR. These results suggest that the AhR plays an important and broad role in obesity and associated complications.

1.1.3 PCBs and type 2 diabetes

1.1.3.1 The pathophysiology of type 2 diabetes

Global estimates indicate 300 million people are affected by diabetes, with type 2 diabetes (T2D) accounting for 90% of diabetes prevalence (90). Moreover, the world-wide diabetes incidence is anticipated to double in the next twenty years in tandem with global population aging, a general decrease in physical activity, and increasing rates of obesity. Women would appear to be at greater risk for developing T2D, as are certain ethnic groups (90-92). Traditionally considered a disease of adults, T2D is increasingly diagnosed in children in parallel with rising obesity rates (90).

T2D is a metabolic disorder that is characterized by high blood glucose in the context of insulin resistance and relative insulin deficiency (93). This is in contrast to diabetes mellitus type 1, where there is an absolute insulin deficiency due to destruction of islet cells in the pancreas (93). Classical T2D symptoms are polyuria, polydypsia, polyphagia, and weight loss (91). Many people, however, have no symptoms during the first few years and are diagnosed on routine testing. Long-term complications from unregulated high blood glucose can include heart disease, strokes, diabetic retinopathy and subsequent blindness, kidney failure which may require dialysis, and poor circulation of limbs leading to amputations (91). The development of T2D is caused by a combination of lifestyle and genetic factors, with obesity believed to be a primary contributing factor (91, 94).

T2D is initially managed by increasing physical activity and improved diet. If blood glucose levels are not adequately lowered by these modifications, medications such as metformin (to suppress hepatic gluconeogenesis and enhance the insulin sensitivity of peripheral tissue) or insulin (in lieu of insufficient endogenous insulin from the pancreas) may be required. For those on insulin, patients must routinely check blood glucose levels.

T2D eventually progresses to insufficient insulin production from beta cells in the pancreas due to chronic insulin resistance (IR) in peripheral tissues (91). IR is typically observed in skeletal muscle, liver, and adipose tissue, and is characterized by the inability of cells to respond adequately to insulin (91). Insulin normally suppresses glucose production and release by the liver. In IR, because

the liver is no longer sensitive to insulin, inappropriate hepatic output of glucose can occur (91). Other potentially significant mechanisms associated with T2D and IR include the increased breakdown of lipids within adipocytes, high blood glucagon levels, increased kidney retention of salt and water, and the inappropriate regulation of metabolism by the central nervous system (93). However, not all people with IR are considered T2D, because an impairment of insulin secretion by pancreatic beta cells is also required (93). For example, prior to the development of T2D, most individuals will exhibit IR and a "pre-diabetic" physiology where in response to IR in peripheral tissues the pancreas will secrete more insulin than necessary. This disregulation of insulin secretion leads to the subsequent beta cell dysfunction present in T2D (93).

1.1.3.2. General characteristics of adipose tissue

Adipose tissue is connective tissue composed primarily of adipocytes, but also containing the stromal vascular fraction (SVF) of cells including preadipocytes, fibroblasts, vascular endothelial cells and variety of immune cells. Adipocytes are derived from preadipocyte stem cells. Adipose tissue stores energy in the form of lipids and acts as a major endocrine organ (95) producing numerous hormones such as adiponectin, estrogen, leptin, and the adipokine TNF-α. Adipose tissue is classified into two distinct types: white adipose tissue (WAT) and brown adipose tissue (BAT). In humans, adipose tissue is located beneath the skin (subcutaneous fat), around internal organs (visceral fat), and in specific locations (adipose depots).

Visceral fat is white adipose tissue located inside the abdominal cavity and is composed of several depots, including mesenteric, epidydmal, and perirenal. An excess of visceral fat is linked to the development of T2D (96), IR (97), inflammatory diseases (98), and other obesity-related diseases (99).

Most of the remaining nonvisceral fat is subcutaneous adipose tissue found below the skin in the hypodermis. Subcutaneous fat is not thought to be related to the development of the classic obesity-related pathologies, such as heart disease and stroke, and some data even suggests it might be protective against metabolic disease pathogenesis (100). Females generally deposit body fat around the hips, thighs, and buttocks in subcutaneous fat depots (termed gynoid distribution) which are believed to pose a lower health risk than visceral fat that is typically present in males (termed android distribution) (100).

A specialized form of adipose tissue is brown adipose tissue (BAT), primarily located near the neck and thorax in humans. This specialized adipose tissue can generate heat via uncoupling of the respiratory chain of oxidative phosphorylation within mitochondria. When protons transit along the electrochemical gradient across the inner mitochondrial membrane, the energy from this process is released as heat instead of being used to generate adenosine triphosphate (ATP). This process is thought to be most critical in neonates exposed to cold which would require thermogenesis to keep warm (101). Until recently, BAT was thought to be found only in infants in humans, but new studies have disproven this hypothesis. Metabolically active tissue with temperature responses similar to BAT was first reported in adults in

2007 (102), and the presence of BAT in adults was later verified by others (103-105). Strategies to direct the differentiation of BAT may become a weight loss therapy of the future.

1.1.3.3. Mechanisms of IR in adipose tissue

Adipocytes have a significant physiological role in sustaining triglyceride and free fatty acid levels, in addition to contributing to IR. Visceral fat is more prone than subcutaneous fat to display IR; thus, central obesity and waist circumference are markers of impaired glucose tolerance (100).

Oxidative stress is the broad term for an imbalance between the systemic expression of reactive oxygen species (ROS) and a biological system's capacity to readily detoxify the reactive intermediates or to repair the resultant damage. Disturbances in the normal redox state of cells can become the origin of toxic effects via the production of peroxides and free radicals that can damage any part of the cell, including proteins, lipids, and DNA. Additionally, some ROS act as cellular messengers in redox signaling, and therefore can cause disruptions in normal cellular signaling processes. The association between oxidative stress and IR, particularly in adipose tissue, has been recognized for some time (106-109). Furukawa et.al. demonstrated that production of ROS increased selectively in the adipose tissue of obese mice, which was abolished by treatment with a NADPH oxidase inhibitor (110). The inhibitor also attenuated the dysregulation of adipocytokines, improved diabetes, and hyperlipidemia in obese mice (110). These results suggest that increased oxidative stress in adipose tissue is an early marker of metabolic syndrome.

Adipokines also play a critical role in the development of adipose tissue IR, with TNF-α being a well recognized modulator of this effect. TNF-α is a multi-functional regulatory cytokine with diverse roles in inflammation, cell apoptosis and survival, cytotoxicity, production of other cytokines, and induction of IR in adipose tissue (111-113). TNF-α is synthesized as a 26 kDa plasma membrane bound monomer (114), and a secreted trimer is formed by proteolytic cleavage of the membrane-bound precursor protein by the TNF-α converting enzyme (TACE, also known as ADAM17) (115-116). Two TNF-α receptors, type I and type II, mediate TNF-α signal transduction (117).

Both mRNA and protein levels of TNF-α are highly induced in the adipose tissue of obese animals (111) and humans (118). Despite the fact that adipose tissue is composed of a variety of cell types which are able to produce cytokines, adipocytes are the principal source of TNF-α in adipose tissue (111, 113, 119), and express both TNF-α receptors. Prolonged exposure of animals (120) to TNF-α induces IR, and conversely neutralization of TNF-α increases insulin sensitivity (121-122). Additionally, TNF-α and TNF-α receptor knock out mice demonstrate improvements in insulin sensitivity in models of obesity (123-124). However, systemic administration of TNF-α neutralizing antibody to obese humans with type 2 diabetes did not improve insulin sensitivity (125). Because adipocyte-derived TNF-α is hypothesized to function principally in an autocrine or paracrine manner in adipose tissue, systemic infusion might not be able to abolish the biological activity of endogenous TNF-α in adipose tissue.

Free fatty acids (FFA) can reduce glucose uptake and metabolism; additionally, increased FFA oxidation can amplify the ratios of mitochondrial acetyl-CoA:CoA and NADH: NAD+, and thus impair insulin-mediated glucose utilization (126-127). FFA also inhibit insulin signaling (128-129) and glycogen synthesis in muscle (130-132), and promote hepatic glucose production (133). Systemic treatment with FFA inhibits glucose uptake in skeletal muscle in a dose-dependent manner (130, 134). Conversely, reducing systemic FFA improved glucose utilization (135-136) and ameliorated hyperinsulinemia in subjects with T2D. Although data suggest elevated blood FFA are involved in IR pathology, mechanisms which increase systemic FFA in T2D subjects are not completely understood. Systemic FFA are a balance between production and utilization, with lipolysis in adipocytes and in triglyceride-rich lipoproteins being principal sources of blood FFA. It has been postulated that systemic FFA levels are linearly correlated to the rate of adipose tissue FFA release (137), and that blockade of adipose tissue FFA release via insulin suppresses systemic FFA (138-139). It has been demonstrated that TNF-α is a significant autocrine/paracrine factor that can promote lipolysis and drive FFA release from adipose tissue (140-141).

Adiponectin is a secreted protein that is expressed primarily by adipocytes and is involved in regulating systemic glucose levels as well as fatty acid breakdown. Insulin stimulates adiponectin secretion in cultured adipocytes (142), however, TNF-α inhibits adiponectin mRNA levels (143). Adiponectin levels are down-regulated in humans and experimental animals with T2D (144-145).

Adiponectin knock out mice develop HF diet induced IR and hyperinsulimia, and have elevated FFA and blood glucose (146-147).

Additionally, adipose tissue is now considered an endocrine organ that can secrete several other bioactive molecules, such as leptin, resistin, IL-6, IL-1ß, adipsin, metalloproteases, plasminogen activator inhibitor-1 (PAI-1), vascular cell adhesion molecule-1 (VCAM-1) and angiotensinogen. While over 50 adipokines have been identified (148), it is probable that adipose tissue secretes additional proteins that have not been identified yet. Taken as a whole, these elements of adipose tissue constitute important factors in whole body energy metabolism and insulin sensitivity.

1.1.3.4. Emerging evidence of a positive correlation between xenobiotic AhR ligand exposure and the development of T2D: Agent Orange and U.S. Vietnam veterans

Agent Orange is the code name for the herbicide used by the U.S. military during the Vietnam War as part of its chemical warfare program known as Operation Ranch Hand. Agent Orange that was extensively sprayed on Vietnam and parts of Cambodia and Laos was later discovered to be contaminated with 2,3,7,8-tetrachlorodibenzodioxin (TCDD). The purpose of Operation Ranch Hand was to defoliate forested and agricultural land for two reasons; to deprive guerrilla combatants of cover and to induce forced draft urbanization of Vietnam's agrarian population to further limit their aid to guerrillas (149).

Numerous studies have examined health effects linked to Agent Orange, its component compounds, and its manufacturing byproducts (150). In 1969, it

was revealed that Agent Orange was contaminated with TCDD and that this was the likely cause of many of the previously unexplained negative health effects which were correlated with exposure to the herbicide (151). Subsequently, TCDD has been heavily studied. The National Toxicology Program has classified TCDD as a known human carcinogen, associated with soft-tissue sarcoma, non-Hodgkin's lymphoma, Hodgkin's lymphoma and chronic lymphocytic leukemia (152).

In 1991, the US Congress enacted the Agent Orange Act, giving the Department of Veterans Affairs the authority to declare certain conditions 'presumptive' to exposure to Agent Orange, which meant veterans who served in Vietnam were eligible to receive treatment and compensation for these conditions (153). Through this process, the list of presumptive conditions has grown to include: prostate cancer, respiratory cancers, multiple myeloma, Hodgkin's disease, non-Hodgkin's lymphoma, soft tissue sarcoma, chloracne and notably, T2D.

U.S. Air Force veterans of the Vietnam war exposed to Agent Orange contaminated with TCDD demonstrate increased risk of diabetes, reduced time-to-onset of disease, and increased diabetes severity (154). Moreover, Fujiyoshi et.al. obtained adipose tissue samples from Agent Orange exposed veterans and unexposed comparison veterans and found a reliable indicator of dioxin-induced diabetes to be the ratio of mRNA of glucose transporter 4 (GLUT4) and nuclear transcription factor kappa B (NFκB) (155). This ratio demonstrated a significant correlation to serum TCDD levels and fasting glucose among the

Agent Orange exposed group. It is interesting to note that very low exposure levels were detected in the Agent Orange group, in fact not much higher than levels found in the general population, implying a need to address current exposure levels linked to the development of diabetes. For further epidemiology studies evaluating Agent Orange exposure and T2D risk, see Table 1.3.

1.1.3.5. Evidence of a positive correlation between PCB exposure and the development of T2D: Anniston, AL Community

As diabetes incidence increases worldwide in tandem with increasing prevalence of obesity and sedentary lifestyles, environmental factors are emerging as a potentially important element of T2D risk. PCBs and dioxins are believed to play a role in diabetes development, based on data from the National Health and Nutrition Examination Survey (NHANES) (Lee 2006; Lee 2007) and studies from the Slovak Republic (Langer 2002), Sweden (Lee 2011), Japan (Uemura 2008), Taiwan (Wang 2008), and the United States (Codru 2007; Lee 2010; Lee 2011; Vasiliu 2006)(see Tables 1.4 and 1.5 for summary of epidemiology studies examining PCB/dioxin exposure and diabetes development); however the results are not always consistent between studies and most focus on mixtures of POPs. Additionally, commentaries (Jones et al. 2008; Porta 2006) have highlighted the need for further research.

PCBs originating from the Monsanto Chemical Company in Anniston, Alabama, leeched into Snow Creek, which then spread to the broader water supply of northern Alabama. Today, the highest pollution levels remain concentrated in Snow and Choccolocco Creeks (156). PCBs were manufactured

at the Monsanto facility from 1929 to 1971. Residents of the Anniston community exhibit some of the highest total body burdens of PCBs than any other location in the world (157), making this unique population a focus of epidemiological study, in particular because this population was exposed primarily to only PCBs (versus exposure to POP mixtures in other studies). In a recent study by Silverstone et.al., 774 residents of Anniston were given physical examinations and serum PCBs were quantified to calculate the odds ratios to assess the relationship between PCBs and diabetes (158). A statistically significant association of serum PCB levels with increased diabetes prevalence was found in the population overall, with women having a stronger association than men. Moreover, the most highly exposed subjects who were more than 55 years old had an elevated risk of diabetes. These findings are consistent with a recent publication by the National Institutes of Environmental Health Sciences (NIEHS) Division of the National Toxicology Program (NTP) which reviewed the bulk of epidemiology studies examining the correlation between PCBs and diabetes and concluded that there is a positive association between these two factors and that more research is needed to understand underlying mechanisms (23)(see Tables 1.4 and 1.5 for summary of epidemiology studies examining dioxin and PCB exposures, respectively, and diabetes development).

Most studies of PCB exposure in humans measure plasma or serum PCB levels as an index of environmental PCB exposure and systemic PCB burden. Efforts to associate PCB exposure with disease risk in many studies of this type are often confounded by the broad range of human PCB exposures and the

impact of statistically more powerful factors on overall disease risk. The Silverstone study is significant for two reasons. First, that it identified PCB exposure as a risk factor for development of T2D independent of other risk factors (158). Second, the study gives clear ranges of serum PCB levels in humans which are positively associated with the development of T2D. Subjects were stratified by serum PCB levels and the adjusted odds ratio comparing the prevalence of diabetes in the fifth versus first quintile of serum PCB levels was 2.78. In this study the fourth and fifth quintiles represented total serum PCB levels (the sum of 35 PCB congeners) in the range of 4.34-170 parts per billion (by weight). Assuming an average molecular weight of 325 and a serum density of 1g/ml this represents serum PCB concentrations of 0.01-0.52 μM.

1.1.3.6. The role of PCBs in oxidative stress and inflammation

Coplanar PCBs exhibit their toxicity by binding to AhR and subsequently increasing CYP1A1 gene expression. Coplanar PCBs can stimulate the production of ROS by uncoupling the catalytic cycle during their metabolism by CYP1A1 (159). Studies have shown that coplanar PCBs, including PCB 77 and PCB 126, are proinflammatory in vascular endothelial cells and can promote NF-κB signaling (160-161). Arsenescu et.al. demonstrated that coplanar PCBs, but not noncoplanar PCBs, can stimulate inflammatory adipokines in adipose tissue (6). Besides stimulating an inflammatory response, PCBs can also promote inflammatory conditions such as obesity and diabetes (6-7).

Many mechanisms and signaling pathways associated with inflammatory diseases can be modulated by both diet and POPs. Several genes induced in

insulin resistant tissues are sensitive to oxidative stress as an initiating stimulus, suggesting that an imbalance in oxidative stress and/or ROS scavenging mechanisms is a significant factor that may mediate effects. There is emerging evidence to suggest that antioxidant nutrients might protect against exposure to environmental pollutants via down-regulation of signaling pathways involved in oxidative stress and inflammatory responses associated with diabetes (162).

1.1.4. PCBs and obesity

1.1.4.1 The pathophysiology of obesity

The World Health Organization classifies people as obese with a body mass index (BMI) greater than 30 and overweight with a BMI of 25-29.9. Data from the NHANES in 2009-2010 indicated that 35.7% of adults and approximately 17% of children in the U.S. are obese (163). Obesity is an element of the metabolic syndrome, a cluster of risk factors that substantially increase the risk for diabetes development and includes increased waist circumference, blood pressure, fasting blood glucose, triglycerides, and reduced HDL (164). Visceral obesity is a primary factor of the metabolic syndrome and is independently associated with each of the other factors (165).

Obesity is thought of as a problem representing an imbalance between energy intake and expenditure, which can be influenced by any number of genetic and environmental factors, including physical activity, regulation of satiety, eating behaviors, hormonal imbalance, fetal programming, or exposure to POPs. Regardless of cause, modifications in adipose tissue growth, function, and remodeling dictate if an obese subject will develop obesity-associated disorders.

In developing obesity, excessive caloric intake drives increases in adipocyte size. Obesity is also correlated with increased macrophage infiltration into adipose tissue (166) due to inappropriate adipose tissue remodeling to make room for hypertrophied adipocytes (167). Chronic adipose tissue inflammation, in combination with ectopic lipid deposition in other tissues, link obesity with other elements of the metabolic syndrome to increase the risk of insulin resistance and the subsequent development of diabetes (168).

1.1.4.2. Polychlorinated biphenyl-77 induces adipocyte differentiation and proinflammatory adipokines and promotes obesity

Due to their lipophilicity, PCBs accumulate in adipose tissue and therefore the total body burden of PCBs increases with obesity (7, 9, 169-170), but the effects of PCBs on adipocytes, adipose tissue, obesity and diabetes are largely undefined.

Arsenescu et.al. examined *in vitro* and *in vivo* effects of coplanar 3,3',4,4'-tetrachlorobiphenyl (PCB-77) on adipocyte differentiation, proinflammatory adipokines, adipocyte morphology, and body weight. 3T3-L1 adipocytes were incubated with PCB-77 either during adipocyte differentiation or in already differentiated adipocytes. Low concentrations of PCB-77 increased adipocyte differentiation and expression of peroxisome proliferator–activated receptor gamma (PPARγ), while higher concentrations inhibited adipocyte differentiation. This result is consistent with adipose wasting effects and reduced preadipocyte differentiation seen at high doses of TCDD in other published in vitro and in vivo studies (171-173). PCB-77 promoted the expression and release of numerous

proinflammatory cytokines from 3T3-L1 adipocytes, including TNF-α. In *in vivo* studies, C57BL/6 wild-type (WT) or AhR deficient (AhR–/–) mice were treated with vehicle or PCB-77 (49 mg/kg, by intraperitoneal injection) and body weights were measured over a six week period. Administration of PCB-77 increased body weight gain in WT but not AhR–/– mice. These findings suggest that PCB-77 may promote the development of obesity and obesity-associated diseases such as T2D.

1.2 Resveratrol

Resveratrol (3,5,4'-trihydroxy-trans-stilbene) is a stilbenoid, a natural polyphenol commonly found in food stuffs such as red wine, grapes, peanuts, and chocolate, albeit in very minute quantities (red wine contains approximately 0.1-14.3 mg/L (174)). Resveratrol can also be chemically (175) and biotechnologically synthesized (176-177), and is sold as a nutritional supplement. The effects of resveratrol are currently a topic of numerous animal and human studies. In animal studies, anticancer (178-181), anti-aging (182-183), anti-inflammatory (184-186), anti-diabetic (182, 187-192), anti-obesity (187, 193-198) and additional beneficial cardiovascular effects (199-211) of resveratrol have been reported. Conversely, a limited number of human studies have reported generally positive effects on measured outcomes, but certainly not the robust disease ablation effects of resveratrol reported from animal studies. Very high doses (3–5 g) of resveratrol used in one small positive human trial significantly lowered blood glucose in T2D patients (212). A larger clinical trial which administered 250 mg/d of resveratrol to sixty-two T2D diabetes patients for 3

months also reported a significant reduction in fasting blood glucose and mean hemoglobin A_{1C} (213). Timmers et.al. reported that in eleven healthy but obese men treated with 150 mg/d of resveratrol for 30 days fasting blood glucose was reduced and HOMA index of insulin sensitivity improved (214). Conversely, a recent study demonstrated that resveratrol had no effect on glucose homeostasis in lean individuals (215), suggesting that resveratrol requires the presence of an existing metabolic disturbance for efficacy in relation to glucose or insulin tolerance. Due to some promising results and the easy availability of resveratrol, research on beneficial effects of the compound are expanding. However, the long-term effects of resveratrol supplementation in humans are not known (174).

1.2.1. General mechanism of action of resveratrol

Resveratrol's effects to increase longevity appear to mimic the biochemical effects of calorie restriction. Resveratrol has been shown to activate Sirtuin 1 (SIRT1) (216) and peroxisome proliferator-activated receptor gamma coactivator 1-alpha (PGC-1α), which are thought to contribute to the compounds effects to improve mitochondrial function (187). However, evidence is conflicting as other studies have not link resveratrol to activation of SIRT1 and effects of calorie restriction (217-219).

Resveratrol has been shown to interfere with the initiation, promotion, and progression of certain cancers. In vitro experiments demonstrate that potential mechanisms could include modulation of the transcription factor NF-κB (220) and inhibition of CYP1A1 (221) (however this mechanism may not be pertinent to CYP1A1-mediated bioactivation of POPs) (222).

Resveratrol also possesses potent antioxidant and anti-inflammatory properties (183, 223). Resveratrol has been shown to increase intracellular glutathione in a nuclear factor (erythroid-derived 2)-like 2 (Nrf2) dependent manner via upregulation of gamma-glutamylcysteine ligase in lung epithelial cells, which subsequently conferred protection against cigarette smoke extract-induced oxidative stress (224). Additionally, a recently published study showed that male C57BL/6 fed a HF diet supplemented with 0.4% resveratrol had lower levels of TNF-α systemically and in adipose tissue (225).

Resveratrol can competitively inhibit key phosphodiesterases, resulting in increased cyclic adenosine monophosphate (cAMP), a second messenger for the activation of the pathway Epac1/CAMMKß/AMPK/SIRT1/PGC-1α. Rising cAMP levels increase fatty acid oxidation, mitochondrial biogenesis, mitochondrial respiration, and gluconeogenesis (226-227).

1.2.2. Resveratrol dosing in rodent and human studies

Approximately 70% of orally administered resveratrol is absorbed by humans; however oral bioavailability is about 1% as a result of extensive hepatic gluconuridation and sulfation (228). When subjects were administered a substantial oral dose of resveratrol (2.5 and 5 g), blood resveratrol levels did not reach the concentration believed to be essential for systemic cancer prevention (229). A proprietary formulation of oral resveratrol, SRT-501 (3 or 5 g), resulted in blood resveratrol levels which were five to eight times higher than those reported by Walle et.al., which did mirror concentrations with demonstrated efficacy in animal and in vitro experiments (212). However, in 2010 GlaxoSmithKline

suspended a small clinical trial of SRT-501 being used as a treatment for patients with multiple myeloma due to safety concerns, and ultimately terminated the study later in the same year when several patients developed kidney failure (230). It should be noted that it is not clear if the kidney failure resulted from SRT-501 administration or from the underlying disease (the type of kidney failure observed in this trial is a common complication of multiple myeloma) (231).

Bioavailability of resveratrol would seem to be dependent in some cases on meal composition. In a pharmacokinetic study of oral resveratrol (2 g) administered twice daily in humans, interactions of resveratrol during concurrent ingestion of ethanol, quercetin, and high fat meals were examined (232). Mean peak serum resveratrol levels were 1,274 ng/ml at steady-state, but this was reduced by 46% when ingested with a high fat meal, although there was no effect of concurrent oral administration of quercetin or ethanol. This study reported no adverse health effects, but was limited by the small number of subjects (8) who were observed in the two week study.

In humans and rats less than 5% of the oral dose has been reported as the parent molecule resveratrol in blood (228, 233-236). The most abundant resveratrol metabolites in humans, rats, and mice are trans-resveratrol-3-O-glucuronide and trans-resveratrol-3-sulfate (237). Walle et.al. hypothesized that sulfate conjugates are the primary source of resveratrol bioactivity (228), Wang et. al. suggest that it is the glucuronides (238), and Boocock et al. emphasize the need for further research on the effects of resveratrol metabolites (233).

Some have suggested that resveratrol from wine might have higher bioavailability than resveratrol from supplements (234). However, this concept has been refuted by several studies (239-240). Studies which have administered moderate amounts of wine to human subjects have only detected trace amounts of resveratrol in blood that are insufficient to explain the French paradox, suggesting that the beneficial effects of wine might require the presence of alcohol (239) or the complex of substances that wine contains (240).

1.2.3. Effects of resveratrol on glucose and insulin tolerance

Resveratrol has well documented anti-diabetic effects in rodents, which has driven a number of clinical trials to utilize the compound as a therapy for diabetes. Resveratrol has been demonstrated to lower blood glucose and lipids in rats with streptozotocin (STZ)-induced diabetes as well as rats with STZ-nicotinamide-induced diabetes (189, 193). In numerous studies in rodents, resveratrol demonstrates antidiabetic effects such as the abolishment of IR and glucose intolerance (182, 187-193). A recent clinical study of T2D patients treated with oral resveratrol supplements for three months reported significant improvements in nearly all biomarkers associated with the disease (213). However, evidence also suggests that resveratrol has no effect in lean individuals (215), or that resveratrol improves adipose tissue glucose homeostasis only under insulin resistant conditions (241). In general, resveratrol has been shown to improve symptoms of T2D via three main mechanisms: reduction of blood glucose, preservation of pancreatic ß cells, and improvement

in insulin action. Studies indicate that the beneficial effects of resveratrol in relation to T2D comprise all these mechanisms.

Maintenance of blood glucose in the physiological range is pivotal for the treatment of T2D, because hyperglycemia causes numerous diabetic complications (242). Thus, treatment with hypoglycemic drugs (metformin or α-glucosidase inhibitors) are administered in clinical practice to lower blood glucose, but these drugs are not without unfavorable side effects (243). Resveratrol has been well documented to lower hyperglycemia in humans and animals, with apparently limited side effects. The blood glucose lowering action of resveratrol has been demonstrated in obese rodents (244) and in two animal models of diabetes: in rats with streptozotocin-induced diabetes or streptozotocin nicotinamide-induced diabetes (189, 192-193, 245-247). Administration of resveratrol to diabetic rats lowered levels of glycosylated hemoglobin (HbA1C), which suggests the prolonged reduction of glycemia (189, 248). The blood glucose lowering effect of resveratrol seen in diabetic animals is believed to stem from a stimulatory action on intracellular glucose transport. Interestingly, in experiments on isolated hepatocytes, adipocytes, and skeletal muscle from diabetic rats, resveratrol stimulated glucose uptake in the absence of insulin (193). Enhanced glucose uptake induced by resveratrol appears to occur due to increased activity of glucose transporters in the plasma membrane. Studies of rats with experimentally induced diabetes administered resveratrol showed increased expression of the insulin-dependent glucose transporter (GLUT4) compared to controls (192, 249).

Development of T2D is a prolonged process, usually accompanied by insulin resistance. Initially, blood glucose is maintained in the physiological range because of the compensatory increase in insulin secretion. Chronic overstimulation of pancreatic ß cells exhausts and degrades these cells, diminishing insulin secretion over time (250). Resveratrol appears to modulate blood insulin concentrations in rodents. Resveratrol effectively reduced blood insulin in animal models of hyperinsulinemia; in mice on a high-fat diet (182, 187, 251-252), in rats on a high cholesterol-fructose diet (188), and in obese Zucker rats (253). *In vitro*, resveratrol reduced insulin secretion by isolated rat pancreatic islets (254-256). The inhibition of insulin secretion caused by resveratrol was shown to result from metabolic changes in pancreatic ß cells. During physiological conditions, glucose-induced insulin secretion from ß cells is predicated on the following series of events: intracellular transport of glucose and its oxidative metabolism, hyperpolarisation of the inner mitochondrial membrane, increased ATP synthesis, closure of ATP-sensitive potassium channels, depolarization of the plasma membrane, opening of voltage-sensitive calcium channels, and the rise in cytosolic calcium ions.The increase in cytosolic calcium ions triggers secretion of insulin (93). In this sequence leading to increased secretion of insulin, resveratrol has been shown to act on ATP formation. Pancreatic islets treated with resveratrol released more lactate, and glucose oxidation was decreased compared to controls (255). It should be noted that the inhibition of insulin secretion by resveratrol was apparently reversible and was not due to permanent changes in pancreatic ß cells (254-255). Because chronic

overstimulation of ß cells is known to stimulate their degradation, inhibition of insulin secretion by resveratrol might attenuate these effects.

Resveratrol may also protect the endocrine pancreas via other mechanisms. *In vitro*, exposure of isolated rat pancreatic islets to cytokines resulted in increased DNA binding of NF-κB, increased production of NO, and expression of iNOS, with all effects being suppressed by resveratrol (257). The protective effect of resveratrol against cytokine-induced dysfunction of ß cells is due in part to the ability of resveratrol to activate NAD+ dependent protein deacetylase SIRT1 (257).

Resveratrol may also protect against T2D via antioxidant activity. Pancreatic ß cells are known to be uniquely sensitive to the oxidative damage (258-259). In a recent study of diabetic rats, the levels of lipid peroxides and protein carbonyls in the pancreatic tissue were significantly increased compared with non-diabetic animals, indicative of oxidative damage; inversely, the activity of enzymes involved in radical scavenging was significantly reduced (260). Administration of resveratrol abolished the oxidative damage and increased the activities of antioxidant responsive enzymes (248).

T2D is typically accompanied by insulin resistance, defined as the impaired action of insulin on target cells, mainly adipocytes, hepatocytes, and skeletal muscle cells. IR develops primarily in overweight or obese individuals with T2D (261), and decreased adiposity improves insulin action (262). Calorie restriction and exercise are clinical recommendations to improve insulin sensitivity in T2D. Numerous animal studies have demonstrated that resveratrol

improves insulin action during diet-induced T2D symptoms, likely by acting as a calorie restriction or exercise mimetic (182, 187, 194, 251, 253).

The improvement in insulin action caused by resveratrol may stem from a variety of effects, including reduced adiposity. High doses of resveratrol reduce body weight / fat mass in rodents on a HF diet (187, 194-198), with effects which are similar to those induced by calorie restriction (183, 263). Consistent with rodent studies, *in vitro* experiments demonstrated decreased ATP content (264) and reduced accumulation of triglycerides in isolated rat adipocytes treated with resveratrol (265). Moreover, resveratrol increased lipolytic response to epinephrine and decreased lipogenesis (266), results that are suggestive as to how resveratrol may contribute to reduced adiposity in rodents. Kennedy et.al. utilized human adipocytes to demonstrate that resveratrol abolished linoleic acid-induced insulin resistance (267). Furthermore, resveratrol suppressed inflammatory cytokines induced by linoleic acid. Potential mechanisms of the protective effects of resveratrol on human adipocytes include the attenuation of oxidative stress, prevention of activation of extracellular signal-related kinase, inhibition of inflammatory gene expression, and increase in peroxisome proliferator-activated receptor γ (PPAR-γ) activity (267).

Resveratrol-induced improvement in insulin action has also been attributed to the activation of SIRT1 and 5'-AMP-activated protein kinase (AMPK) (182, 187, 195-196, 257). In AMPK-deficient mice fed a high-fat diet, resveratrol had no effect and neither reduced body fat nor improved insulin action (194). However, contrary findings have been reported by Pacholec *et al*., which

demonstrated that resveratrol is not a direct activator of SIRT1, which would suggest that the role of SIRT1 in the mechanism of resveratrol action should be reconsidered. While the exact mechanism of resveratrol action is still poorly understood, there is ample evidence that this compound is able to improve insulin action in a variety of animal models of insulin resistance.

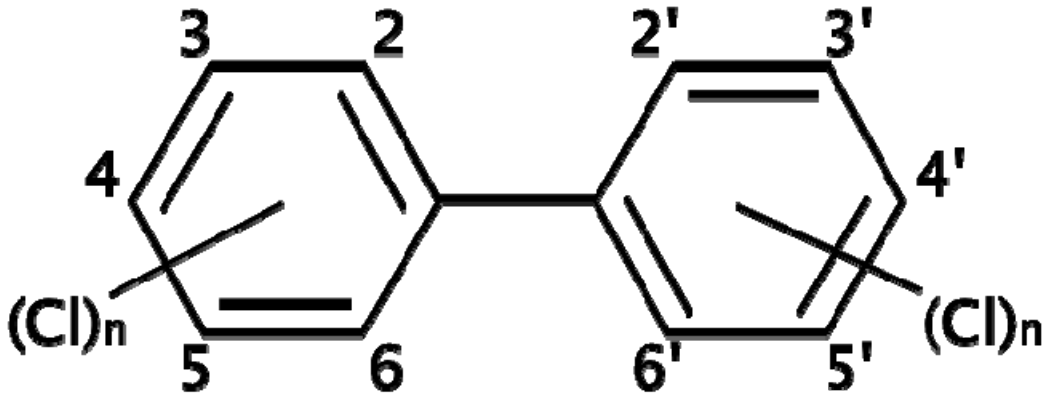

Figure 1.1 Chemical Structure of PCBs

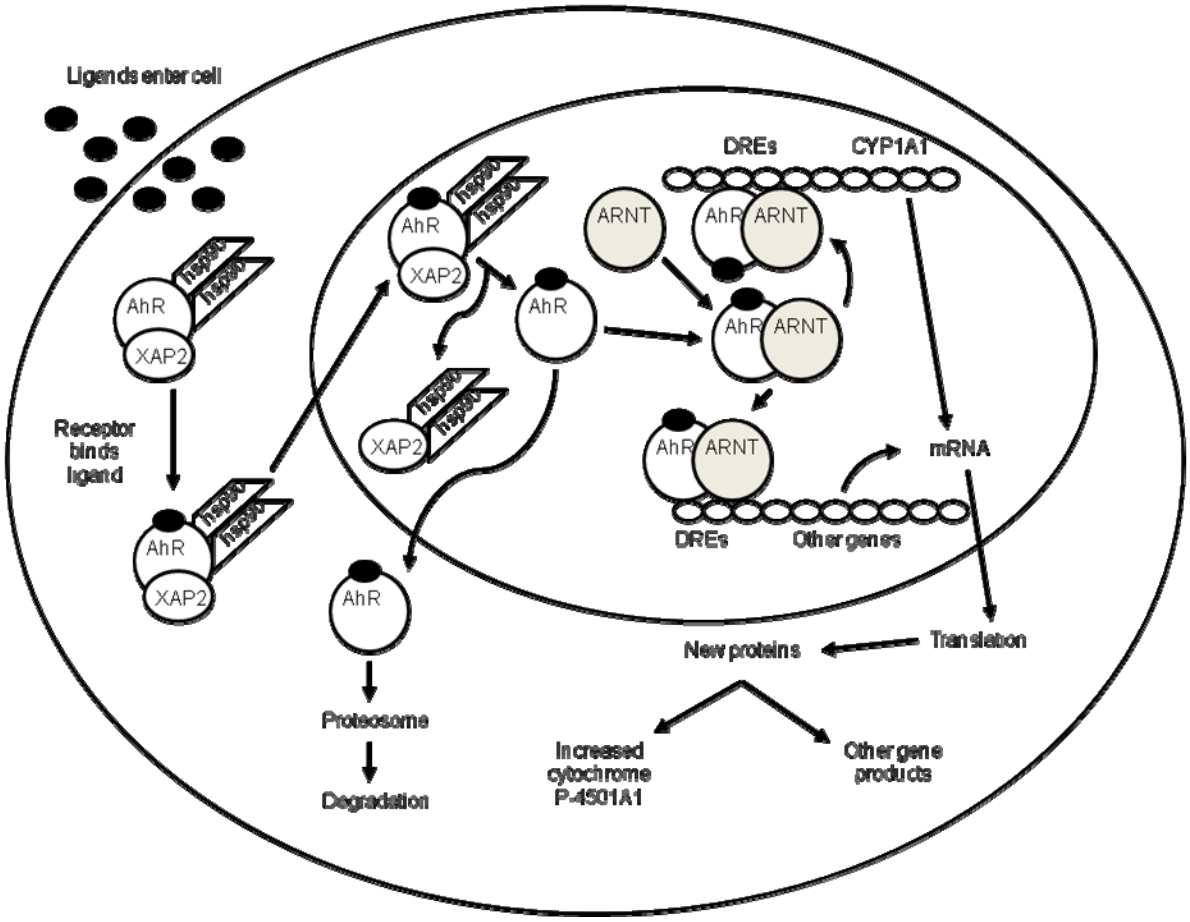

Figure 1.2 AhR Signaling Pathway

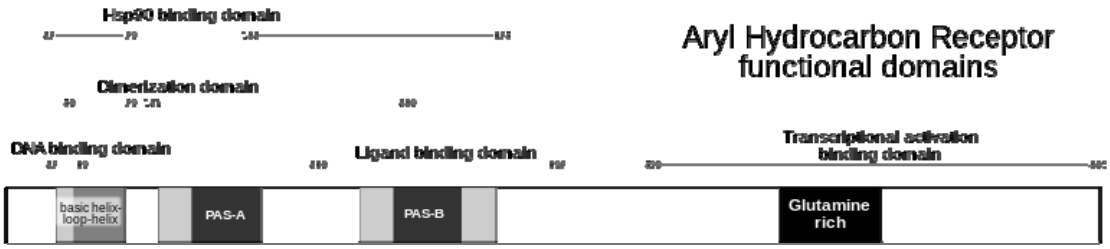

Figure 1.3 Protein functional domains of AhR

Compound	WHO TEF
2,3,7,8-TCDD	1
3,3',4,4'-tetraCB (PCB-77)	0.0001
3,3',4,4',5-pentaCB (PCB-126)	0.1

Table 1.1 World Health Organization TEF values of TCDD and selected PCBs

Synthetic	Naturally Occuring
2,3,7,8-TCDD	Derivatives of tryptophan
Coplanar PCBs	Lipoxin A4
Polychlorinated dibenzofurans	Bilirubin
Benzo (a) pyrene	Prostaglandin G2
Benzoflavones	Curcumin
Benzanthracenes	Modified low-density lipoprotein

Table 1.2 Synthetic and naturally occuring AhR ligands

Publication	Population	Diagnosis	Exposure	Risk Estimate
ADVA 2005b	Vietnam veterans	Diabetes (death certificate)	Vietnam service	SMR = 0.52 (Vietnam veterans vs. general population)
ADVA 2005a	Vietnam veterans	Diabetes (death certificate)	Agent Orange	SMR = 0.3 (deployed vs. non-deployed)
AFHS 2005	Vietnam veterans	Diabetes (verified history)	Agent Orange	RR = 1.3 (within Ranch Hand veterans, adjusted for prior TCDD measurements)
CDC 1988	Vietnam veterans	Diabetes (self report)	Vietnam service	adjOR = 1.2 (deployed vs. non-deployed)
Fujiyoshi 2006	Vietnam veterans	Diabetes (physican diagnosed)	TCDD	r = 0.07, p = 0.40 (Operation Ranch Hand veterans vs. non-Ranch Hand veterans)
Henriksen 1997	Vietnam veterans	Diabetes (physican diagnosed)	TCDD	RR = 1.5 (time to develop diabetes decreased with high TCDD exposure)
Kang 2006	Vietnam veterans	Diabetes (self report)	Vietnam service	OR = 1.50 (sprayed herbicides in Vietnam vs. never)
Kim 2003	Vietnam veterans	Diabetes (clinical exam)	Agent Orange	OR = 2.69 (Vietnam veterans vs. non-veterans)
Kern 2004	Vietnam veterans	Insulin sensitivity (ivGTT,QUICKI)	TCDD	ß = -0.00639, p = 0.02 (w/in pair differences for lower insulin sensitivity in Operation Ranch Hand veterans)
Longnecker 2000	Vietnam veterans	Diabetes (self report)	TCDD	adjOR = 1.56 (4th quartile of TCDD exposure, Operation Ranch Hand veterans vs. non-Ranch Hand veterans)
Michalek 2003	Vietnam veterans	Diabetes (physican diagnosed)	TCDD	no relationship after adjustment for covariates (diabetic Operation Ranch Hand veterans vs. non-diabetic Ranch Hand veterans)
Michalek 2008	Vietnam veterans	Diabetes (physican diagnosed)	TCDD	RR = 1.21, p = 0.16 (Operation Ranch Hand veterans vs. non-Ranch Hand veterans)
Steenland 2001	Vietnam veterans	Diabetes (physican diagnosed)	TCDD	OR = 1.18, (TCDD exposed Operation Ranch Hand veterans vs. non-exposed Ranch Hand veterans)

SMR = standardized mortality ratio

RR = relative risk

adjOR = adjusted odds ratio

Table 1.3 Summary of studies investigating the correlation between Agent Orange/TCDD exposure in Vietnam veterans and the development of type 2 diabetes.

Publication	Population	Diagnosis	Exposure	Risk Estimates
Bertazzi 2001	Residents of Seveso during 1976 incident	Diabetes (death certificate)	TCDD	RR = 1.7 (males), RR = 0.8 (females) (cause of death vs. reference population)
Calvert 1999	Workers employed at plants in NJ and MO	Diabetes (physician diagnosis)	TCDD	adjOR = 1.97 (4th quartile of TCDD exposure vs. unexposed workers)
Chang 2010	Residents living near dioxin factory	Non-diabetics w/ metabolic syndrome	dioxins	adjOR = 1.7 (insulin resistance in lowest 3 quartiles vs. 4th quartile of TCDD exposure)
Chen 2006	Recidents living near municipal waste incinerators in Tiawan	Diabetes (physician diagnosis)	PCDDs, PCDFs	adjOR = 2.44 (PCDD/PCDF concentration and diabetes vs. non-diabetics)
Chen 2008	Non-diabetic pregnant women living near incinerators in Tiawan	Non-diabetics	PCDDs, PCDFs, PCBs	no significant correlations with serum insulin or QUICKI results in adjusted models
Collins 2009	Plant workers w/ occupational exposure vs. US population	Diabetes (death certificate)	TCDD	SMR = 1.1 (workers vs. US population)
Consonni 2008	Residents of Seveso during 1976 incident	Diabetes (death certificate)	TCDD	RR = 1.03 (Zone A), 1.32 (Zone B), 1.26 (Zone R) (reference territory vs. Zones A, B, and R)
Cranmer 2000	Residents living near AK Superfund site	Fasting insulin and glucose; OGTT	TCDD	adjOR = 8.5 (high fasting insulin for highest exposure percentile vs. lowest exposure percentile)
Fierens 2003	Residents living near Belgium industrial sites vs. rural areas	Diabetes (self report)	dioxins, PCBs	adjOR = 5.07 (17 dioxins or PCDD/Fs), 13.3 (4 coplanar PCBs [77, 81, 126, 169]), 7.58 (12 other PCBs [3, 8, 28, 52, 101, 118, 138, 153, 180, 194, 206, 209]) (highest percentile for dioxin vs. all other percentiles)
Lee 2007	Adults from NHANES 1999 - 2002	Insulin sensitivity (HOMA)	PCDDs, PCDFs, coplanar PCBs, noncoplanar PCBs, OC pesticides	adjOR = 2.3 (PCDD), 1.4 (coplanar PCBs), 2.3 (noncoplanar PCBs) (highest percentile vs. lowest percentile)
Pesatori 1998	Residents of Seveso during 1976 incident	Diabetes (death certificate)	TCDD	RR = 1.1 (males, Zone R), 1.2 (females, Zone R) (Zone R vs. population of Lombardy region)
Steenland 1999	Workers from 12 US plants that produced TCDD-contaminated products	Diabetes (death certificate)	TCDD	SMR = 1.08 (diabetes, multiple causes and beyond) (total cohort industrial cohorts vs. US population)
Sweeney 1997	Workers from NJ and MO plants that produced TCDD-contaminated products	Diabetes (medical exam)	TCDD	OR = 1.12 (workers [mean 220 pg/g lipid] vs. referents [mean 7 pg/g lipid])
Turunen 2008	Finnish fishermen and fishermen's wives	Diabetes (death certificate)	dioxins, PCBs	SMR = 0.43 (males), 0.83 (females)
Uemura 2008	General population of Japan from urban, agrarian, and fishing areas	Diabetes (self report)	7 PCDDs, 10 PCDFs, 12 coplanar PCBs	adjOR = 2.21 (highest tertile for PCDDs+PCDFs), 6.82 (highest tertile for coplanar PCBs), 3.81 (highest tertile for total dioxins)
Vena 1998	Research on Cancer International (IARC) study of herbicide production workers	Diabetes (death certificate)	TCDD	RR = 2.25 (Poisson regression analysis of diabetes mortality)

Table 1.4 Summary of studies investigating the correlation between dioxin exposure and the development of type 2 diabetes.

Publication	Population	Diagnosis	Exposure	Risk Estimates
Chen 2008	Non-diabetic pregnant women	Non-diabetics	PCDDs, PCDFs, PCBs	no significant correlations with serum insulin or QUICKI results in adjusted models
Codru 2007	Mohawks from Akwesasne River for ≥ 5 years	Diabetes (use of diabetes medication)	PCBs, PCB-153, PCB-74, DDE, mirex, HCB	OR = 3.2 (total PCBs), 2.4 (PCB-153), 4.5 (PCB-74) (Diabetes, highest tertile vs. lowest tertile)
Everett 2007	NHANES 1999 – 2002 (adults)	Diabetes (self report)	PCB-126, p,p'-DDT, HxCDD	adjOR = 1.67 (PCB-126) (total diagnosed and undiagnosed diabetes)
Fierens 2003	Belgians living near industrial sites vs. rural areas	Diabetes (self report)	dioxins, PCBs	adjOR = 5.07 (17 dioxins or PCDD/Fs), 13.3 (4 coplanar PCBs [77, 81, 126, 169]), 7.58 (12 other PCBs [3, 8, 28, 52, 101, 118, 138, 153, 180, 194, 206, 209])
Jorgensen 2008	Greenlanders from three areas of West Greenland	Diabetes (OGTT or FBG; IR by HOMA)	Coplanar (3) and noncoplanar (10) PCBs, 11 OC pesticides	adjOR = 1.2 (coplanar PCBs [105, 118, 156]), 1.2 (noncoplanar PCBs [28, 52, 99, 101, 128, 138, 153, 163, 170, 180]) (1st [referent] vs. 4th quartile)
Langer 2002	Workers from a PCB factory vs. residents of rural East Slovakia	Anti-GAD antibody serum levels > 1.21 U/mL	PCBs	40.4% vs. 10.5% (frequency of anti-GAD antibodies in exposed workers vs. unexposed rural dwellers)
Langer 2009	Adults from industrial areas of Slovakia	glucose, insulin, lipids, BMI	PCBs	chi-square = 110.55, p < 0.0001 (increased FG), 11.89, p = 0.0182 (increased fasting insulin)
Lee 2006	Adults from NHANES 1999 - 2002	Diabetes (self report)	PCB-153, DDE, HpCDD	adjOR = 6.8 (PCB-153) (diabetes in highest percentile vs. non detectable)
Lee 2007	Adults from NHANES 1999 - 2002	Insulin sensitivity (HOMA)	PCDDs, PCDFs, PCBs, OC pesticides	adjOR = 2.3 (PCDD), 1.4 (coplanar PCBs), 2.3 (noncoplanar PCBs) (highest percentile vs. lowest percentile)
Lee 2010	Young Adults CARDIA cohort	Diabetes (use of diabetes medication)	55 POPs	OR = 2.8 (PCB-74), 2.0 (PCB-153), 2.2 (PCB-170), 2.8 (PCB-180) (2nd quartile vs. 1st quartile of incident diabetes)
Mullerova 2008	Obese women vs. non-obese women	HOMA index; fasting glucose and insulin	PCB-153	no correlation between PCB-153 and study group (p > 0.05)
Patel 2010	NHANES 1999 - 2006 (total of four cohorts)	Diabetes (FG ≥ 126 mg/dL)	heptachlor epoxide, PCB-170	OR for PCB-170 = 2.3, p = 0.02 (1999-2000 cohort), 4.5, p = 0.01 (2003-2004 cohort), 2.2, p < 0.001 (1999-2004, 3 cohorts)
Rignell-Hydbom 2009	Fisherman's wives from the Swedish east and west coasts	Diabetes (self report)	PCB-153, p,p'-DDE	OR = 1.4 (PCB-153) (PCB-153 per 100 ng/g lipid increase in serum level)
Rignell-Hydbom 2007	Participants of WHILA diagnosed w/ T2D	Diabetes (OGTT)	PCB-153, p,p'-DDE	OR = 1.6 (PCB-153) (> 7 years after baseline)
Rylander 2005	Swedish fisherman and fisherman's wives	Diabetes (self report)	PCB-153, p,p'-DDE	OR = 1.20 (men, PCB-153), 1.06 (women, PCB-153) (PCB-153 per 100 ng/g lipid increase in serum level)
Turunen 2008	Finnish fishermen	Diabetes (death certificate)	dioxins, PCBs	SMR = 0.43 (males), 0.83 (females)
Turyk 2009a	Participants of GLCHA	Diabetes (self report)	DDE, total PCBs	RR = 1.8 (total PCBs)
Turyk 2009b	Participants of GLCHA	Diabetes (self report)	DDE, total PCBs	OR = 1.9 (highest quartile for total PCBs), 2.1 (highest tertile for total coplanar PCBs)
Uemura 2008	Japanese from urban, agrarian, and fishing areas	Diabetes (self report)	7 PCDDs, 10 PCDFs, 12 coplanar PCBs	adjOR = 2.21 (highest tertile for PCDDs+PCDFs), 6.82 (highest tertile for coplanar PCBs), 3.81 (highest tertile for total dioxins)
Vasiliu 2006	Adults in the Michigan PBB cohort	Diabetes (self report)	PBBs, PCBs	Incidence density ratio = 1.74 (males, highest PCB quartile), 2.33 (females, highest PCB quartile)
Wang 2008	Yucheng cohort study	Diabetes (self report)	PCBs	OR = 1.7 (males), 5.5 (females)

Table 1.5 Summary of studies investigating the correlation between PCB exposure and the development of type 2 diabetes.

STATEMENT OF THE PROBLEM

Emerging evidence supports a link between exposures to polychlorinated biphenyls (PCBs) and the development of type 2 diabetes (T2D). However, mechanisms for this link are unclear. Because of their lipophilicity, PCBs accumulate markedly in adipose lipids. Thus, obesity increases the body burden of PCBs. Notably, studies have demonstrated that weight loss results in redistribution of PCBs to the systemic circulation, and this redistribution is associated with adverse health effects. However, it is unclear if release of greater quantities of PCBs stored in adipose tissue of obese subjects following weight loss adversely influences the control of glucose homeostasis. Moreover, it is unclear if therapeutic strategies can be developed to mitigate harmful effects of liberated PCBs on glucose homeostasis.

Previous studies in our laboratory demonstrated that coplanar PCBs that are ligands of the aryl hydrocarbon receptor (AhR) promote the expression and release of proinflammatory cytokines from cultured adipocytes. Tumor necrosis factor-α (TNF-α), an inflammatory cytokine known to exert several effects that impair insulin sensitivity, was increased by PCB-77 in 3T3-L1 adipocytes. However, mechanisms for PCB-induced increases in inflammatory cytokine expression in adipocytes and the pathophysiologic consequences of this effect on glucose homeostasis are unknown.

The purpose of this study was to determine mechanisms linking coplanar PCB exposures to the development of T2D. We initially defined effects of coplanar PCBs (dose-dependency, sustainability) on measures of glucose homeostasis in

lean mice. To determine potential sites for PCB-induced impairment of glucose homeostasis, we quantified effects of PCBs on TNF-α expression in adipose tissue, liver and muscle, tissues that are major sites of insulin-mediated glucose uptake. Since obesity is a well known contributor to the development of T2D, we defined effects of a coplanar PCB on measures of glucose homeostasis during the weight gain phase in mice with diet-induced obesity. Moreover, we examined effects of PCBs administered during the weight gain phase of obesity on glucose homeostasis during weight loss. We hypothesized that release of increased body burdens of PCBs in obese mice experiencing weight loss would impair glucose homeostasis. To determine if effects of coplanar PCBs to impair glucose homeostasis were adipose-specific and AhR-mediated, we examined effects of PCBs on glucose homeostasis in lean and obese mice (during the weight gain and weight loss phase) lacking AhR specifically in adipocytes. Finally, we used supplemental doses of resveratrol as a therapeutic entity to prevent PCB-induced impairment of glucose homeostasis in lean mice. We also defined mechanisms of resveratrol to protect against PCB-induced oxidative stress, impairment of glucose uptake and disruptions in insulin signaling. We focused on stimulation of anti-oxidant pathways by resveratrol.

The overall hypothesis of this dissertation is that coplanar PCBs act at adipocyte AhR to impair insulin signaling and glucose uptake and that resveratrol protects against PCB-induced impairment of glucose homeostasis. The following specific aims were designed to test this hypothesis:

Specific Aim 1: Define effects of coplanar PCBs (PCB-77, PCB-126) on glucose homeostasis in lean versus obese C57BL/6 mice.

A. Define effects (dose-dependency, sustainability) of PCB-77 on glucose homeostasis in lean mice.

B. Define effects of PCB-77 on glucose homeostasis in mice during the weight gain versus weight loss phases of diet-induced obesity.

C. Define mechanisms for PCB-induced impairment of glucose homeostasis in 3T3-L1 adipocytes.

Specific Aim 2: Determine if dietary administration of resveratrol is an effective nutritional therapy against PCB-77 induced diabetes in lean C57BL/6 mice.

A. Determine the effect of resveratrol supplementation in mice with acute PCB-77 exposure.

B. Determine the effect of resveratrol on oxidative stress and glucose uptake in 3T3-L1 adipocytes exposed to PCB-77.

Specific Aim 3: Determine the role of the adipocyte AhR on the development of PCB-77 induced diabetes.

A. Determine the effect of adipocyte-AhR deficiency on parameters of glucose and insulin tolerance in lean versus obese (with and without weight loss) mice administered vehicle or PCB-77.

SECTION II. SPECIFIC AIM 1

2.1 Summary

Previous studies demonstrated that coplanar polychlorinated biphenyls (PCBs) promote proinflammatory gene expression in adipocytes. PCBs are highly lipophilic and accumulate in adipose tissue, a site of insulin resistance in persons with type 2 diabetes. We investigated the *in vitro* and *in vivo* effects of coplanar PCBs on adipose expression of tumor necrosis factor α (TNF-α) and on glucose and insulin homeostasis in lean and obese mice.

We quantified glucose and insulin tolerance, as well as TNF-α levels, in liver, muscle, and adipose tissue of male C57BL/6 mice administered vehicle, PCB-77, or PCB-126 and fed a low fat (LF) diet. Another group of mice administered vehicle or PCB-77 were fed a high fat (HF) diet for 12 weeks; the diet was then switched from HF to LF for 4 weeks to induce weight loss. We quantified glucose and insulin tolerance and adipose TNF-α expression in these mice. In addition, we used *in vitro* and *in vivo* studies to quantify aryl hydrocarbon receptor (AhR)-dependent effects of PCB-77 on parameters of glucose homeostasis.

Treatment with coplanar PCBs resulted in sustained impairment of glucose and insulin tolerance in mice fed the LF diet. In PCB-77–treated mice, TNF-α expression was increased in adipose tissue but not in liver or muscle. PCB-77 levels were strikingly higher in adipose tissue than in liver or serum. Antagonism of AhR abolished both *in vitro* and *in vivo* effects of PCB-77. In

obese mice, PCB-77 had no effect on glucose homeostasis, but glucose homeostasis was impaired after weight loss.

Coplanar PCBs impaired glucose homeostasis in lean mice and in obese mice following weight loss. Adipose-specific elevations in TNF-α expression by PCBs may contribute to impaired glucose homeostasis.

2.2 Introduction

Type 2 diabetes (T2D) affects 300 million people, and diabetes prevalence is anticipated to double world-wide over the next 20 years (90). Recent epidemiological studies suggested that exposure to low concentrations of polychlorinated biphenyls (PCBs) similar to current exposure levels in humans increases diabetes risk (268). Multiple cross-sectional analyses of National Health and Nutrition Examination Survey (NHANES) cohorts from 1999–2006 found concentrations of PCB-170 in urine or blood with an adjusted odds ratio of 4.5 for T2D, predicting up to 15% risk (269). Remarkably, this increased risk appeared in individuals who were not overweight or obese (270). Similar observations linking PCB exposures to T2D have been reported in other populations (271-272). Recently, a significant association between elevated PCB levels and diabetes was found in the Anniston Community Health Survey (158). Collectively, accumulating evidence supports a link between PCB exposure levels and the development of diabetes, but mechanisms linking PCBs to diabetes are largely unknown.

Because of their lipophilicity, PCBs accumulate in lipid stores of adipose tissue (8), suggesting that adipocytes experience continuous low-grade exposures to PCBs. Extension of these findings to the setting of obesity suggests that the total body burden of PCBs would increase in obese subjects because of the inherent lipophilicity of these compounds. Recent studies demonstrated an inverse relationship between serum levels of several PCBs and body mass index, suggesting that sequestration of PCBs in adipose tissue is enhanced by

obesity (273). It is unclear whether this enhanced sequestration limits effects of PCBs systemically. Given the epidemic of obesity and T2D in the United States, a large percentage of the population strives to lose weight. Weight loss, through dietary restriction or increased physical activity, typically reduces adipose tissue mass through liberation of lipid stores (274). Lim et al. (275) reported that plasma concentrations of organochlorines were increased and significantly correlated to reductions in body mass index in obese subjects undergoing a weight-loss program. Further, Pelletier et al. (276) found that plasma concentrations of 13 of 17 organochlorines in serum increased in obese subjects experiencing weight loss. The consequences of increased liberation of PCBs following weight loss in obese subjects with T2D are unknown.

Previous studies in our laboratory demonstrated that low concentrations of coplanar PCB-77 (3,3´,4,4´-tetrachlorobiphenyl), a ligand of the aryl hydrocarbon receptor (AhR), promoted adipocyte differentiation and the production of proinflammatory adipokines (6). Recent studies showed that PCB-126 (3,3´,4,4´,5-pentachlorobiphenyl), a coplanar AhR ligand, promoted inflammatory gene expression in human preadipocytes and adipocytes, and also increased inflammatory gene expression in adipose tissue from wild-type, but not AhR-deficient, mice (277). Among several inflammatory cytokines stimulated by coplanar PCBs in adipocytes (6, 277), tumor necrosis α (TNF-α) is a recognized contributor to insulin resistance (278-279). TNF-α promotes insulin resistance through downstream alternative phosphorylation of the insulin receptor (IR) docking protein, insulin receptor substrate-1 (IRS-1) (280), which prevents

phosphorylation of protein kinase B (Akt) (281) and impairs transport of glucose transporter type 4 vesicles in skeletal muscle and adipose tissue to the plasma membrane (282). TNF-α can indirectly contribute to adipocyte insulin resistance by promoting lipolysis (283) and/or by inhibiting differentiation (284).

In the present study, we defined dose-dependent effects of coplanar PCBs on glucose homeostasis in lean mice. To define mechanisms for PCB-induced impairment of glucose and insulin tolerance, we quantified expression levels of TNF-α in organs contributing to insulin resistance. Moreover, we defined the sustainability of PCB-induced impairment of glucose homeostasis in lean mice in reference to organ and serum concentrations of PCBs. To delineate the role of AhR in effects of PCBs, we examined *in vitro* and *in vivo* effects of an AhR antagonist on parameters of glucose homeostasis. Because T2D is frequently associated with obesity, we examined effects of a coplanar PCB on glucose homeostasis in obese mice. In addition, because PCBs redistribute from adipose tissue to the circulation during weight loss, we determined effects of previous PCB exposures on glucose homeostasis in obese mice experiencing weight loss.

2.3 Materials and Methods

2.3.1 Chemicals

We purchased PCB-77 and PCB-126 from AccuStandard Inc. (New Haven, CT). 2-Methyl-2H-pyrazole-3-carboxylic acid (2-methyl-4-*o*-tolylazo-phenyl-amide; CH-223191) was a generous gift from H. Swanson (University of Kentucky, Lexington, KY).

2.3.2 Animal treatments and sample collection

All experimental procedures met the approval of the Animal Care and Use Committee of the University of Kentucky. We treated animals humanely and with regard for alleviation of suffering. Male C57BL/6 mice (2 months of age; The Jackson Laboratory, Bar Harbor, ME) were given *ad libitum* access to food and water and housed in a pathogen-free environment. Initial studies examined glucose and insulin tolerance in mice administered vehicle (tocopherol-stripped safflower oil), PCB-77 (2.5, 50, or 248 mg/kg; by oral gavage given as two separate doses over 2 weeks; n = 10 mice/group), or PCB-126 (0.3, 1.6, or 3.3 mg/kg once by oral gavage; n = 10 mice/group). Mice in dose–response studies were fed a low fat diet (LF; 10% kcal as fat; Research Diets Inc., New Brunswick, NJ).

To define the sustainability of PCB effects, we performed temporal studies in mice fed a LF diet. Mice were administered vehicle or PCB-77 (50 mg/kg by oral gavage) once in week 1 and once in week 2. For mice examined at later time points (12 weeks), a second set of treatment by oral gavages was administered in weeks 9 and 10. Mice in each treatment group (vehicle or PCB-77) were

examined at weeks 2, 4, or 12 after onset of feeding with LF diet. Body weights were quantified weekly in all studies. At the study end point, mice were anesthetized (ketamine/xylazine, 10/100 mg/kg, by intraperitoneal (ip) injection] for exsanguination and tissue harvest (liver, soleus muscle, and visceral adipose). A subset of mice (*n* = 5/group) in each treatment group were administered insulin [10 U/kg (285)] 10 min before exsanguination to elicit insulin signaling pathways.

For studies examining obesity and weight loss, male C57BL/6 mice (2 months of age; *n* = 10/group) were fed a high fat diet (HF; 60% kcal as fat; Research Diets Inc.) for 12 weeks and administered vehicle or PCB-77 (50 mg/kg by oral gavage) at weeks 1, 2, 9, and 10. Body weight was quantified weekly. At 12 weeks of HF feeding, a subset of mice (*n* = 3/group) was anesthetized for exsanguination and tissue harvest. The remaining mice in each treatment group were then fed the LF diet for 4 weeks to induce weight loss.

To determine whether *in vivo* effects were AhR-mediated, we fed male C57BL/6 mice (2 months of age; *n* = 7/group) the LF diet and orally gavaged them with vehicle or CH-223191 daily (10 mg/kg/day) (286-287) starting 1 week before administration of vehicle or PCB-77 and through the remainder of the study. After 1 week of pretreatment with CH-233191, mice were administered vehicle or PCB-77 (50 mg/kg by oral gavage, given as two separate doses in weeks 1 and 2). Within 48 hr after the last dose of vehicle/PCB-77, we performed glucose and insulin tolerance tests.

2.3.3 Glucose tolerance tests (GTT) and insulin tolerance tests (ITT)

Mice were fasted for 6 hr or 4 hr prior to quantification of GTT or ITT, respectively. Blood collected from the tail vein was tested for glucose concentration using a handheld glucometer (Freedom Freestyle Lite; Abbott Laboratories, Abbott Park, IL). Mice were injected with d-glucose (20% in saline, ip) or human insulin (Novolin, 0.0125 μM/g body weight, ip) and blood glucose was quantified at 0–120 min. Total area under the curve (AUC; arbitrary units), which is obtained without the presence of a baseline, calculates the area below the observed concentrations and, in comparison studies, was reported to compare favorably to the positive incremental area method for statistical analyses of glucose tolerance data (288).

2.3.4 Quantification of PCBs

Frozen tissue samples (epididymal adipose tissue, liver, and skeletal muscle) or mouse sera were spiked with surrogate standards (100 μL of 0.35 ng/μL PCB-166 in isooctane). After the addition of 1.0 g of diatomaceous earth, the mixture was grained into fine powders and transferred into an extraction cell filled with Ottawa Sands (Thermo Fisher Scientific, Pittsburgh, PA). Extraction with hexane (30 mL) was performed using an ASE 200 accelerated solvent extractor (Dionex Corporation, Sunnyvale, CA). Lipids were removed by the addition of an equal volume of concentrated sulfuric acid. For adipose samples containing high lipid content, hexane extracts were subjected to delipidation by passing them over a Florisil SPE column, according to the manufacturer's instructions, before acid treatment. The hexane layer containing PCBs was

collected and concentrated to 2 mL using a Heidolph Synthesis1 evaporator (Heidolph, Schwabach, Germany) and then to 100 μL using a gentle stream of nitrogen. Then, 10 μL of of internal standard PCB-209 (1.0 ng/μL) was added.

Gas chromatographic analysis was performed with a gas chromatography (GC)–mass spectrometry (MS) system (Agilent 6890N GC, G2913A auto sampler, and 5975 MS detector; Agilent Technologies, Santa Clara, CA) using an HP-5MS 5% phenyl methyl siloxane column (30 m length, 0.25 mm internal diameter, 0.25 μm film thickness). The column temperature was held at 60°C for 1 min, increased to 200°C at a rate of 40°C/min, followed by a rate of 4°C/min to 280°C, and then held for 5.5 min. The injector temperature was 250°C. The carrier gas was ultrapure helium, and the makeup gas was nitrogen. PCBs were identified on the basis of their retention times relative to standards. Quantification was achieved based on calibration curves obtained using PCB standards. The recovery efficiency was calculated from the surrogates and the sample weight.

2.3.5 Quantification of plasma components

We quantified plasma insulin concentrations using a commercial ELISA (Crystal Chem, Downers Grove, IL). Plasma TNF-α and interleukin-6 (IL-6) concentrations were quantified using a commercial Milliplex MAP Mouse Serum Adipokine kit (Millipore, St. Charles, MO).

2.3.6 Extraction of RNA and quantification of mRNA abundance using real-time polymerase chain reaction (PCR)

Total RNA was extracted from tissues using the SV Total RNA Isolation System kit (Promega Corporation, Madison, WI) (6). RNA concentrations were

quantified and cDNA was synthesized from total RNA and amplified using an iCycler (Bio-Rad, Hercules, CA) with the Perfecta SYBR Green Fastmix for iQ (20 μL; Quanta Biosciences, Gaithersburg, MD). Using the difference from 18S rRNA (reference gene) and the ΔΔCt method, we calculated the relative quantification of gene expression. The PCR reaction was 94°C for 5 min, 40 cycles at 94°C for 15 sec, 58°C or 64°C (based on tested primer efficiency) for 40 sec, 72°C for 10 min, and 100 cycles from 95°C to 45.5°C for 10 sec. Primer sequences were as follows: 18S, forward 5´AGTCGGCATCGTTTATGGTC-3´, reverse 5´-CGAAAGCATTTGCCAAGAAT-3´; *CYP1A1* (cytochrome P450 1A1), forward 5´AGTCAATCTGAGCAATGAGTTTGG-3´, reverse 5´-GGCATCCAGGGAA GAGTTAGG-3´; *F4/80* (macrophage marker), forward 5´-CTTTGGCTATGGGCTTCCAGTC-3´, reverse 5´-GCAAGGAGGACAGAGTTTATCGTG-3´; *TNF*-α, forward 5´-CCCACTCTGACCCCTTTACTC-3´, reverse 5´-TCACTGTCCCAGCATCTTGT-3´.

2.3.7 Western blotting

Tissues (liver, soleus muscle, and epididymal adipose tissue) were homogenized in mammalian protein extraction reagent (M-PER; Thermo Scientific, Rockford, IL), sonicated, and centrifuged, and supernatants were used to quantify protein. Proteins were resolved on 4–15% precast polyacrylamide gels (Bio-Rad) and transferred onto a polyvinylidene difluoride transfer membrane (GE Healthcare, Buckinghamshire, UK); nonspecific proteins were blocked for 1 hr at room temperature [5% nonfat milk in phosphate-buffered saline (PBS)

in 0.1% Tween-20 for 60 min at 25°C]. Membranes were then incubated with primary antibody: rabbit anti-TNF-α (1:1,000; Novus Biologicals, Littleton, CO), mouse β-actin (1:5,000; Cell Signaling Technology, Beverly, MA) in diluted PBS overnight at 4°C. After stripping primary antibody, membranes were incubated with secondary goat anti-rabbit IgG horseradish peroxidase–linked antibody (1:5,000; Cell Signaling Technology) for 1 hr at room temperature. Protein levels were quantified using Kodak Molecular Imaging Software (Carestream Health Inc., Rochester, NY).

2.3.8 Cell culture

3T3-L1 mouse preadipocytes, obtained from American Type Culture Collection (Manassas, VA) were cultured as described previously (6). Differentiation was induced by incubating cells for 2 days with media containing insulin (0.1 μM; Sigma Chemical Co., St. Louis, MO), dexamethasone (1 μM; Sigma), and isobutylmethyl xanthine (IBMX; 0.5 mM; Sigma), and then incubating with insulin for 1 additional day. Assays (n = 3/group) were performed on duplicate wells of cells. Differentiated adipocytes (day 8) were incubated with vehicle [0.03% dimethyl sulfoxide (DMSO)] or PCB-77 (3.4 μM) for 24 hr (6). The concentration of PCB-77 was based on the maximum serum level of PCB-77 (0.84 μg/g, converted to ≈ 3 μM) measured in experimental mice, as described above, at week 2 after administration of PCB-77 (50 mg/kg). Adipocytes from each treatment group were incubated with the AhR antagonist α-naphthoflavone (α-NF; 20 μM) for 30 min before adding vehicle or PCB-77 (3.4 μM).

2.3.9 Statistical analysis

Data are represented as mean ± SE. Total AUC and mRNA abundance data were log-transformed. We used one-way analysis of variance (ANOVA; SigmaPlot, version 12.0; Systat Software Inc., Chicago, IL) to define treatment effects of different doses of PCBs and for studies using CH-223191. In studies examining sustainability of PCB effects in lean mice, total AUC was analyzed using two-way ANOVA with the Holm-Sidak method for post hoc analysis. In studies of obese mice and mice undergoing weight loss, we performed a mixed model analysis of repeated measures and analyzed total AUC using two-way ANOVA (JMP, version 10; SAS Institute Inc., Cary, NC). Statistical significance was defined as $p < 0.05$.

2.4 Results

2.4.1 Coplanar PCBs dose-dependently impair glucose and insulin tolerance in LF-fed mice in an AhR-dependent manner

We defined dose-dependent effects of two coplanar PCBs (PCB-77 and PCB-126)—both of which are prevalent in the environment (289) and/or linked to T2D (270, 290)—on glucose and insulin tolerance in LF-fed mice. Forty-eight hours after the final dose, animals treated with PCB-77 (50 mg/kg) or PCB-126 (1.6 mg/kg) showed a significant increase in blood glucose concentrations, compared with controls, in response to a bolus of administered glucose (Figure 2.1A and B, respectively; $p < 0.05$). The total AUC for blood glucose concentrations was significantly increased in mice treated with PCB-77 or PCB-126 (Figure 2.1C and D, respectively; $p < 0.05$). Similarly, blood glucose concentrations in response to insulin administration were significantly increased in mice administered PCB-77 (50 mg/kg) or PCB-126 (3.3 mg/kg) (Figure 2.2A and B, respectively; $p < 0.05$), resulting in a significant increase in total AUC (Figure 2.2C and D, respectively; $p < 0.05$). Fasting plasma insulin concentrations were similar in mice administered vehicle (mean ± SE, 0.18 ± 0.10) or PCB-77 (0.19 ± 0.09 ng/ml; $p > 0.05$). On the basis of a higher prevalence of PCB-77 in food compared with PCB-126 (291), we used PCB-77 in further studies examining mechanisms of glucose and insulin intolerance.

To determine whether *in vivo* effects of PCB-77 are AhR-mediated, we defined effects of CH-223191, an AhR antagonist, on PCB-77–induced impairment of glucose and insulin tolerance in LF-fed mice. Administration of

PCB-77 significantly impaired glucose and insulin tolerance compared with vehicle, and these effects of PCB-77 were abolished in mice administered CH-223191 (Figure 2.3; $p < 0.05$).

2.4.2 PCB-77 treatment results in sustained impairment of glucose and insulin tolerance in LF-fed mice

To define the duration of PCB-induced impairment of glucose tolerance, we administered vehicle or PCB-77 (50 mg/kg) to LF-fed (12 weeks) male C57BL/6 mice in two doses in weeks 1 and 2 of LF feeding, and then again in weeks 9 and 10 of LF feeding. Body weight was not significantly different in mice administered vehicle (mean ± SE, 27 ± 1 g) or PCB-77 (28 ± 1 g; $p > 0.05$). Glucose tolerance was significantly impaired in PCB-77–treated mice compared with controls from weeks 2 to 12 of LF feeding (Figure 2.4A). Insulin tolerance was significantly impaired in PCB-77–treated mice compared with controls on weeks 2 and 4 (Figure 2.4B).

Due to their lipophilicity, PCBs accumulate in adipose tissue (8). We quantified levels of PCB-77 in retroperitoneal white adipose (RPF), liver, skeletal muscle, and serum following administration of PCB-77. PCB-77 levels were undetectable in tissues or serum from vehicle-treated mice; in addition, PCB-77 was not detected in skeletal muscle from either treatment group. At week 2, PCB-77 levels in RPF (mean ± SE, 192 ± 36 μg/g) were 10 and 384 times those in liver or serum (19 ± 1 and 0.5 ± 0.2 μg/g, respectively). At week 3, PCB-77 levels in RPF (91 ± 37 μg/g) were decreased (by 53%) compared with those in week 2 (192 ± 36 μg/g) and were markedly decreased by weeks 4 and 12.

Previous studies showed that PCB-77 increased *TNF*-α mRNA abundance in 3T3-L1 adipocytes (6). Thus, we contrasted effects of PCB-77 on *TNF*-α expression in adipose tissue compared with liver and skeletal muscle. As evidence of AhR activation by PCB-77, mRNA abundance of *CYP1A1*, an AhR target gene (32), was significantly increased in adipose tissue from PCB-77–treated mice compared with controls (Figure 2.5A). By comparison, *CYP1A1* mRNA abundance was significantly increased in livers of PCB-77–treated mice compared with controls at week 2 but not at later time points (Figure 2.5B). Although *TNF*-α mRNA expression in adipose tissue of PCB-77–treated mice did not reach statistically significant levels (Figure 2.6A), TNF-α protein was significantly increased at week 4 (Figure 2.7; $p < 0.05$). Plasma concentrations of TNF-α were significantly increased in PCB-77–treated mice compared with controls (Figure 2.8A; $p < 0.05$). Plasma concentrations of IL-6 were significantly increased at week 12 in mice administered PCB-77 compared with vehicle controls (Figure 2.8B; $p < 0.05$).

Infiltration of macrophages into adipose tissue has been suggested as a mechanism contributing to low-grade inflammation from obesity and the development of insulin resistance (292). Adipose tissue from mice administered PCB-77 exhibited statistically similar mRNA abundance of the macrophage marker F4/80 compared with controls (Figure 2.6B).

2.4.3 Effects of PCB-77 to promote glucose and insulin intolerance are lost in mice with diet-induced obesity, but manifest when obese mice lose weight

Obesity is associated with the development of insulin resistance in T2D (293). Moreover, obesity increases the total body burden of lipophilic PCBs (9). Thus, we examined effects of PCB-77 on glucose and insulin tolerance in mice fed a HF diet for 12 weeks (weight gain phase). In addition, we examined effects of PCB-77 on glucose and insulin tolerance in HF-fed obese mice (12 weeks) that were switched to the LF diet for 4 weeks to induce weight loss (weight loss phase). During the weight gain phase, PCB-77 treatment had no significant effect on body weight in mice fed either the LF or HF diet compared with controls (Figure 2.9A). Surprisingly, PCB-77 treatment had no effect on glucose or insulin tolerance in HF-fed mice (weeks 4 or 12; Figure 2.10A and B; weight gain phase). Moreover, abundance of *TNF*-α mRNA in adipose tissue was not significantly different in PCB-77–treated mice compared with controls (Figure 2.11). At 12 weeks, adipose tissue levels of PCB-77 (1.8 ± 0.5 μg/g tissue, wet weight) in mice fed the HF diet were 2 times those observed in adipose tissue from LF-fed mice.

Previous studies showed that plasma concentrations of PCBs increased in obese subjects experiencing weight loss (294). Thus, we defined effects of PCB-77 administered during the weight gain phase of HF feeding on glucose homeostasis during weight loss. Administration of PCB-77 during the weight gain phase had no effect on body weight reductions during the weight loss phase (Figure 2.9B). Glucose tolerance was significantly improved by weight loss in

vehicle- or PCB-77–treated mice (week 16 vs. week 12; Figure 2.10A; $p < 0.05$). Insulin tolerance was also significantly improved by weight loss in vehicle-treated mice (week 16 vs. week 12; Figure 2.10B; $p < 0.05$). However, compared with controls, mice administered PCB-77 exhibited impaired glucose (Figure 2.10A; $p < 0.05$) and insulin tolerance (Figure 2.10B; $p < 0.05$) during the weight loss phase. Weight loss resulted in a significant decrease in *TNF*-α mRNA abundance in adipose tissue from mice administered vehicle or PCB-77 (Figure 2.11; $p < 0.05$). However, PCB-77–treated mice had significantly increased *TNF*-α mRNA abundance in adipose tissue during weight loss (Figure 2.11; $p < 0.05$).

2.4.4 PCB-77 results in an AhR-dependent increase in expression of TNF-α in 3T3-L1 adipocytes

Previous studies demonstrated that PCB-77 increased mRNA abundance of *TNF*-α in 3T3-L1 adipocytes (6). TNF-α is an intermediate in reactive oxygen species generated by 2,3,7,8-tetrachloro-dibenzo-*p*-dioxin (TCDD), an AhR ligand (295). To define mechanisms for effects of coplanar PCBs to promote glucose and insulin intolerance, we examined effects of PCB-77 on *TNF*-α expression in 3T3-L1 adipocytes. Moreover, to determine whether effects of PCB-77 are AhR-mediated, we incubated cells with an AhR antagonist, α-NF. Incubation of differentiated 3T3-L1 adipocytes with PCB-77 significantly increased *CYP1A1* mRNA abundance, indicative of AhR activation (Figure 2.12A; $p < 0.05$), which was abolished by α-NF. Similarly, PCB-77-induced increases in *TNF*-α mRNA were abolished by α-NF in 3T3-L1 adipocytes (Figure 2.12B; $p < 0.05$).

2.5 Discussion

Results from this study indicate that coplanar PCBs induce rapid and sustained glucose and insulin intolerance in lean mice in an AhR-dependent manner. These effects were associated with pronounced accumulation of PCB to adipose tissue, most likely contributing to adipose-specific increases in expression of TNF-α. Remarkably, in PCB-exposed mice that became obese from consumption of a HF diet, the harmful effects of the toxicant promotion of glucose and insulin intolerance were lost. However, when the PCB-exposed obese mice lost weight, glucose and insulin tolerance were impaired, mitigating the beneficial effects of weight loss to improve glucose homeostasis. Moreover, adipose expression levels of *TNF*-α, while not influenced by PCB-77 during the weight gain phase of HF feeding, were increased upon weight loss. In cultured adipocytes, PCB-77 promoted *TNF*-α expression through an AhR-dependent mechanism. These results suggest that PCBs could promote insulin resistance through adipose-specific increases in TNF-α. Moreover, these results suggest that in obese mice with a greater body burden of PCBs, the concentration of PCB was increased in adipose tissue, resulting in increased adipose *TNF*-α expression and insulin resistance upon liberation of PCBs during weight loss.

Increasing evidence suggests that background exposure to persistent organic pollutants is linked to the development of T2D. U.S. Air Force veterans of the Vietnam War who were exposed to Agent Orange contaminated with dioxin had increased risk of diabetes, reduced time-to-onset of disease, and increased diabetes severity (154). In a cross-sectional study among the general population

of Japan and covering the years 2002–2006, blood levels representing the highest quartiles of PCB-126 and PCB-105 had adjusted odds ratios of 9.1 and 7.3, respectively (296). Recent results from the Anniston Community Health Survey demonstrated significant associations between elevated PCB levels and diabetes (158). Serum levels of PCB-77 in the present study (≈ 3 μM) were similar to levels (1.43 ppb, equivalent to ≈ 0.5 μM) observed in the lowest quartile of subjects from the Anniston study (158). Our results demonstrate that lean mice respond to coplanar PCBs with impaired glucose and insulin tolerance, supporting an interaction between PCB exposures and the development of insulin resistance. We used this mouse model of PCB-induced glucose and insulin intolerance to define mechanisms linking PCB exposures to dysregulated glucose homeostasis.

In the present study we demonstrated that PCB-77, a coplanar PCB abundant in the environment (289), as well as PCB-126, a coplanar PCB that has been linked to diabetes (290), both resulted in dose-dependent rapid impairment of glucose and insulin tolerance in lean mice. Interestingly, mice exposed to the highest dose of either PCB did not have impaired glucose or insulin tolerance; however, these mice demonstrated abnormal behavior (lethargy, tremors), polyuria, and gained minimal weight (unpublished observations), suggesting that higher doses of PCB had deleterious health consequences. Recent studies demonstrated that consumption of farmed salmon containing persistent organic pollutants, including increased levels of seven different PCBs, promoted glucose intolerance associated with elevations in adipose tissue expression of TNF-α in

HF-fed mice (88). Interestingly, when levels of pollutants were decreased by feeding farm-raised salmon purified fish oil, glucose tolerance improved and adipose expression levels of TNF-α decreased. Our results are in agreement with these findings, and extend these studies by demonstrating that individual coplanar PCBs promote glucose and insulin intolerance associated with adipose-specific elevations in expression of TNF-α. Moreover, similar to previous findings (88), adipose contained markedly higher PCB levels than did liver and serum, suggesting that chronic exposures of adipocytes to PCBs most likely contributed to selective increases in TNF-α expression in adipose tissue but not in liver or muscle.

Previous studies in our laboratory demonstrated that coplanar PCBs increased abundance of *TNF*-α mRNA in cultured adipocytes (6). Results from the present study demonstrate that PCB-77–induced increases in *TNF*-α expression are AhR mediated. Moreover, the concentrations (3.4 μM) of PCB-77 used in our *in vitro* studies with cultured adipocytes were comparable to serum levels (3 μM) of PCB-77 that induced glucose and insulin intolerance in mice. Kim et al. (277) reported that exposures of 3T3-L1 adipocytes to dioxin increased mRNA abundance of several proinflammatory factors, including TNF-α receptors. In that study, when dioxin was administered to mice fed standard mouse diet, abundance of *TNF*-α mRNA in adipose tissue was markedly increased, and this effect was abolished in AhR deficient mice. Results of the present study confirm and extend previous studies by demonstrating that *in vivo* effects of PCB-77 to impair glucose homeostasis are AhR mediated. An interesting finding of our

study was that levels of PCB-77 in adipose tissue were markedly decreased 4 weeks after the last dose; however, mice continued to exhibit glucose and insulin intolerance. PCB-induced activation of AhR induces *CYP1A1* gene expression, which hydroxylates the toxicant to increase water solubility for elimination. Our findings of rapid declines in levels of PCB-77, in the face of sustained impairment of glucose homeostasis, suggest that metabolites of PCB-77 may have contributed to long-lasting impairment of glucose and insulin intolerance in mice.

In this study, although PCB-77 impaired glucose and insulin tolerance in lean mice, these effects were lost when mice were fed a HF diet. The lipophilic nature of PCBs results in their accumulation in adipocyte lipid-containing droplets. For example, in humans, body mass index is inversely correlated with serum levels of PCBs, supporting the concept that an expanded adipose mass results in redistribution of PCBs away from the circulating compartment (273). In support, Kim et al. (9) reported an increased (2.9-fold) total body burden of PCBs in obese subjects. Thus, sequestration of PCB-77 in adipocyte lipid pools, as demonstrated by higher levels in adipose tissue from HF-fed mice in the present study, most likely resulted in restricted access to AhR, contributing to a lack of effect of PCB-77 on glucose and/or insulin tolerance in obese mice. Alternatively, effects of PCB-77 to impair glucose homeostasis may have become apparent with longer durations of HF-feeding. Previous studies found that plasma levels of 13 of 17 measured organochlorines in human serum increased with weight loss (276). Similarly, obese subjects experiencing drastic weight loss from bariatric surgery had increased serum levels of PCBs, which decreased the beneficial

effects of weight loss (9). In agreement with previous findings, our results demonstrate that beneficial effects of weight loss to improve glucose and insulin tolerance in mice were blunted in mice administered PCB-77. Moreover, our results extend previous findings by showing that elevations in TNF-α in adipose tissue may have contributed to impaired glucose and insulin tolerance in PCB-exposed mice experiencing weight loss.

Results from this study demonstrate that coplanar PCBs cause rapid and sustained impairment of glucose and insulin tolerance in mice through an AhR-dependent mechanism associated with an adipose-specific increase in TNF-α expression. Although harmful effects of PCB-77 on glucose and insulin tolerance were absent in obese mice, beneficial effects of weight loss to improve glucose and insulin tolerance were mitigated in mice previously exposed to PCB-77. These results suggest that sequestration of lipophilic coplanar PCBs to adipose tissue may contribute to AhR-mediated increases in TNF-α and the development of adipocyte insulin resistance, an effect manifest in lean conditions as well as during weight loss when adipose-derived toxicants may be liberated.

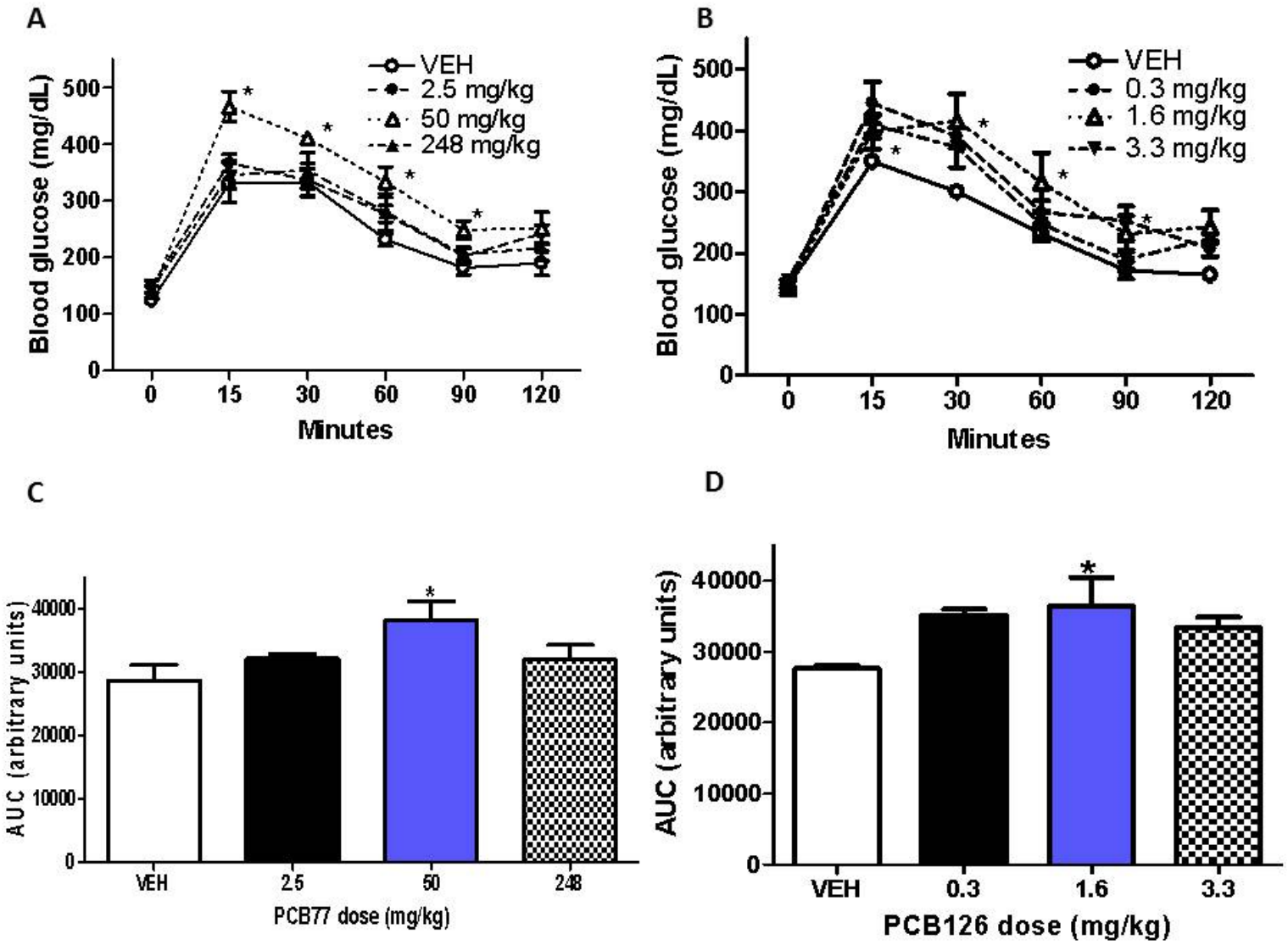
A
Blood glucose (mg/dL)
500
400
300
200
100
0
0
15
30
60
90
120
Minutes
VEH
2.5 mg/kg
50 mg/kg
248 mg/kg
B
Blood glucose (mg/dL)
Minutes
VEH
0.3 mg/kg
1.6 mg/kg
3.3 mg/kg
C
AUC (arbitrary units)
40000
30000
20000
10000
0
VEH
2.5
50
248
PCB77 dose (mg/kg)
D
AUC (arbitrary units)
VEH
0.3
1.6
3.3
PCB126 dose (mg/kg)

Figure 2.1. PCB-77 (A) and PCB-126 (B) impair glucose tolerance in LF-fed mice. (A), Blood glucose concentrations following a bolus of glucose in mice administered vehicle (VEH), 2.5, 50 or 248 mg/kg of PCB-77 (48 hours after the second dose). (B), Blood glucose concentrations following a bolus of glucose in mice administered vehicle, 0.3, 1.6 or 3.3 mg/kg of PCB-126 (48 hours after the second dose). Data are mean ± SEM from n = 5 mice/dose of PCB. *, $P < 0.05$ compared to VEH within a time point. (C,D), Quantification of total area under the curve (AUC) for data in A, B, respectively. *, $P < 0.05$ compared to VEH.

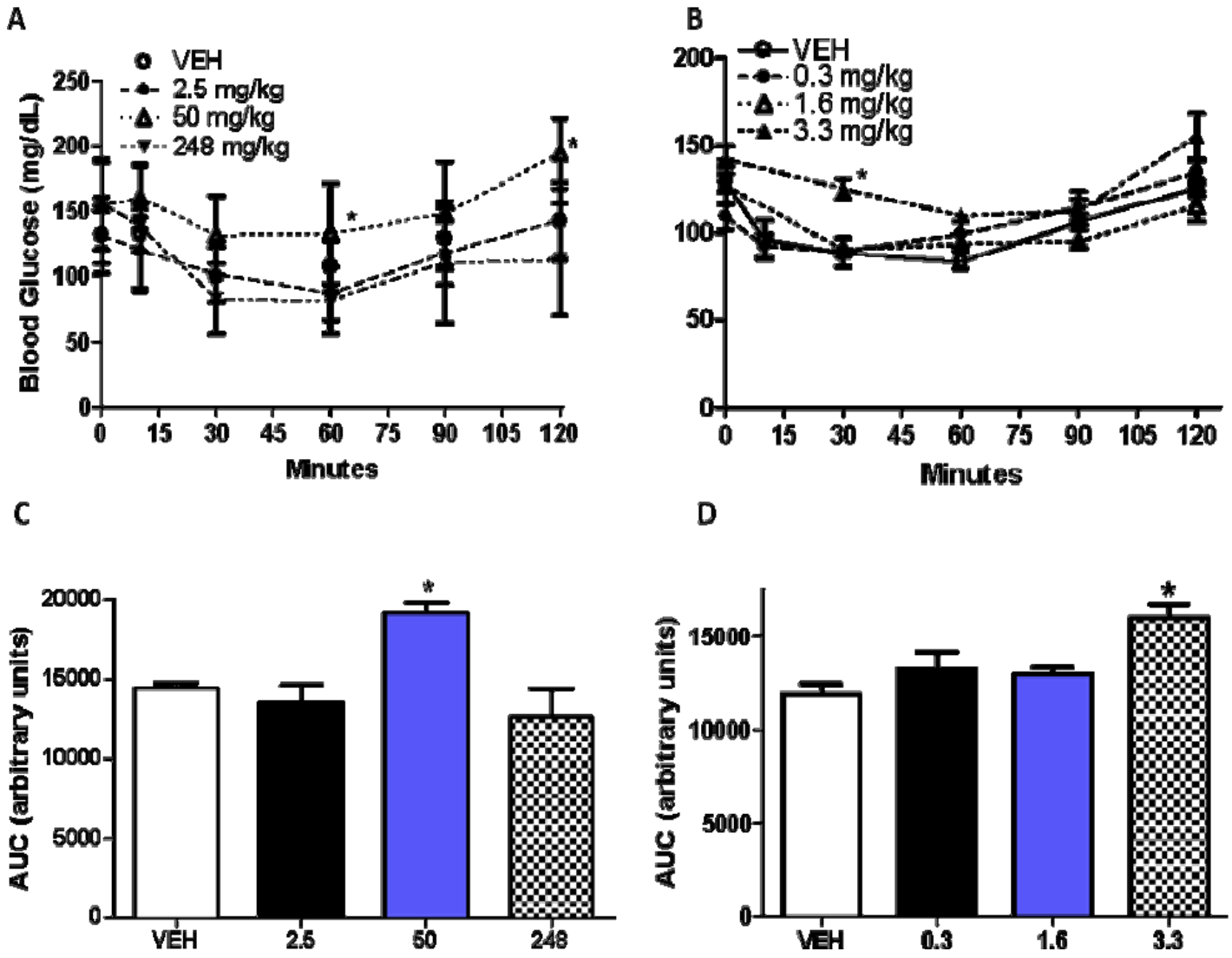
A
VEH
2.5 mg/kg
50 mg/kg
248 mg/kg
Blood Glucose (mg/dL)
Minutes
B
VEH
0.3 mg/kg
1.6 mg/kg
3.3 mg/kg
Minutes
C
AUC (arbitrary units)
VEH
2.5
50
248
D
AUC (arbitrary units)
VEH
0.3
1.6
3.3

Figure 2.2. Insulin tolerance tests in mice administered vehicle (VEH), PCB-77 (2.5, 50 or 248 mg/kg, A) or PCB-126 (0.3, 1.6 or 3.3 mg/kg, B). At 48 hours after the last dose, insulin (0.0125 μM/gm body weight) was administered to mice from each treatment group and blood glucose concentrations quantified at several time points. (C, D), Total area under the curve (AUC) for data in A, B, above. Data are mean ± SEM from n = 5 mice/group. *, $P < 0.05$ compared to vehicle.

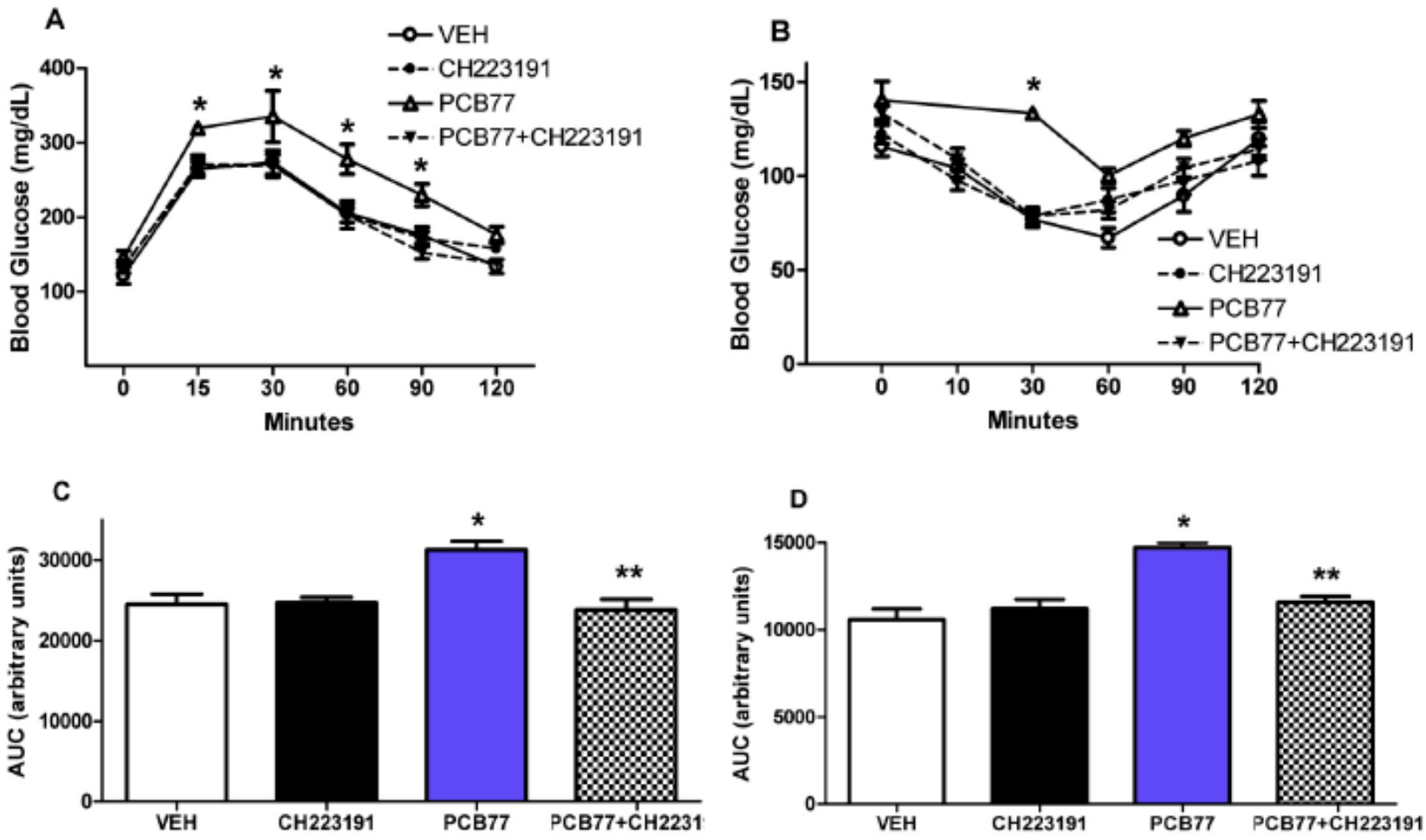
A
VEH
CH223191
PCB77
PCB77+CH223191
Blood Glucose (mg/dL)
400
300
200
100
0
15
30
60
90
120
Minutes
B
Blood Glucose (mg/dL)
150
100
50
0
10
Minutes
C
AUC (arbitrary units)
30000
20000
10000
D
15000
5000
VEH
CH223191
PCB77
PCB77+CH223191

Figure 2.3. Glucose (A) and insulin (B) tolerance tests in mice administered vehicle (VEH), CH-223191 (10 mg/kg/day), or PCB-77 (50 mg/kg). (C, D) Total area under the curve (AUC) for data in A, B, above. Data are mean ± SEM from n ≥ 7 mice/group. *, $P < 0.05$ compared to vehicle. **, $P < 0.05$ compared to PCB77.

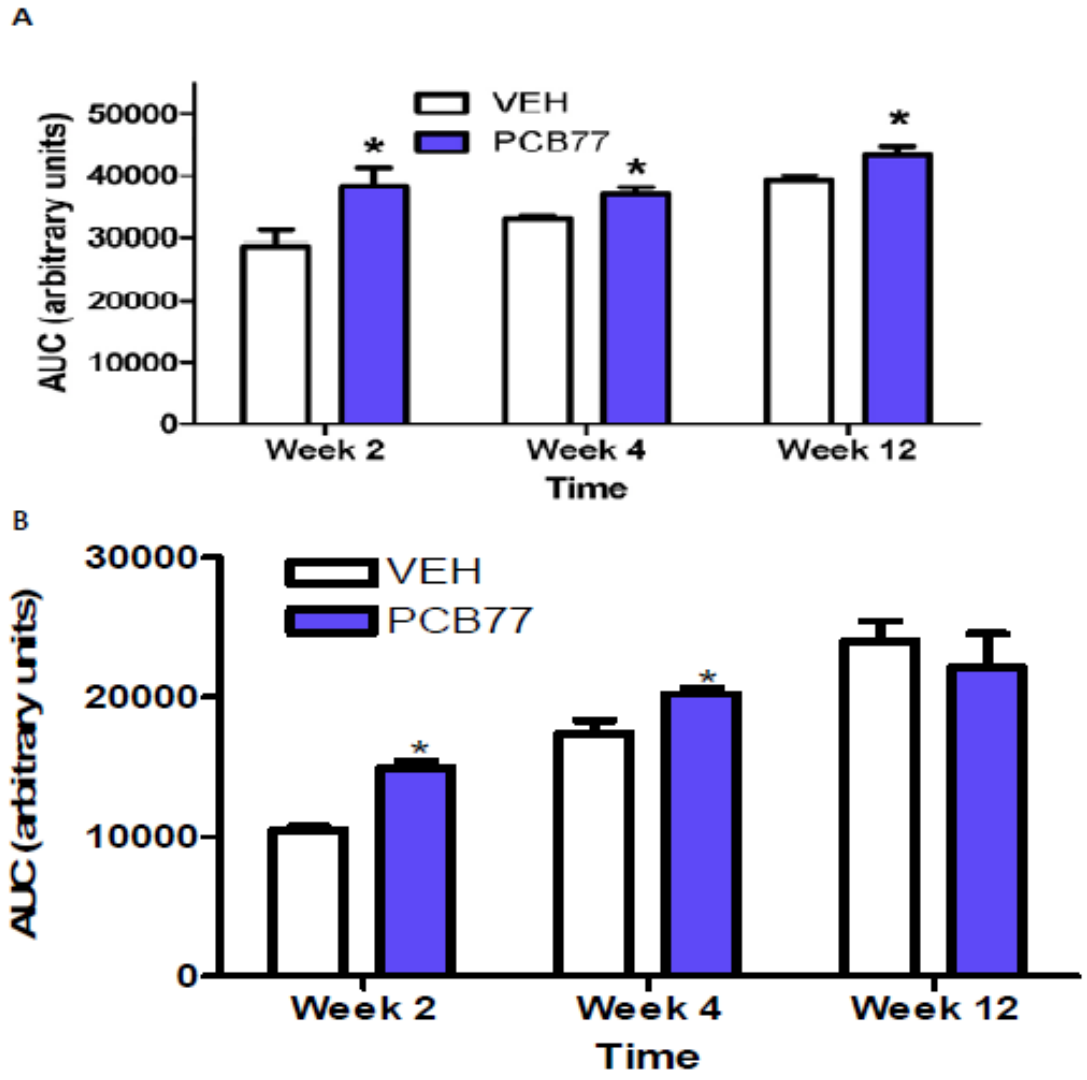

Figure 2.4. PCB-77 results in sustained impairment of glucose (A) and insulin (B) tolerance in LF-fed mice. Mice were administered vehicle (VEH) or PCB-77 (50 mg/kg, two divided doses during weeks 1 and 2, a second set of 2 doses during weeks 9 and 10 for mice studied at 12 weeks). At 2, 4 or 12 weeks, mice in each treatment group were administered a bolus of glucose (20% glucose, A) or insulin (0.0125 μM/gm body weight, B) and blood glucose

concentrations were quantified. Total area under the curve (AUC) for blood glucose concentrations were quantified. Data are mean ± SEM from n $\geq$ 5 mice/group. *, $P < 0.05$ compared to VEH within time point.

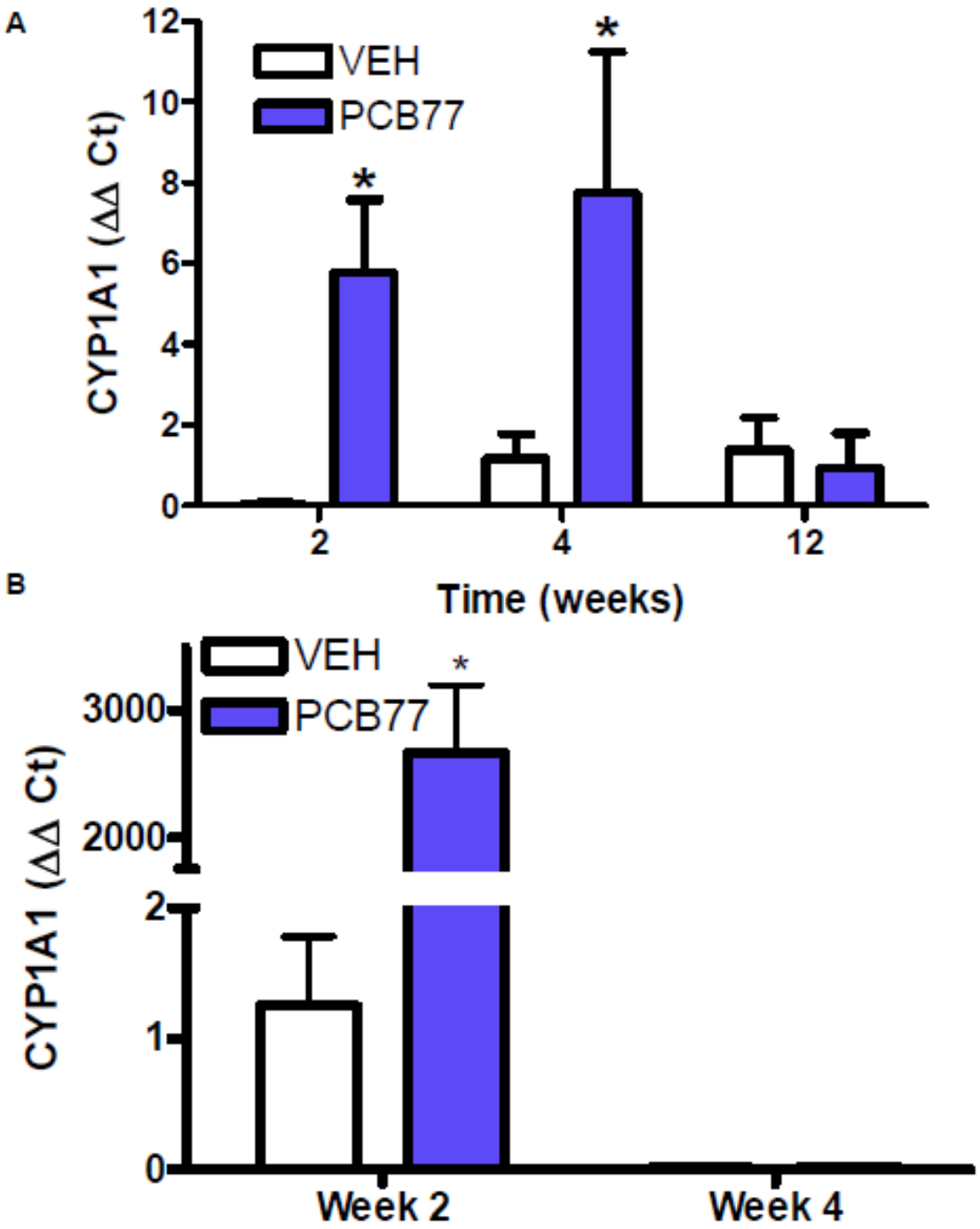

Figure 2.5. PCB-77 increases mRNA abundance of CYP1A1 in adipose (A) and liver (B) of LF-fed mice. Mice were administered vehicle (VEH) or PCB-77 (50 mg/kg, 2 doses in weeks 1 and 2, second 2 doses in weeks 9 and 10 for 12 week mice). (A), CYP1A1 mRNA abundance was increased in adipose at 1 and

4 weeks, but not 12 weeks after PCB-77 administration. (B), CYP1A1 mRNA abundance was increased in liver at week 2, but not week 4 after PCB-77 administration. Data are mean ± SEM from n $\geq$ 3 mice/group. *, $P < 0.05$ compared to VEH.

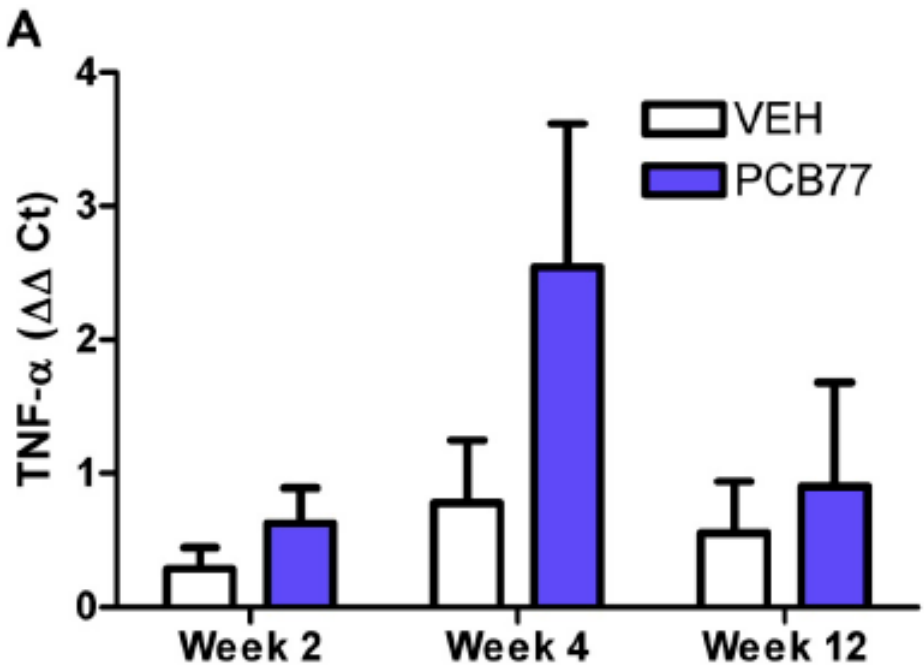
A
TNF-α (ΔΔ Ct)
4
3
2
1
0
VEH
PCB77
Week 2
Week 4
Week 12

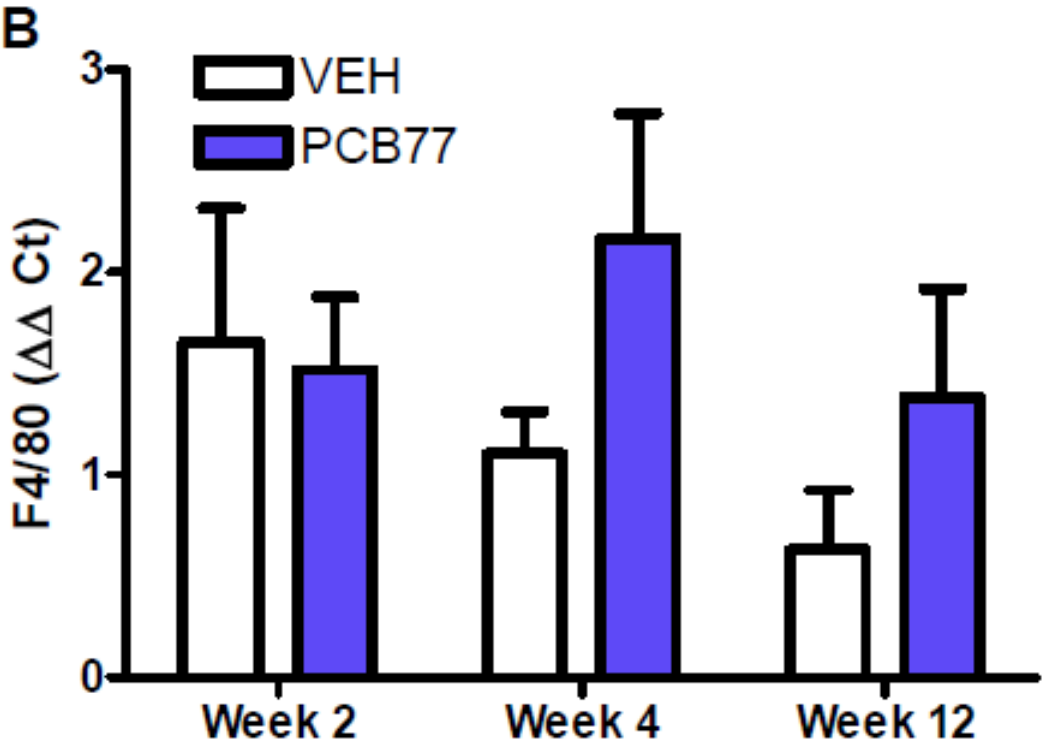
B
F4/80 (ΔΔ Ct)
3
2
1
0
VEH
PCB77
Week 2
Week 4
Week 12

Figure 2.6. TNF-α (A) and F4/80 (B) mRNA abundance in adipose from mice administered vehicle (VEH) or PCB-77 (50 mg/kg, 2 doses in weeks 1, 2, and then in weeks 9, 10 for mice euthanatized at week 12). Data are mean ± SEM from n = 6 mice/group.

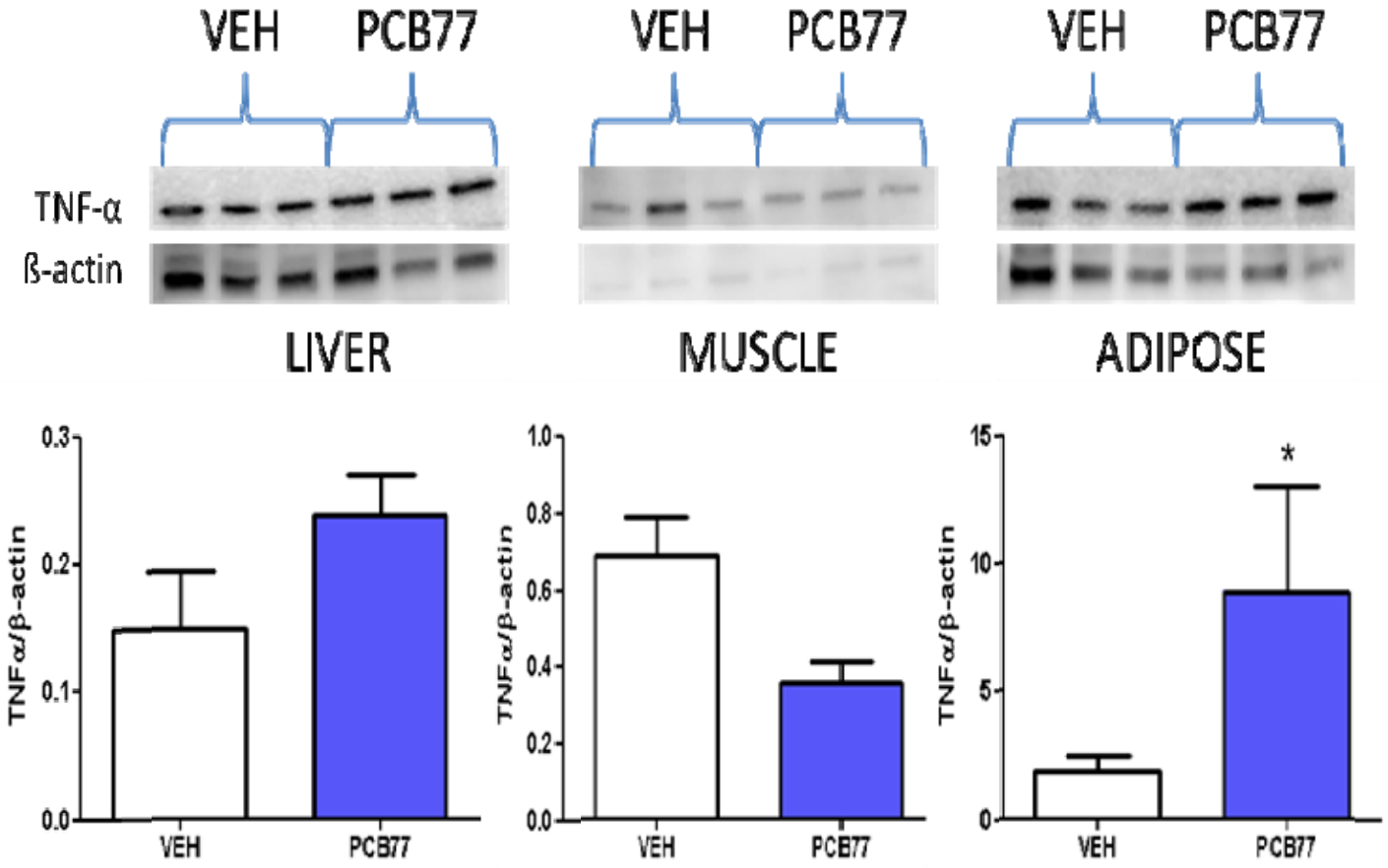
VEH
PCB77
VEH
PCB77
VEH
PCB77
TNF-α
ß-actin
LIVER
MUSCLE
ADIPOSE
TNFα/β-actin
0.3
0.2
0.1
0.0
VEH
PCB77
TNFα/β-actin
1.0
0.8
0.6
0.4
0.2
0.0
VEH
PCB77
TNFα/β-actin
15
10
5
0
*
VEH
PCB77

Figure 2.7. PCB-77 results in elevated TNF-α expression in adipose, but not in liver or soleus muscle of LF-fed mice. Mice were administered vehicle (VEH) or PCB-77 (50 mg/kg, 2 doses) and expression levels of TNF-α quantified in adipose, liver or soleus muscle 2 weeks later (week 4). Data are mean ± SEM from n = 3 mice/group. *, $P < 0.05$ compared to VEH.

A

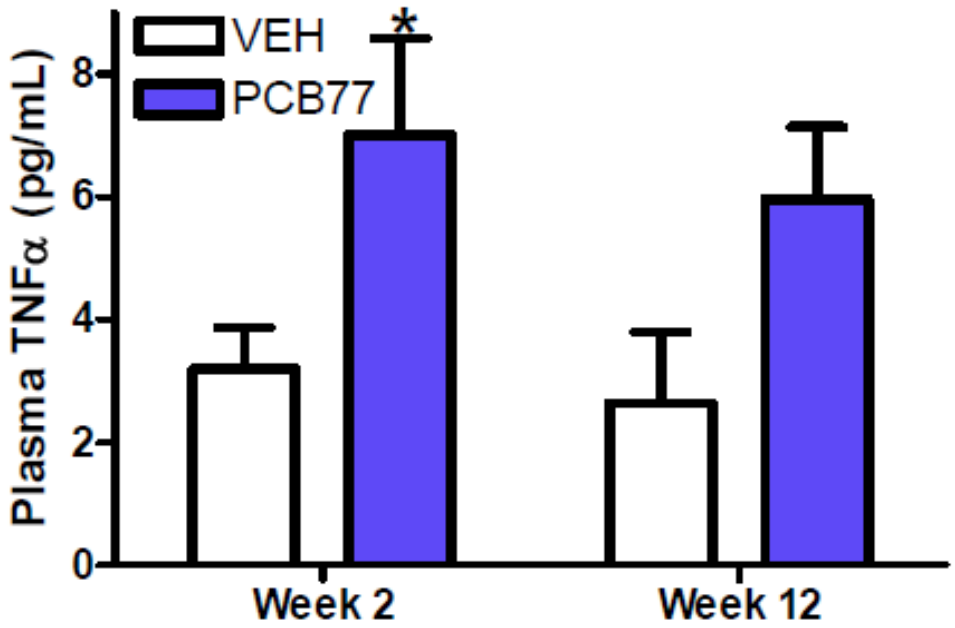
VEH
PCB77
*
Plasma TNFα (pg/mL)
0
2
4
6
8
Week 2
Week 12

B

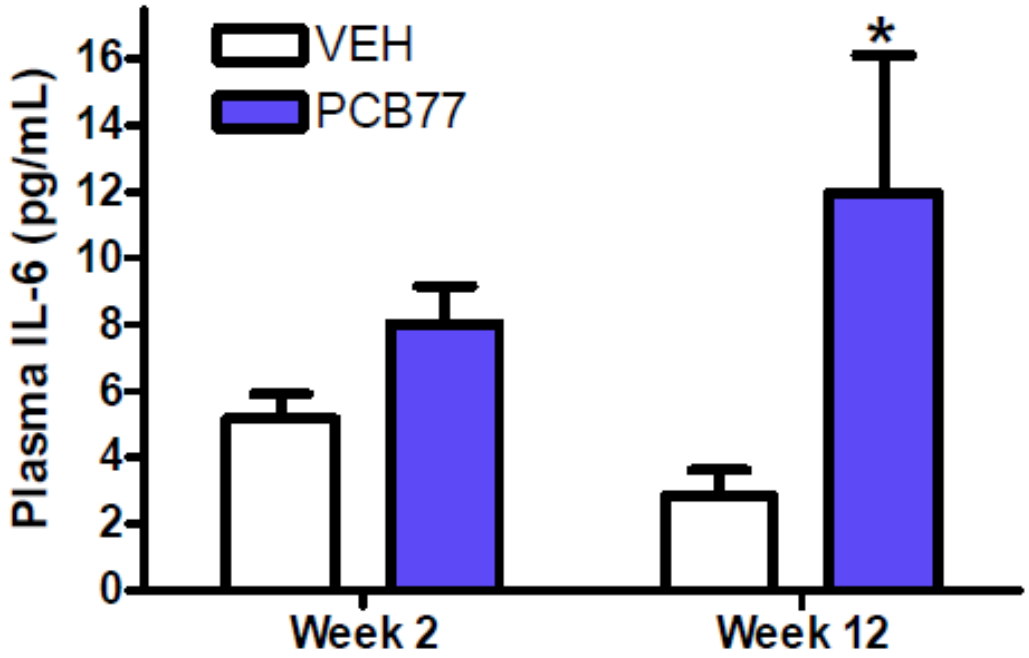
VEH
PCB77
*
Plasma IL-6 (pg/mL)
0
2
4
6
8
10
12
14
16
Week 2
Week 12

Figure 2.8. Plasma concentrations of TNF-α (A) and IL-6 (B) following administration of vehicle (VEH) or PCB-77 (50 mg/kg, 2 doses in weeks 1 and 2, second 2 doses in weeks 9 and 10). Data are mean ± SEM from n = 10 mice/group. *, $P < 0.05$ compared to VEH.

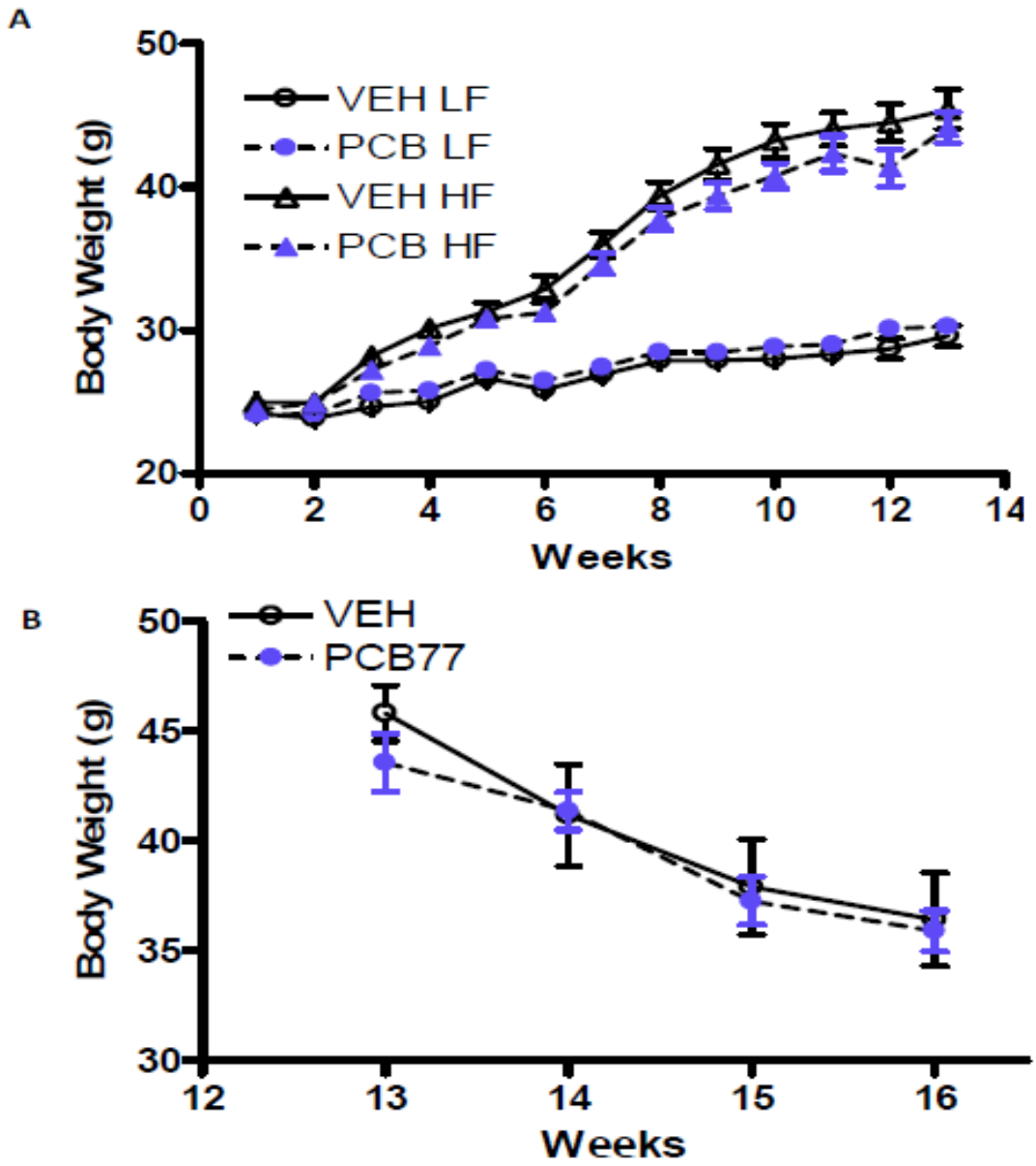

Figure 2.9. Body weight in LF and HF-fed mice administered vehicle (VEH) or PCB-77 (50 mg/kg, doses in weeks 1, 2, 9, and 10) during the weight gain phase of HF feeding (A), and after mice are switched to a LF diet at week 12 – 16 to induce weight loss (B). Body weight was increased in HF compared to LF-fed mice beginning on week 4 (A). Data are mean ± SEM from n $\geq$ 5 mice/group.

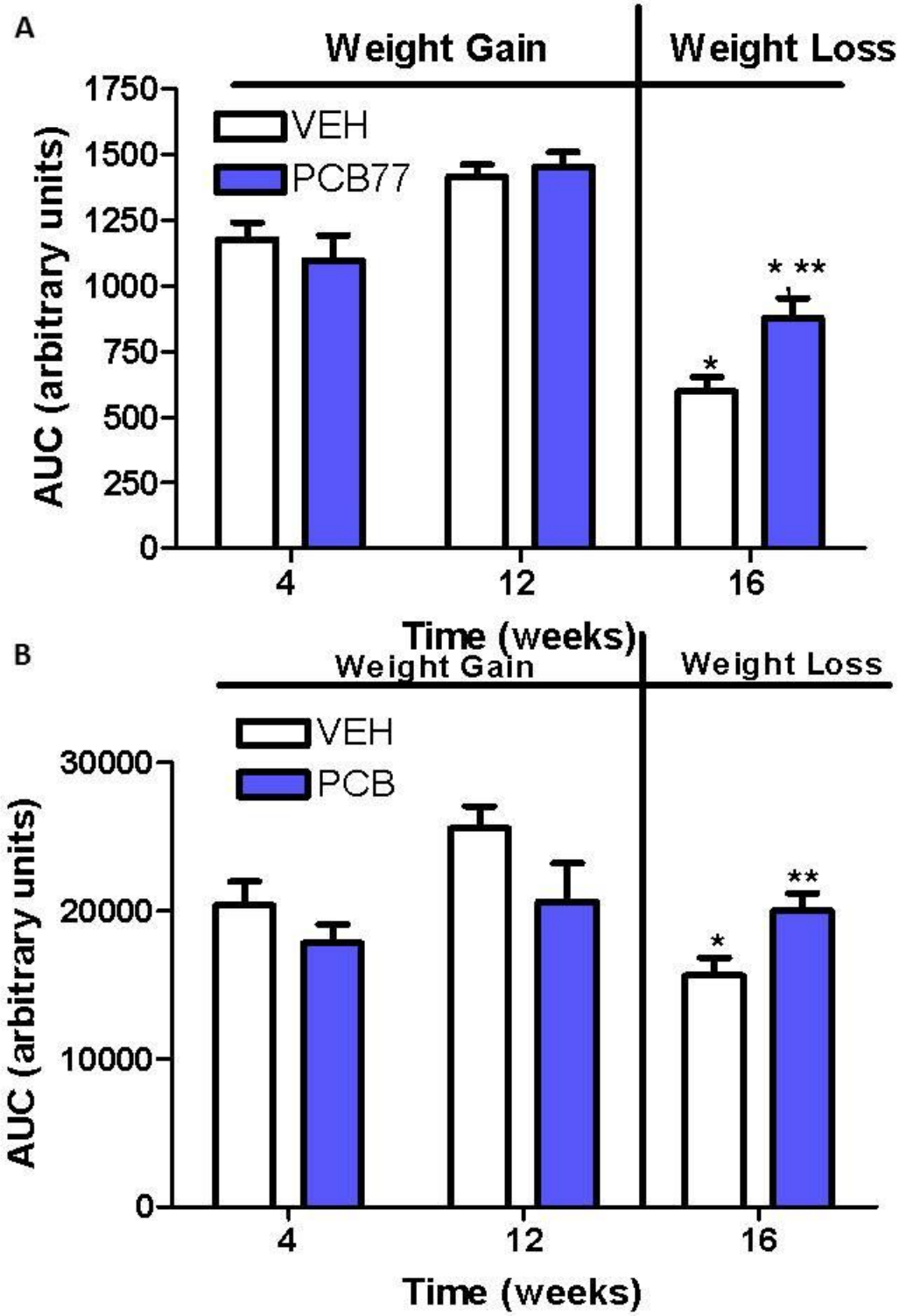

Figure 2.10. PCB-77 has no effect on glucose (A) or insulin (B) tolerance in HF-fed mice during weight gain, but impairs glucose homeostasis during

weight loss. (A), Total area under the curve (AUC) for glucose tolerance in mice administered vehicle (VEH) or PCB-77 (50 mg/kg, 2 doses during weeks 1 and 2 and a second 2 doses during weeks 9 and 10) during weight gain (weeks 4, 12 of HF feeding) or weight loss (at week 16 after mice are switched to a LF diet). Data are mean ± SEM from $n \geq 5$ mice/group. *, $P < 0.05$ compared to week 12 within treatment group. **, $P < 0.05$ compared to VEH within time point.

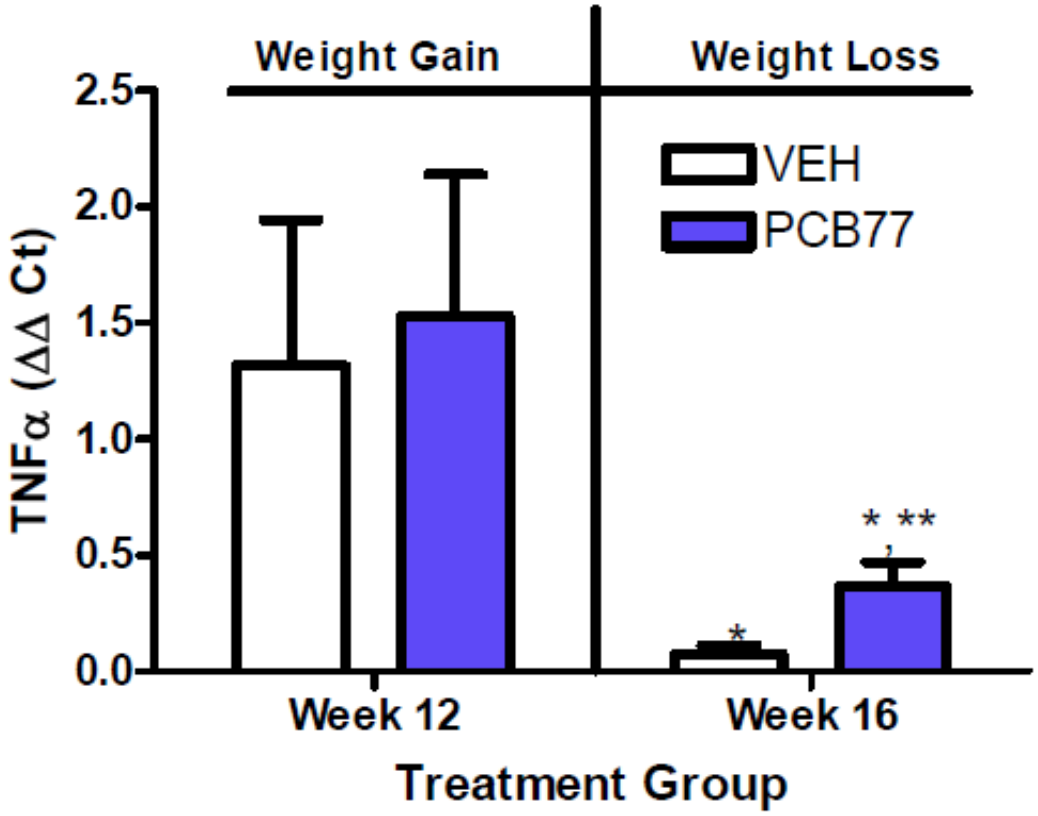

Figure 2.11. TNF-α mRNA abundance in adipose from mice during weight gain (week 12 of HF feeding), and after mice are switched to a LF diet to induce weight loss (week 16). Data are mean ± SEM from n ≥ 3 mice/group. *, $P < 0.05$ compared to week 12 within treatment group. **, $P < 0.05$ compared to VEH within time point.

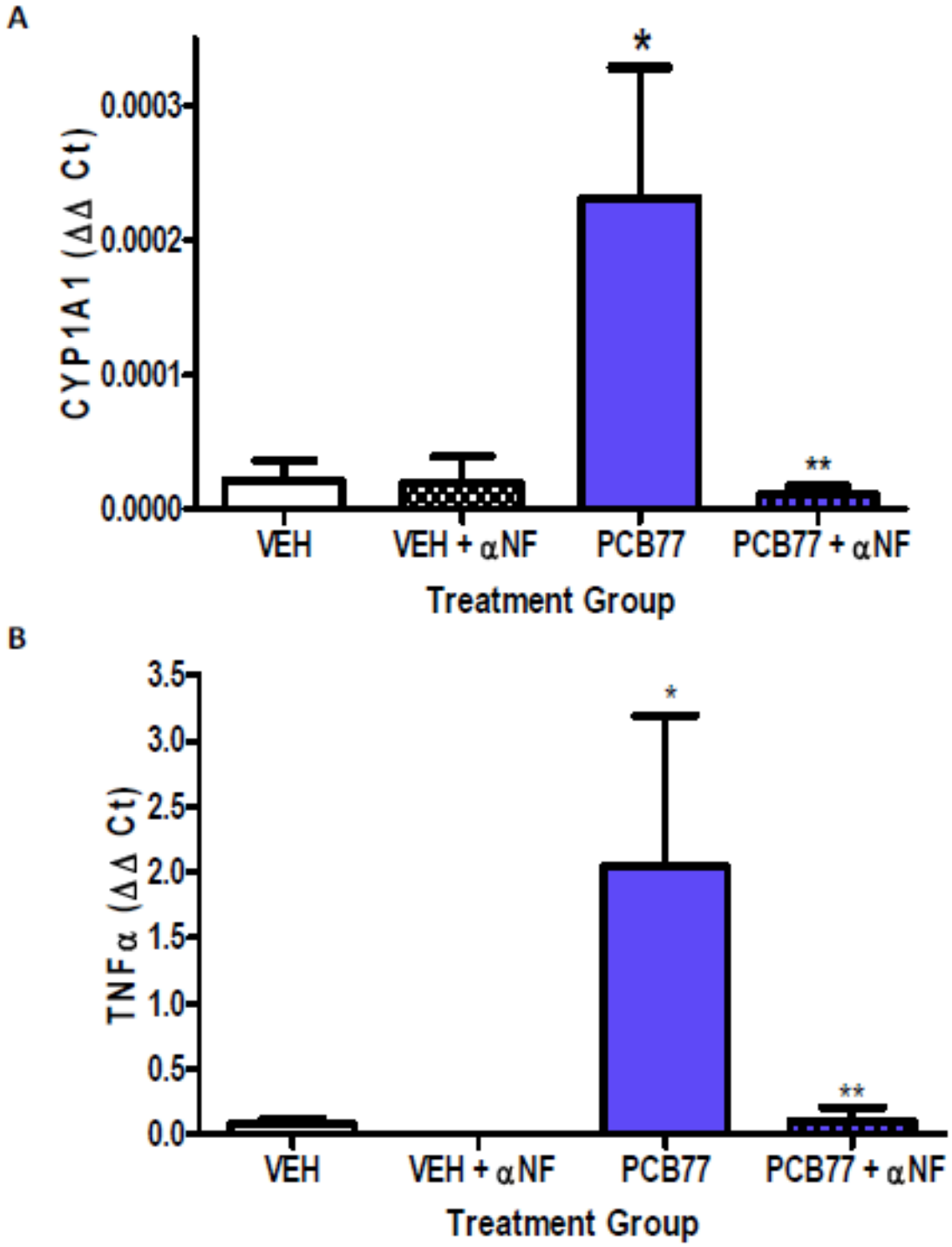
A
CYP1A1 (ΔΔ Ct)
0.0003
0.0002
0.0001
0.0000
*
**
VEH
VEH + αNF
PCB77
PCB77 + αNF
Treatment Group
B
TNFα (ΔΔ Ct)
3.5
3.0
2.5
2.0
1.5
1.0
0.5
0.0
*
**
VEH
VEH + αNF
PCB77
PCB77 + αNF
Treatment Group

Figure 2.12. CYP1A1 (A) and TNF-α (B) mRNA abundance in 3T3-L1 adipocytes incubated with vehicle, α-NF, PCB-77, or PCB-77 + α-NF. Data are mean ± SEM from n = 3 experiments. *, $P < 0.05$ compared to vehicle. **, $P < 0.05$ compared to PCB-77.

SECTION III. SPECIFIC AIM 2

3.1 Summary

Resveratrol (RSV) is a plant polyphenol that exhibits several favorable effects on glucose homeostasis in adipocytes. Recent studies from our laboratory demonstrated that coplanar polychlorinated biphenyls (PCBs) that are ligands of the aryl hydrocarbon receptor (AhR) impair glucose homeostasis in mice. PCB-induced impairment of glucose homeostasis was associated with augmented expression of inflammatory cytokines in adipose tissue, a site for accumulation of lipophilic PCBs. This study determined if RSV protects against PCB-77 induced impairment of glucose disposal *in vitro* and *in vivo*, and if these beneficial effects are associated with enhanced nuclear factor erythoid 2-related factor 2 (Nrf2) signaling in adipose tissue. PCB-77 increased oxidative stress and abolished insulin stimulated 2-deoxy-D-glucose (2DG) uptake in 3T3-L1 adipocytes. These effects were restored by RSV, which resulted in a concentration-dependent increase in NAD(P)H:quinone oxidoreductase 1 (NQO1), a downstream target of Nrf2 signaling. We quantified glucose and insulin tolerance and components of Nrf2 and insulin signaling cascades in adipose tissue of male C57BL/6 mice administered vehicle or PCB-77 (50 mg/kg) and fed a diet with or without resVida® (0.1%, or 160 mg/kg/day). PCB-77 impaired glucose and insulin tolerance, and these effects were reversed by RSV. PCB-77 induced reductions in insulin signaling in adipose tissue were also abolished by RSV, which increased NQO1 expression. These results demonstrate that coplanar PCB-induced impairment of glucose homeostasis in

mice can be prevented by RSV, potentially through stimulation of Nrf2 signaling and enhanced insulin stimulated glucose disposal in adipose tissue.

3.2 Introduction

Polychlorinated biphenyls (PCBs) are persistent organic pollutants that are highly lipophilic and tend to bio-accumulate in the environment. Although industrial use of these compounds was banned in the U.S. in the 1970's, recent studies have estimated that the average American is exposed to approximately 33 ng of PCBs per day through the diet (11). Several epidemiological studies suggest that exposure to low concentrations of PCBs may promote type 2 diabetes (T2D) in humans (268, 297). Notably, recent results from the Anniston Community Health Survey demonstrated significant associations between elevated PCB levels and diabetes risk (158). Largely resulting from accumulating evidence linking PCB exposures to diabetes, the National Institute of Environmental Health Studies (NIEHS), Division of the National Toxicology Program (NTP) hosted a workshop to review approximately seventy-five different epidemiology studies linking persistent organic pollutants (POPs), including coplanar PCBs, to T2D outcomes. A publication from the workshop concluded that there is evidence for a positive association between POP exposures and the development of T2D (23). The summary of the workshop also called for additional studies to define mechanisms linking PCBs and other POPs to increased risk for diabetes.

We recently demonstrated that coplanar PCBs that are ligands of the aryl hydrocarbon receptor (AhR) impair glucose homeostasis in C57BL/6 mice (7). These effects were associated with inflammation in adipose tissue, a site for pronounced PCB accumulation (7). Similarly, recent studies demonstrated that

2,3,7,8-tetrachloro-dibenzo-*p*-dioxin (TCDD), an AhR ligand, promoted low grade inflammation in adipocytes in vitro and in vivo (277). Generation of reactive oxygen species (ROS) by AhR ligands such as TCDD or PCBs in adipocytes may contribute to low grade inflammation and the development of insulin resistance (298).

The plant polyphenol, resveratrol (RSV), exerts several protective effects in adipocytes. In 3T3-L1 adipocytes RSV inhibited stimulation of inflammatory adipokines (265, 299-304). As a mechanism for protective effects of RSV, reductions in oxidative stress by RSV are associated with activation of nuclear factor erythoid 2-related factor 2 (Nrf2) (247, 305-306), a component of the anti-oxidant pathway. RSV had been demonstrated to protect against insulin resistance in cultured adipocytes (241). Moreover, administration of RSV improves glucose tolerance and reduces insulin resistance resulting from consumption of a high fat diet (182, 187, 307), in genetically obese rodents (253, 308-309) and in humans with T2D (213). Notably, RSV interacts with the AhR, resulting in translocation of the receptor to the nucleus; however this interaction does not appear to result in transactivation (310-311). Accordingly, RSV attenuates toxic effects of AhR ligands in vitro and in vivo (310, 312-315). However, it is unclear if protective effects of RSV extend to PCB ligands of AhR, and whether this protection includes restoration of measures of insulin sensitivity in adipocytes, a primary site for PCB-induced activation of inflammatory cytokines that are linked to the development of insulin resistance (6-7).

In this study, we tested the hypothesis that RSV protects against in vitro and in vivo effects of a coplanar PCB (PCB-77) to induce measures of insulin resistance. We selected coplanar PCB-77 for these studies based on its high toxicity and abundance within the food chain (289, 291). Since PCBs accumulate markedly in adipose tissue and have been demonstrated to promote inflammatory cytokines linked to insulin resistance (6-7), we focused on adipocytes as the cell target of PCBs and/or RSV to regulate glucose homeostasis. As a mechanism for effects of PCB and/or RSV, we quantified oxidative stress and induction of the Nrf2 anti-oxidant signaling pathway. Our results suggest that RSV may provide therapeutic benefit against PCB-induced dysregulation of glucose homeostasis and the development of diabetes.

3.3 Materials and Methods

3.3.1 Materials

3,3',4,4'-tetrachlorobiphenyl (PCB-77) was purchased from AccuStandard Inc. (New Haven, CT). 2-deoxyglucose (2DG), bovine insulin (0.1 μM for adipocyte differentiation), dexamethasone (1 μM), and isobutylmethyl xanthine (0.5 mM, IBMX) were obtained from Sigma Aldrich (St. Louis, MO). The resVida® (>99% pure trans-resveratrol) was provided by DSM Nutrition Products, Inc (Heerlen, NL).

3.3.2 Quantification of PCB-77, RSV, and metabolites in serum and tissues

PCB-77, hydroxyPCB-77 and RSV were measured using a Shimadzu UFLC coupled with an AB Sciex 4000-Qtrap hybrid linear ion trap triple quadrupole mass spectrometer in multiple reaction monitoring (MRM) mode. d6-PCB-77 was used as internal standard for PCB-77 and hydroxyPCB-77 measurements. D4-RSV was used as an internal standard for resveratrol and its metabolite measurements. The mass spectrometer was operated in the positive APCI mode for PCB-77 measurements and in negative ESI mode for hydroxyPCB-77 and RSV measurements with optimal ion source settings determined by synthetic standards. PCB-77 was analyzed using Kinetex 2.6 u C18, 100 A, 100 X 2.10 mm (Phenomenex) column. The mobile phase consisted of water as solvent A and acetonitrile as solvent B. For the analysis of PCBs the separation was achieved using a gradient of 20 % B to 60 % B for 1 min, 60% B to 100% B in the next 7 min, and maintained at 100% B for the last 2 min with a flow rate of 0.25 ml/min. MRM transitions monitored were as follows: 291.9/

222.1 and 291.9/220 for PCB-77; and 297.9/228.1 and 297.9/226.2 for d6-PCB-77. In the MRM ion transition the precursor ion represents the $M^{+\cdot}$ and the product ion represents either $[M-Cl]^{+}$ or $[M-2Cl]^{+}$.

HydroxyPCB-77 was analyzed using Luna 3 u C18 (2), 100 A, 250 X 2.00 mm (Phenomenex) column with a flow rate of 0.25 mL/min. The mobile phase consisted of 75/25 of methanol/ water with formic acid (0.5%) and 5 mM ammonium formate (0.1%) as solvent A and 99/1of methanol/ water with formic acid (0.5%) and 5 mM ammonium formate (0.1%) as solvent B. HydroxyPCB-77 was eluted using a gradient of 10 % B to 100 % B in 4 min and maintained at 100% B for the next 11 min. MRM transitions monitored were as follows: 352.8/306.9 for hydroxyPCB-77 and 368.8/322.9 for dihydroxyPCB-77. Precursor ion of the ion transition is a formic acid adduct: [M+FA-H]- and product ion is [M-H]-.

3.3.3 Cell culture

3T3-L1 mouse preadipocytes purchased from Zen-Bio (Research Triangle Park, NC) were cultured in standard Dulbecco's modified Eagle's medium (DMEM; Invitrogen, Carlsbad, CA) enriched with 10% fetal bovine serum (FBS; Gemini Bio-Products, Woodland, CA) and 1% penicillin/streptomycin in 6-well culture dishes. Cells (passage number 5 or lower) were grown to 100% confluence at 37°C in a humidified 5% CO2 atmosphere. Differentiation to mature adipocytes was induced as previously described (7). Assays (n = 2/group) were performed in triplicate.

To examine the effects of PCBs, we incubated differentiated adipocytes (day 8) with vehicle [0.03% dimethyl sulfoxide (DMSO)] or PCB-77 (3.4 μM (6-7)) for 24 hours in the absence or presence of RSV (0.1 μM, 1 μM, or 10 μM). RSV was added to culture media 30 minutes prior to the addition of vehicle or PCB-77. Cells were harvested for glucose uptake and oxidative stress assays in addition to mRNA quantification of gene expression.

3.3.4 Measurement of insulin-stimulated uptake of 2DG

To measure uptake of 2DG, differentiated 3T3-L1 adipocytes were incubated with appropriate treatments in serum-free media for 6 hours. Cells were washed three times and then incubated with insulin (1 μM) in glucose-free Krebs buffer (pH 7.4) containing 2% bovine serum albumin for 20 minutes at 37°C. 2DG (1 mM) was added to each well and incubated at 37°C for 20 minutes. Cells were washed three times with buffer, and 10 mM Tris-HCl was added to each well. Following sonication, cell lysates were collected and 2DG uptake was quantified per the manufacturer's instructions (2-Deoxyglucose Uptake Measurement kit, Cosmo Bio Co. Ltd., Tokyo, Japan). 2DG uptake was normalized to cellular protein.

3.3.5 Measurement of oxidative stress

To measure oxidative stress, differentiated 3T3-L1 adipocytes were incubated with appropriate treatments for 24 hours. Cellular oxidation was determined by 2',7'-dichlorofluorescein (DCF) fluorescence via the Oxiselect^{TM} Intracellular ROS Assay kit (Cell Biolabs, Inc., San Diego, CA). Briefly, this method is based on the conversion of 2',7'-dichlorofluorescin into fluorescent DCF through oxidation by

reactive oxygen species, including super oxide radicals and peroxides. Following appropriate treatments, cells were incubated with 100 μM 2',7'-dichlorofluorescin diacetate for 30 minutes. A multi-well fluorescent plate reader (Molecular Devices, CA) was utilized for measuring relative oxidative stress; excitation and emission wavelengths were 480 and 530 nm, respectively.

3.3.6 Animals and experimental diets

All experimental procedures met the approval of the Animal Care and Use Committee of the University of Kentucky. Two month old, male, C57BL/6 mice (The Jackson Laboratory, Bar Harbor, ME) were housed in a pathogen-free environment and given ad libutum access to water and standard mouse diet in the absence or presence of 0.1% resVida® (#5SSG, 14.6% kcal as fat, TestDiet, Richmond, IN). Mice were pre-fed diets for 1 week prior to administration of vehicle (tocopherol stripped safflower oil, Dyets Inc., 10 μL/g of body weight) or PCB-77 (49.6 mg/kg)(n=10 mice/group), given in two divided doses during weeks 1 and 2. Body weights were recorded bi-weekly. Glucose and insulin tolerance tests were performed within 48 hours after the second dose as described below. At study endpoint, mice were fasted for 4 hours and anesthetized with ketamine/xylazine (100/10 mg/kg intraperitoneal (ip) injection). Following ketamine injection, a sub-set of mice in each group were injected (i.p.) with 10 U/kg body weight human insulin (Novolin) to stimulate insulin signaling pathways, using methods as described previously (285).

3.3.7 Glucose tolerance test (GTT) and insulin tolerance test (ITT)

For glucose (GTT) and insulin tolerance tests (ITT), sub-sets of mice in each group were examined within 48 hours after the second dose. Mice were fasted for 4 or 6 hours for ITT or GTT, respectively, and fasted blood glucose was measured by tail vein using a hand held glucometer (Freedom Freestyle Lite, Abbott Laboratories, Abbott Park, IL). Mice were injected (i.p.) with D-glucose (Sigma, 20% in saline, 10 μL/g of body weight) for GTT and blood glucose was measured at 15, 30, 60, 90, and 120 minutes later. For ITT, mice were injected (i.p.) with human insulin (Novolin, 0.0125 μM in saline/g of body weight), and plasma glucose was measured at 30, 60, 90, and 120 minutes later. Total area under the curve (AUC; arbitrary units) was calculated as previously described (7).

3.3.8 Quantification of adipose tissue Akt and P-Akt.

Epididymal adipose tissue was homogenized and centrifuged, and supernatants were stored in 1X Cell Lysis Buffer (Cell Signaling, Danvers, MA). Akt and p-Akt concentrations were quantified as per the manufacturer's instructions using a commercial ELISA (Cell Signaling, Beverly, MA), and normalized to adipose tissue protein.

3.3.9 RNA isolation and gene expression analysis using real-time polymerase chain reaction (PCR)

Total RNA was extracted from epididymal adipose tissue using the SV Total RNA Isolation System kit (Promega Corporation, Madison, WI), per the manufacturer's instructions. RNA from 3T3-L1 cells was extracted in Trizol.

RNA concentrations were determined using a NanoDrop 2000 spectophotometer and associated software (Thermo Scientific, Logan, UT). cDNA was synthesized from 0.4 µg total RNA with qScript cDNA SuperMix (Quanta Biosciences, Gaithersburg, MD) in the following reaction: 25°C for 5 minutes, 42°C for 30 minutes, and 85°C for 5 minutes. The cDNA was diluted 1:50 to achieve a concentration of 0.4 ng/µL. The diluted cDNA was amplified with an iCycler (Bio-Rad, Hercules, CA) and the Perfecta SYBR Green Fastmix for iQ (Quanta Biosciences, Gaithersburg, MD). Components of the PCR reaction were as follows: Perfecta SYBR Green FastMix (10 µL), forward and reverse primers (0.125 µL), nuclease free water (4.75 µL), and diluted cDNA (5 µL for 2 ng of cDNA/reaction). Using the difference from GAPDH (glyceraldehydes 3-phosphate dehydrogenase) rRNA (reference gene) and the comparative Ct method, the relative quantification of gene expression in each sample was calculated. Primers (Eurofins MWG Operon, Huntsville, AL) were designed using the primer design program available from PubMed.gov (sequences presented in Table 3.1). The PCR reaction was as follows: 94°C for 5 minutes, 40 cycles at 94°C for 15 seconds, 58°C or 64°C (based on tested primer efficiency) for 40 seconds, 72°C for 10 minutes, and 100 cycles from 95°C to 45.5°C for 10 seconds.

3.3.10 Statistical analysis

Data are represented as mean ± standard error of the mean (SEM). Data was log transformed prior to statistical analysis. A one-way or two-way analysis of variance (ANOVA; SigmaPlot, version 12.0; Systat Software Inc., Chicago, IL)

were used as appropriate to determine statistical significance, which was defined as $p < 0.05$. Glucose and insulin tolerance tests were analyzed using repeated measure, two-way ANOVA. Holm-Sidak method was used for post-hoc analyses, except in Figures 3.1D and 3.4B which used Dunnett's method and basal and non-insulin stimulated groups as controls for comparison, respectively.

3.4 Results

3.4.1 RSV promotes Nrf2 signaling, suppresses oxidative stress, and restores insulin-stimulated glucose uptake in PCB-77 treated adipocytes.

RSV has been demonstrated to promote the anti-oxidant Nrf2 signaling pathway and reduce oxidative stress in a variety of cell types (247, 306, 316). We quantified effects of PCB-77 on Nrf2 and one of its downstream signaling targets, NQO1, and oxidative stress in the absence or presence of increasing concentrations of RSV in 3T3-L1 adipocytes. In the absence of RSV, PCB-77 had no significant effect on mRNA abundance of Nrf2 or NQO1 in 3T3-L1 adipocytes (Fig. 3.1A,B, respectively). However, in the presence of PCB-77, RSV significantly increased mRNA abundance of Nrf2 and NQO1 in a concentration-dependent manner (Fig. 3.1A,B; $P<0.05$). PCB-77 significantly increased fluorescence of DCF as a measure of oxidative stress, and this effect was abolished by RSV (1 μM; Fig. 3.1C, $P<0.05$).

To determine if PCB-77-induced oxidative stress influenced glucose homeostasis in 3T3-L1 adipocytes, and whether RSV could restore adipocyte function, we quantified 2DG uptake. In the presence of insulin, 2DG uptake increased 4-fold in 3T3-L1 adipocytes (DMSO *versus* basal; Fig. 1D, $P<0.05$). However, PCB-77 totally abolished 2DG uptake in insulin-stimulated adipocytes (Fig. 3.1D). Effects of PCB-77 to impair glucose uptake by adipocytes were reversed in a concentration-dependent manner by RSV (Fig. 3.1D, $P<0.05$).

3.4.2 RSV has no effect on tissue levels of PCB-77 or PCB-77 metabolites.

RSV has been demonstrated to have AhR antagonist properties (310-311), which could influence metabolism of PCBs by cytochrome P-450 1A1 (CYP1A1). We quantified mRNA abundance of CYP1A1 as an index of AhR activation in adipose tissue of mice administered PCB-77 in the absence or presence of RSV. PCB-77 resulted in a significant increase in CYP1A1 mRNA abundance in adipose tissue of mice administered vehicle (VEH) or RSV (Fig. 3.2; $P<0.05$). We then quantified levels of PCB-77 and its major metabolites (hydroxyPCB-77, dihydroxyPCB-77) in serum, liver or adipose tissue from mice in each treatment group. Similarly, we quantified levels of the parent compound, trans-RSV, and 2 metabolites (RSV-3-O-glucuoride, trans-RSV-3-O-sulfate). As demonstrated previously (7), adipose tissue concentrations of PCB-77 were markedly higher than liver or serum (Table 3.2). Moreover, the ratio of PCB-77 to its quantified metabolites was greater in adipose tissue (5:1) than liver (0.02:1). Significantly higher concentrations of RSV metabolites were detected in serum, liver and adipose tissue than the parent molecule, RSV. However, there was no significant effect of RSV on levels of PCB-77 or its metabolites. In addition, administration of PCB-77 had no significant effect on levels of RSV or its metabolites.

3.4.3 RSV improves glucose tolerance and insulin signaling in adipose tissue of mice administered PCB-77

There was no significant effect of PCB-77 or RSV on body weight (data not shown). As reported previously (7), PCB-77 significantly impaired glucose

and insulin tolerance (Fig. 3.3A,B, respectively), as indicated by a significant increase in the area under the curve (AUC) for blood glucose levels following administration of glucose (GTT) or insulin (ITT) (Fig. 3.3C,D, respectively). While RSV had no effect on either glucose or insulin tolerance in mice administered vehicle, RSV totally abolished effects of PCB-77 to impair glucose and insulin tolerance. Based on findings from 3T3-L1 adipocytes demonstrating that RSV stimulated the Nrf2 signaling cascade (Fig. 3.1A), we quantified mRNA abundance of Nrf2 and NQO1 in epididymal adipose tissue from insulin-stimulated mice. There were no significant effects of PCB-77 or RSV on Nrf2 mRNA abundance in adipose tissue (data not shown). However, in mice administered PCB-77, RSV resulted in a significant increase in mRNA abundance of NQO1 (Fig. 3.4A, $P<0.05$). We quantified levels of phosphorylated Akt (pAkt, normalized to total Akt) as an index of the insulin signaling pathway in adipose tissue of mice administered insulin. Administration of insulin significantly increased pAkt expression in adipose tissue, which was totally abolished by PCB-77 (Fig. 3.4B, $P<0.05$). While RSV had no effect in the absence of PCB-77, it totally restored insulin-stimulated levels of pAkt in adipose tissue (Fig. 3.4B, $P<0.05$).

3.5 Discussion

Results from this study demonstrate that supplementation with RSV in the diet totally prevents PCB-77 induced impairment of glucose and insulin tolerance in mice. Notably, PCB-77 resulted in pronounced suppression of insulin-stimulated levels of pAkt in adipose tissue, and this effect was abolished by RSV. In cultured adipocytes, PCB-77 increased oxidative stress and reduced insulin-stimulated glucose uptake, and these effects were attenuated in a concentration-dependent manner by RSV. Mechanisms of RSV to protect against PCB-induced oxidative stress and impairment of glucose uptake in 3T3-L1 adipocytes may involve activation of the anti-oxidant Nrf2 signaling pathway, as RSV stimulated Nrf2 and/or NQO1 expression in cultured adipocytes and elevated NQO1 expression in adipose tissue of mice. In contrast, RSV did not alter systemic or tissue distribution of PCB-77 and/or its major metabolites, or levels of CYP1A1 in adipose tissue, suggesting that regulation of PCB metabolism did not contribute to effectiveness of RSV. These results demonstrate that RSV can attenuate PCB-77-induced insulin resistance in adipose tissue potentially by stimulating the NRF2 pathway and preventing oxidative damage. RSV may provide an effective therapy to protect against PCB-induced dysregulation of glucose homeostasis.

Increasing evidence suggests that exposures to environmental pollutants, including PCBs, may be a contributing factor for an increased risk of T2D development. Similar to recent findings (7), in the present study administration of PCB-77 to C57BL/6 mice resulted in impaired glucose and insulin tolerance.

Results from this study extend previous findings by demonstrating that PCB-77 administration totally abolished levels of phosphorylated Akt in adipose tissue as an index of insulin signaling. We recently reported that serum levels of PCB-77 in experimental mice are lower than total serum PCB levels in populations with known accidental exposures (7). In the present study, mice administered PCB-77 had serum levels of approximately 0.07 $\pm$ 0.01 μM, consistent with total PCB levels reported in subjects from the highest quintile of the Anniston Community Health Survey Population that exhibit an increased odds ratio for T2D (158). Moreover, as reported previously (7-8), PCB-77 accumulated markedly in adipose tissue compared to serum or liver. An interesting finding of the present study was the higher ratio of parent PCB-77 compound to its metabolites in adipose tissue, as compared to liver. These results suggest that in comparison to liver where PCBs are predominately metabolized through CYP1A1 activation, sequestration of the parent PCB-77 molecule in adipose lipids may hinder effective metabolism of the toxin. However, upon release of sequestered PCBs from adipose tissue during lipolysis, adipocytes may experience more pronounced effects of the toxin at adipocyte AhR.

In the present study, serum RSV concentrations (0.6 nM) in 4 hour fasted mice were lower than concentrations (1 μM) that effectively abolished PCB-77 induced oxidative stress and impaired glucose uptake by 3T3-L1 adipocytes. Previous investigators demonstrated that fasted (4 hrs) C57BL/6 mice administered 100 mg/kg of RSV via oral gavage had appreciable amounts of the RSV-3-O-glucuronide metabolite (317). These results suggest that protective

effects of RSV observed during fasting of mice in this study may have resulted from RSV metabolites. Importantly, neither levels of RSV and metabolites, nor levels of PCB-77 and metabolites, were influenced by co-administration of these compounds to mice, suggesting that protective effects of RSV against PCB-induced impairment of glucose homeostasis did not result from changes in distribution or metabolism of either compound.

In the present study we demonstrated that supplementation with RSV effectively protected against the diabetogenic effects of PCB-77 in vitro and in vivo. A recent clinical study of T2D patients treated with oral RSV supplements for three months reported significant improvements in nearly all biomarkers associated with the disease (213). However, other groups have not been able to show improvements in insulin sensitivity or glucose regulation with RSV (215, 318). The dietary dose of RSV used in this study (approx. 160 mg/kg/day) equates to a human equivalent dose of just under 800 mg/day for a 60 kg individual (319). This dose of RSV would not be achievable in humans without the aid of supplementation. A potential RSV treatment therapy in PCB exposed populations should be regarded cautiously, since the drug interaction potential of the high doses of RSV typically utilized in clinical trials remains poorly understood (320). Interestingly, plant food sources that are high in RSV also tend to be conversely low in PCBs, as total PCB concentrations in food tend to be higher in meats and fish than other sources (11). This would suggest that a diet that enhances consumption of vegetables and limits PCB containing foods

(e.g., meat) would simultaneously confer antioxidant protection and lower the total body burden of these environmental contaminants.

Another interesting finding from this study was that RSV had little effect on any measured parameter in the absence of PCB-77 administration. This finding is consistent with recent studies that demonstrate that RSV had no effect in lean individuals (215), or that RSV improved adipose tissue glucose homeostasis only under insulin resistant conditions (241). These results suggest that RSV would not adversely influence glucose homeostasis in the absence of an insult, in this case, exposure to an environmental toxin. Indeed, protective pathways (e.g., NQO1) targeted by RSV are typically quiescent and become activated in response to an external stimuli (e.g., PCB-77).

Mechanisms for protective effects of RSV in the present study include reductions in oxidative stress associated with stimulation of the anti-oxidant Nrf2 signaling pathway. Several studies have demonstrated that RSV stimulates Nrf2 expression in various cell types (247, 306, 316). As described above, RSV stimulated Nrf2 and NQO1 gene expression only in adipocytes incubated with PCB-77, suggesting that stimulation of the anti-oxidant system by RSV requires induction of oxidative stress by a damaging stimulus. These results are consistent with in vivo data from the present study demonstrating that RSV favorably influenced a measure of insulin signaling and NQO1 gene expression in adipose tissue only when mice were exposed to PCB-77.

In conclusion, results from this study indicate that RSV reduces PCB-77 induced oxidative stress in adipose tissue by enhancing Nrf2 signaling, protecting

against PCB-77-induced impairment of glucose and insulin tolerance. These results suggest that supplementation with resveratrol may be a potential therapy for populations with known PCB exposures to lower the risk of developing diabetes.

Gene	Forward	Reverse
CYP1A1	AGTCAATCTGAGCAATGAGTTTGG	GGCATCCAGGGAAGAGTTAGG
GAPDH	GCCAAAAGGGTCATCATCTC	GGCCATCCACAGTCTTCT
NQO1	AGGATGGGAGGTACTCGAATC	TGCTAGAGATGACTCGGAAGG
Nrf2	CCATATTCCATTCCCTGTCG	TAAGTGGCCCAAGTCTTGCT

Abbreviations: CYP1A1, cytochrome P-450 1A1; GAPDH, glyceraldehyde 3-phosphate dehydrogenase; NQO1, NAD(P)H:quinone oxidoreductase 1; Nrf2, nuclear factor erythoid 2-related factor 2.

Table 3.1. Primer sequences for real-time PCR.

PCB77 (µM)					
Tissue type	VEH	VEH+RSV	PCB77	PCB77+RSV	p-value
Serum	N.D.	N.D.	0.07 ± 0.02	0.08 ± 0.02	0.249
Liver	N.D.	N.D.	4.78 ± 2.88	3.16 ± 2.19	0.347
RPF	N.D.	N.D.	29.90 ± 10.44	19.12 ± 8.65	0.113
Hydroxy PCB77 (µM)					
Tissue type	VEH	VEH+RSV	PCB77	PCB77+RSV	p-value
Serum	N.D.	N.D.	1.53 ± 0.38	1.73 ± 0.48	0.492
Liver	N.D.	N.D.	216.19 ± 301.58	75.22 ± 69.03	0.338
RPF	N.D.	N.D.	4.25 ± 0.98	3.14 ± 0.17	0.282
Dihydroxy PCB77 (µM)					
Tissue type	VEH	VEH+RSV	PCB77	PCB77+RSV	p-value
Serum	N.D.	N.D.	0.31 ± 0.08	0.45 ± 0.14	0.096
Liver	N.D.	N.D.	1.50 ± 2.07	2.39 ± 4.47	0.695
RPF	N.D.	N.D.	1.77 ± 1.11	1.21 ± 0.33	0.346
trans-Resveratrol (nM)					
Tissue type	VEH	VEH+RSV	PCB77	PCB77+RSV	p-value
Serum	N.D.	0.60 ± 0.17	N.D.	0.75 ± 0.15	0.174
Liver	N.D.	0.08 ± 0.07	N.D.	0.06 ± 0.10	0.819
RPF	N.D.	0.57 ± 0.71	N.D.	2.87 ± 3.44	0.181
Resveratrol-3-O-glucuronide (nM)					
Tissue type	VEH	VEH+RSV	PCB77	PCB77+RSV	p-value
Serum	N.D.	22.44 ± 8.21	N.D.	76.90 ± 52.18	0.059
Liver	N.D.	13.15 ± 24.13	N.D.	7.24 ± 3.76	0.603
RPF	N.D.	1.11 ± 0.54	N.D.	1.97 ± 1.02	0.134
trans-Resveratrol-3-O-sulfate (nM)					
Tissue type	VEH	VEH+RSV	PCB77	PCB77+RSV	p-value
Serum	N.D.	34.06 ± 19.93	N.D.	30.95 ± 9.15	0.759
Liver	N.D.	17.34 ± 19.22	N.D.	62.63 ± 83.76	0.272
RPF	N.D.	0.99 ± 0.64	N.D.	3.58 ± 3.31	0.125

Table 3.2. Levels of PCB-77, RSV, and their metabolites in serum, liver, and retroperitoneal fat of mice. Values are mean ± SEM from n = 5/group. P-values established via Student's t-test of independendent means comparing detectable groups. N.D., Not detected; VEH, vehicle; RSV, resveratrol; RPF, retroperitoneal fat.

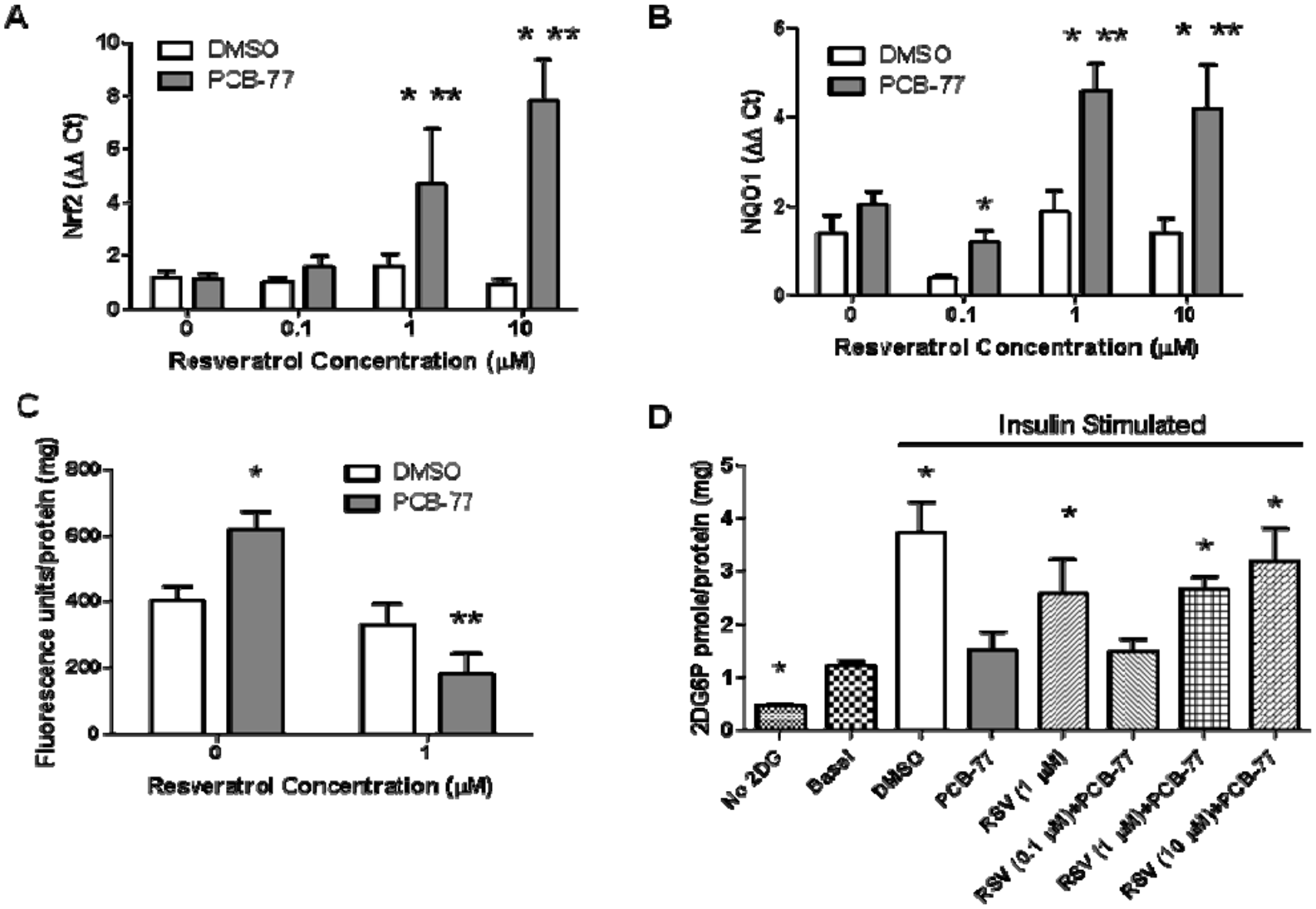
A
DMSO
PCB-77
Nrf2 (ΔΔ Ct)
Resveratrol Concentration (μM)
B
DMSO
PCB-77
NQO1 (ΔΔ Ct)
Resveratrol Concentration (μM)
C
DMSO
PCB-77
Fluorescence units/protein (mg)
Resveratrol Concentration (μM)
D
Insulin Stimulated
2DG6P pmole/protein (mg)
No 2DG
Basal
DMSO
PCB-77
RSV (1 μM)
RSV (0.1 μM)+PCB-77
RSV (1 μM)+PCB-77
RSV (10 μM)+PCB-77

Figure 3.1. Resveratrol protects 3T3-L1 adipocytes against PCB-77-induced oxidative stress and impaired glucose uptake. A, RSV results in a concentration-dependent increase in Nrf2 mRNA abundance in 3T3-L1 adipocytes incubated with PCB-77 (3.4 μM). B, RSV (1, 10 μM) promotes NQO1 mRNA abundance in 3T3-L1 adipocytes incubated with PCB-77. C, PCB-77 increases DCF fluorescence as an index of oxidative stress, which is abolished by RSV (1 μM). D, PCB-77 abolishes insulin-stimulated 2DG uptake in 3T3-L1 adipocytes, and RSV restores insulin-stimulated glucose uptake. Data are mean ± SEM from n = 2 experimental triplicates. *, $P<0.05$ compared to DMSO within RSV concentration or compared to basal in Figure 3.1D; **, $P<0.05$ compared to 0 within treatment.

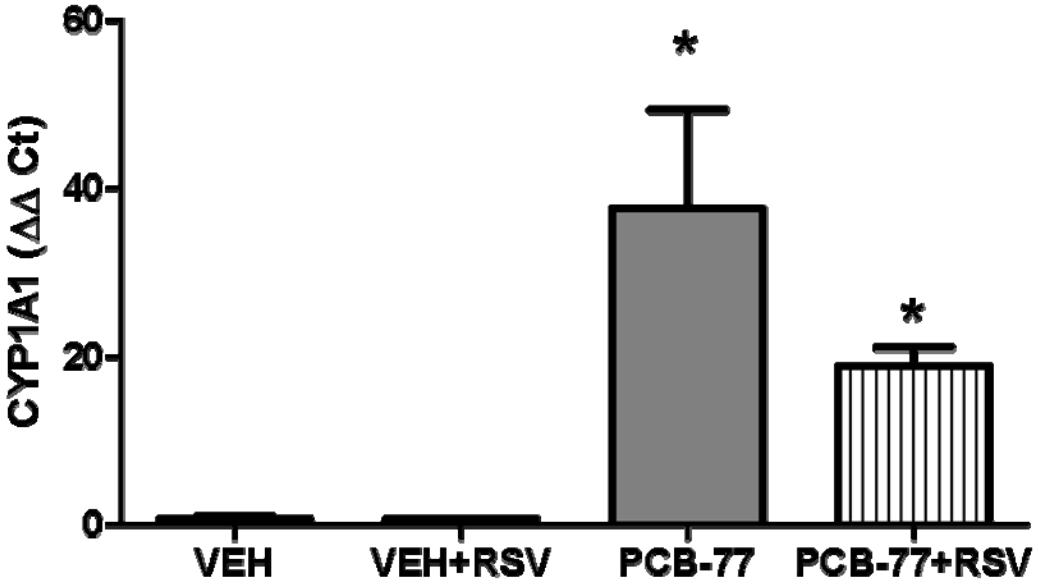

Figure 3.2. PCB-77 increases CYP1A1 mRNA abundance in adipose tissue. Mice were administered vehicle (VEH) or PCB-77 (50 mg/kg) in 2 divided doses and fed standard mouse diet without and with RSV (0.1%). At 48 hours after the second PCB-77 dose, adipose tissue was harvested for quantification of gene expression. PCB-77 administration significantly increased CYP1A1 mRNA abundance in adipose tissue of mice in each diet group. Data are mean ± SEM from n = 5 mice/group. *, $P<0.05$ compared to VEH within diet group.

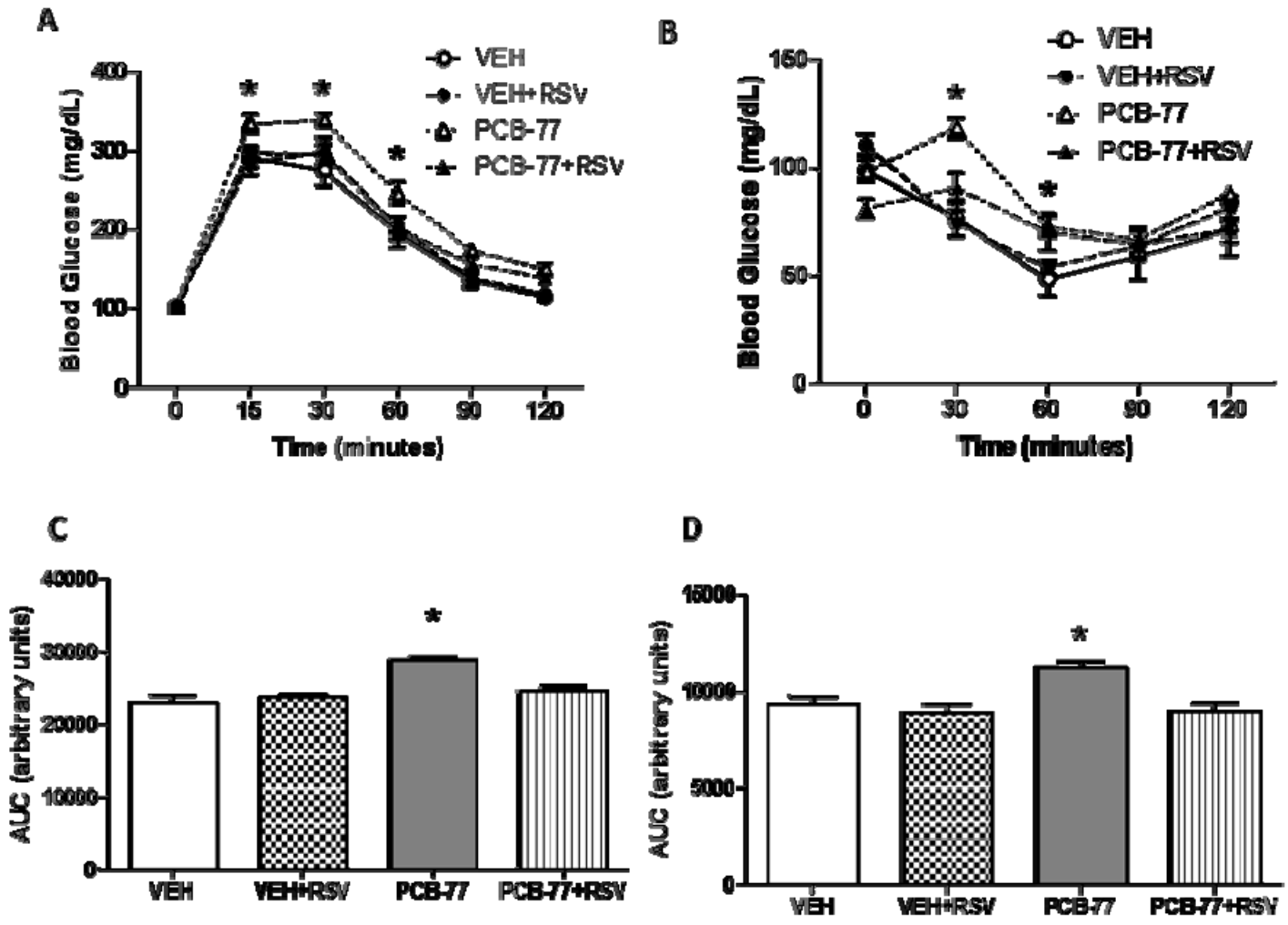
A
Blood Glucose (mg/dL)
400
300
200
100
0
0
15
30
60
90
120
Time (minutes)
VEH
VEH+RSV
PCB-77
PCB-77+RSV
B
Blood Glucose (mg/dL)
150
100
50
0
0
30
60
90
120
Time (minutes)
VEH
VEH+RSV
PCB-77
PCB-77+RSV
C
AUC (arbitrary units)
40000
30000
20000
10000
0
VEH
VEH+RSV
PCB-77
PCB-77+RSV
D
AUC (arbitrary units)
15000
10000
5000
0
VEH
VEH+RSV
PCB-77
PCB-77+RSV

Figure 3.3. RSV prevents PCB-77-induced impairment of glucose or insulin tolerance. Mice were administered vehicle (VEH) or PCB-77 (50 mg/kg) in 2 divided doses. Mice in each treatment group were fed either standard mouse diet or diet enriched with Resvida™ (RSV, 0.1%). A, Blood glucose levels after administration of glucose. B, Blood glucose levels after administration of insulin. C, Area under the curve (AUC) for data in A. D, AUC for data in B. Data are mean ± SEM from n = 5 mice/group. *, $P<0.05$ compared to PCB77+RSV (A,B) or compared to VEH (C,D).

A

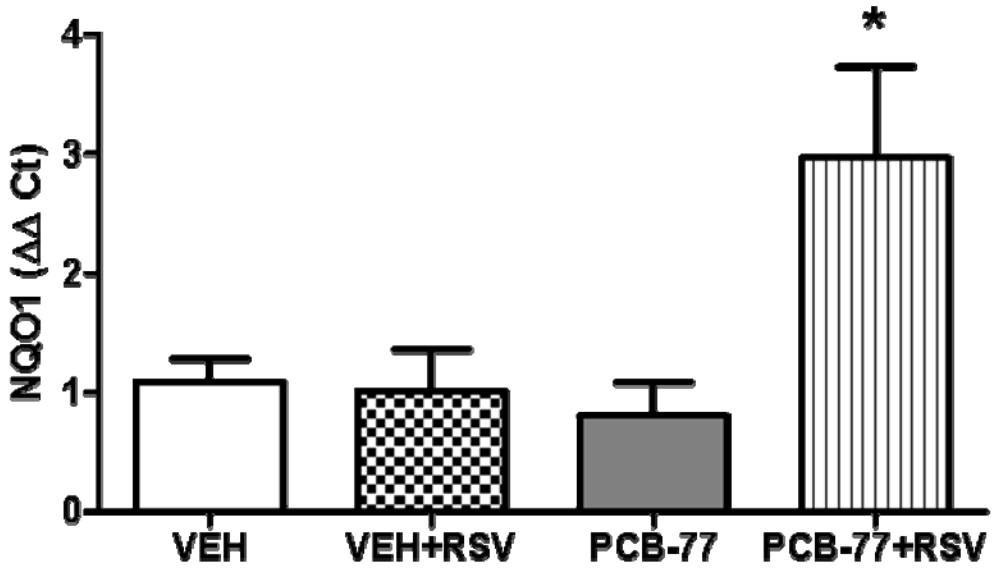
NQO1 (ΔΔ Ct)
4
3
2
1
0
*
VEH
VEH+RSV
PCB-77
PCB-77+RSV

B

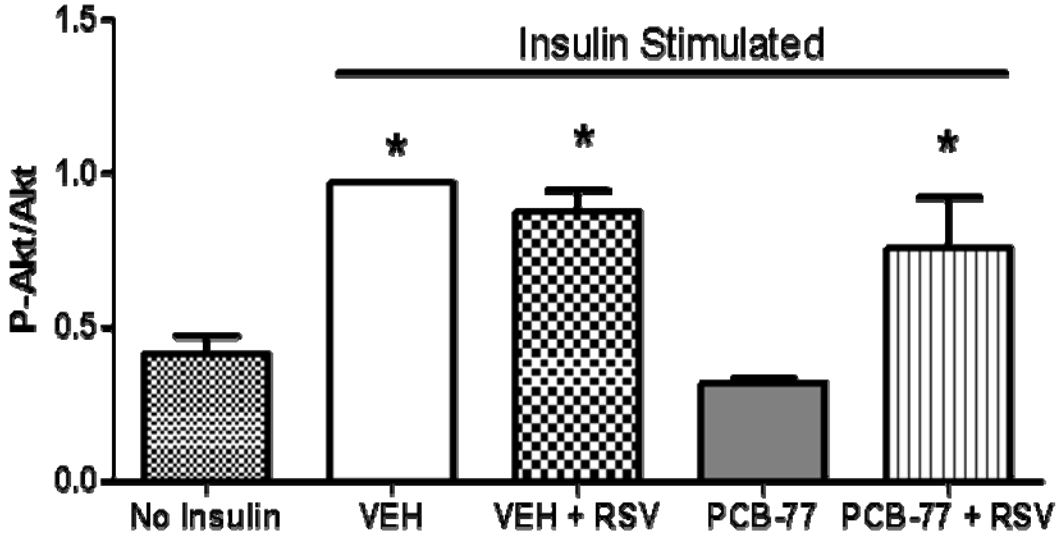
P-Akt/Akt
1.5
1.0
0.5
0.0
Insulin Stimulated
*
*
*
No Insulin
VEH
VEH + RSV
PCB-77
PCB-77 + RSV

Figure 3.4. RSV promotes the anti-oxidant NRF2 target, NQO1, and reverses PCB-77-induced impairment of insulin signaling in adipose tissue. Mice were administered vehicle (VEH) or PCB-77 (50 mg/kg) in 2 divided doses, and fed either standard mouse diet or a diet enriched with RSV (0.01%). A, NQO1 mRNA abundance in adipose tissue from mice in each treatment group. B, Levels of phosphorylated Akt (pAkt), normalized to total Akt, in adipose tissue from mice in each treatment group in the absence (no insulin) or presence of insulin. Data are mean ± SEM from n = 5 mice/group. *, $P<0.05$ compared to VEH (A) or compared to no insulin (B).

SECTION IV. SPECIFIC AIM 3

4.1 Summary

Previous studies in our laboratory demonstrated that coplanar polychlorinated biphenyls (PCBs) promote adipose tissue inflammation and impair glucose homeostasis in mice in an aryl hydrocarbon receptor (AhR)-dependent manner. PCBs are highly lipophilic, accumulating in adipose tissue, a recognized site of insulin resistance in type 2 diabetes (T2D). The current study tested the hypothesis that adipocyte AhR deficiency confers a protective effect on PCB-77 induced impairments of glucose disposal *in vivo*. We determined the effects of adipocyte AhR deficiency on responsiveness to PCB-77 (50 mg/kg)-induced disruptions in glucose homeostasis in mice fed low-fat (LF) or high-fat (HF) diets, as well as in obese mice undergoing weight loss. Mice expressing transgenic Cre recombinase under the control of the adiponectin (AdQ) promoter were bred with AhR-floxed mice to generate littermate controls ($AhR^{fl/fl}$) and adipocyte AhR deficient mice (AhR^{AdQ}). AhR mRNA abundance was reduced significantly in both white and brown adipose tissue from AhR^{AdQ} mice compared to $AhR^{fl/fl}$ mice. Adipocyte AhR deficiency resulted in greater fat mass and reduced lean mass in two month old, chow-fed mice, but this did not significantly influence body weight. However, when AhR^{AdQ} mice were challenged with a HF diet, body weight was significantly increased compared to $AhR^{fl/fl}$ controls. Notably, body weight increases in HF-fed AhR^{AdQ} mice were associated with greater deposition of subcutaneous adipose tissue. HF-fed AhR^{AdQ} mice had significantly increased numbers of adipocytes in both visceral and subcutaneous

adipose tissue compared to control. Importantly, adipocyte AhR deficiency protected against PCB-77 induced impairments in glucose and insulin tolerance following both acute and chronic exposure. We also examined effects of adipocyte AhR deficiency on PCB-77-induced impairment of glucose homeostasis during weight loss in obese mice. During LF feeding and post weight loss, AhR^{AdQ} mice had greater total fat mass than littermate controls. Additionally, AhR^{AdQ} mice dosed with PCB-77 during obesity and then subjected to weight loss had decreased levels of PCB-77 metabolites in adipose tissue, as well as decreased expression of cytochrome P450 1A1 (CYP1A1) and tumor necrosis factor-alpha (TNF-α) in adipose tissue compared to littermate controls. These results suggest that PCB-77 sequesters to the expanded adipocyte lipid pools present during obesity, and that weight loss facilitates the interaction of contaminants with the adipocyte AhR and facilitates subsequent metabolism. These results demonstrate that the adipocyte AhR is critical in mediating the disruptive effects of coplanar PCBs on glucose homeostasis, and that the adipocyte AhR might have novel importance in the regulation of obesity and body fat deposition.

4.2 Introduction

The aryl-hydrocarbon receptor (AhR) has well-established roles in toxicology and phase I drug metabolism, and also influences developmental cell proliferation and differentiation (67). Studies have demonstrated that adipose tissue can store xenobiotic ligands of AhR, namely coplanar PCBs (289), likely contributing to a low-grade internal source of PCBs which can act in an autocrine or paracrine manner. Adipocytes express AhR, and are likely chronically exposed to ingested lipophilic POPs given that this cell type stores most triglyceride in the body (32, 169). Moreover, storage of lipophilic PCBs in adipose tissue suggests that tonic low grade exposures may influence adipocyte differentiation and/or inflammation (6-7). While results have demonstrated that adipocyte AhR influence adipocyte differentiation and expression of inflammatory cytokine (6, 277, 321), the precise role that this receptor plays in normal or disease-related dysfunction of adipose tissue is unclear. Previous studies demonstrated that whole body deficiency of AhR resulted in improved insulin sensitivity and glucose tolerance in mice (87), suggesting that the endogenous AhR influences whole body glucose metabolism. However, the contribution of adipocyte AhR to effects of whole body AhR deficiency on glucose homeostasis are unclear.

Studies in humans undergoing weight loss have demonstrated that serum values of PCBs are inversely correlated with BMI (275-276), and that obese individuals store a greater body burden of total PCBs than lean counterparts (294). PCBs stored in adipose tissue may be released to blood to act

systemically, or alternately interact with the cytosolic adipocyte AhR. We have previously demonstrated that obese mice administered PCB-77 and subsequently subjected to weight loss experienced impaired glucose and insulin tolerance; this effect was also observed in lean mice acutely exposed to PCB-77 (7). One possible explanation for this observation is that weight loss results in release of hydrophobic PCBs from lipid pools during lipolysis of adipocytes. Indeed, levels of PCB-77 in adipose tissue were increased by obesity, but reduced to non-detectable levels following weight loss (7).

Interaction of coplanar PCBs with the adipocyte AhR could impact adipose tissue insulin sensitivity via several potential mechanisms. Alsharif et. al. demonstrated that mice exposed to 2,3,7,8-tetrachlorodibenzo-p-dioxin (TCDD) experienced an AhR-dependent increase in superoxide anion (295). Cytochrome P450, family 1, member A1 (CYP1A1), the detoxifying enzyme activated by AhR, is known to produce superoxide anion and hydrogen peroxide as part of the catalytic cycle of xenobiotic hydroxylation (322-323). The association between oxidative stress and insulin resistance, particularly in adipose tissue, has been recognized for some time (106-109). However, the role of adipocyte AhR as a contributor to oxidative stress of adipocytes has not been well defined.

An additional mechanism of PCB-induced insulin resistance mediated by the adipocyte AhR may stem from the promotion of chronic, low-grade inflammation in adipose tissue by these toxicants. Previous studies in our laboratory demonstrated that coplanar PCBs result in concentration-dependent increases in expression of several proinflammatory cytokines in 3T3-L1

adipocytes (6). Moreover, administration of PCB-77 to lean mice impaired glucose and insulin tolerance, and these effects were associated with adipose-specific elevations in expression of tumor necrosis factor-α (TNF-α) (7). PCB-induced impairment of glucose homeostasis was lost when mice were made obese from consumption of a high fat (HF) diet. However, when obese mice exposed to PCB-77 were subjected to weight loss they did not demonstrate the same degree of improvement in adipose levels of TNF-α compared to control (7). Collectively, these results suggest that coplanar PCBs act at adipocyte AhR to influence glucose homeostasis.

In this study, we hypothesized that coplanar PCBs promote insulin resistance in adipose tissue through direct effects at adipocyte AhR. To test this hypothesis, we examined effects of PCB-77 in lean and obese mice (with and without weight loss) on glucose homeostasis in mice lacking AhR in adipocytes. Results from these studies may have therapeutic implications for populations exposed to PCBs (from environmental accidents, or from higher levels due to obesity). In addition, results from these studies suggest that PCBs released from adipose stores during weight loss act at adipocyte AhR to blunt beneficial effects of weight loss.

4.3 Materials and Methods

4.3.1 Chemical Procurement

3,3',4,4'-tetrachlorobiphenyl (PCB-77) was purchased from AccuStandard Inc. (New Haven, CT).

4.3.2 Quantification of PCB-77 and hydroxylated metabolites in serum and tissues

Tissue samples were weighed and homogenized in dH_20. Cold acetonitrile and 50 µL of internal standard (10 µM 13C labeled d6-PCB-77) were added to homogenates and vortexed, sonicated, and centrifuged at 15,000 rpm for 5 minutes. Supernatants were transferred to glass vials and cold acetonitrile was added to the pellets and vortexed, sonicated, and centrifuged. Supernatants were transferred again and 50:50 acetonitrile:dH_20 was added to the pellet and repeated vortex, sonication, and centrifugation. All supernatants were pooled and dried under nitrogen. The dried samples were reconstituted in 100 µL of 99/1 methanol/dH_20 and 0.5% formic acid and 0.1% ammonium formate solution.

PCB-77 was measured using a Shimadzu UFLC coupled with an AB Sciex 4000-Qtrap hybrid linear ion trap triple quadrupole mass spectrometer in multiple reaction monitoring (MRM) mode. d6-PCB-77 was used as internal standards. PCBs were separated using Kinetex 2.6 u C18, 100 A, 100 X 2.10 mm (Phenomenex) column. The mobile phase consisted of water as solvent A and acetonitrile as solvent B. For the analysis of PCBs the separation was achieved using a gradient of 20% B to 60% B for 1 min, 60% B to 100% B in the next 7 min, and maintained at 100% B for the last 2 min with a flow rate of 0.25 ml/min.

Column was equilibrated back to the initial conditions in 3 min. Column temperature was maintained at 30 °C. The sample injection volume was 10 µL. The mass spectrometer was operated in the positive APCI mode with optimal ion source settings determined by synthetic standards of PCB-77 and d6-PCB-77 with a declustering potential of 36 V, entrance potential of 10 V, collision energy of 53 V, collision cell exit potential of 10 V, curtain gas of 20 psi, nebulizer current of 3, ion source gas1 of 40 psi and temperature of 550 °C. MRM transitions monitored were as follows: 291.9/ 222.1 and 291.9/220 for PCB-77 and 297.9/228.1 and 297.9/226.2 for d6-PCB-77. In the MRM ion transition the precursor ion represents the $M^{+\cdot}$ and the product ion represents either $[M\text{-}Cl]^+$ or $[M\text{-}2Cl]^+$.

Hydroxy PCB-77 was analyzed using Luna 3 u C18 (2), 100 A, 250 X 2.00 mm (Phenomenex) column. The mobile phase consisted of 75/25 of methanol/ water with formic acid (0.5%) and 5 mM ammonium formate (0.1%) as solvent A and 99/1of methanol/ water with formic acid (0.5%) and 5 mM ammonium formate (0.1%) as solvent B. Hydroxy PCB-77 was eluted using a gradient of 10% B to 100% B in 4 min and maintained at 100% B for the next 11 min. Column was equilibrated back to the initial conditions in 3 min. The flow rate was 0.25 mL/min with a column temperature of 30 °C. The sample injection volume was 10 µL. The mass spectrometer was operated in the negative ESI mode with optimal ion source settings determined by synthetic standards of 2-hydroxy-2', 3', 5', 6'-tetrachlorobiphenyl with a declustering potential of -60 V, entrance potential of -10 V, collision energy of -6 V, collision cell exit potential of -7 V, curtain gas of

20 psi, ion spray voltage of -4200 V, ion source gas1/gas2 of 40 psi and temperature of 550 °C. MRM transitions monitored were 352.8/306.9 for hydroxy PCB-77. Precursor ion of the ion transition is a formic acid adduct: $[M+FA-H]^-$ and product ion is $[M-H]^-$.

4.3.3 Animals and experimental diets

All experiments met the approval of the Animal Care and Use Committee of the University of Kentucky. AhR-floxed (*AhR*$^{fl/fl}$) mice were a generous gift of Dr. Mary Walker, University of New Mexico. Female *AhR*$^{fl/fl}$ mice were bred to hemizygous transgenic male Cre mice under control of an adiponectin/promoter/enhancer (B6;FVB-Tg(Adipoq-cre)1Evdr/J; The Jackson Laboratory, Bar Harbor, ME). Male *AhR*$^{fl/fl}$ littermates were used for comparison to mice with adipocyte AhR deficiency. Initial studies examined effects of adipocyte AhR deficiency on PCB-induced impairment of glucose homeostasis in lean mice. Male mice (8-9 weeks of age) of each genotype were administered vehicle (tocopherol-stripped safflower oil) or PCB-77 (50 mg/kg; by oral gavage given as two separate doses over 2 weeks; n = 3-8 mice/group and were fed a low fat diet (LF; 10% kcal as fat, D12450B; Research Diets, New Brunswick, NJ) for 2 or 4 weeks.

Follow up studies examined glucose and insulin tolerance in male mice administered vehicle or PCB-77 (50 mg/kg; by oral gavage given as 4 doses in weeks 1,2, 9, and 10; n = 6-8 mice/group) and fed a HF diet (60% kcal as fat, D12492; Research Diets) for 12 weeks to promote the development of obesity. After 12 weeks of HF feeding, subsets of mice from each genotype/treatment

group were euthanatized for tissue harvest. Remaining subsets of mice were placed on the LF diet for 4 additional weeks to induce weight loss.

Body weights were quantified weekly in all studies. At study end point, mice were anesthetized (ketamine/xylazine, 10/100 mg/kg, ip) for exsanguination and tissue harvest (liver, soleus muscle, and visceral adipose).

4.3.4 Measurement of body composition

Body weights of mice were recorded weekly. The body composition of mice was determined by nuclear magnetic resonance spectroscopy [EchoMRI (magnetic resonance imaging)] before mice began study diets and within 1 week of study endpoint.

4.3.5 Measurement of glucose and insulin tolerance

For glucose (GTT) and insulin tolerance tests (ITT), mice were examined at week 2 (LF), 4 (LF), 12 (HF) and 16 (HF then switched to LF diet from week 12-16). Mice were fasted for 4 or 6 hours for ITT or GTT, respectively, and fasted blood glucose was quantified by tail vein puncture using a hand held glucometer (Freedom Freestyle Lite, Abbott Laboratories, Abbott Park, IL). Mice were injected i.p. with D-glucose (Sigma, 20% in saline, 10 μL/g of body weight) for GTT and blood glucose was quantified at 15, 30, 60, 90, and 120 minutes post the bolus injection. For ITT, mice were injected i.p. with human insulin (Novolin, 0.0125 μM in saline/g of body weight), and plasma glucose was quantified at 30, 60, 90, and 120 minutes post ip injection. Total area under the curve (AUC; arbitrary units) was calculated as previously described (7). The GTT and ITT results of two vehicle treated mice were excluded from the acute (2 week) PCB-

77 findings when adipose tissue from these animals was found to be contaminated with PCB-77.

4.3.6 Quantification of mRNA abundance

Total RNA was extracted from tissues using the SV Total RNA Isolation System kit (Promega Corporation, Madison, WI), per the manufacturer's instructions. RNA from 3T3-L1 cells was extracted in Trizol. RNA concentrations were determined using NanoDrop 2000 spectophotometer and associated software (Thermo Scientific, Logan, UT). cDNA was synthesized from 0.4 µg total RNA with qScript cDNA SuperMix (Quanta Biosciences, Gaithersburg, MD) in the following reaction: 25°C for 5 minutes, 42°C for 30 minutes, and 85°C for 5 minutes. The cDNA was diluted 1:50 for a concentration of 0.4 ng/µL. The diluted cDNA was amplified with an iCycler (Bio-Rad, Hercules, CA) and the Perfecta SYBR Green Fastmix for iQ (Quanta Biosciences, Gaithersburg, MD). The components of the PCR reaction were as follows: Perfecta SYBR Green FastMix (10 µL), forward and reverse primers (0.125 µL), nuclease free water (4.75 µL), and diluted cDNA (5 µL for 2 ng of cDNA/reaction). Using the difference from GAPDH rRNA (reference gene) and the comparative Ct method, the relative quantification of gene expression in each sample was calculated. Primers (Eurofins MWG Operon, Huntsville, AL) were designed using the primer design program available from PubMed.gov (sequences presented in Table 1). The PCR reaction was as follows: 94°C for 5 minutes, 40 cycles at 94°C for 15 seconds, 58°C or 64°C (based on tested primer efficiency) for 40 seconds, 72°C for 10 minutes, and 100 cycles from 95°C to 45.5°C for 10 seconds. Primer sequences

were as follows: *CYP1A1*, forward 5'-AGTCAATCTGAGCAATGAGTTTGG-3', reverse 5'-GGCATCCAGGGAAGAGTTAGG-3'; *GAPDH*, forward 5'-GCCAAAAGGGTCATCATCTC-3', reverse 5'-GGCCATCCACAGTCTTCT-3'; *TNF-α*, forward 5'-CCCACTCTGACCCCTTTACTC-3', reverse 5'-TCACTGTCCCAGCATCTTGT-3'.

4.3.7 Determination of adipocyte size and cell number

Sections of formalin (10% wt/vol) fixed pieces of epidydmal or subcutaneous adipose tissue were stained with hematoxylin and eosin. Images of slides were taken at 10× magnification. Via use of the "detect edges" setting, image threshold, and object count features of NIS Elements software (Nikon Instruments, Inc., Tokyo, Japan), the area of each adipocyte and the number of adipocytes within a 700 × 700 μm measurement frame were quantified. Adipocyte size and number were calculated on three measurement frames within each section of adipose tissue (n = 3 sections/mouse) from mice in each group (n = 3 mice/group).

4.3.8 Differentiation of preadipocytes from SVC

Subcutaneous adipose tissue was taken from the inguinal region, minced, and incubated in basal medium (OM-BM; Zenbio, Research Triangle Park, NC) supplemented with collagenase (1 mg/ml) and penicillin/streptomyocin mixture (5%) for 1 h with shaking at 37°C as previously described (324). Two days after cells had reached 100% confluence, media was changed to differentiation medium (OM-DM; Zenbio) and changed every other day for 8 days. Cells were harvested for RNA using TRIzol.

4.3.9 Statistical analysis

Data are represented as mean ± SEM. Data was log transformed prior to statistical analysis. A two-way analysis of variance (ANOVA; SigmaPlot, version 12.0; Systat Software Inc., Chicago, IL) was used to determine statistical significance, which was defined as $p < 0.05$. Glucose and insulin tolerance tests were analyzed using repeated measure, two-way ANOVA. Holm-Sidak method was used for post-hoc analyses.

4.4 Results

4.4.1 Generation of mice with adipocyte AhR deficiency.

To confirm effective and specific deletion of exon 2 of AhR in adipocytes, AhR mRNA abundance was quantified in adipose tissues, liver, brain, heart, and kidneys from mice fed standard laboratory diet (2 months of age). AhR mRNA abundances were not significantly different in liver, kidney, or brains from $AhR^{fl/fl}$ compared to AhR^{AdQ} mice (Figure 1A; P>0.05). In heart, AhR mRNA abundance was reduced in AhR^{AdQ} compared to $AhR^{fl/fl}$ mice, but did not meet criteria for statistical significance (p = 0.08) (Figure 4.1A). In retroperitoneal (RPF) white adipose tissue and brown adipose tissue (BAT), AhR mRNA abundance was decreased significantly in AhR^{AdQ} compared to $AhR^{fl/fl}$ mice (Figure 4.1A; P<0.05). While no significant difference between genotypes was detected in AhR mRNA abundance in stromal vascular cells (SVCs) , AhR^{AdQ} mice had no detectable AhR mRNA in isolated adipocyte fractions from epidydmal adipose tissue compared to $AhR^{fl/fl}$ mice (Figure 4.1B; P<0.05).

We examined the ability of preadipocytes within SVCs isolated from mice of each genotype to differentiate into mature adipocytes. No visual differences in cell morphology or size were noted at any day during differentiation (data not shown). AhR mRNA abundance was significantly decreased in adipocytes (day 8) differentiated from SVCs of AhR^{AdQ} mice compared to $AhR^{fl/fl}$ controls (Figure 4C, $AhR^{fl/fl}$, 1.46 ± 0.27; AhR^{AdQ}, 0.60 ± 0.31, △△ Ct method, 18S used as reference gene; P < 0.05).

Chow-fed, two month old male *AhR*^{AdQ} mice did not have significant differences in body weight compared to littermate controls (Figure 4.2A); however, these mice had significantly increased fat mass and reduced lean mass compared to age-matched *AhR*$^{fl/fl}$ mice (Figure 4.2B; $P<0.05$). Additionally, chow-fed *AhR*^{AdQ} mice had significantly larger visceral adipose depots and moderately larger subcutaneous adipose depots (Figure 4.2C). Because differences in body fat deposition could potentially affect glucose and insulin tolerance in the absence of PCB and/or diet, we conducted baseline glucose and insulin tolerance tests in chow-fed male mice. Neither glucose nor insulin tolerance were influenced by adipocyte AhR deficiency in chow-fed mice (data not shown).

4.4.2 Adipocyte AhR deficiency improves glucose and insulin tolerance in lean mice acutely exposed to PCB-77.

We have previously demonstrated that lean mice acutely exposed to PCB-77 develop impaired glucose and insulin tolerance within 48 hours of the last dose (7). To determine the role of adipocyte AhR in mediating the acute effects of PCB-77 on glucose homeostasis, LF-fed *AhR*^{AdQ} mice and littermate controls were dosed twice with vehicle or PCB-77 (50 mg/kg) and glucose and insulin tolerance tests (GTT and ITT) were performed. *AhR*$^{fl/fl}$ mice, but not *AhR*^{AdQ} mice, exposed to PCB-77 had impaired glucose and insulin tolerance compared to vehicle treated controls (Figures 4.3A and 4.3B, respectively; $P<0.05$). Surprisingly, regardless of treatment (vehicle, PCB-77), adipocyte deficiency of AhR resulted in improved insulin tolerance compared to *AhR*$^{fl/fl}$ controls, as shown by the area under the curve (AUC) for ITT (Figure 4.3C; $P<0.05$). An

additional unexpected finding was an effect of PCB-77 to increase total fat mass, regardless of genotype (Figure 4.3D; $P<0.05$).

Due to their lipophilicity, PCBs accumulate in adipose tissue (8). We quantified levels of PCB-77 and the metabolite hydroxy PCB-77 in retroperitoneal white adipose (RPF) and serum of *AhR*$^{fl/fl}$ and *AhR*^{AdQ} mice following administration of PCB-77. At week 2 following acute PCB-77 exposure, PCB-77 levels in serum or RPF of *AhR*$^{fl/fl}$ mice (mean ± SE, serum: 0.77 ± 0.09 μM; RPF: 74.35 ± 7.91 μM) were not significantly different from values measured in *AhR*^{AdQ} mice (serum: 0.61 ± 0.07 μM, P = 0.61 compared to *AhR*$^{fl/fl}$ mice; RPF: 53.89 ± 4.65, P = 0.06 compared to *AhR*$^{fl/fl}$ mice). Additionally, serum and RPF levels of hydroxy PCB-77 were not significantly different in *AhR*$^{fl/fl}$ mice (serum: 0.01 ± 0.01 μM; RPF: 0.69 ± 0.26 μM) and *AhR*^{AdQ} mice (serum: 0.01 ± 0.01 μM, P = 0.84 compared to *AhR*$^{fl/fl}$ mice; RPF: 0.41 ± 0.15 μM, P = 0.35 compared to *AhR*$^{fl/fl}$ mice) with acute PCB-77 exposure.

4.4.3 Adipocyte AhR deficiency promotes the development of obesity during HF-feeding and alters body fat distribution.

Given that lean mice with adipocyte AhR deficiency displayed increased fat mass when fed chow diet (Figure 4.2B) in the absence of PCB exposure, we examined effects of adipocyte AhR deficiency on the development of obesity. Interestingly, deficiency of adipocyte AhR resulted in significant increases in the development of obesity (Figure 4.4A,B; $P<0.05$). There was a trend for adipocyte AhR deficient mice to exhibit impairments of glucose and insulin tolerance (Figure 4.5A,B), with

these findings tracking body weight differences between groups (i.e., heavier groups were more glucose and insulin intolerance than leaner groups).

4.4.4 Adipocyte AhR deficiency resulted in adipose depot-specific changes in adipocyte cell number in HF-fed mice.

In subcutaneous adipose tissue from HF-fed *AhR*^{AdQ} mice, adipocytes were larger in size resulting in fewer number of cells per field compared to tissue from *AhR*$^{fl/fl}$ mice (Figure 4.6A,B; $P<0.05$). In epidydmal adipose tissue, similar trends were observed with increased adipocyte size of HF-fed *AhR*^{AdQ} mice compared to control (Figure 4.6B); however, these increases did not reach statistical significance in epididymal adipose. Notably, epididymal adipose tissue from HF fed *AhR*^{AdQ} mice exhibited pronounced macrophage infiltration, as evidenced by increased mRNA abundance of F4/80 as a macrophage marker compared to adipose tissue from *AhR*$^{fl/fl}$ controls (Figure 4.6C; $P<0.05$). Increased macrophage infiltration was observed in epididymal, but not in subcutaneous adipose tissue from either group.

4.4.5 Adipocyte AhR deficiency protects against PCB-77 induced disruptions in glucose homeostasis and adipose tissue inflammation during weight loss.

To examine if adipocyte AhR deficiency would protect against PCB-77 induced disruptions in glucose homeostasis during weight loss, *AhR*^{AdQ} mice and littermate controls were fed the HF diet for 12 weeks and orally gavaged with vehicle or PCB-77 (50 mg/kg) in weeks 1, 2, 9, and 10. Following the weight gain portion of the study, mice were then fed the LF diet for 4 weeks to promote weight loss. Even though *AhR*^{AdQ} mice gained more weight when fed the HF diet

(Figure 4.4), all groups reached statistically similar body weights following 4 weeks of weight loss (Figure 4.7).

Similar to previous findings (7), administration of PCB-77 during the weight gain phase of the study resulted in significant impairments of glucose and insulin tolerance following weight loss in *AhR*$^{fl/fl}$ mice (Figure 4.8A-D; $P<0.05$). In contrast, effects of PCB-77 to impair glucose (Figure 4.8A,C) and insulin tolerance (Figure 4.8 B,D) during weight loss were mitigated in *AhR*^{AdQ} mice. As indicated by area under the curve quantification of blood glucose levels following glucose or insulin administration, adipocyte AhR deficiency conferred partial protection from PCB-77 induced disruptions in glucose tolerance (Figure 4.8C), and totally prevented PCB-77-induced impairment of insulin tolerance (Figure 4.8D; $P<0.05$).

We quantified adipose levels of PCB-77 and the metabolite hydroxy PCB-77 mice of both genotypes administered PCB-77, in obese mice of both genotypes at week 12 and post weight loss at week 16. HF-fed *AhR*^{AdQ} mice accumulated significantly higher levels of PCB-77, but not hydroxyl PCB-77 in adipose tissue (Figure 4.9A,B), potentially related to increased body weights and fat mass of these mice. With weight loss, both genotypes of mice exhibited reductions in adipose tissue levels of PCB-77 (Figure 4.9A), and increased levels of the metabolite hydroxyl PCB-77 (Figure 4.9B), suggesting that weight loss promoted liberation of PCB-77 from adipose lipids with potential CYP1A1-mediated metabolism to hydroxyl PCB-77. In addition, adipocyte AhR deficient mice undergoing weight loss exhibited significantly lower levels of metabolite

hydroxyl PCB-77 compared to controls (Figure 4.9B; $P<0.05$), suggesting that AhR-mediated induction of CYP1A1 contributed to metabolism of the parent toxin.

To determine the extent of AhR activation in mice of each genotype, we quantified epidydmal adipose tissue mRNA abundance of CYP1A1. Administration of PCB-77 significantly increased mRNA abundance of CYP1A1 in $AhR^{fl/fl}$, but not AhR^{AdQ} mice (Figure 4.10A; $P<0.05$). Similarly, mRNA abundance of TNF-α was significantly increased by administration of PCB-77 in adipose tissue of $AhR^{fl/fl}$, but not AhR^{AdQ} mice (Figure 4.10B; $P<0.05$).

4.5 Discussion

Results from this study demonstrate that the adipocyte AhR mediates effects of PCB-77 to impair glucose and insulin tolerance in lean mice, and in obese mice experiencing weight loss. Consistent with previously reported findings (7), PCB-77 impaired glucose homeostasis in lean wild type mice (week 2 of LF feeding), effects that were abolished in adipocyte AhR deficient mice. Furthermore, PCB-77 had no effect on glucose or insulin tolerance in obese mice of either genotype (week 12 of HF feeding). However, PCB-77 exposed wild type mice undergoing weight loss demonstrated previously reported impairments in glucose homeostasis, an effect which was not observed in AhR^{AdQ} mice (week 16, concluding 4 week LF feeding weight loss period). We uncovered the surprising finding that adipocyte AhR deficiency, in the absence of toxin administration, promoted an increase in fat mass in mice fed a LF or HF diet. These results suggest that location of this receptor to adipocytes influences the distribution of fat mass. Our results confirm previous findings that obese mice exhibit greater adipose levels of PCB-77(7), and extend these findings to demonstrate that sequestration to adipose lipids most likely protects the parent PCB-77 molecule from metabolism and detoxification. However, with weight loss adipose levels of the parent toxin decrease while metabolite levels increase, and these effects are most likely mediated through adipocyte AhR-induction of CYP1A1. Moreover, PCB-mediated induction of TNF-α expression in adipose tissue following weight loss was abolished in mice with adipocyte AhR deficiency. Reductions in adipose TNF-α expression most likely contributed to improved glucose and

insulin tolerance with weight loss in adipocyte AhR deficient mice previously exposed to PCB-77. These results indicate a pivotal role for adipocyte AhR in diabetes-inducing effects of PCB-77.

AhR^{AdQ} mice fed HF diet for 12 weeks demonstrated significant increases in macrophage infiltration to epidydmal adipose tissue compared to littermate controls, as shown by mRNA abundance of macrophage marker F4/80. Epidydmal adipocytes from obese *AhR*^{AdQ} mice were larger than controls, however this increase in size did not meet criteria for statistical significance. Increased macrophage recruitment to epidydmal adipose tissue may have occurred as a result of this modest epidydmal adipocyte hypertrophy. Alternatively, the adipocyte AhR may have undocumented effects on the regulation of macrophage recruitment signaling in adipocytes, which could be the basis of future studies.

An unexpected finding of the present study was that adipocyte AhR deficiency led to increased body weight and adipose depot-specific changes to adipocyte size and cell number during HF feeding. Interestingly, two month old, male *AhR*^{AdQ} mice fed standard chow diet also had increased body fat mass and larger visceral adipose depots, despite displaying no significant differences in body weights. These findings suggest that the adipocyte AhR plays a previously unrecognized role in body fat deposition, perhaps in an adipose depot-specific manner, and that this role becomes more important under HF feeding conditions. These intriguing findings warrant further study. Currently, there are several putative endogenous AhR ligands that could have contributed to these findings,

including arachidonic acid and one of its ecosanoid products, such as lipoxin A4 or prostaglandin G2 (325-326). Bui et. al. demonstrated that treatment of wild type mice with TCDD led to a significant increase in liver ecosanoids (unfortunately, adipose tissue was not examined in this study), but this effect was not observed in mice with whole body AhR deficiency. The authors concluded that TCDD-mediated binding of AhR resulted in antagonism of the receptors interaction with endogenous ecosanoid ligands, leading to an increase of these products in examined tissues (326). Our laboratory has previously demonstrated that coplanar PCB exogenous ligands of the AhR promoted adipocyte differentiation when incubated with predipocytes (6). It should be noted that AhR expression was present in the stromal vascular fraction from mice with adipocyte AhR deficiency; however, AhR expression levels were reduced in mature adipocytes that would experience increased expression of the Cre-driven promoter, adiponectin. Therefore, increased adipocyte size in mice with adipocyte AhR deficiency was most likely not the result of regulation of adipocyte differentiation by an endogenous ligand.

Another potential explanation for the unusual phenotype observed in *AhR*^{AdQ} mice may relate to crosstalk between the adipocyte AhR and other nuclear receptors or transcription factors. Interestingly, recent studies characterized a mouse model with adipocyte-specific deficiency of aryl-hydrocarbon receptor nuclear translocator-like, ARNTL (also known as BMAL1 or MOP3)(327). Not only has signaling between the circadian protein ARNTL and AhR been postulated to have metabolic effects on glucose and insulin tolerance

(87), but the adipocyte-specific ARNTL knock out mice demonstrated a similar phenotype in response to HF feeding as observed in the present study (327).

Crosstalk between AhR and estrogen receptor-alpha (ERα) and estrogen receptor-beta (ERß) has been recognized for some time (328-332), with several studies demonstrating that activation of AhR by synthetic ligands effectively mutes ER signaling, and vice versa (328-332). Moreover, PCB-77 and its metabolites can demonstrate both estrogenic or anti-estrogenic properties that may have influenced findings of the present study (333-334). CYP1B1, a member of the classical AhR gene battery, is a known monooxygenase activator of 17beta-estradiol. CYP1B1 hydroxylates 17beta-estradiol to generate catechol estrogen metabolites with carcinogenic and estrogenic potential (331). Although the present studies were conducted utilizing male mice, adipose tissue expresses aromatase and could therefore convert androgens to estrogens. It is possible that a combination of these factors are contributing to the gynoid pattern of fat distribution (i.e. larger subcutaneous adipose depots) demonstrated by male AhR^{AdQ} mice.

Another potential mechanism for the increased fat mass phenotype observed in AhR^{AdQ} mice might be that removing AhR from adipocytes then frees the AhR dimerization partner, aryl-hydrocarbon receptor translocator (ARNT) to interact with other adipocyte transcription factors. Hypoxia has been shown to inhibit AhR activity in an ARNT-dependent fashion (335), while conversely AhR activation has been shown to suppress the expression of hypoxia inducible factor 1 alpha (HIF1-α), a transcription factor that is also dependent on ARNT for gene

regulation (336). Taken together, these findings suggest that activation of AhR or HIF1-α would tend to sequester ARNT away from the opposing pathway, effectively muting downstream cellular pathways. Interestingly, Jiang et. al. demonstrated that adipocyte-specific HIF1-α deficient mice gained less weight than controls during HF feeding (337). It is possible that deficiency of adipocyte AhR resulted in increased interaction between ARNT and HIF1-α, functionally increasing HIF1-α activity and increasing body weight.

In conclusion, the adipocyte AhR may represent a novel therapeutic target for individuals from PCB exposed populations, or overweight subjects attempting to lose weight in general. This therapeutic should be cautiously considered until the mechanisms behind adipocyte AhR regulation of body weight and adipose tissue deposition are more clearly delineated.

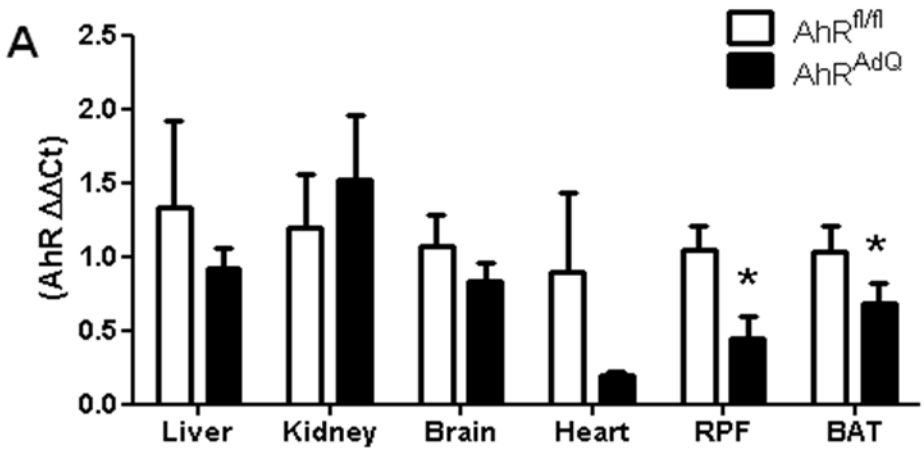
A
AhR$^{fl/fl}$
AhR^{AdQ}
(AhR ΔΔCt)
2.5
2.0
1.5
1.0
0.5
0.0
*
*
Liver
Kidney
Brain
Heart
RPF
BAT

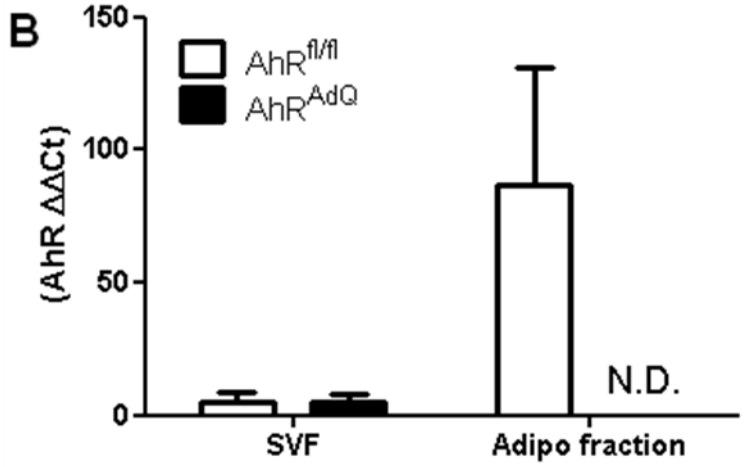
B
AhR$^{fl/fl}$
AhR^{AdQ}
(AhR ΔΔCt)
150
100
50
0
N.D.
SVF
Adipo fraction

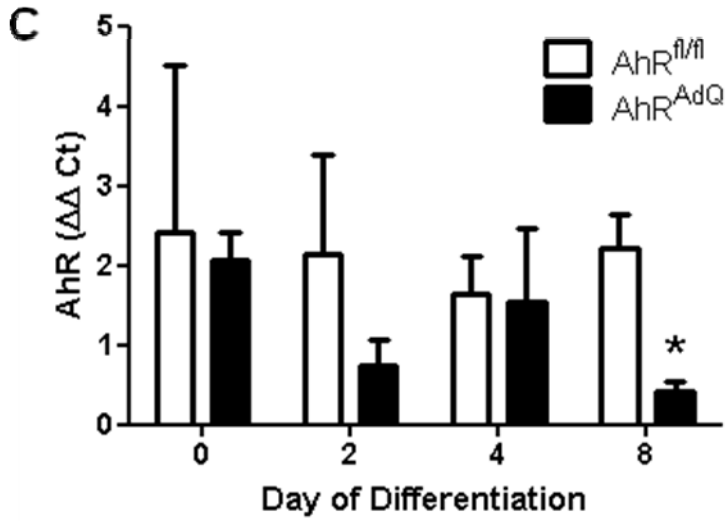
C
AhR$^{fl/fl}$
AhR^{AdQ}
AhR (ΔΔ Ct)
5
4
3
2
1
0
*
0
2
4
8
Day of Differentiation

Figure 4.1. Development of mice with adipocyte deficiency of AhR. A, AhR mRNA abundance was analyzed in liver, kidney, brain, heart, retroperitoneal fat (RPF), and brown adipose tissue (BAT). B, mRNA abundance of AhR in stromal vascular fractions (SVF) and adipocyte fractions from epidydmal adipose tissue of each genotype. C, AhR mRNA abundance in SVF cells isolated from subcutaneous adipose tissue of mice from each genotype that were then differentiated to mature adipocytes. Data are mean ± SEM from n = 4-6 mice/group. *, $P < 0.05$ compared to $AhR^{fl/fl}$.

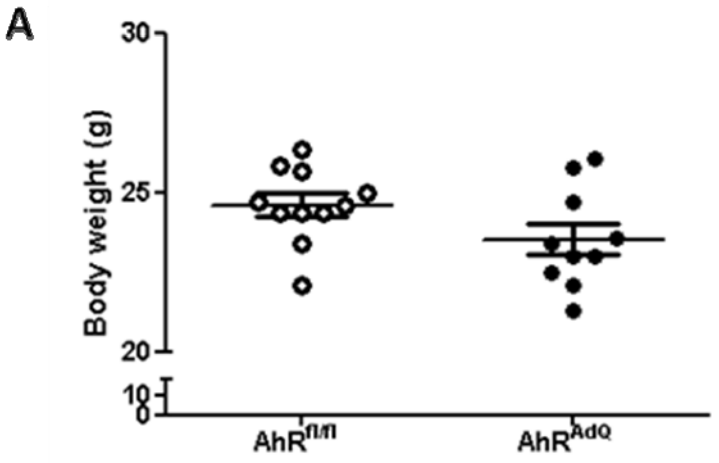
A
Body weight (g)
30
25
20
10
0
AhR^fl/fl
AhR^AdQ

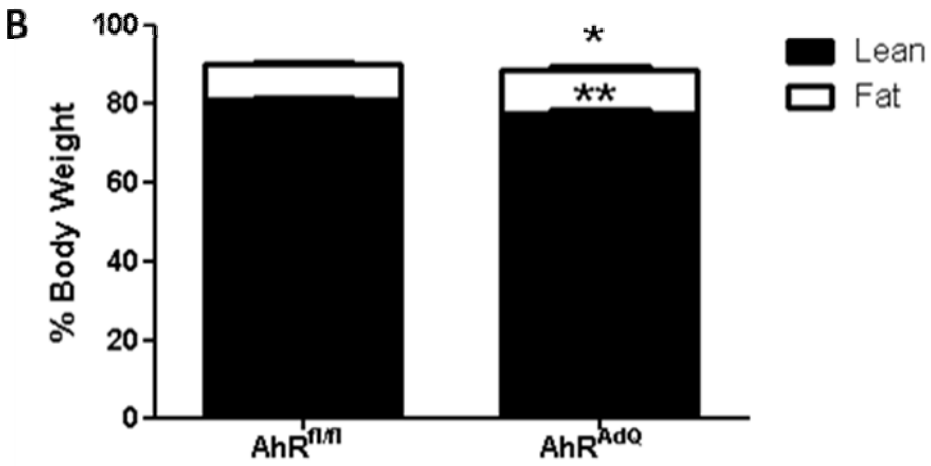
B
% Body Weight
100
80
60
40
20
0
*
**
Lean
Fat
AhR^fl/fl
AhR^AdQ

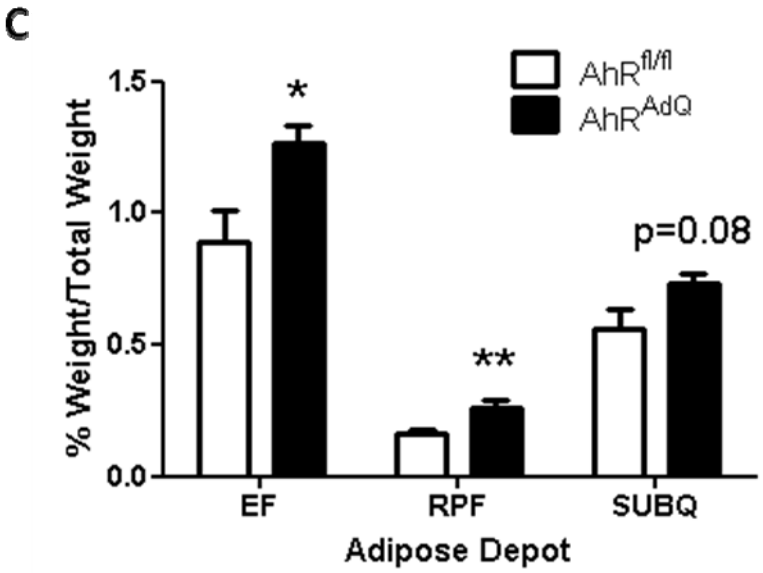
C
% Weight/Total Weight
1.5
1.0
0.5
0.0
*
**
p=0.08
AhR^fl/fl
AhR^AdQ
EF
RPF
SUBQ
Adipose Depot

Figure 4.2. Body weight and composition of adipocyte AhR deficient mice. A, Body weights from 2 month old, chow-fed male *AhR*^{AdQ} mice versus littermate controls. Circles represent individual mice with mean ± SEM represented as the horizontal line. B, Body composition from male *AhR*^{AdQ} mice versus littermate controls. C, Percent weight of adipose depots normalized as a percentage of total body weight from *AhR*^{AdQ} mice compared to littermate controls. Data are mean ± SEM from n = 10 mice/group. *, $P < 0.05$ compared to *AhR*$^{fl/fl}$; **, $P < 0.01$ compared to *AhR*$^{fl/fl}$.

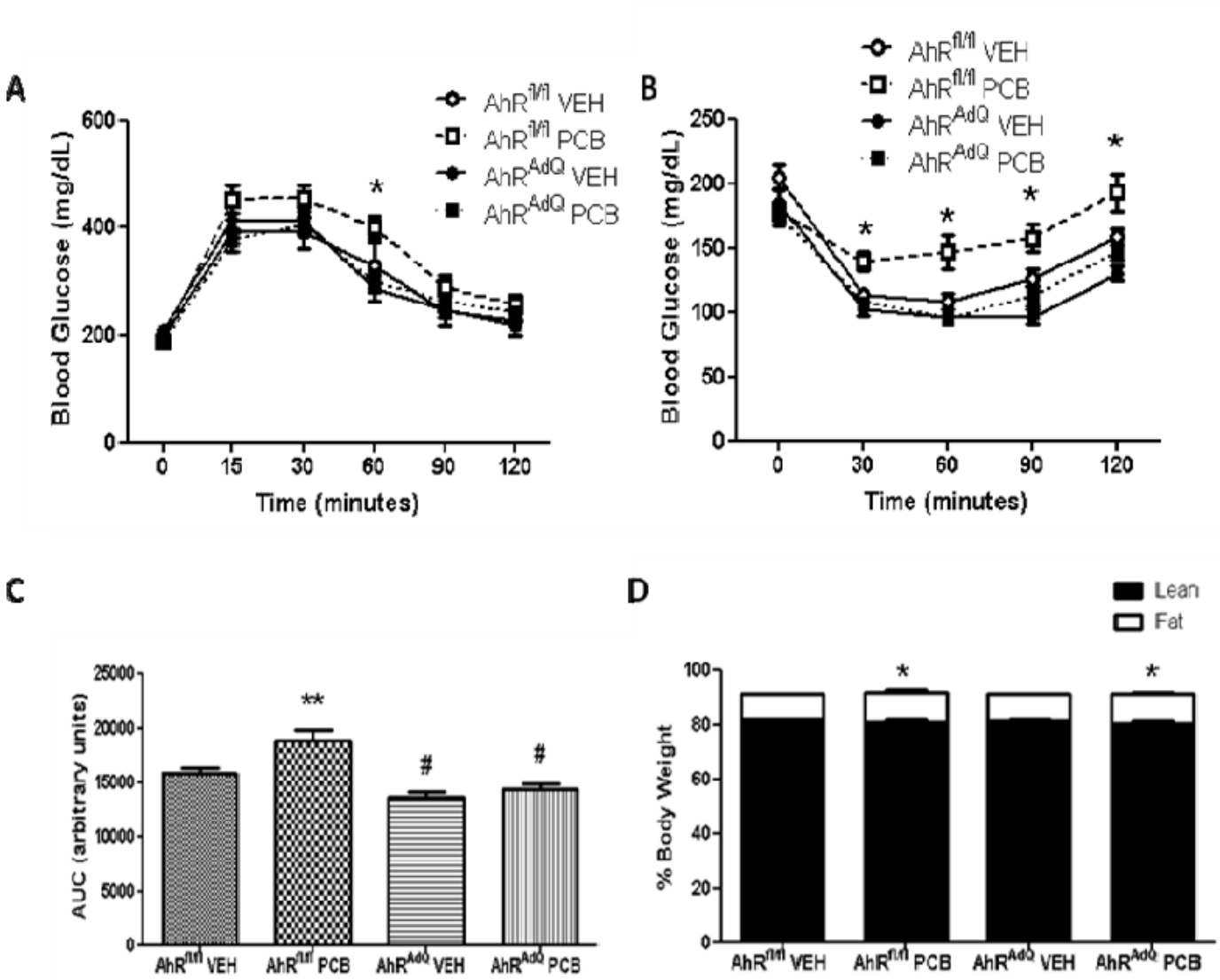
A
Blood Glucose (mg/dL)
Time (minutes)
AhR fl/fl VEH
AhR fl/fl PCB
AhR AdQ VEH
AhR AdQ PCB
B
Blood Glucose (mg/dL)
Time (minutes)
C
AUC (arbitrary units)
AhR fl/fl VEH
AhR fl/fl PCB
AhR AdQ VEH
AhR AdQ PCB
D
Lean
Fat
% Body Weight
AhR fl/fl VEH
AhR fl/fl PCB
AhR AdQ VEH
AhR AdQ PCB

Figure 4.3. Adipocyte AhR deficiency abolishes PCB-77-induced impairment of glucose and insulin tolerance in lean mice. A, Blood glucose levels following administration of glucose. B, Blood glucose levels following administration of insulin. C, Area under the curve (AUC) for insulin tolerance test (ITT) in panel B. D, Body composition of AhR^{AdQ} mice compared to littermate controls. Data are mean ± SEM from n = 6-8 mice/group. *, $P < 0.05$ compared to vehicle treated $AhR^{fl/fl}$; **, $P < 0.01$ compared to vehicle treated $AhR^{fl/fl}$; #, $P < 0.05$ effect of genotype.

A

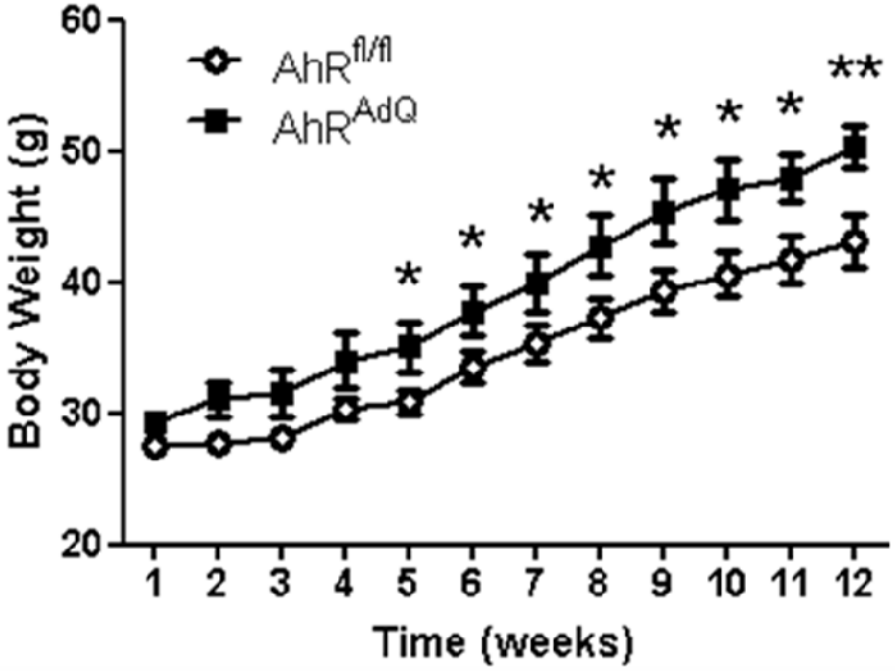
AhR$^{fl/fl}$
AhR^{AdQ}
Body Weight (g)
Time (weeks)
60
50
40
30
20
1
2
3
4
5
6
7
8
9
10
11
12
*
**

B

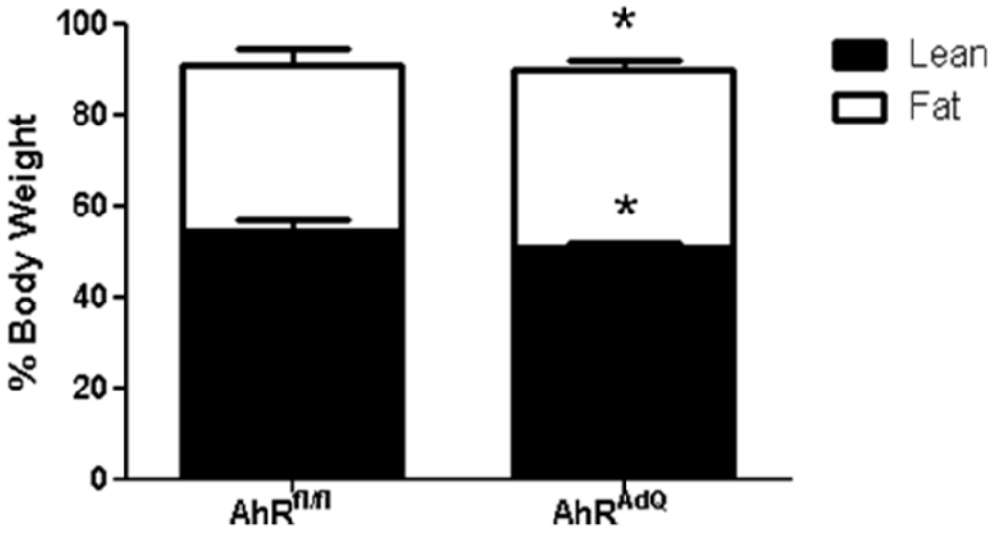
% Body Weight
100
80
60
40
20
0
AhR$^{fl/fl}$
AhR^{AdQ}
Lean
Fat
*
*

Figure 4.4. Adipocyte AhR deficiency promotes the development of obesity. A, Body weights during 12 weeks of HF feeding in each genotype. B, Body composition after 12 weeks of HF feeding in each genotype. Data are mean ± SEM from n = 6-8 mice/group. *, $P < 0.05$ compared to $AhR^{fl/fl}$; **, $P < 0.01$ compared to $AhR^{fl/fl}$.

A

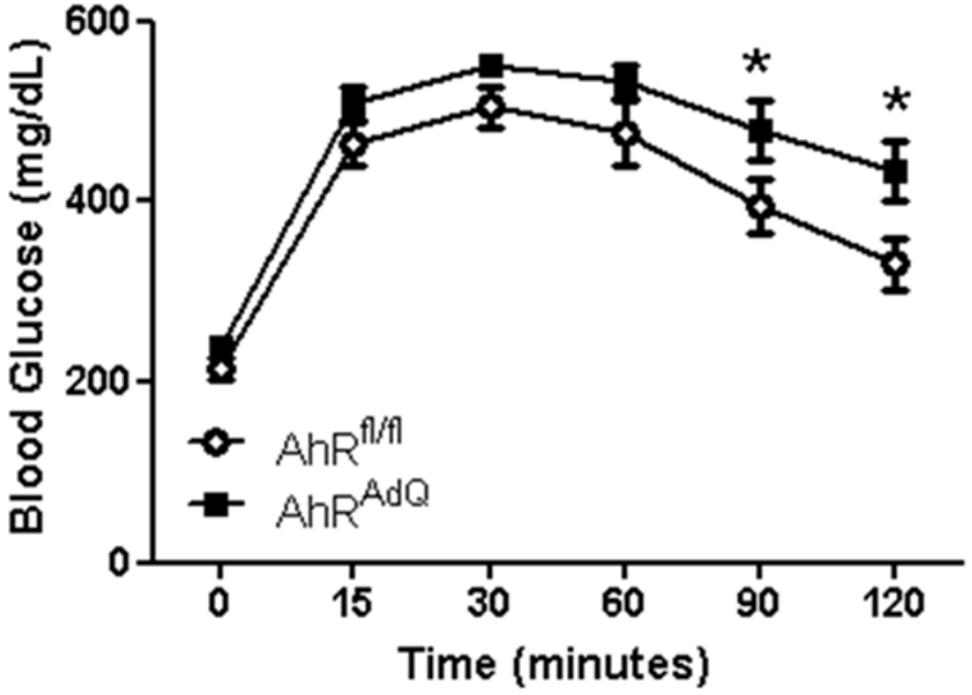
600
400
200
0
Blood Glucose (mg/dL)
*
*
AhR^fl/fl
AhR^AdQ
0
15
30
60
90
120
Time (minutes)

B

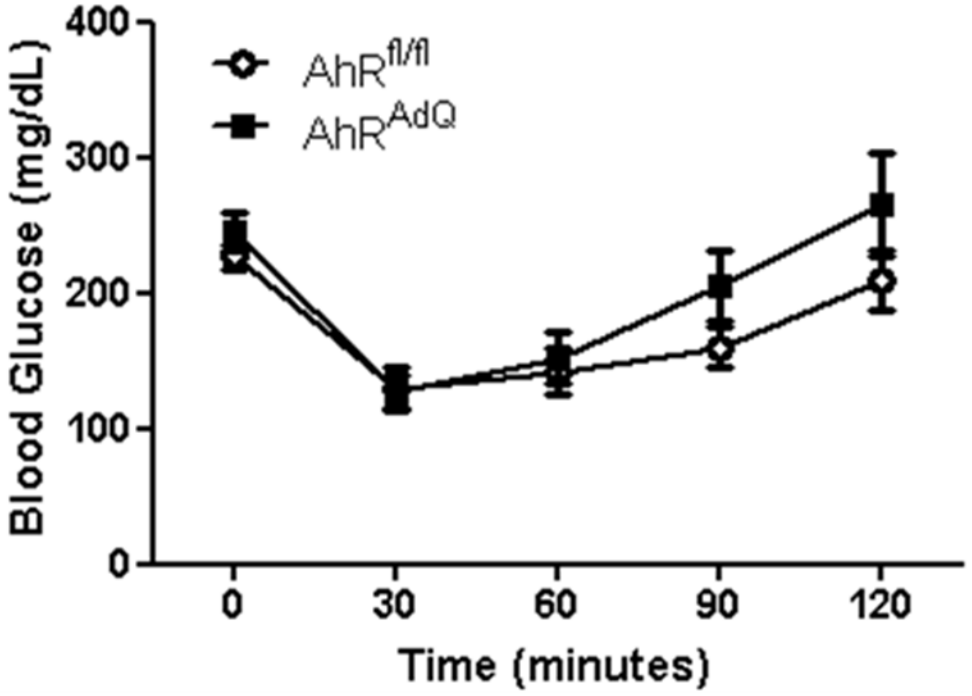
400
300
200
100
0
Blood Glucose (mg/dL)
AhR^fl/fl
AhR^AdQ
0
30
60
90
120
Time (minutes)

Figure 4.5. Adipocyte AhR deficiency modestly impairs glucose tolerance. A, Glucose tolerance test. B, Insulin tolerance test. Data are mean ± SEM from n = 6-8 mice/group. *, $P < 0.05$ compared to *AhR*$^{fl/fl}$.

A

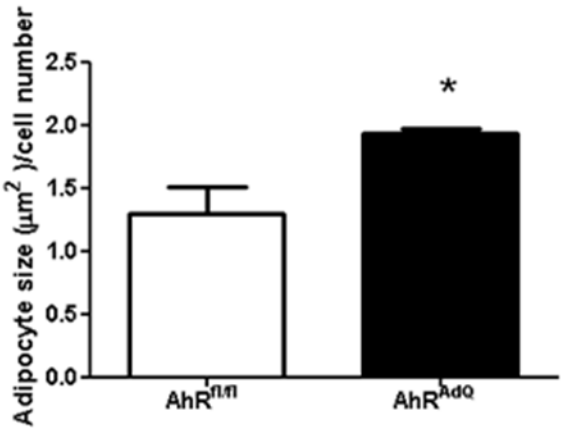
Adipocyte size (μm2)/cell number
2.5
2.0
1.5
1.0
0.5
0.0
*
AhRfl/fl
AhRAdQ

B

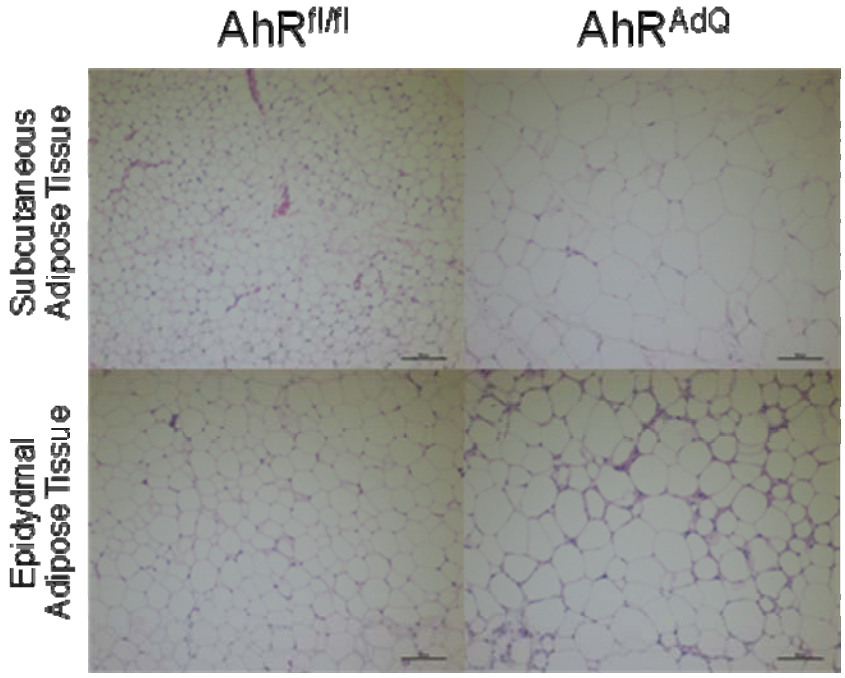
AhRfl/fl
AhRAdQ
Subcutaneous Adipose Tissue
Epidydmal Adipose Tissue

C

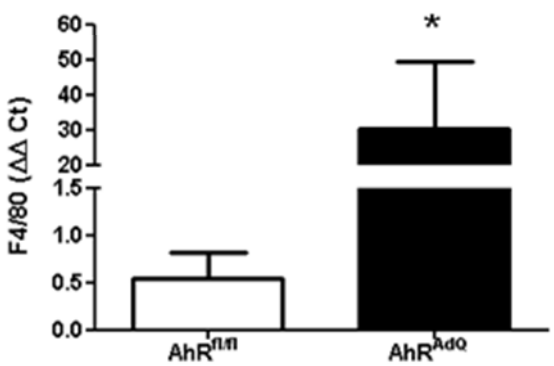
F4/80 (ΔΔ Ct)
60
50
40
30
20
1.5
1.0
0.5
0.0
*
AhRfl/fl
AhRAdQ

Figure 4.6. Adipocyte AhR deficiency promotes adipocyte hypertrophy and increases adipose F4/80 gene expression. A, Quantification of adipocyte size normalized to number of adipocytes/field in subcutaneous adipose tissue from each genotype. B, Representative subcutaneous and epidydmal adipose tissue sections. C, Epidydmal adipose tissue F4/80 mRNA abundance. Data are mean ± SEM from n = 3 mice/group for adipocyte quantifications, n = 5 for RT-PCR measurements. *, $P < 0.05$ compared to vehicle treated $AhR^{fl/fl}$.

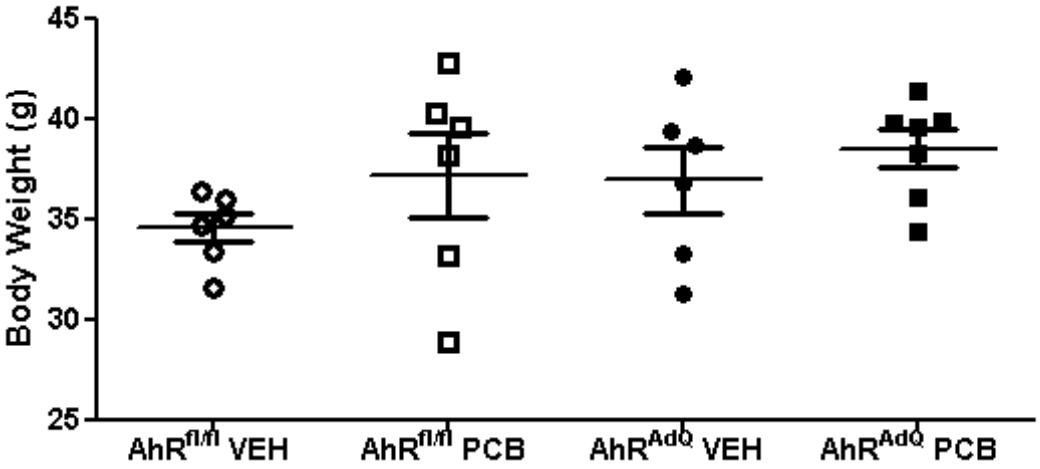

Figure 4.7. Following weight loss body weight is similar between genotypes and treatments. Body weights following 4 weeks of weight loss in mice of each genotype and treatment group. Data are mean ± SEM from n = 6-7 mice/group.

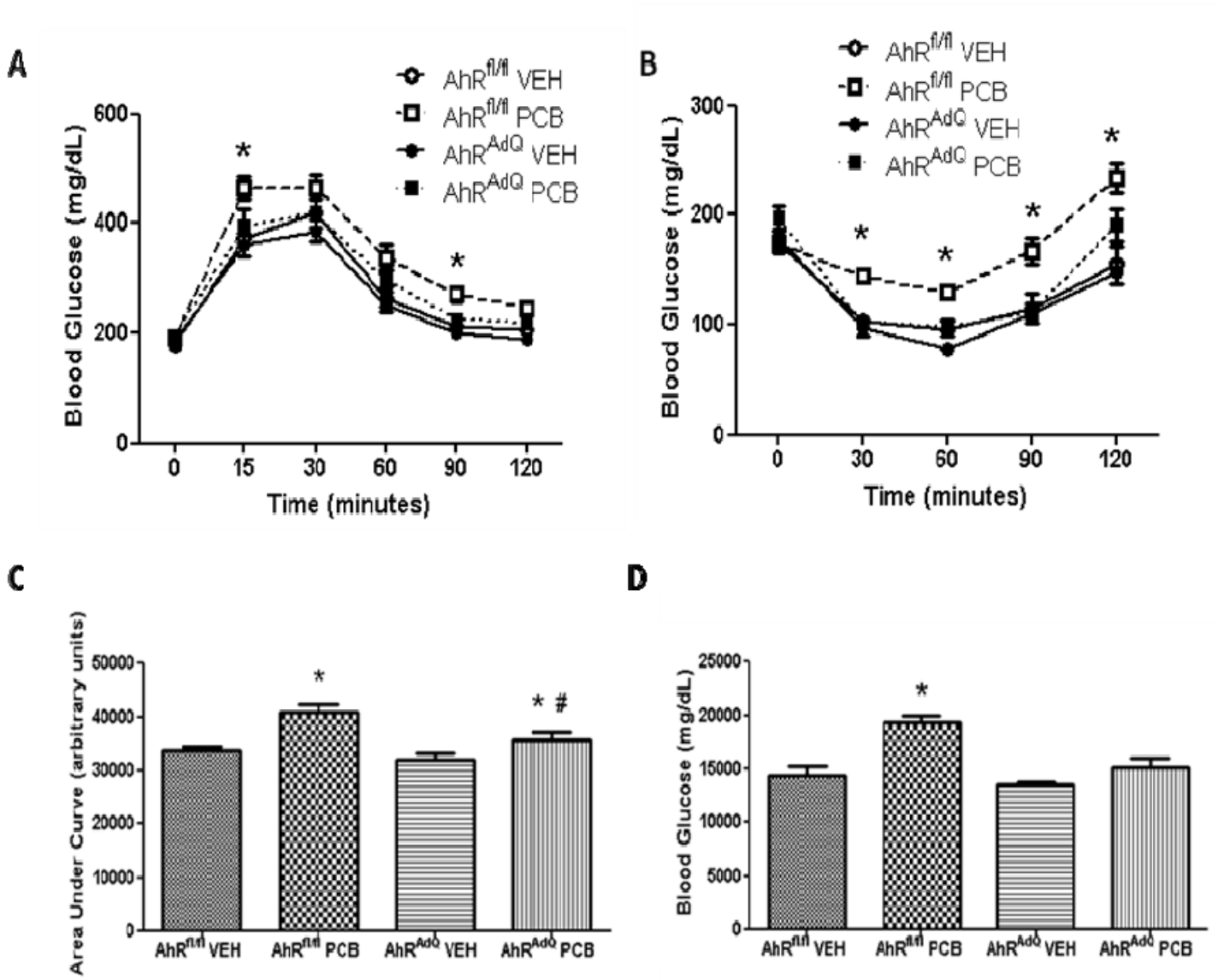
A
Blood Glucose (mg/dL)
600
400
200
0
0
15
30
60
90
120
Time (minutes)
AhR fl/fl VEH
AhR fl/fl PCB
AhR AdQ VEH
AhR AdQ PCB
B
Blood Glucose (mg/dL)
300
200
100
0
0
30
60
90
120
Time (minutes)
AhR fl/fl VEH
AhR fl/fl PCB
AhR AdQ VEH
AhR AdQ PCB
C
Area Under Curve (arbitrary units)
50000
40000
30000
20000
10000
0
AhR fl/fl VEH
AhR fl/fl PCB
AhR AdQ VEH
AhR AdQ PCB
D
Blood Glucose (mg/dL)
25000
20000
15000
10000
5000
0
AhR fl/fl VEH
AhR fl/fl PCB
AhR AdQ VEH
AhR AdQ PCB

Figure 4.8. Adipocyte AhR deficiency prevents PCB7-77-induced impairment of glucose and insulin tolerance following weight loss. A, Blood glucose levels following administration of glucose. B, Blood glucose levels following administration of insulin. C, Area under the curve (AUC) of glucose tolerance test (GTT) data in panel A. D, AUC of insulin tolerance test (ITT) data in panel B. Data are mean ± SEM from n = 6-8 mice/group. *, $P < 0.05$ compared to vehicle treated *AhR*$^{fl/fl}$; #, $P < 0.05$ effect of genotype.

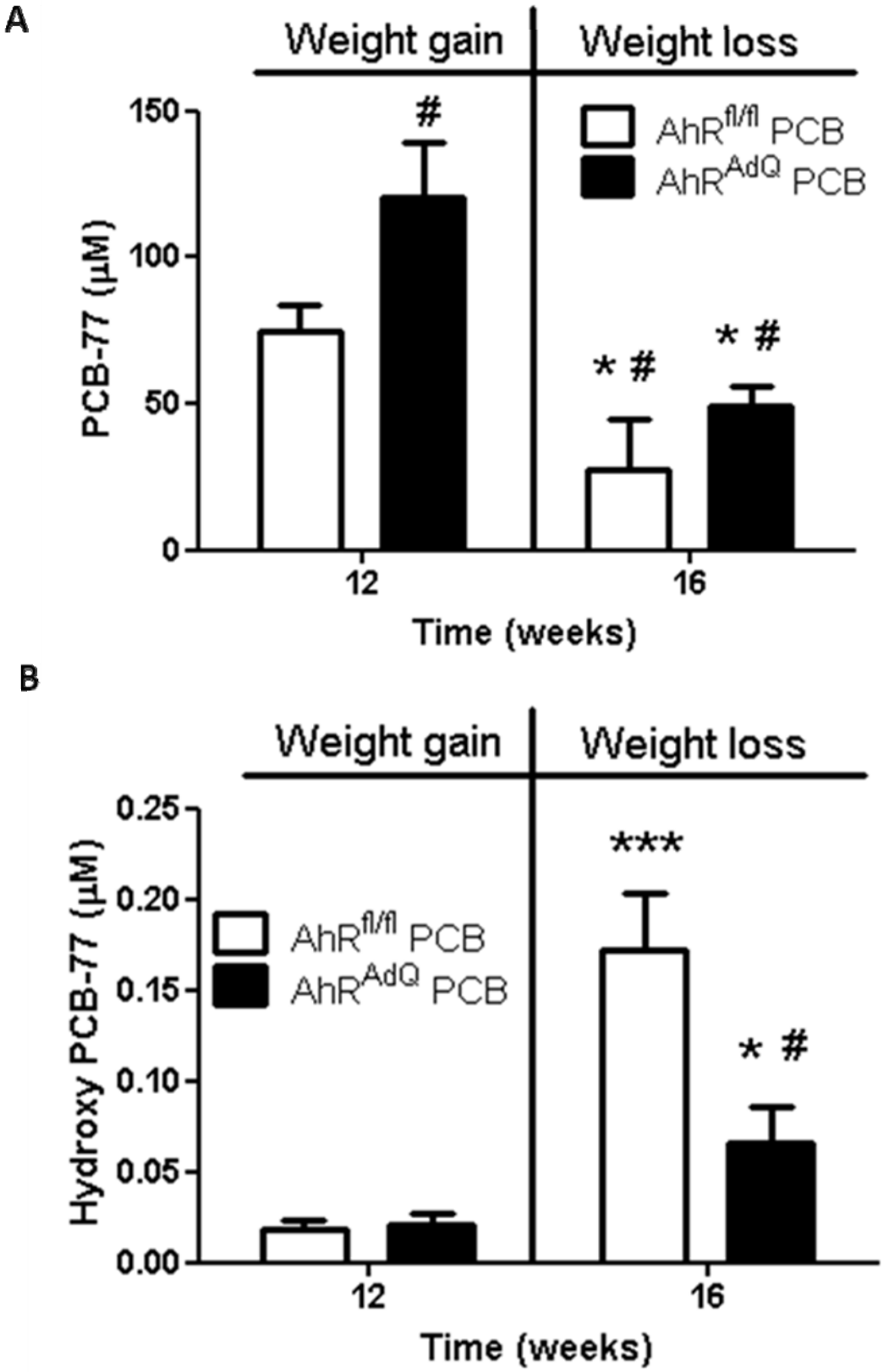
A
Weight gain
Weight loss
150
100
50
0
PCB-77 (µM)
#
* #
* #
AhR^fl/fl PCB
AhR^AdQ PCB
12
16
Time (weeks)
B
Weight gain
Weight loss
0.25
0.20
0.15
0.10
0.05
0.00
Hydroxy PCB-77 (µM)
***
* #
AhR^fl/fl PCB
AhR^AdQ PCB
12
16
Time (weeks)

Figure 4.9. Adipose levels of PCB-77 and hydroxy PCB-77 metabolite in obese mice (week 12 of HF feeding) and after 4 weeks of weight loss. A, PCB-77 levels in epidydmal adipose tissue from mice of each genotype and treatment group at weeks 12 and 16. B, Hydroxy PCB-77 levels in epidydmal adipose tissue from mice of each genotype and treatment group at weeks 12 and 16. Data are mean ± SEM from n = 5 mice/group. *, $P < 0.05$ compared to *AhR*$^{fl/fl}$; ***, $P < 0.001$ compared to *AhR*$^{fl/fl}$; #, $P < 0.05$ effect of genotype.

A

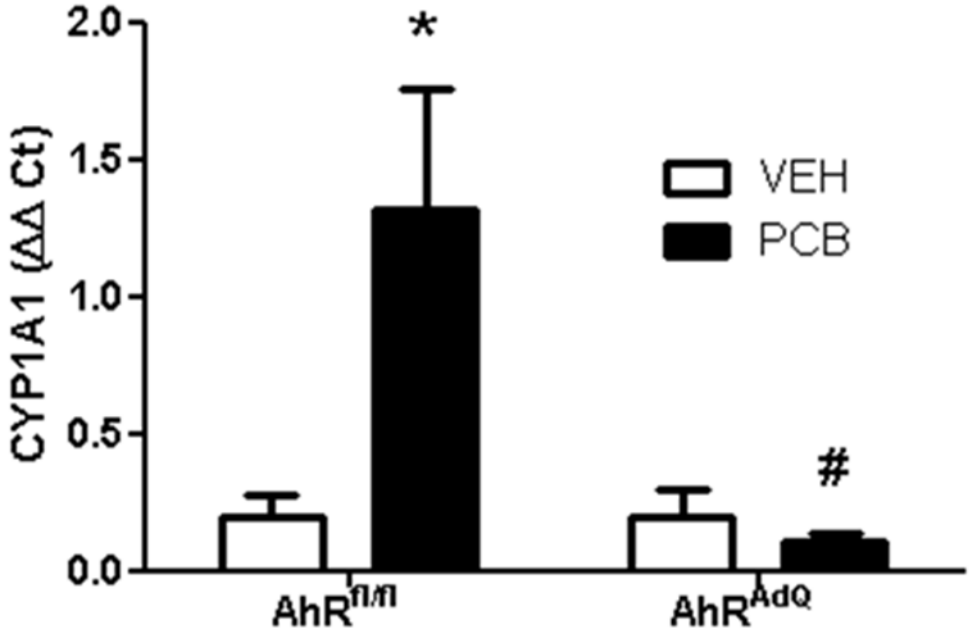
2.0
1.5
1.0
0.5
0.0
CYP1A1 (ΔΔ Ct)
*
#
VEH
PCB
AhR fl/fl
AhR ΔdQ

B

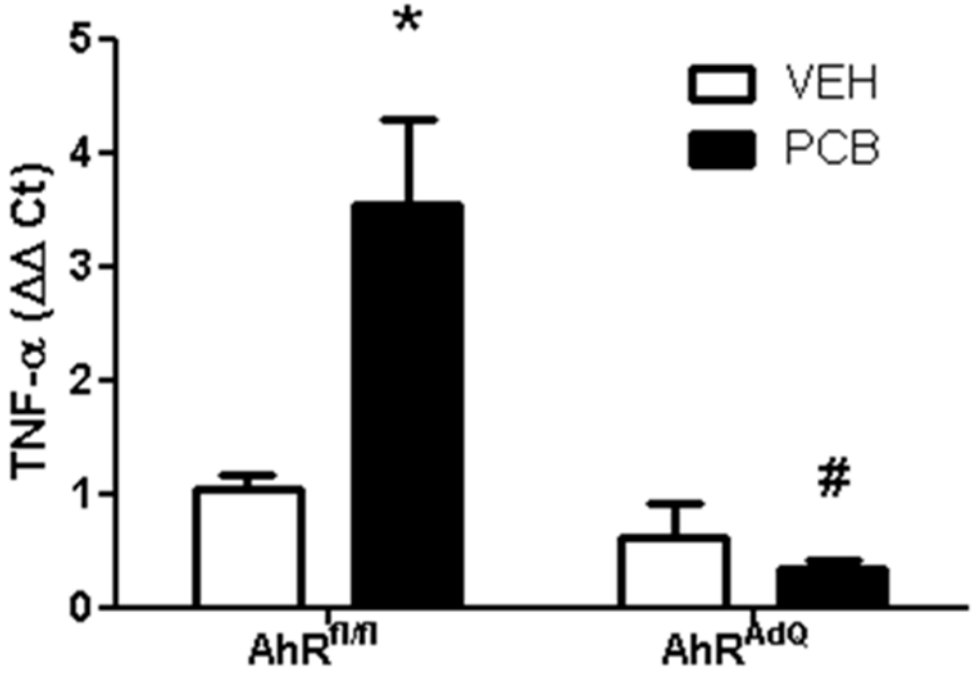
5
4
3
2
1
0
TNF-α (ΔΔ Ct)
*
#
VEH
PCB
AhR fl/fl
AhR ΔdQ

Figure 4.10. PCB-77-induced increases in mRNA abundance of CYP1A1 and TNF-α are abolished in mice with adipocyte AhR deficiency. A, Epidydmal adipose tissue CYP1A1 mRNA abundance in mice of each genotype and treatment group. B, Epidydmal adipose tissue TNF-α mRNA abundance in mice of each genotype and treatment group. Data are mean ± SEM from n = 5 mice/group. *, $P < 0.05$ compared to vehicle treated $AhR^{fl/fl}$; #, $P < 0.05$ effect of genotype.

SECTION V: GENERAL DISCUSSION

5.1 Summary

The purpose of the studies described in this dissertation was to test the hypothesis that PCB-77 regulates adipose tissue glucose homeostasis and inflammation through the adipocyte AhR, and that resveratrol would protect adipose tissue against PCB-77 induced insulin resistance. A mouse model of PCB-77 induced diabetes was developed in lean mice and in obese mice undergoing weight loss. PCB-77 had no effect on glucose or insulin tolerance in the context of obesity. In lean mice and obese mice undergoing weight loss, PCB-77 induced impairments in glucose homeostasis were associated with increased levels of TNF-α specifically in adipose tissue. Administration of resveratrol supplementation improved glucose homeostasis in lean PCB-77 treated mice, and simultaneously promoted NRF2 activity and restored insulin signaling pathways in adipose tissue of these mice. Moreover, 3T3-L1 adipocytes demonstrated a dose dependent increase in NRF2 signaling during cotreatment with PCB-77 and resveratrol. Also in vitro, resveratrol protected from PCB-77 induced oxidative stress and restored glucose uptake in PCB-77 treated cells in a concentration-dependent manner. A mouse model of adipocyte-AhR deficiency was developed using the Cre/LoxP system to investigate the potential roles of the adipocyte-AhR in mediating toxicities of PCB-77 in lean and obese mice, as well as obese mice undergoing weight loss. Lean AhR^{AdQ} mice fed a LF diet and acutely exposed to PCB-77 demonstrated a modest improvement in glucose tolerance and a more pronounced improvement in insulin sensitivity than $AhR^{fl/fl}$

mice. *AhR*^{AdQ} mice fed HF diet for 3 months unexpectedly gained more weight, had greater fat mass, and deposited more subcutaneous adipose tissue than littermate controls; however, PCB-77 had no effect on glucose homeostasis in obese mice of either genotype. During weight loss, obese *AhR*^{AdQ} mice exhibited partial protection against PCB-77 during glucose tolerance test and total protection from PCB-77 induced insulin resistance (see Figure 5.1 for a summary of these findings).

5.2 The interplay between adipose tissue and persistent organic pollutants: Insights from mouse models of PCB-77 induced diabetes

5.2.1. PCB distribution in the body

During exposure to PCBs, these lipophilic pollutants are stored in liver and adipose tissue (169, 289). This may avert the action of these pollutants in other susceptible tissues and might be protective to a certain extent or under some metabolic conditions (i.e. obesity) (7, 338). PCBs released from their storage in adipose tissue may also represent a source of low-level internal exposure or may act on the adipocyte directly as obesogens or disruptors of adipose tissue structure and function (6, 9). Strong evidence from both *in vivo* and *in vitro* studies suggests that PCBs can influence the development of adipose tissue, principally through the promotion of preadipocyte differentiation at low doses, and conversely preventing differentiation at high doses (6). Furthermore, storage of PCBs in adipose tissue could impact offspring via fetal programming, probably through epigenetic mechanisms, impacting the development of diseases in adulthood (339-340). Additionally PCBs might alter adipose tissue function and

structure later in life, primarily through metabolic disruption and inflammation, conditions which favor the development of metabolic diseases (6-7).

The findings described herein would suggest that obesity could adversely impact overall health in that expanded adipose stores might improve storage of lipophilic POPs, thus increasing total body burden of environmental contaminants. If obese subjects subsequently lose weight, this enhanced store of POPs can then be released from adipose tissue via lipolysis, where they may have effects systemically or on adipocytes directly. Observations in humans suggest that pollutants released from adipose tissue are a significant source of blood POPs. Many studies have demonstrated an increase in blood POPs after weight loss by either dietary changes alone or coupled with bariatric surgery (9, 341). The importance of fat mass in the regulation of POP blood levels was additionally reported by Lim et al. (275) who showed an inverse correlation between long-term weight changes and POP serum concentrations.

An important question is if the release of POPs from adipose tissue during weight loss could negatively impact other organs and tissues. A limited amount of data is available in humans from weight loss studies. Studies have demonstrated that increased serum POPs due to weight loss are associated with impairments in resting metabolic rates, thermogenesis, and oxidative capacity of skeletal muscle (276, 342-343). Kim et al. reported that individuals undergoing weight loss had improved blood lipid and liver toxicity parameters, but those with the highest serum POP levels had delayed improvement of these metabolic parameters (9). Thus POPs may counteract the beneficial effects of weight loss.

5.2.2. Potential target organs of coplanar PCB induced diabetes

5.2.2.1. Adipose tissue

As previously discussed, we have demonstrated that adipose tissue can be a critical target organ of PCB induced insulin resistance in male C57BL/6 mice (7). It should be noted that our studies only examined molecular pathways of impaired insulin signaling in adipose tissue which were dependent on increased levels of TNF-α expression or reactive oxygen species. Insulin resistance in adipose tissue can also be regulated by lipolysis and relative free fatty acid levels, adiponectin, and other proinflammatory cytokines. Kim et. al. dosed C57BL/6 mice and AhR-KO mice with a single i.p. injection of TCDD (10 μg/kg) and harvested adipose tissue 48 hours later (277). TCDD significantly increased a number of additional proinflammatory adipokines associated with insulin resistance, such as IL-1ß, in wild type mice but not AhR-KO mice, demonstrating that these effects were AhR-dependent. Additionally, the method of POP dosing and the metabolic state of experimental animals appears to be a critical factor in studies of adipose-specific effects of POPs. In a study by Ibrahim et. al. (88), male C57BL/6J mice were fed a HF diet enriched with low concentrations of POPs for 8 weeks and glucose and insulin tolerance were measured. Contrary to findings reported here, obese mice in this study demonstrated significantly impaired glucose and insulin tolerance in response to POP feeding. Taken with the findings presented here, this would suggest that the method POP dosing and metabolic state of experimental animals may have differential effects on POP-induced impairment of glucose homeostasis. Future studies could examine the

kinetics of different types of PCB dosing and how this modulates subsequent PCB metabolism and body partitioning. Other modulators of insulin resistance, influenced by PCBs in adipose tissue could also be explored in future studies.

5.2.2.2. Liver

The liver is also a potential site of insulin resistance, and highly active in the metabolism of coplanar PCBs. While our efforts to quantify hepatic inflammation did not yield significant results (7), it is plausible that coplanar PCBs reduce insulin sensitivity in the liver via other mechanisms, and /or alter hepatic glucose output, contributing to the PCB-77 induced diabetes observed in male mice. A consistent observation of the experiments described in this dissertation were that PCB-77 treated mice demonstrated hepatomegaly due to high levels of ectopic lipid accumulation in the liver (6). This factor alone could have unexplored consequences on overall insulin resistance, given that fatty liver is a condition of other pathologies associated with T2D, such as non-alcoholic fatty liver disease (NALFD).

Attempts were made in these studies to determine the effect of PCB-77 administration on hepatic gluconeogenesis. Surprisingly, RT-PCR results for mRNA abundance of an array of gluconeogenic enzymes, in particular phosphoenol pyruvate carboxykinase (PEPCK), found that expression of all enzymes were decreased in PCB-77 treated animals compared to controls (Figure 5.2), suggesting that enhanced hepatic glucose output was not the mechanism behind impaired glucose tolerance in those mice. This observation

using PCB-77 is consistent with AhR-dependent effects of TCDD reported by others (344-345).

In a recent study, Wang et.al. examined glucose tolerance, insulin resistance, hepatic expression of peroxisome proliferator–activated receptor-α (PPAR-α), and genes affecting glucose metabolism and fatty acid oxidation rhythms in wild-type (WT) versus AhR-deficient [knockout (KO)] mice (87). In this study, KO mice displayed enhanced insulin sensitivity and improved glucose tolerance, accompanied by decreased hepatic peroxisome proliferator activated receptor-α (PPAR-α) and key gluconeogenic and fatty acid oxidation enzymes, indicating a link between AhR signaling and glucose metabolism. The authors further conclude that hepatic activation of the PPAR-α pathway might be a mechanism underlying AhR-mediated insulin resistance. Findings presented here would suggest that the adipocyte AhR is a critical mediator of PCB-induced insulin resistance, as insulin resistance was completely abolished in AhR^{AdQ} mice treated with PCB-77 both acutely and chronically (unfortunately the study by Wang et. al. did not treat experimental mice with either AhR agonists or POPs (87), making comparison to the studies described here difficult).

Nault et.al. utilized livers from chow-fed C57BL/6 mice for gene microarray, 1, 3 and 7 days after a single oral gavage of 30 μg/kg TCDD (85). Administration of TCDD resulted in robust activation of not only genes involved in the xenobiotic response, but also genes associated with steroid, phospholipid, fatty acid, and carbohydrate metabolism. Arzuaga et.al. performed gene DNA analysis on livers from C57BL/6 mice fed diets enriched with high-linoleic acid

oils (20% and 40% as calories), with half of each group exposed to PCB-77 (84). This study demonstrated a significant interaction between dietary fat and PCB exposure, such that deregulated genes were organized into patterns describing the interaction of diet and PCB exposure. Control animals demonstrated a significant high-fat mediated induction of genes associated with fatty acid metabolism, triacylglycerol synthesis and cholesterol catabolism, but this effect was down-regulated in animals exposed to PCB-77. Several of these genes are regulated by PPAR-α and as predicted, changes in PPAR-α gene expression followed the same pattern as described above, demonstrating that dietary fat can interact with environmental pollutants to compromise lipid metabolism. Taken together, the results of these gene microarray studies would suggest not only that there is a distinctive role for the AhR in lipid and glucose metabolism, but that overall nutritional status and the presence of lipids can modulate the interaction between AhR and exogenous ligands. These findings would suggest that the liver could be the subject of future research for its complex roles in PCB detoxification and nutrient metabolism.

5.2.2.3. Skeletal Muscle

Skeletal muscle can be a potential site of insulin resistance, but was not a major focus of these studies utilizing PCB-77, given that detectable amounts of PCB-77 were not found in skeletal muscle from treated mice. Additionally PCB-77 treated mice in our study did not demonstrate differences from controls in skeletal muscle TNF-α protein levels, a well known contributor to insulin resistance. In a recent study by Trumble et.al., muscle and blubber samples were collected from

Weddell seals in Antarctica and measured for 41 different persistent organic pollutants, including PCBs (346). The greatest distribution of POPs were found in blubber and reduced amounts found in skeletal muscle; however the muscle samples demonstrated similar orders of POP prevalence. The author's further suggest that POPs may exert local effects on skeletal muscle via their attraction to intramuscular lipid. An additional possibility is that POPs stored in blubber may be released over time and constitute a source of low-level internal exposure that might chronically damage other tissues including skeletal muscle. The chronic effects of PCB dosing on skeletal muscle were not included in the present study, but could certainly be examined in future studies.

5.2.2.4. Pancreas

The pancreas is a glandular organ in the digestive and endocrine system, producing several important hormones, including insulin, glucagon, pancreatic polypeptide, as well as pancreatic juice which contains digestive enzymes that assist the absorption of nutrients. These enzymes aid in the breakdown of carbohydrates, proteins, and lipids. Given that pancreatic beta cell secretion of insulin is impaired in T2D, PCB toxicities in the pancreas might represent a further area of study utilizing these mouse models. In our LF diet time course study in male C57BL/6 mice, mice were administered two or four oral doses (weeks 1, 2, 9, and 10) of vehicle or PCB-77 (50 mg/kg) and sacrificed at weeks 2, 4, and 12. At weeks 2 and 4, no significant difference in fasting plasma insulin was observed between treatment groups; however at week 12, PCB-77 treated mice had a significant decrease in fasting plasma insulin compared to controls

(Figure 5.3). A possible explanation may be that in longer term PCB dosing studies, coplanar PCBs may exert beta cell damaging effects, or through some other mechanism inhibit insulin secretion. Furthermore, it has been previously reported that pancreatic beta cell lines exposed to TCDD experience high degrees of cytotoxicity in addition to reduced levels of glucose-stimulated insulin secretion (347). Taken together, these studies would suggest that pancreatic beta cell destruction might be an additional mechanism of PCB induced diabetes.

5.2.3. The progression of adipose inflammation in LF time course studies

5.2.3.1. ROS as the initiating event for adipose inflammation

An interesting finding of these studies is that PCBs contribute to a progression of inflammation in adipose tissue. In time course studies of mice fed a LF diet and dosed with vehicle or PCB-77 (50 mg/kg, oral gavage), PCB treated mice experienced an AhR-dependent and adipose-specific increase in TNF-α protein at week 4 (2 weeks post final PCB dose) which was correlated with observed impairments in glucose and insulin tolerance (7). However, no difference was found in adipose TNF-α mRNA abundance in PCB treated mice at week 2 (48 hours post final PCB dose), despite the fact that these animals also exhibited impaired glucose homeostasis. In subsequent studies using resveratrol as a therapeutic against coplanar PCB-induced diabetes, mice sacrificed 48 hours after the last dose of PCB-77 also displayed no difference in adipose TNF-α expression levels; however, these mice displayed glucose intolerance and insulin resistance consistent with previously reported findings (7). These results suggest that acute effects of PCB-77 to increase oxidative stress and impair downstream

insulin signaling in adipose tissue contribute to deficits in glucose homeostasis, and these acute effects were ablated by supplementation with resveratrol (7).

It has been hypothesized by others that AhR activation by synthetic ligands induces oxidative stress in target tissues via the upregulation of xenobiotic metabolizing enzymes such as CYP1A1 (162, 348). CYP1A1 can produce hydrogen peroxide and super oxide anions as a byproduct of xenobiotic catalyzing activity (159, 322-323). However, our results did not define if progressive increases in adipose tissue TNF-α are dependent on initial dysregulation of oxidative stress. An informative experiment could utilize the existing experimental design of PCB induced diabetes with CYP1A1 deficient mice (or adipose-specific CYP1A1 deficient mice) to better understand the mechanisms linking AhR, oxidative stress, and inflammation. Conversely, CYP1A1 si-RNA could be utilized to inhibit enzyme activity *in vitro* and determine effects on PCB-induced regulation of oxidative stress and insulin signaling in adipocytes.

5.2.3.2. Potential role of PCB-77 metabolites

An additional question raised but not directly answered by the present studies are the potential impact of PCB-77 metabolites on the observed impairments in glucose homeostasis and adipose inflammation. It is interesting to note that in both the LF diet time course study as well as the obesity/weight loss time course study there was no difference in adipose TNF-α mRNA abundance when extremely high adipose concentrations of the parent molecule PCB-77 detected in adipose tissue (LF diet time course, week 2). Conversely, the highest levels of

adipose TNF-α expression occurred in tandem with extremely low adipose concentrations of parentPCB-77 (LF time course, week 4; obesity/weight loss time course, week 16) (7). These data suggest that PCB-77 metabolites contribute to adipose tissue inflammation. Unfortunately, in early studies of this project, facilities were not available to quantify PCB-77 metabolites in serum or tissues. It should also be noted that the current mass spectrometry protocol for PCB-77 metabolite detection only screens for hydroxy and dihydroxy metabolites of PCB-77, but not the larger pool of potential metabolites such as glucuronidated or sulfated variants. To more comprehensively address the role of PCB-77 metabolites, future studies could utilize two different approaches. The most direct would be to utilize the aforementioned CYP1A1 deficient mice in the previously established PCB induced diabetes experimental design. However, this approach ignores other metabolizing enzymes in the AhR gene battery and would not control for alternate PCB-77 metabolites. An alternative approach could utilize the existing mouse model of PCB-77 induced diabetes, but instead dose mice with commercially available PCB-77 metabolite analogues (available from Canadian distributors).

5.3. The potential therapeutic benefits of resveratrol supplementation in PCB exposed populations: Insights from resveratrol supplementation mouse model of PCB-77 induced diabetes

5.3.1. Resveratrol intervention in populations with known PCB exposures

The data presented herein suggest that supplementation with resveratrol or potentially other AhR antagonizing nutrients or pharmaceuticals may be a

therapeutic for populations with known coplanar PCB exposures. It should be noted that a limitation of our study is that it only examined effects of resveratrol against acute PCB-77 exposure, and that mice were pre fed resveratrol for one week prior to initiating the study. An experiment with greater implications for comparison to human exposures would be to dose mice with PCB-77 and then supplement the diet with resveratrol, because in reality, humans are unlikely to take large doses of resveratrol as a preventative measure against possible PCB exposure.

5.3.2. General use of resveratrol supplements for weight loss

This study would more generally suggest that resveratrol might be a beneficial supplement for patients post bariatric surgery, or even subjects more generally involved in weight loss programs, given that nearly all individuals are exposed to persistent organic pollutants on a daily basis via food or air (11), and likely have significant adipose stores of PCBs to release with increased lipolysis (23). A relevant follow up experiment would be to dose obese mice with PCB-77, and then feed a resveratrol enriched LF diet to induce weight loss, and determine if resveratrol ameliorates the negative effects of PCBs during weight loss. The ability of PCBs to attenuate the beneficial effects of weight loss might explain in part why most individuals find sustained weight loss incredibly challenging, and why compliance in weight loss programs is generally low. For example, hyperinsulinemia in response to insulin resistance in peripheral tissues can promote feelings of hunger (91, 93), which may potentially derail an individual's

motivation in regards to weight loss. Blunting the effects of POPs released with weight loss might improve weight loss program outcomes.

5.3.3. Pharmaceutical resveratrol analogues and resveratrol use in tandem with other nutritional supplements

Because the levels of resveratrol endogenously available in food are limited, it would be worthwhile to consider the use of pharmaceutical resveratrol analogues, should future research demonstrate that this compound is a clinically relevant strategy for treating PCB exposed populations. A benefit of utilizing pharmaceutical analogues would be that the compound could be conjugated to or formulated as a mixture with other nutrients that might protect against PCB exposure. For example, the fat substitute Olestra has been shown previously to effectively lower adipose burdens of Arochlor in humans (349). Olestra is a fat substitute that is resistant to lipases in the human digestive tract; because of Olestra's fatty acid-like molecular structure, it has been shown that it can create a lipophilic 'sink' in the intestinal lumen and thereby promote enhanced elimination of stored PCBs and organochlorines. A pharmaceutical preparation of resveratrol and Olestra might present a "two-pronged" strategy for protecting against PCB exposure. However, an interesting study by Arguin et.al. compared plasma organochlorine concentrations in subjects on vegan, omnivorous, and a fat-substituted Olestra diet, and found the significant improvement on plasma PCB levels only in the vegan diet group (350). Because the vegan diet group did not gain weight over the study, which could promote organochlorine partitioning from blood to adipose tissue, it is possible that the vegans ate greater amounts of

plants containing antioxidants and fewer PCB laden foods (i.e. high fat dairy and meats) (351). It may also be suggested by this study that a pharmaceutical blend of antioxidants might confer more PCB protective effects than Olestra; however drug forms of antioxidants are unlikely to change food related behaviors, and thus the efficacy of this drug in lowering body burdens of PCB might be limited if users continued to ingest food high in organochlorines. Future research should determine if this is a clinically relevant avenue of potential drug development.

5.4. Adipose AhR: Role in mediating PCB-77 induced diabetes, and a potentially novel role in regulating body weight, body composition, and fat deposition

5.4.1 Limitations of the model of adipocyte-AhR deficiency

5.4.1.1. Non-specific reductions in AhR mRNA abundance

The model of adipocyte-AhR deficiency used in these studies was developed using the Cre/LoxP system, in which exon 2 of the AhR gene was flanked by LoxP sites and mice were bred to transgenic mice expressing Cre recombinase driven by the adiponectin (AdQ) promoter. Adiponectin was originally described as an adipocyte-specific protein and thus the promoter was used by several groups to reduce gene expression in adipocytes. However, as more models using this promoter have been developed, it has become clear that the adiponectin gene is also expressed in other tissues, such as cardiomyocytes. Indeed, mRNA abundance of AhR in AhR^{AdQ} mice was reduced in the heart, but these reductions fell short of statistical significance. Quantification of heart weight to body weight ratios as a measure of cardiac hypertrophy revealed no differences between $AhR^{fl/fl}$ and AhR^{AdQ} mice (Figure 5.4). Additionally, given that

these mice were utilized for glucose and insulin tolerance studies and not examined for cardiovascular parameters *per se*, it is unknown if AhR deficiency in the heart impacted other physiologic measures, but it is unlikely to have influenced study endpoints.

5.4.1.2. Model validation

AhR mRNA abundance was quantified in whole adipose tissue lysates, the adipocyte fraction of collagenase-digested adipose tissue, as well as in subcutaneous adipocytes differentiated from isolated stromal vascular cells. Some level of residual AhR mRNA abundance was detected in all of these adipocyte sources from AhR^{AdQ} mice. This may reflect sub-optimal efficiency of Cre recombinase enzyme activity at the LoxP sites surrounding exon 2 of the AhR gene. Given that there was total deletion of AhR mRNA abundance in adipocyte fractions from visceral adipose tissue, the minimal AhR expression seen in subcutaneous adipocytes at Day 8 might suggest residual receptor turnover.

5.4.2. HF diet induced phenotype in adipose AhR deficient mice

5.4.2.1 Differential expression of AhR in LF versus HF feeding

Preliminary studies in our lab examined if there were diet-induced changes in AhR gene expression in adipose tissue, liver, and kidney. Tissues were taken from C57BL/6 mice fed either a LF or HF diet for three months, and RNA was extracted for subsequent RT-PCR measurements. In liver and kidney, AhR mRNA abundance did not change between LF and HF feeding (Figure 5.5). However, in subcutaneous, epidydmal, and brown adipose tissue, HF feeding

significantly increased AhR mRNA abundance (Figure 5.5). While it should be noted that the sample size for these preliminary studies was small (n = 3-4/group), this data may lend support to the hypothesis that the endogenous AhR ligand is a fatty acid or fatty acid derivative, given that HF feeding would increase the influx of fatty acids to adipose tissue.

5.4.2.2. Arachidonic acid or ecosanoid metabolites as a potential endogenous AhR ligand

The unexpected increased body weight phenotype of HF-fed adipocyte AhR deficient mice may be due to a number or combination of different factors. Currently, the endogenous AhR ligand(s) remains unknown; however, some studies have suggested ligands may include arachidonic acid or one of its eicosanoid products, such as lipoxin A4 or prostaglandin G2 (326, 352). Bui et. al. demonstrated that treatment with TCDD in wild type mice led to a significant increase in liver eicosanoids , but this effect was not observed in whole body AhR deficient mice, demonstrating AhR dependency. The authors concluded that AhR binding with TCDD antagonized receptor interaction with endogenous eicosanoid ligands, leading to an increase of these products in examined tissues (326). Further studies utilizing AhR^{AdQ} mice and lipid profiling techniques may provide novel insight into the endogenous AhR ligand.

5.5. Further exploration of the adipose AhR: Dietary manipulations

In our studies, adipocyte-AhR deficiency was studied under several conditions including lean mice, obese mice, and obese mice undergoing weight loss. The most striking effects of PCB-77 induced impairments on glucose homeostasis

were observed in obese mice undergoing weight loss, suggesting that the effects of adipocyte-AhR deficiency may be most relevant when the kinetics of PCB dosing favor rapid sequestration to expanded adipose stores, and subsequent chronic release with weight loss. Interestingly, effects of adipocyte-AhR deficiency on body weight, body composition, and fat deposition were only seen on the HF diet (60% fat by calories). Dietary manipulations could be performed in future studies to examine how fatty acid composition of the diet impact effects of adipocyte-AhR deficiency.

For example, it has been suggested that the polyunsaturated, omega 6 arachidonic acid or eicosanoid metabolites lipoxin A4 or prostaglandin G2 may be endogenous AhR ligands (35), perhaps leading to the phenotype observed in HF fed AhR^{AdQ} mice. However, it has also been published by Hennig et.al. that omega 6 fatty acids can enhance PCB toxicity, whereas polyunsaturated omega 3 fatty acids can protect against the harmful effects of PCBs (348, 354). AhR^{AdQ} mice and littermate controls could be dosed with PCB-77 during HF feeding of diets with modified ratios of omega 3 and omega 6 polyunsaturated fatty acids, and then tested for glucose and insulin tolerance following a weight loss period. By this method, a dose-response to arachidonic acid in adipocyte-AhR deficient mice could be observed during obesity, and conversely it could be determined if omega 3 fatty acids conferred a protective effect against PCB-77 induced diabetes during weight loss in $AhR^{fl/fl}$ mice.

5.6. Additional future directions

5.6.1. The role of noncoplanar PCBs in the development of diabetes

An important question raised by this research is the effect that noncoplanar PCBs might have on the development of T2D and obesity, especially given that noncoplanar PCBs are also positively associated with T2D in epidemiology studies (271, 355-357). Mechanistic studies of these compounds would likely prove challenging given that noncoplanar PCBs can activate both the CAR and PXR signaling pathways (358). PXR activation by noncoplanar PCBs might be a more critical pathway in the development of PCB-induced diabetes than the CAR pathway, given that studies have shown that CAR activation during HF feeding improves insulin sensitivity (359), whereas PXR ablation alleviates diet induced and genetic obesity and insulin resistance in mice (360). Furthermore, studies in our lab using 3T3-L1 adipocytes demonstrated that exposure to noncoplanar PCB-153 had no effect on inflammation or insulin-stimulated glucose uptake (6)(Figure 5.6). This would suggest that noncoplanar PCBs might exert their effects on organs other than adipose tissue, or that this particular cell line is not responsive to PCB-153. Finally, Shi et.al. have reported that the metabolic effects of PCB-153 are highly dependent on macronutrient interactions during HF feeding (361), which might be an additional complicating factor in studies of this nature.

5.6.2. The role of mixtures of persistent organic pollutants in the development of diabetes

A limitation of this data is that only two coplanar PCB congeners were studied; in reality, it is highly unusual for human subjects to be exposed to only one congener of PCB. In fact, given that nearly all individuals are exposed to a variety of persistent organic pollutants on a daily basis via food or air (11), and that obesity is rapidly increasing in the U.S. (362-363), it is likely that many people have significant and variable distributions of an assortment of lipophilic POPs stored in adipose tissue. Ibrahim et. al. pioneered the use of a “POP diet” (88), in which Atlantic salmon were fed fish feed enriched with low concentrations of POPs. Salmon were filleted after 8 weeks of feeding, and fillets were homogenized and fish oil extracted. Fish oil extracts were added to purified rodent diets (72% kcal as fat), which were subsequently fed to male C57BL/6J mice for 8 weeks. Interestingly, obese mice in this chronic feeding study demonstrated dramatically impaired glucose and insulin tolerance in response to POP exposure compared to controls. This finding, taken with the findings described in this dissertation, are suggestive that the method of POP exposure and the metabolic state of experimental mice have a significant impact on the kinetics of POP body distribution and / or metabolism and the POP-induced impairment of glucose and insulin tolerance. Experiments utilizing the “POP diet” developed by Ibrahim et. al. and examining a variety of metabolic states would be beneficial in determining the efficacy or potential toxicity of resveratrol supplementation in populations exposed to POP mixtures. Furthermore, feeding

a similar diet to *AhR*^{AdQ} mice and littermate controls could give a more complete understanding of the overall importance of the adipocyte AhR in mediating PCB-induced diabetes during chronic POP exposure through feeding.

5.6.3. Potential gender differences in development of PCB or POP associated diabetes

Some epidemiology studies, including the Anniston community survey by Silverstone et.al., have indicated that PCB exposure has a stronger positive association with development of T2D in females than males (158, 364-365); however, other clinical studies show no impact of gender on the positive correlation between POP exposure and diabetes risk or severity (268, 271, 290, 366-368). Whether gender-specific responses to PCB exposure are due to interaction with additional environmental or genetic factors remains unknown. Furthermore, it is possible that there are gender differences in AhR expression, activation, activity, gene regulation, signaling pathways, or receptor turnover, which could present an alternate avenue of future study. However, it is more likely that gender differences in response to PCBs stem from AhR crosstalk with other steroid receptors, particularly by AhR induced inhibition of the estrogen receptor (369-370). We repeated the experimental design using two oral doses of either vehicle or PCB-77 (50 mg/kg) administered to female LF-fed mice, and quantified glucose and insulin tolerance within 48 hours of the second dose (Figure 5.7A and 5.7B, respectively). At 48 hours post gavage, females exposed to PCB-77 had a more robust impairment to glucose tolerance than that observed in males; conversely, females had no impairment of insulin tolerance,

contrary to what has previously been observed in males (7). While not having significantly different body weights, PCB-77 treated females had greater fat mass than controls which was associated with enlarged visceral and subcutaneous adipose depots, an effect that was not observed in male C57BL/6 mice in experiments described in this dissertation (Figure 5.8). Gender differences relating to the AhR represent an important and clinically relevant direction for future research.

5.7 Clinical Implications

The data presented here raise broad clinical implications. Firstly, our data suggest that supplementation with resveratrol or potentially other AhR antagonizing nutrients or pharmaceuticals may be a therapeutic for populations with known coplanar PCB exposures. It should be noted that our study only examined effects of resveratrol to protect against acute PCB-77 exposure, and that mice were pre fed resveratrol for one week prior to initiating the study. An important and informative experiment would be to dose mice with PCB-77 and then supplement the diet with resveratrol, as this would more closely mirror the therapeutic potential of the compound in subjects with known, accidental exposures to PCBs. As previously noted, it is unusual for human subjects to be exposed to only one congener of PCB; experiments examining resveratrol supplementation utilizing the “POP diet” developed by Ibrahim et. al. (88) would be beneficial in determining the efficacy or potential toxicity of resveratrol in populations exposed to POP mixtures. Secondly, it would suggest that resveratrol might be a beneficial supplement for patients post bariatric surgery, or

even subjects more generally involved in weight loss programs, given that nearly all individuals are exposed to persistent organic pollutants on a daily basis via food or air (11), and likely have significant adipose stores of POPs to release with increased lipolysis (7). An interesting follow up experiment would be to dose obese mice with PCB-77, and then feed resveratrol enriched LF diet to induce weight loss, and determine if resveratrol ameliorates the negative effects of PCBs during weight loss. The ability of POPs to attenuate the beneficial effects of weight loss might explain in part why most individuals find sustained weight loss incredibly challenging, and why compliance in weight loss programs is generally low. For example, hyperinsulinemia in response to insulin resistance in peripheral tissues can promote feelings of hunger (91, 93), which may potentially derail an individual's motivation in regards to weight loss. Blunting the effects of POPs released with weight loss might improve weight loss program compliance and outcomes. Finally, study in greater detail of adipocyte AhR regulation of body weight, body mass, and fat deposition may have significant implications both clinically or in pharmaceutical research.

5.8 Concluding remarks

Overall these studies suggest a critical role of coplanar PCB-bound AhRs on adipocytes to promote insulin resistance in adipose tissue during lean and weight loss conditions, and a more general and novel role in regulating body mass and fat deposition. The consequences on glucose homeostasis of PCB-77 acting through adipocyte AhRs are most prominent in lean/weight loss conditions and are absent in the setting of obesity, lending further credence to the hypothesis

that lipophilic pollutants are sequestered to lipid pools during obesity and freed during weight loss. Future studies should explore resveratrol supplementation in the weight loss model of PCB-77 induced diabetes and investigate the feasibility of clinical resveratrol supplementation studies in PCB exposed Kentucky populations. Additionally, the impact of adipocyte AhR deficiency on body weight, fat mass, and fat deposition should be studied in greater detail. Furthermore, this model of adipocyte AhR deficiency may provide important clues to the identity of the endogenous AhR ligand, which would perhaps have far reaching clinical implications.

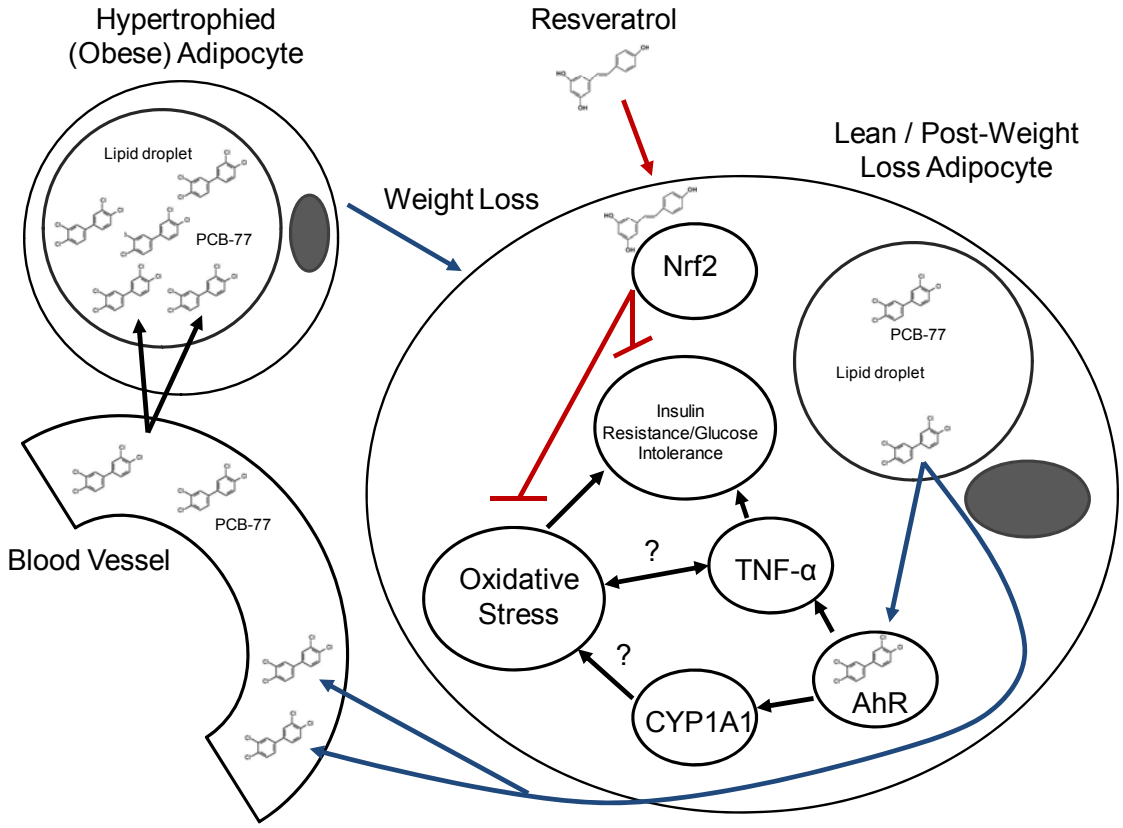

Figure 5.1. Summary of findings: Proposed mechanism of PCB-77 induced adipocyte mediated T2D and inhibition with resveratrol. PCB-77 is transported in blood and highly attracted to expanded lipid pools present in hypertrophied adipocytes during obesity. During lean or weight loss conditions (blue pathway), PCB-77 is released from adipocyte lipid droplets with lipolysis, and returns to blood to act systemically and / or act at the cytosolic adipocyte AhR. AhR activation leads to increased expression of CYP1A1 and TNF-α, and the generation of reactive oxygen species. The culmination of these changes induces glucose intolerance and insulin resistance in adipocytes. Resveratrol stimulates Nrf2 signaling to suppress oxidative stress and restore insulin sensitivity and glucose tolerance to adipocytes (red pathway).

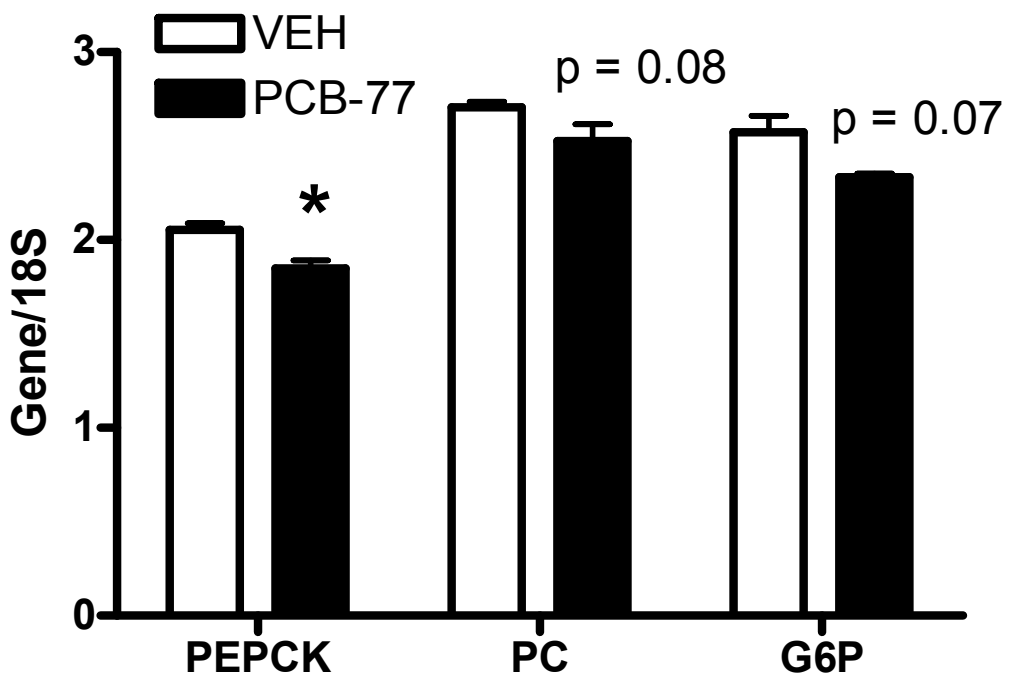

Figure 5.2. PCB-77 treatment decreases hepatic mRNA abundance of gluconeogenic enzymes. Mice were administered vehicle (VEH) or PCB-77 (50 mg/kg, two divided doses during weeks 1 and 2). At week 4, hepatic mRNA abundance of phosphoenolpyruvate carboxykinase (PEPCK), pyruvate carboxylase (PC), and glucose 6-phosphatase (G6P) were measured. Genes were normalized to reference gene 18S. Data are mean ± SEM from n = 4 mice/group. *, $P < 0.05$ compared to VEH within gene of interest.

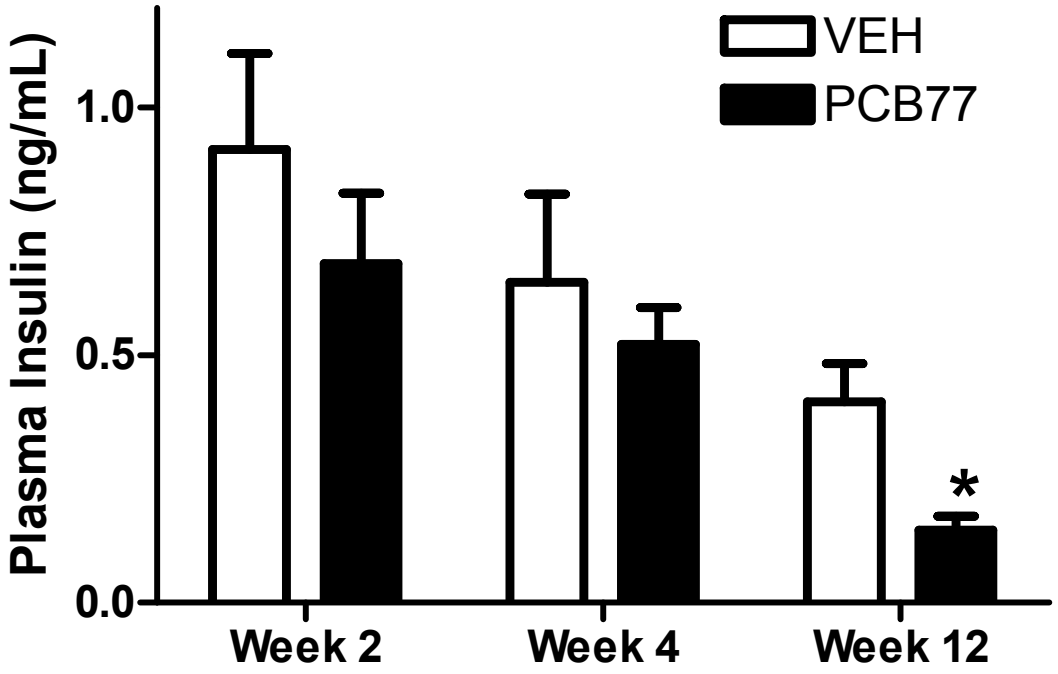

Figure 5.3. PCB-77 treatment decreases fasted plasma insulin in LF fed mice. Mice were administered vehicle (VEH) or PCB-77 (50 mg/kg, two divided doses during weeks 1 and 2, a second set of 2 doses during weeks 9 and 10 for mice studied at 12 weeks). At 2, 4 or 12 weeks, mice in each treatment group were fasted for 4 hours prior to sacrifice, and plasma was collected for commercial insulin ELISA. Data are mean ± SEM from n $\geq$ 5 mice/group. *, P < 0.05 compared to VEH within time point.

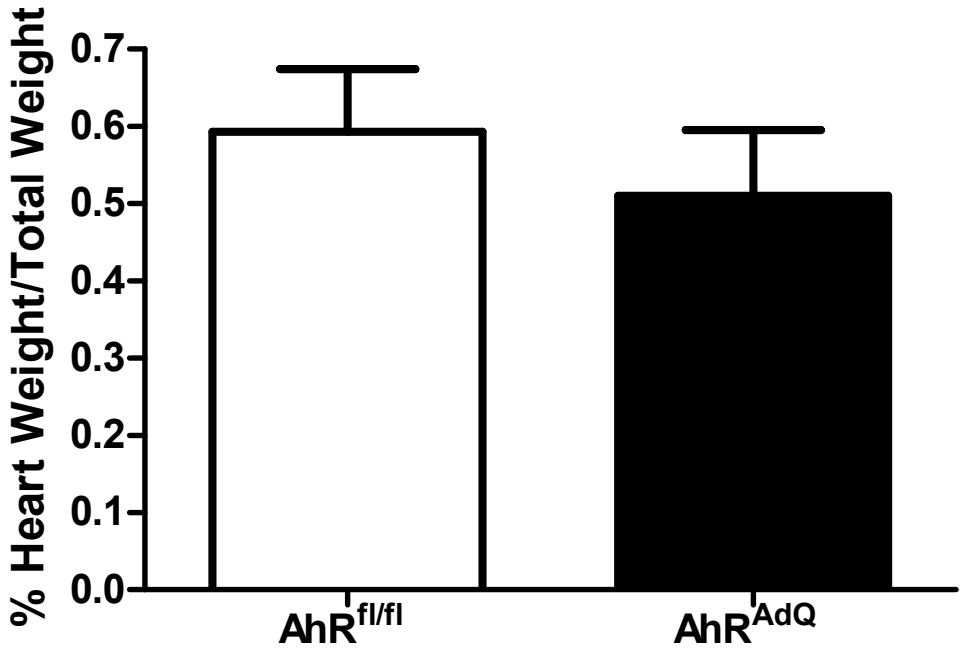

Figure 5.4. Adipocyte AhR deficiency does not affect heart weight. Hearts were harvested from two month old, male *AhR*^{AdQ} mice and littermate controls. Data are mean ± SEM from n = 6 to 8 mice/group.

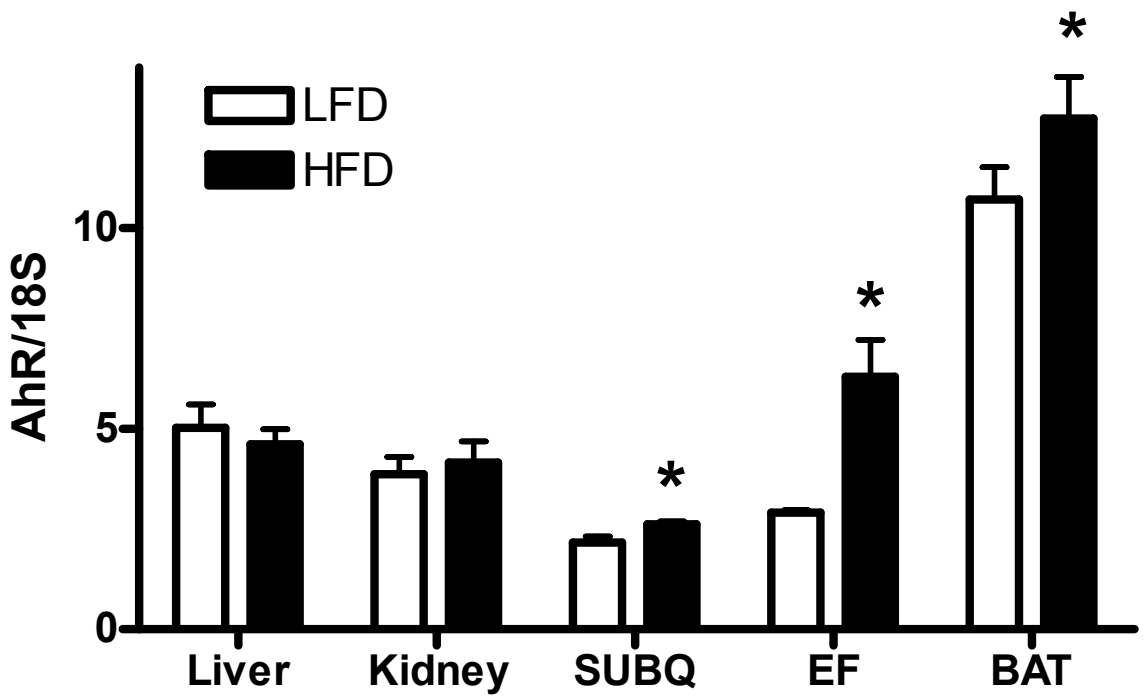

Figure 5.5. Differential expression of AhR in adipose tissue during LF vs. HF feeding. Male C57BL/6 mice were fed either LFD (10% kcal as fat) or HFD (60% kcal as fat) for 3 months. AhR mRNA abundance was quantified in liver, kidney, subcutaneous adipose tissue (SUBQ), epidydmal adipose tissue (EF), and brown adipose tissue (BAT). Genes were normalized to reference gene 18S. Data are mean ± SEM from n = 3 to 4 mice/group. *, $P < 0.05$ compared to VEH within tissue type.

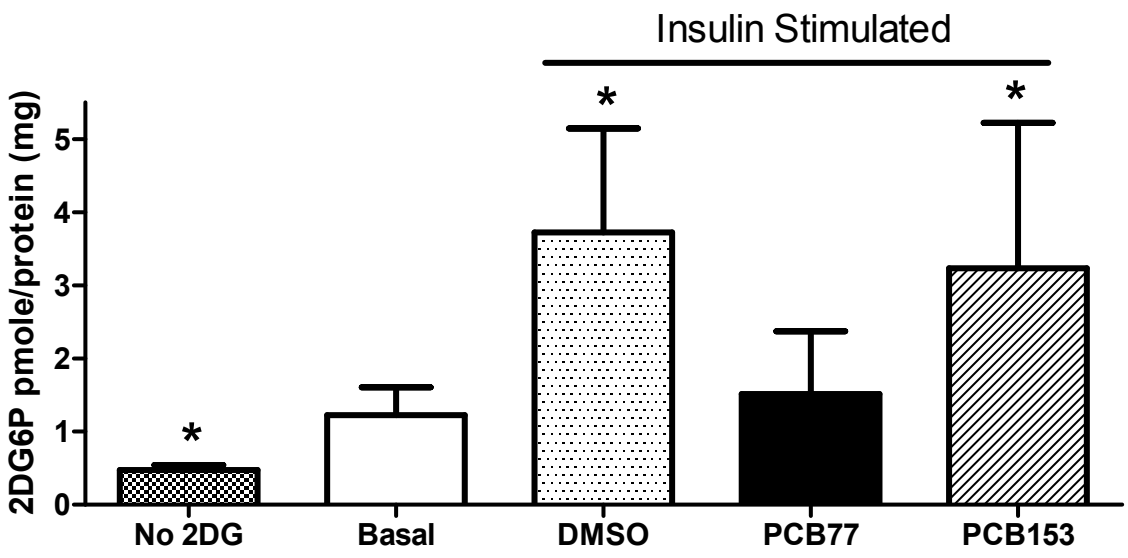

Figure 5.6. PCB-153 has no effect on insulin-stimulated glucose uptake in 3T3-L1 adipocytes. Coplanar PCB-77 abolishes insulin-stimulated 2DG uptake in 3T3-L1 adipocytes, while PCB-153 has no effect on insulin-stimulated glucose uptake. Data are mean ± SEM from n = 2 experimental triplicates. *, $P<0.05$ compared to basal.

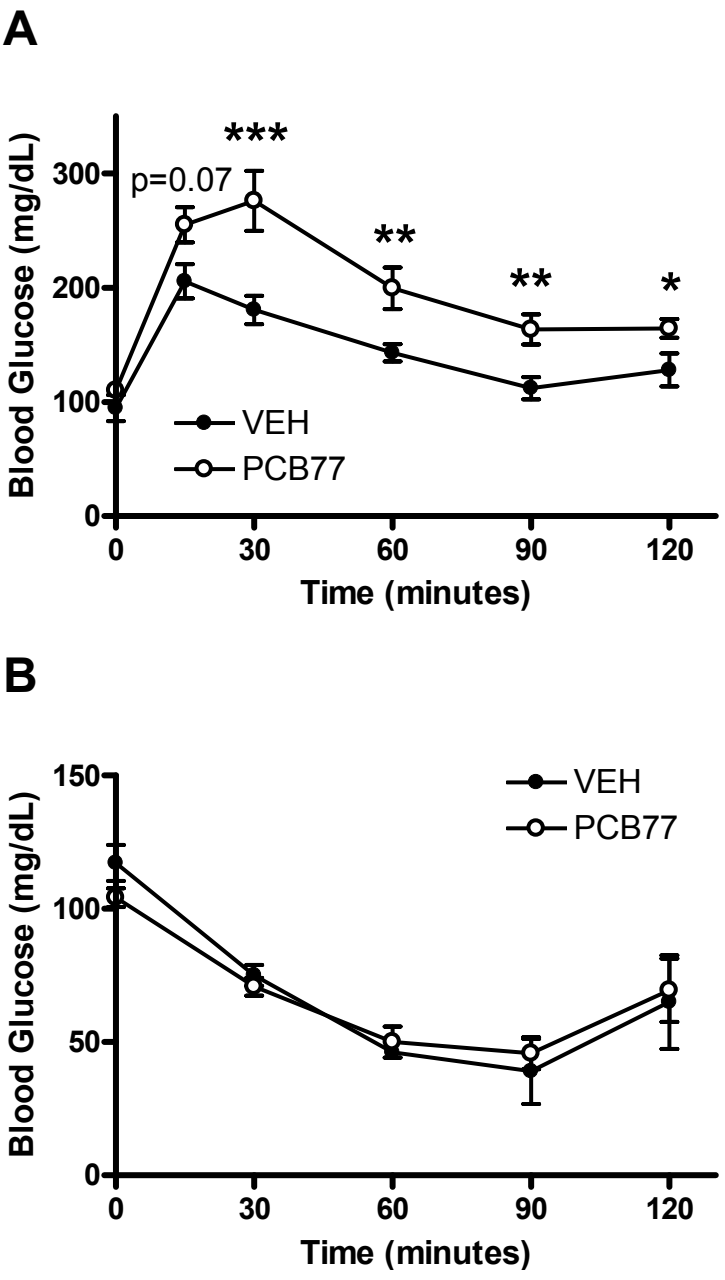

Figure 5.7. PCB-77 impairs glucose tolerance (A) in female C57BL/6 mice, but has no effect on insulin tolerance (B). Mice were administered vehicle (VEH) or PCB-77 (50 mg/kg, two divided doses during weeks 1 and 2). 48 hours post-second gavage administration, mice in each treatment group were administered a bolus of glucose (20% glucose, A) or insulin (0.0125 μM/gm body

weight, B) and blood glucose concentrations were quantified. Data are mean ± SEM from n = 5 mice/group. *, $P < 0.05$ compared to VEH within time point. **, $P < 0.01$ compared to VEH within time point. ***, $P < 0.001$ compared to VEH within time point.

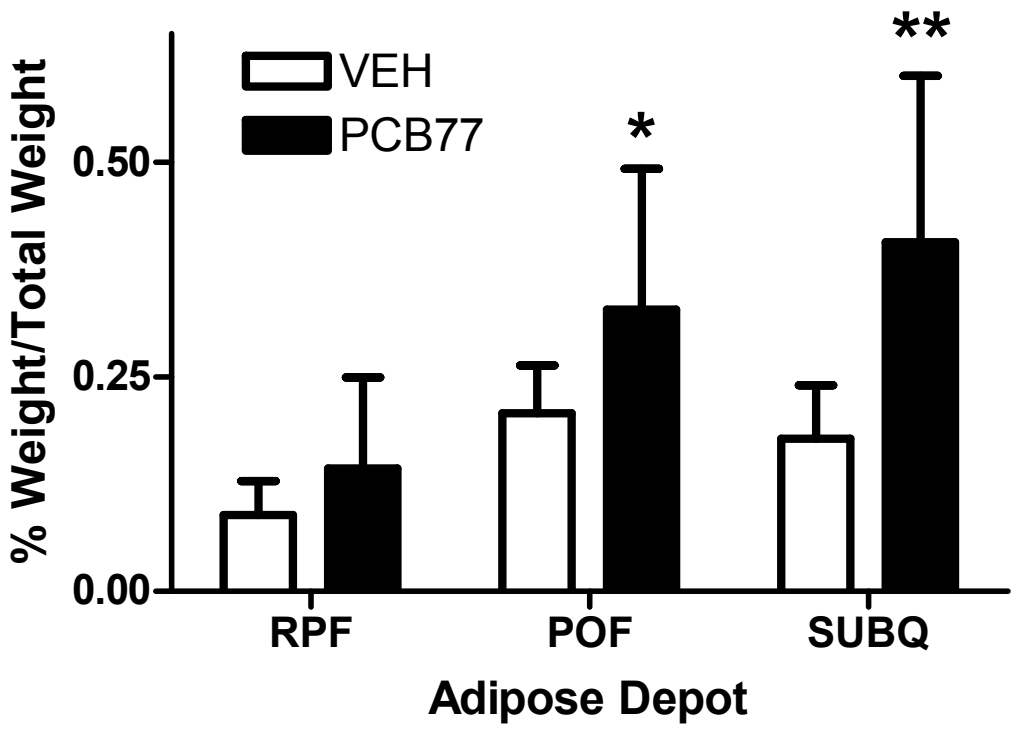

Figure 5.8. PCB-77 increases adipose depot weight of female C57BL/6 mice. Mice were administered vehicle (VEH) or PCB-77 (50 mg/kg, two divided doses during weeks 1 and 2). Mice were sacrificed at week 4 and adipose depot weights in retroperitoneal fat (RPF), periovarian fat (POF), and subcutaneous adipose tissue (SUBQ) were quantified. Data are mean ± SEM from n = 10 mice/group. *, $P < 0.05$ compared to VEH within tissue type.

REFERENCES

1. Fisher BE. Most unwanted. Environ Health Perspect. 1999 Jan;107:A18-23.

2. Smith MA. Reassessment of the carcinogenicity of polychlorinated biphenyls (PCBs). J Toxicol Environ Health. 1997 Apr 25;50:567-79.

3. Kramer S, Hikel SM, Adams K, Hinds D, Moon K. Current status of the epidemiologic evidence linking polychlorinated biphenyls and non-hodgkin lymphoma, and the role of immune dysregulation. Environ Health Perspect. 2012 Aug;120:1067-75.

4. Polychlorinated biphenyls (PCBs). Rep Carcinog. 2004;11:III218-9.

5. Boate A. Chemistry of PCBs. 2004.

6. Arsenescu V, Arsenescu RI, King V, Swanson H, Cassis LA. Polychlorinated biphenyl-77 induces adipocyte differentiation and proinflammatory adipokines and promotes obesity and atherosclerosis. Environ Health Perspect. 2008 Jun;116:761-8.

7. Baker NA, Karounos M, English V, Fang J, Wei Y, Stromberg A, Sunkara M, Morris AJ, Swanson HI, Cassis LA. Coplanar polychlorinated biphenyls impair glucose homeostasis in lean C57BL/6 mice and mitigate beneficial effects of weight loss on glucose homeostasis in obese mice. Environ Health Perspect. 2013 Jan;121:105-10.

8. Kodavanti PR, Ward TR, Derr-Yellin EC, Mundy WR, Casey AC, Bush B, Tilson HA. Congener-specific distribution of polychlorinated biphenyls in brain

regions, blood, liver, and fat of adult rats following repeated exposure to Aroclor 1254. Toxicol Appl Pharmacol. 1998 Dec;153:199-210.

9. Kim MJ, Marchand P, Henegar C, Antignac JP, Alili R, Poitou C, Bouillot JL, Basdevant A, Le Bizec B, et al. Fate and complex pathogenic effects of dioxins and polychlorinated biphenyls in obese subjects before and after drastic weight loss. Environ Health Perspect. 2011 Mar;119:377-83.

10. Van den Berg M, Birnbaum L, Bosveld AT, Brunstrom B, Cook P, Feeley M, Giesy JP, Hanberg A, Hasegawa R, et al. Toxic equivalency factors (TEFs) for PCBs, PCDDs, PCDFs for humans and wildlife. Environ Health Perspect. 1998 Dec;106:775-92.

11. Schecter A, Colacino J, Haffner D, Patel K, Opel M, Papke O, Birnbaum L. Perfluorinated compounds, polychlorinated biphenyls, and organochlorine pesticide contamination in composite food samples from Dallas, Texas, USA. Environ Health Perspect. 2010 Jun;118:796-802.

12. Hayward D, Wong J, Krynitsky AJ. Polybrominated diphenyl ethers and polychlorinated biphenyls in commercially wild caught and farm-raised fish fillets in the United States. Environ Res. 2007 Jan;103:46-54.

13. Wong MH, Armour MA, Naidu R, Man M. Persistent toxic substances: sources, fates and effects. Rev Environ Health. 2012 Oct 17;0:1-7.

14. Vigh E, Colombo A, Benfenati E, Hakansson H, Berglund M, Bodis J, Garai J. Individual breast milk consumption and exposure to PCBs and PCDD/Fs in Hungarian infants: A time-course analysis of the first three months of lactation. Sci Total Environ. 2013 Feb 21;449C:336-44.

15. Wong TW, Wong AH, Nelson EA, Qiu H, Ku SY. Levels of PCDDs, PCDFs, and dioxin-like PCBs in human milk among Hong Kong mothers. Sci Total Environ. 2012 Aug 29.

16. Tsukimori K, Uchi H, Tokunaga S, Yasukawa F, Chiba T, Kajiwara J, Hirata T, Furue M. Blood levels of PCDDs, PCDFs, and coplanar PCBs in Yusho mothers and their descendants: association with fetal Yusho disease. Chemosphere. 2013 Feb;90:1581-8.

17. Masuda Y. [Toxic effects of PCB/PCDF to human observed in Yusho and other poisonings]. Fukuoka Igaku Zasshi. 2009 May;100:141-55.

18. Bertrand KA, Spiegelman D, Aster JC, Altshul LM, Korrick SA, Rodig SJ, Zhang SM, Kurth T, Laden F. Plasma organochlorine levels and risk of non-Hodgkin lymphoma in a cohort of men. Epidemiology. 2010 Mar;21:172-80.

19. Hardell K, Carlberg M, Hardell L, Bjornfoth H, Ericson Jogsten I, Eriksson M, Van Bavel B, Lindstrom G. Concentrations of organohalogen compounds and titres of antibodies to Epstein-Barr virus antigens and the risk for non-Hodgkin lymphoma. Oncol Rep. 2009 Jun;21:1567-76.

20. Nesaretnam K, Corcoran D, Dils RR, Darbre P. 3,4,3',4'-Tetrachlorobiphenyl acts as an estrogen in vitro and in vivo. Mol Endocrinol. 1996 Aug;10:923-36.

21. Donato F, Zani C. [Chronic exposure to organochlorine compounds and health effects in adults: cancer, non-Hodgkin lymphoma. Review of literature]. Ann Ig. 2010 Jul-Aug;22:357-67.

22. Gray MN, Aylward LL, Keenan RE. Relative cancer potencies of selected dioxin-like compounds on a body-burden basis: comparison to current toxic equivalency factors (TEFs). J Toxicol Environ Health A. 2006 May;69:907-17.

23. Thayer KA, Heindel JJ, Bucher JR, Gallo MA. Role of environmental chemicals in diabetes and obesity: a National Toxicology Program workshop review. Environ Health Perspect. 2012 Jun;120:779-89.

24. Burbach KM, Poland A, Bradfield CA. Cloning of the Ah-receptor cDNA reveals a distinctive ligand-activated transcription factor. Proc Natl Acad Sci U S A. 1992 Sep 1;89:8185-9.

25. Fukunaga BN, Probst MR, Reisz-Porszasz S, Hankinson O. Identification of functional domains of the aryl hydrocarbon receptor. J Biol Chem. 1995 Dec 8;270:29270-8.

26. Jones S. An overview of the basic helix-loop-helix proteins. Genome Biol. 2004;5:226.

27. Ema M, Sogawa K, Watanabe N, Chujoh Y, Matsushita N, Gotoh O, Funae Y, Fujii-Kuriyama Y. cDNA cloning and structure of mouse putative Ah receptor. Biochem Biophys Res Commun. 1992 Apr 15;184:246-53.

28. Coumailleau P, Poellinger L, Gustafsson JA, Whitelaw ML. Definition of a minimal domain of the dioxin receptor that is associated with Hsp90 and maintains wild type ligand binding affinity and specificity. J Biol Chem. 1995 Oct 20;270:25291-300.

29. Goryo K, Suzuki A, Del Carpio CA, Siizaki K, Kuriyama E, Mikami Y, Kinoshita K, Yasumoto K, Rannug A, et al. Identification of amino acid residues

in the Ah receptor involved in ligand binding. Biochem Biophys Res Commun. 2007 Mar 9;354:396-402.

30. Kumar MB, Ramadoss P, Reen RK, Vanden Heuvel JP, Perdew GH. The Q-rich subdomain of the human Ah receptor transactivation domain is required for dioxin-mediated transcriptional activity. J Biol Chem. 2001 Nov 9;276:42302-10.

31. Denison MS, Pandini A, Nagy SR, Baldwin EP, Bonati L. Ligand binding and activation of the Ah receptor. Chem Biol Interact. 2002 Sep 20;141:3-24.

32. Denison MS, Nagy SR. Activation of the aryl hydrocarbon receptor by structurally diverse exogenous and endogenous chemicals. Annu Rev Pharmacol Toxicol. 2003;43:309-34.

33. Adachi J, Mori Y, Matsui S, Takigami H, Fujino J, Kitagawa H, Miller CA, 3rd, Kato T, Saeki K, Matsuda T. Indirubin and indigo are potent aryl hydrocarbon receptor ligands present in human urine. J Biol Chem. 2001 Aug 24;276:31475-8.

34. Sinal CJ, Bend JR. Aryl hydrocarbon receptor-dependent induction of cyp1a1 by bilirubin in mouse hepatoma hepa 1c1c7 cells. Mol Pharmacol. 1997 Oct;52:590-9.

35. Seidel SD, Winters GM, Rogers WJ, Ziccardi MH, Li V, Keser B, Denison MS. Activation of the Ah receptor signaling pathway by prostaglandins. J Biochem Mol Toxicol. 2001;15:187-96.

36. McMillan BJ, Bradfield CA. The aryl hydrocarbon receptor is activated by modified low-density lipoprotein. Proc Natl Acad Sci U S A. 2007 Jan 23;104:1412-7.

37. Denis M, Cuthill S, Wikstrom AC, Poellinger L, Gustafsson JA. Association of the dioxin receptor with the Mr 90,000 heat shock protein: a structural kinship with the glucocorticoid receptor. Biochem Biophys Res Commun. 1988 Sep 15;155:801-7.

38. Perdew GH. Association of the Ah receptor with the 90-kDa heat shock protein. J Biol Chem. 1988 Sep 25;263:13802-5.

39. Cox MB, Miller CA, 3rd. Cooperation of heat shock protein 90 and p23 in aryl hydrocarbon receptor signaling. Cell Stress Chaperones. 2004 Mar;9:4-20.

40. Kazlauskas A, Poellinger L, Pongratz I. Evidence that the co-chaperone p23 regulates ligand responsiveness of the dioxin (Aryl hydrocarbon) receptor. J Biol Chem. 1999 May 7;274:13519-24.

41. Kazlauskas A, Sundstrom S, Poellinger L, Pongratz I. The hsp90 chaperone complex regulates intracellular localization of the dioxin receptor. Mol Cell Biol. 2001 Apr;21:2594-607.

42. Shetty PV, Bhagwat BY, Chan WK. P23 enhances the formation of the aryl hydrocarbon receptor-DNA complex. Biochem Pharmacol. 2003 Mar 15;65:941-8.

43. Meyer BK, Pray-Grant MG, Vanden Heuvel JP, Perdew GH. Hepatitis B virus X-associated protein 2 is a subunit of the unliganded aryl hydrocarbon

receptor core complex and exhibits transcriptional enhancer activity. Mol Cell Biol. 1998 Feb;18:978-88.

44. Ma Q, Whitlock JP, Jr. A novel cytoplasmic protein that interacts with the Ah receptor, contains tetratricopeptide repeat motifs, and augments the transcriptional response to 2,3,7,8-tetrachlorodibenzo-p-dioxin. J Biol Chem. 1997 Apr 4;272:8878-84.

45. Carver LA, Bradfield CA. Ligand-dependent interaction of the aryl hydrocarbon receptor with a novel immunophilin homolog in vivo. J Biol Chem. 1997 Apr 25;272:11452-6.

46. Pongratz I, Mason GG, Poellinger L. Dual roles of the 90-kDa heat shock protein hsp90 in modulating functional activities of the dioxin receptor. Evidence that the dioxin receptor functionally belongs to a subclass of nuclear receptors which require hsp90 both for ligand binding activity and repression of intrinsic DNA binding activity. J Biol Chem. 1992 Jul 5;267:13728-34.

47. Whitelaw M, Pongratz I, Wilhelmsson A, Gustafsson JA, Poellinger L. Ligand-dependent recruitment of the Arnt coregulator determines DNA recognition by the dioxin receptor. Mol Cell Biol. 1993 Apr;13:2504-14.

48. Carver LA, LaPres JJ, Jain S, Dunham EE, Bradfield CA. Characterization of the Ah receptor-associated protein, ARA9. J Biol Chem. 1998 Dec 11;273:33580-7.

49. Petrulis JR, Hord NG, Perdew GH. Subcellular localization of the aryl hydrocarbon receptor is modulated by the immunophilin homolog hepatitis B virus X-associated protein 2. J Biol Chem. 2000 Dec 1;275:37448-53.

50. Petrulis JR, Kusnadi A, Ramadoss P, Hollingshead B, Perdew GH. The hsp90 Co-chaperone XAP2 alters importin beta recognition of the bipartite nuclear localization signal of the Ah receptor and represses transcriptional activity. J Biol Chem. 2003 Jan 24;278:2677-85.

51. Pollenz RS, Barbour ER. Analysis of the complex relationship between nuclear export and aryl hydrocarbon receptor-mediated gene regulation. Mol Cell Biol. 2000 Aug;20:6095-104.

52. Whitelaw ML, Gottlicher M, Gustafsson JA, Poellinger L. Definition of a novel ligand binding domain of a nuclear bHLH receptor: co-localization of ligand and hsp90 binding activities within the regulable inactivation domain of the dioxin receptor. EMBO J. 1993 Nov;12:4169-79.

53. Hoffman EC, Reyes H, Chu FF, Sander F, Conley LH, Brooks BA, Hankinson O. Cloning of a factor required for activity of the Ah (dioxin) receptor. Science. 1991 May 17;252:954-8.

54. Probst MR, Reisz-Porszasz S, Agbunag RV, Ong MS, Hankinson O. Role of the aryl hydrocarbon receptor nuclear translocator protein in aryl hydrocarbon (dioxin) receptor action. Mol Pharmacol. 1993 Sep;44:511-8.

55. Reyes H, Reisz-Porszasz S, Hankinson O. Identification of the Ah receptor nuclear translocator protein (Arnt) as a component of the DNA binding form of the Ah receptor. Science. 1992 May 22;256:1193-5.

56. Dolwick KM, Swanson HI, Bradfield CA. In vitro analysis of Ah receptor domains involved in ligand-activated DNA recognition. Proc Natl Acad Sci U S A. 1993 Sep 15;90:8566-70.

57. Shen ES, Whitlock JP, Jr. Protein-DNA interactions at a dioxin-responsive enhancer. Mutational analysis of the DNA-binding site for the liganded Ah receptor. J Biol Chem. 1992 Apr 5;267:6815-9.

58. Lusska A, Shen E, Whitlock JP, Jr. Protein-DNA interactions at a dioxin-responsive enhancer. Analysis of six bona fide DNA-binding sites for the liganded Ah receptor. J Biol Chem. 1993 Mar 25;268:6575-80.

59. Yao EF, Denison MS. DNA sequence determinants for binding of transformed Ah receptor to a dioxin-responsive enhancer. Biochemistry. 1992 Jun 2;31:5060-7.

60. Bacsi SG, Reisz-Porszasz S, Hankinson O. Orientation of the heterodimeric aryl hydrocarbon (dioxin) receptor complex on its asymmetric DNA recognition sequence. Mol Pharmacol. 1995 Mar;47:432-8.

61. Swanson HI, Chan WK, Bradfield CA. DNA binding specificities and pairing rules of the Ah receptor, ARNT, and SIM proteins. J Biol Chem. 1995 Nov 3;270:26292-302.

62. Boutros PC, Moffat ID, Franc MA, Tijet N, Tuomisto J, Pohjanvirta R, Okey AB. Dioxin-responsive AHRE-II gene battery: identification by phylogenetic footprinting. Biochem Biophys Res Commun. 2004 Aug 27;321:707-15.

63. Sogawa K, Numayama-Tsuruta K, Takahashi T, Matsushita N, Miura C, Nikawa J, Gotoh O, Kikuchi Y, Fujii-Kuriyama Y. A novel induction mechanism of the rat CYP1A2 gene mediated by Ah receptor-Arnt heterodimer. Biochem Biophys Res Commun. 2004 Jun 4;318:746-55.

64. Hahn ME, Karchner SI, Evans BR, Franks DG, Merson RR, Lapseritis JM. Unexpected diversity of aryl hydrocarbon receptors in non-mammalian vertebrates: insights from comparative genomics. J Exp Zool A Comp Exp Biol. 2006 Sep 1;305:693-706.

65. Duncan DM, Burgess EA, Duncan I. Control of distal antennal identity and tarsal development in Drosophila by spineless-aristapedia, a homolog of the mammalian dioxin receptor. Genes Dev. 1998 May 1;12:1290-303.

66. Emmons RB, Duncan D, Estes PA, Kiefel P, Mosher JT, Sonnenfeld M, Ward MP, Duncan I, Crews ST. The spineless-aristapedia and tango bHLH-PAS proteins interact to control antennal and tarsal development in Drosophila. Development. 1999 Sep;126:3937-45.

67. Tijet N, Boutros PC, Moffat ID, Okey AB, Tuomisto J, Pohjanvirta R. Aryl hydrocarbon receptor regulates distinct dioxin-dependent and dioxin-independent gene batteries. Mol Pharmacol. 2006 Jan;69:140-53.

68. Gasiewicz TA, Singh KP, Casado FL. The aryl hydrocarbon receptor has an important role in the regulation of hematopoiesis: implications for benzene-induced hematopoietic toxicity. Chem Biol Interact. 2010 Mar 19;184:246-51.

69. Kiss EA, Vonarbourg C, Kopfmann S, Hobeika E, Finke D, Esser C, Diefenbach A. Natural aryl hydrocarbon receptor ligands control organogenesis of intestinal lymphoid follicles. Science. 2011 Dec 16;334:1561-5.

70. Li Y, Innocentin S, Withers DR, Roberts NA, Gallagher AR, Grigorieva EF, Wilhelm C, Veldhoen M. Exogenous stimuli maintain intraepithelial lymphocytes via aryl hydrocarbon receptor activation. Cell. 2011 Oct 28;147:629-40.

71. Quintana FJ, Basso AS, Iglesias AH, Korn T, Farez MF, Bettelli E, Caccamo M, Oukka M, Weiner HL. Control of T(reg) and T(H)17 cell differentiation by the aryl hydrocarbon receptor. Nature. 2008 May 1;453:65-71.

72. Akahoshi E, Yoshimura S, Ishihara-Sugano M. Over-expression of AhR (aryl hydrocarbon receptor) induces neural differentiation of Neuro2a cells: neurotoxicology study. Environ Health. 2006;5:24.

73. Walisser JA, Glover E, Pande K, Liss AL, Bradfield CA. Aryl hydrocarbon receptor-dependent liver development and hepatotoxicity are mediated by different cell types. Proc Natl Acad Sci U S A. 2005 Dec 6;102:17858-63.

74. Israel DI, Whitlock JP, Jr. Induction of mRNA specific for cytochrome P1-450 in wild type and variant mouse hepatoma cells. J Biol Chem. 1983 Sep 10;258:10390-4.

75. Israel DI, Whitlock JP, Jr. Regulation of cytochrome P1-450 gene transcription by 2,3,7, 8-tetrachlorodibenzo-p-dioxin in wild type and variant mouse hepatoma cells. J Biol Chem. 1984 May 10;259:5400-2.

76. Ko HP, Okino ST, Ma Q, Whitlock JP, Jr. Dioxin-induced CYP1A1 transcription in vivo: the aromatic hydrocarbon receptor mediates transactivation, enhancer-promoter communication, and changes in chromatin structure. Mol Cell Biol. 1996 Jan;16:430-6.

77. Nebert DW, Roe AL, Dieter MZ, Solis WA, Yang Y, Dalton TP. Role of the aromatic hydrocarbon receptor and [Ah] gene battery in the oxidative stress response, cell cycle control, and apoptosis. Biochem Pharmacol. 2000 Jan 1;59:65-85.

78. Lensu S, Tuomisto JT, Tuomisto J, Viluksela M, Niittynen M, Pohjanvirta R. Immediate and highly sensitive aversion response to a novel food item linked to AH receptor stimulation. Toxicol Lett. 2011 Jun 24;203:252-7.

79. Harrigan JA, Vezina CM, McGarrigle BP, Ersing N, Box HC, Maccubbin AE, Olson JR. DNA adduct formation in precision-cut rat liver and lung slices exposed to benzo[a]pyrene. Toxicol Sci. 2004 Feb;77:307-14.

80. Linden J, Lensu S, Tuomisto J, Pohjanvirta R. Dioxins, the aryl hydrocarbon receptor and the central regulation of energy balance. Front Neuroendocrinol. 2010 Oct;31:452-78.

81. Martinez JM, Afshari CA, Bushel PR, Masuda A, Takahashi T, Walker NJ. Differential toxicogenomic responses to 2,3,7,8-tetrachlorodibenzo-p-dioxin in malignant and nonmalignant human airway epithelial cells. Toxicol Sci. 2002 Oct;69:409-23.

82. Vezina CM, Walker NJ, Olson JR. Subchronic exposure to TCDD, PeCDF, PCB126, and PCB153: effect on hepatic gene expression. Environ Health Perspect. 2004 Nov;112:1636-44.

83. Ovando BJ, Vezina CM, McGarrigle BP, Olson JR. Hepatic gene downregulation following acute and subchronic exposure to 2,3,7,8-tetrachlorodibenzo-p-dioxin. Toxicol Sci. 2006 Dec;94:428-38.

84. Arzuaga X, Ren N, Stromberg A, Black EP, Arsenescu V, Cassis LA, Majkova Z, Toborek M, Hennig B. Induction of gene pattern changes associated with dysfunctional lipid metabolism induced by dietary fat and exposure to a persistent organic pollutant. Toxicol Lett. 2009 Sep 10;189:96-101.

85. Nault R, Kim S, Zacharewski TR. Comparison of TCDD-elicited genome-wide hepatic gene expression in Sprague-Dawley rats and C57BL/6 mice. Toxicol Appl Pharmacol. 2013 Mar 1;267:184-91.

86. Swedenborg E, Kotka M, Seifert M, Kanno J, Pongratz I, Ruegg J. The aryl hydrocarbon receptor ligands 2,3,7,8-tetrachlorodibenzo-p-dioxin and 3-methylcholanthrene regulate distinct genetic networks. Mol Cell Endocrinol. 2012 Oct 15;362:39-47.

87. Wang C, Xu CX, Krager SL, Bottum KM, Liao DF, Tischkau SA. Aryl hydrocarbon receptor deficiency enhances insulin sensitivity and reduces PPAR-alpha pathway activity in mice. Environ Health Perspect. 2011 Dec;119:1739-44.

88. Ibrahim MM, Fjaere E, Lock EJ, Naville D, Amlund H, Meugnier E, Le Magueresse Battistoni B, Froyland L, Madsen L, et al. Chronic consumption of farmed salmon containing persistent organic pollutants causes insulin resistance and obesity in mice. PLoS One. 2011;6:e25170.

89. Kerley-Hamilton JS, Trask HW, Ridley CJ, Dufour E, Ringelberg CS, Nurinova N, Wong D, Moodie KL, Shipman SL, et al. Obesity is mediated by differential aryl hydrocarbon receptor signaling in mice fed a Western diet. Environ Health Perspect. 2012 Sep;120:1252-9.

90. Shaw JE, Sicree RA, Zimmet PZ. Global estimates of the prevalence of diabetes for 2010 and 2030. Diabetes Res Clin Pract. 2010 Jan;87:4-14.

91. Vijan S. Type 2 diabetes. Ann Intern Med. 2010 Mar 2;152:ITC31-15; quiz ITC316.

92. Abate N, Chandalia M. Ethnicity and type 2 diabetes: focus on Asian Indians. J Diabetes Complications. 2001 Nov-Dec;15:320-7.

93. Silverthorn DU. Human Physiology: An Integrated Approach. San Francisco, CA: Pearson/Benjamin Cummings; 2009.

94. Riserus U, Willett WC, Hu FB. Dietary fats and prevention of type 2 diabetes. Prog Lipid Res. 2009 Jan;48:44-51.

95. Kershaw EE, Flier JS. Adipose tissue as an endocrine organ. J Clin Endocrinol Metab. 2004 Jun;89:2548-56.

96. Montague CT, O'Rahilly S. The perils of portliness: causes and consequences of visceral adiposity. Diabetes. 2000 Jun;49:883-8.

97. Kern PA, Ranganathan S, Li C, Wood L, Ranganathan G. Adipose tissue tumor necrosis factor and interleukin-6 expression in human obesity and insulin resistance. Am J Physiol Endocrinol Metab. 2001 May;280:E745-51.

98. Marette A. Molecular mechanisms of inflammation in obesity-linked insulin resistance. Int J Obes Relat Metab Disord. 2003 Dec;27 Suppl 3:S46-8.

99. Mokdad AH, Ford ES, Bowman BA, Dietz WH, Vinicor F, Bales VS, Marks JS. Prevalence of obesity, diabetes, and obesity-related health risk factors, 2001. JAMA. 2003 Jan 1;289:76-9.

100. Porter SA, Massaro JM, Hoffmann U, Vasan RS, O'Donnel CJ, Fox CS. Abdominal subcutaneous adipose tissue: a protective fat depot? Diabetes Care. 2009 Jun;32:1068-75.

101. Himms-Hagen J. Brown adipose tissue thermogenesis: interdisciplinary studies. FASEB J. 1990 Aug;4:2890-8.

102. Nedergaard J, Bengtsson T, Cannon B. Unexpected evidence for active brown adipose tissue in adult humans. Am J Physiol Endocrinol Metab. 2007 Aug;293:E444-52.

103. Virtanen KA, Lidell ME, Orava J, Heglind M, Westergren R, Niemi T, Taittonen M, Laine J, Savisto NJ, et al. Functional brown adipose tissue in healthy adults. N Engl J Med. 2009 Apr 9;360:1518-25.

104. van Marken Lichtenbelt WD, Vanhommerig JW, Smulders NM, Drossaerts JM, Kemerink GJ, Bouvy ND, Schrauwen P, Teule GJ. Cold-activated brown adipose tissue in healthy men. N Engl J Med. 2009 Apr 9;360:1500-8.

105. Cypess AM, Lehman S, Williams G, Tal I, Rodman D, Goldfine AB, Kuo FC, Palmer EL, Tseng YH, et al. Identification and importance of brown adipose tissue in adult humans. N Engl J Med. 2009 Apr 9;360:1509-17.

106. Urakawa H, Katsuki A, Sumida Y, Gabazza EC, Murashima S, Morioka K, Maruyama N, Kitagawa N, Tanaka T, et al. Oxidative stress is associated with adiposity and insulin resistance in men. J Clin Endocrinol Metab. 2003 Oct;88:4673-6.

107. Matsuzawa-Nagata N, Takamura T, Ando H, Nakamura S, Kurita S, Misu H, Ota T, Yokoyama M, Honda M, et al. Increased oxidative stress precedes the onset of high-fat diet-induced insulin resistance and obesity. Metabolism. 2008 Aug;57:1071-7.

108. Findeisen HM, Pearson KJ, Gizard F, Zhao Y, Qing H, Jones KL, Cohn D, Heywood EB, de Cabo R, Bruemmer D. Oxidative stress accumulates in adipose tissue during aging and inhibits adipogenesis. PLoS One. 2011;6:e18532.

109. Xu XJ, Gauthier MS, Hess DT, Apovian CM, Cacicedo JM, Gokce N, Farb M, Valentine RJ, Ruderman NB. Insulin sensitive and resistant obesity in humans: AMPK activity, oxidative stress, and depot-specific changes in gene expression in adipose tissue. J Lipid Res. 2012 Apr;53:792-801.

110. Furukawa S, Fujita T, Shimabukuro M, Iwaki M, Yamada Y, Nakajima Y, Nakayama O, Makishima M, Matsuda M, Shimomura I. Increased oxidative stress in obesity and its impact on metabolic syndrome. J Clin Invest. 2004 Dec;114:1752-61.

111. Hotamisligil GS, Shargill NS, Spiegelman BM. Adipose expression of tumor necrosis factor-alpha: direct role in obesity-linked insulin resistance. Science. 1993 Jan 1;259:87-91.

112. Spiegelman BM, Hotamisligil GS. Through thick and thin: wasting, obesity, and TNF alpha. Cell. 1993 May 21;73:625-7.

113. Kern PA, Saghizadeh M, Ong JM, Bosch RJ, Deem R, Simsolo RB. The expression of tumor necrosis factor in human adipose tissue. Regulation by obesity, weight loss, and relationship to lipoprotein lipase. J Clin Invest. 1995 May;95:2111-9.

114. Kriegler M, Perez C, DeFay K, Albert I, Lu SD. A novel form of TNF/cachectin is a cell surface cytotoxic transmembrane protein: ramifications for the complex physiology of TNF. Cell. 1988 Apr 8;53:45-53.

115. Maskos K, Fernandez-Catalan C, Huber R, Bourenkov GP, Bartunik H, Ellestad GA, Reddy P, Wolfson MF, Rauch CT, et al. Crystal structure of the

catalytic domain of human tumor necrosis factor-alpha-converting enzyme. Proc Natl Acad Sci U S A. 1998 Mar 31;95:3408-12.

116. Black RA, Rauch CT, Kozlosky CJ, Peschon JJ, Slack JL, Wolfson MF, Castner BJ, Stocking KL, Reddy P, et al. A metalloproteinase disintegrin that releases tumour-necrosis factor-alpha from cells. Nature. 1997 Feb 20;385:729-33.

117. Wallach D, Varfolomeev EE, Malinin NL, Goltsev YV, Kovalenko AV, Boldin MP. Tumor necrosis factor receptor and Fas signaling mechanisms. Annu Rev Immunol. 1999;17:331-67.

118. Hotamisligil GS, Arner P, Caro JF, Atkinson RL, Spiegelman BM. Increased adipose tissue expression of tumor necrosis factor-alpha in human obesity and insulin resistance. J Clin Invest. 1995 May;95:2409-15.

119. Montague CT, Prins JB, Sanders L, Zhang J, Sewter CP, Digby J, Byrne CD, O'Rahilly S. Depot-related gene expression in human subcutaneous and omental adipocytes. Diabetes. 1998 Sep;47:1384-91.

120. Lang CH, Dobrescu C, Bagby GJ. Tumor necrosis factor impairs insulin action on peripheral glucose disposal and hepatic glucose output. Endocrinology. 1992 Jan;130:43-52.

121. Hotamisligil GS, Murray DL, Choy LN, Spiegelman BM. Tumor necrosis factor alpha inhibits signaling from the insulin receptor. Proc Natl Acad Sci U S A. 1994 May 24;91:4854-8.

122. Hotamisligil GS, Spiegelman BM. Tumor necrosis factor alpha: a key component of the obesity-diabetes link. Diabetes. 1994 Nov;43:1271-8.

123. Uysal KT, Wiesbrock SM, Marino MW, Hotamisligil GS. Protection from obesity-induced insulin resistance in mice lacking TNF-alpha function. Nature. 1997 Oct 9;389:610-4.

124. Uysal KT, Wiesbrock SM, Hotamisligil GS. Functional analysis of tumor necrosis factor (TNF) receptors in TNF-alpha-mediated insulin resistance in genetic obesity. Endocrinology. 1998 Dec;139:4832-8.

125. Ofei F, Hurel S, Newkirk J, Sopwith M, Taylor R. Effects of an engineered human anti-TNF-alpha antibody (CDP571) on insulin sensitivity and glycemic control in patients with NIDDM. Diabetes. 1996 Jul;45:881-5.

126. Randle PJ, Garland PB, Hales CN, Newsholme EA. The glucose fatty-acid cycle. Its role in insulin sensitivity and the metabolic disturbances of diabetes mellitus. Lancet. 1963 Apr 13;1:785-9.

127. Randle PJ, Garland PB, Newsholme EA, Hales CN. The glucose fatty acid cycle in obesity and maturity onset diabetes mellitus. Ann N Y Acad Sci. 1965 Oct 8;131:324-33.

128. Kruszynska YT, Worrall DS, Ofrecio J, Frias JP, Macaraeg G, Olefsky JM. Fatty acid-induced insulin resistance: decreased muscle PI3K activation but unchanged Akt phosphorylation. J Clin Endocrinol Metab. 2002 Jan;87:226-34.

129. Yu Y, Zhu J, Wu Y, Baron AD. [Insulin mitigates the effect of free fatty acid to cause endothelial dysfunction in rat aortic rings]. Zhonghua Yi Xue Za Zhi. 2002 Mar 25;82:422-5.

130. Boden G, Chen X, Ruiz J, White JV, Rossetti L. Mechanisms of fatty acid-induced inhibition of glucose uptake. J Clin Invest. 1994 Jun;93:2438-46.

131. Boden G, Jadali F, White J, Liang Y, Mozzoli M, Chen X, Coleman E, Smith C. Effects of fat on insulin-stimulated carbohydrate metabolism in normal men. J Clin Invest. 1991 Sep;88:960-6.

132. Shulman GI, Rothman DL, Jue T, Stein P, DeFronzo RA, Shulman RG. Quantitation of muscle glycogen synthesis in normal subjects and subjects with non-insulin-dependent diabetes by 13C nuclear magnetic resonance spectroscopy. N Engl J Med. 1990 Jan 25;322:223-8.

133. Saloranta C, Franssila-Kallunki A, Ekstrand A, Taskinen MR, Groop L. Modulation of hepatic glucose production by non-esterified fatty acids in type 2 (non-insulin-dependent) diabetes mellitus. Diabetologia. 1991 Jun;34:409-15.

134. Boden G. Fatty acids and insulin resistance. Diabetes Care. 1996 Apr;19:394-5.

135. Reaven GM, Chang H, Hoffman BB. Additive hypoglycemic effects of drugs that modify free-fatty acid metabolism by different mechanisms in rats with streptozocin-induced diabetes. Diabetes. 1988 Jan;37:28-32.

136. Boden G. Free fatty acids (FFA), a link between obesity and insulin resistance. Front Biosci. 1998 Feb 15;3:d169-75.

137. Bonadonna RC, Groop L, Kraemer N, Ferrannini E, Del Prato S, DeFronzo RA. Obesity and insulin resistance in humans: a dose-response study. Metabolism. 1990 May;39:452-9.

138. Laws A, Hoen HM, Selby JV, Saad MF, Haffner SM, Howard BV. Differences in insulin suppression of free fatty acid levels by gender and glucose tolerance status. Relation to plasma triglyceride and apolipoprotein B

concentrations. Insulin Resistance Atherosclerosis Study (IRAS) Investigators. Arterioscler Thromb Vasc Biol. 1997 Jan;17:64-71.

139. Skowronski R, Hollenbeck CB, Varasteh BB, Chen YD, Reaven GM. Regulation of non-esterified fatty acid and glycerol concentration by insulin in normal individuals and patients with type 2 diabetes. Diabet Med. 1991 May;8:330-3.

140. Rosenstock M, Greenberg AS, Rudich A. Distinct long-term regulation of glycerol and non-esterified fatty acid release by insulin and TNF-alpha in 3T3-L1 adipocytes. Diabetologia. 2001 Jan;44:55-62.

141. Zhang HH, Halbleib M, Ahmad F, Manganiello VC, Greenberg AS. Tumor necrosis factor-alpha stimulates lipolysis in differentiated human adipocytes through activation of extracellular signal-related kinase and elevation of intracellular cAMP. Diabetes. 2002 Oct;51:2929-35.

142. Bogan JS, McKee AE, Lodish HF. Insulin-responsive compartments containing GLUT4 in 3T3-L1 and CHO cells: regulation by amino acid concentrations. Mol Cell Biol. 2001 Jul;21:4785-806.

143. Ruan H, Hacohen N, Golub TR, Van Parijs L, Lodish HF. Tumor necrosis factor-alpha suppresses adipocyte-specific genes and activates expression of preadipocyte genes in 3T3-L1 adipocytes: nuclear factor-kappaB activation by TNF-alpha is obligatory. Diabetes. 2002 May;51:1319-36.

144. Arita Y, Kihara S, Ouchi N, Takahashi M, Maeda K, Miyagawa J, Hotta K, Shimomura I, Nakamura T, et al. Paradoxical decrease of an adipose-specific

protein, adiponectin, in obesity. Biochem Biophys Res Commun. 1999 Apr 2;257:79-83.

145. Combs TP, Wagner JA, Berger J, Doebber T, Wang WJ, Zhang BB, Tanen M, Berg AH, O'Rahilly S, et al. Induction of adipocyte complement-related protein of 30 kilodaltons by PPARgamma agonists: a potential mechanism of insulin sensitization. Endocrinology. 2002 Mar;143:998-1007.

146. Kubota N, Terauchi Y, Yamauchi T, Kubota T, Moroi M, Matsui J, Eto K, Yamashita T, Kamon J, et al. Disruption of adiponectin causes insulin resistance and neointimal formation. J Biol Chem. 2002 Jul 19;277:25863-6.

147. Maeda N, Shimomura I, Kishida K, Nishizawa H, Matsuda M, Nagaretani H, Furuyama N, Kondo H, Takahashi M, et al. Diet-induced insulin resistance in mice lacking adiponectin/ACRP30. Nat Med. 2002 Jul;8:731-7.

148. Leal Vde O, Mafra D. Adipokines in obesity. Clin Chim Acta. 2013 Apr 18;419:87-94.

149. Kolko G. Anatomy of a War: Vietnam, the United States, and the Modern Historical Experiences: New Press; 1994.

150. Frumkin H. Agent Orange and cancer: an overview for clinicians. CA Cancer J Clin. 2003 Jul-Aug;53:245-55.

151. Young AL. The History, Use, Deposition, and Environmental Fate of Agent Orange. New York, NY: Springer; 2009.

152. 2,3,7,8-Tetrachlorodibenzo-p-dioxin. Rep Carcinog. 2011;12:396-8.

153. Affairs USDoV. Veterans' Diseases Associated with Agent Orange - Public Health. 2012 October 3, 2012 [cited 2013 May 15]; Available from: http://www.publichealth.va.gov/exposures/agentorange/diseases.asp

154. Henriksen GL, Ketchum NS, Michalek JE, Swaby JA. Serum dioxin and diabetes mellitus in veterans of Operation Ranch Hand. Epidemiology. 1997 May;8:252-8.

155. Fujiyoshi PT, Michalek JE, Matsumura F. Molecular epidemiologic evidence for diabetogenic effects of dioxin exposure in U.S. Air force veterans of the Vietnam war. Environ Health Perspect. 2006 Nov;114:1677-83.

156. Rypel AL, Findlay RH, Mitchell JB, Bayne DR. Variations in PCB concentrations between genders of six warmwater fish species in Lake Logan Martin, Alabama, USA. Chemosphere. 2007 Aug;68:1707-15.

157. Hansen LG. PCB congener comparisons reveal exposure histories for residents of Anniston, Alabama, USA. Fresenius Envir Bull 2003;12:181-90.

158. Silverstone AE, Rosenbaum PF, Weinstock RS, Bartell SM, Foushee HR, Shelton C, Pavuk M. Polychlorinated biphenyl (PCB) exposure and diabetes: results from the Anniston Community Health Survey. Environ Health Perspect. 2012 May;120:727-32.

159. Schlezinger JJ, Struntz WD, Goldstone JV, Stegeman JJ. Uncoupling of cytochrome P450 1A and stimulation of reactive oxygen species production by co-planar polychlorinated biphenyl congeners. Aquat Toxicol. 2006 May 25;77:422-32.

160. Han SG, Eum SY, Toborek M, Smart E, Hennig B. Polychlorinated biphenyl-induced VCAM-1 expression is attenuated in aortic endothelial cells isolated from caveolin-1 deficient mice. Toxicol Appl Pharmacol. 2010 Jul;246:74-82.

161. Majkova Z, Smart E, Toborek M, Hennig B. Up-regulation of endothelial monocyte chemoattractant protein-1 by coplanar PCB77 is caveolin-1-dependent. Toxicol Appl Pharmacol. 2009 May 15;237:1-7.

162. Hennig B, Ettinger AS, Jandacek RJ, Koo S, McClain C, Seifried H, Silverstone A, Watkins B, Suk WA. Using nutrition for intervention and prevention against environmental chemical toxicity and associated diseases. Environ Health Perspect. 2007 Apr;115:493-5.

163. Ogden CL, Carroll MD, Kit BK, Flegal KM. Prevalence of obesity in the United States, 2009-2010. NCHS Data Brief. 2012 Jan:1-8.

164. Alberti KG, Eckel RH, Grundy SM, Zimmet PZ, Cleeman JI, Donato KA, Fruchart JC, James WP, Loria CM, Smith SC, Jr. Harmonizing the metabolic syndrome: a joint interim statement of the International Diabetes Federation Task Force on Epidemiology and Prevention; National Heart, Lung, and Blood Institute; American Heart Association; World Heart Federation; International Atherosclerosis Society; and International Association for the Study of Obesity. Circulation. 2009 Oct 20;120:1640-5.

165. Carr DB, Utzschneider KM, Hull RL, Kodama K, Retzlaff BM, Brunzell JD, Shofer JB, Fish BE, Knopp RH, Kahn SE. Intra-abdominal fat is a major

determinant of the National Cholesterol Education Program Adult Treatment Panel III criteria for the metabolic syndrome. Diabetes. 2004 Aug;53:2087-94.

166. Weisberg SP, McCann D, Desai M, Rosenbaum M, Leibel RL, Ferrante AW, Jr. Obesity is associated with macrophage accumulation in adipose tissue. J Clin Invest. 2003 Dec;112:1796-808.

167. Sun K, Kusminski CM, Scherer PE. Adipose tissue remodeling and obesity. J Clin Invest. 2011 Jun;121:2094-101.

168. Monteiro R, Azevedo I. Chronic inflammation in obesity and the metabolic syndrome. Mediators Inflamm. 2010;2010.

169. La Merrill M, Emond C, Kim MJ, Antignac JP, Le Bizec B, Clement K, Birnbaum LS, Barouki R. Toxicological function of adipose tissue: focus on persistent organic pollutants. Environ Health Perspect. 2013 Feb;121:162-9.

170. La Rocca C, Alivernini S, Badiali M, Cornoldi A, Iacovella N, Silvestroni L, Spera G, Turrio-Baldassarri L. TEQ(S) and body burden for PCDDs, PCDFs, and dioxin-like PCBs in human adipose tissue. Chemosphere. 2008 Aug;73:92-6.

171. Brodie AE, Azarenko VA, Hu CY. 2,3,7,8-Tetrachlorodibenzo-p-dioxin (TCDD) inhibition of fat cell differentiation. Toxicol Lett. 1996 Jan;84:55-9.

172. Brodie AE, Azarenko VA, Hu CY. Inhibition of increases of transcription factor mRNAs during differentiation of primary rat adipocytes by in vivo 2,3,7,8-tetrachlorodibenzo-p-dioxin (TCDD) treatment. Toxicol Lett. 1997 Feb 7;90:91-5.

173. Phillips M, Enan E, Liu PC, Matsumura F. Inhibition of 3T3-L1 adipose differentiation by 2,3,7,8-tetrachlorodibenzo-p-dioxin. J Cell Sci. 1995 Jan;108 (Pt 1):395-402.

174. Baur JA, Sinclair DA. Therapeutic potential of resveratrol: the in vivo evidence. Nat Rev Drug Discov. 2006 Jun;5:493-506.

175. Farina A, Ferranti C, Marra C. An improved synthesis of resveratrol. Nat Prod Res. 2006 Mar;20:247-52.

176. Trantas E, Panopoulos N, Ververidis F. Metabolic engineering of the complete pathway leading to heterologous biosynthesis of various flavonoids and stilbenoids in Saccharomyces cerevisiae. Metab Eng. 2009 Nov;11:355-66.

177. Wang H, Liu L, Guo YX, Dong YS, Zhang DJ, Xiu ZL. Biotransformation of piceid in Polygonum cuspidatum to resveratrol by Aspergillus oryzae. Appl Microbiol Biotechnol. 2007 Jun;75:763-8.

178. Jang M, Cai L, Udeani GO, Slowing KV, Thomas CF, Beecher CW, Fong HH, Farnsworth NR, Kinghorn AD, et al. Cancer chemopreventive activity of resveratrol, a natural product derived from grapes. Science. 1997 Jan 10;275:218-20.

179. Athar M, Back JH, Tang X, Kim KH, Kopelovich L, Bickers DR, Kim AL. Resveratrol: a review of preclinical studies for human cancer prevention. Toxicol Appl Pharmacol. 2007 Nov 1;224:274-83.

180. Li ZG, Hong T, Shimada Y, Komoto I, Kawabe A, Ding Y, Kaganoi J, Hashimoto Y, Imamura M. Suppression of N-nitrosomethylbenzylamine (NMBA)-induced esophageal tumorigenesis in F344 rats by resveratrol. Carcinogenesis. 2002 Sep;23:1531-6.

181. Kimura Y, Okuda H. Resveratrol isolated from Polygonum cuspidatum root prevents tumor growth and metastasis to lung and tumor-induced

neovascularization in Lewis lung carcinoma-bearing mice. J Nutr. 2001 Jun;131:1844-9.

182. Baur JA, Pearson KJ, Price NL, Jamieson HA, Lerin C, Kalra A, Prabhu VV, Allard JS, Lopez-Lluch G, et al. Resveratrol improves health and survival of mice on a high-calorie diet. Nature. 2006 Nov 16;444:337-42.

183. Pearson KJ, Baur JA, Lewis KN, Peshkin L, Price NL, Labinskyy N, Swindell WR, Kamara D, Minor RK, et al. Resveratrol delays age-related deterioration and mimics transcriptional aspects of dietary restriction without extending life span. Cell Metab. 2008 Aug;8:157-68.

184. Gentilli M, Mazoit JX, Bouaziz H, Fletcher D, Casper RF, Benhamou D, Savouret JF. Resveratrol decreases hyperalgesia induced by carrageenan in the rat hind paw. Life Sci. 2001 Feb 2;68:1317-21.

185. Tsai SH, Lin-Shiau SY, Lin JK. Suppression of nitric oxide synthase and the down-regulation of the activation of NFkappaB in macrophages by resveratrol. Br J Pharmacol. 1999 Feb;126:673-80.

186. Elmali N, Baysal O, Harma A, Esenkaya I, Mizrak B. Effects of resveratrol in inflammatory arthritis. Inflammation. 2007 Apr;30:1-6.

187. Lagouge M, Argmann C, Gerhart-Hines Z, Meziane H, Lerin C, Daussin F, Messadeq N, Milne J, Lambert P, et al. Resveratrol improves mitochondrial function and protects against metabolic disease by activating SIRT1 and PGC-1alpha. Cell. 2006 Dec 15;127:1109-22.

188. Deng JY, Hsieh PS, Huang JP, Lu LS, Hung LM. Activation of estrogen receptor is crucial for resveratrol-stimulating muscular glucose uptake via both insulin-dependent and -independent pathways. Diabetes. 2008 Jul;57:1814-23.

189. Palsamy P, Subramanian S. Resveratrol, a natural phytoalexin, normalizes hyperglycemia in streptozotocin-nicotinamide induced experimental diabetic rats. Biomed Pharmacother. 2008 Nov;62:598-605.

190. Sharma S, Anjaneyulu M, Kulkarni SK, Chopra K. Resveratrol, a polyphenolic phytoalexin, attenuates diabetic nephropathy in rats. Pharmacology. 2006;76:69-75.

191. Schmatz R, Mazzanti CM, Spanevello R, Stefanello N, Gutierres J, Correa M, da Rosa MM, Rubin MA, Chitolina Schetinger MR, Morsch VM. Resveratrol prevents memory deficits and the increase in acetylcholinesterase activity in streptozotocin-induced diabetic rats. Eur J Pharmacol. 2009 May 21;610:42-8.

192. Penumathsa SV, Thirunavukkarasu M, Zhan L, Maulik G, Menon VP, Bagchi D, Maulik N. Resveratrol enhances GLUT-4 translocation to the caveolar lipid raft fractions through AMPK/Akt/eNOS signalling pathway in diabetic myocardium. J Cell Mol Med. 2008 Dec;12:2350-61.

193. Su HC, Hung LM, Chen JK. Resveratrol, a red wine antioxidant, possesses an insulin-like effect in streptozotocin-induced diabetic rats. Am J Physiol Endocrinol Metab. 2006 Jun;290:E1339-46.

194. Um JH, Park SJ, Kang H, Yang S, Foretz M, McBurney MW, Kim MK, Viollet B, Chung JH. AMP-activated protein kinase-deficient mice are resistant to the metabolic effects of resveratrol. Diabetes. 2010 Mar;59:554-63.

195. Shang J, Chen LL, Xiao FX. [Resveratrol improves high-fat induced nonalcoholic fatty liver in rats]. Zhonghua Gan Zang Bing Za Zhi. 2008 Aug;16:616-9.

196. Shang J, Chen LL, Xiao FX, Sun H, Ding HC, Xiao H. Resveratrol improves non-alcoholic fatty liver disease by activating AMP-activated protein kinase. Acta Pharmacol Sin. 2008 Jun;29:698-706.

197. Rocha KK, Souza GA, Ebaid GX, Seiva FR, Cataneo AC, Novelli EL. Resveratrol toxicity: effects on risk factors for atherosclerosis and hepatic oxidative stress in standard and high-fat diets. Food Chem Toxicol. 2009 Jun;47:1362-7.

198. Macarulla MT, Alberdi G, Gomez S, Tueros I, Bald C, Rodriguez VM, Martinez JA, Portillo MP. Effects of different doses of resveratrol on body fat and serum parameters in rats fed a hypercaloric diet. J Physiol Biochem. 2009 Dec;65:369-76.

199. Kopp P. Resveratrol, a phytoestrogen found in red wine. A possible explanation for the conundrum of the 'French paradox'? Eur J Endocrinol. 1998 Jun;138:619-20.

200. Ferrero ME, Bertelli AE, Fulgenzi A, Pellegatta F, Corsi MM, Bonfrate M, Ferrara F, De Caterina R, Giovannini L, Bertelli A. Activity in vitro of resveratrol on granulocyte and monocyte adhesion to endothelium. Am J Clin Nutr. 1998 Dec;68:1208-14.

201. Rotondo S, Rajtar G, Manarini S, Celardo A, Rotillo D, de Gaetano G, Evangelista V, Cerletti C. Effect of trans-resveratrol, a natural polyphenolic

compound, on human polymorphonuclear leukocyte function. Br J Pharmacol. 1998 Apr;123:1691-9.

202. Haider UG, Roos TU, Kontaridis MI, Neel BG, Sorescu D, Griendling KK, Vollmar AM, Dirsch VM. Resveratrol inhibits angiotensin II- and epidermal growth factor-mediated Akt activation: role of Gab1 and Shp2. Mol Pharmacol. 2005 Jul;68:41-8.

203. Wang Z, Chen Y, Labinskyy N, Hsieh TC, Ungvari Z, Wu JM. Regulation of proliferation and gene expression in cultured human aortic smooth muscle cells by resveratrol and standardized grape extracts. Biochem Biophys Res Commun. 2006 Jul 21;346:367-76.

204. Poussier B, Cordova AC, Becquemin JP, Sumpio BE. Resveratrol inhibits vascular smooth muscle cell proliferation and induces apoptosis. J Vasc Surg. 2005 Dec;42:1190-7.

205. Duffy SJ, Vita JA. Effects of phenolics on vascular endothelial function. Curr Opin Lipidol. 2003 Feb;14:21-7.

206. Wallerath T, Deckert G, Ternes T, Anderson H, Li H, Witte K, Forstermann U. Resveratrol, a polyphenolic phytoalexin present in red wine, enhances expression and activity of endothelial nitric oxide synthase. Circulation. 2002 Sep 24;106:1652-8.

207. Chen CK, Pace-Asciak CR. Vasorelaxing activity of resveratrol and quercetin in isolated rat aorta. Gen Pharmacol. 1996 Mar;27:363-6.

208. Olas B, Wachowicz B, Majsterek I, Blasiak J. Resveratrol may reduce oxidative stress induced by platinum compounds in human plasma, blood platelets and lymphocytes. Anticancer Drugs. 2005 Jul;16:659-65.

209. Stef G, Csiszar A, Lerea K, Ungvari Z, Veress G. Resveratrol inhibits aggregation of platelets from high-risk cardiac patients with aspirin resistance. J Cardiovasc Pharmacol. 2006 Aug;48:1-5.

210. Wang Z, Huang Y, Zou J, Cao K, Xu Y, Wu JM. Effects of red wine and wine polyphenol resveratrol on platelet aggregation in vivo and in vitro. Int J Mol Med. 2002 Jan;9:77-9.

211. Fremont L, Belguendouz L, Delpal S. Antioxidant activity of resveratrol and alcohol-free wine polyphenols related to LDL oxidation and polyunsaturated fatty acids. Life Sci. 1999;64:2511-21.

212. Elliott PJ, Jirousek M. Sirtuins: novel targets for metabolic disease. Curr Opin Investig Drugs. 2008 Apr;9:371-8.

213. Bhatt JK, Thomas S, Nanjan MJ. Resveratrol supplementation improves glycemic control in type 2 diabetes mellitus. Nutr Res. 2012 Jul;32:537-41.

214. Timmers S, Konings E, Bilet L, Houtkooper RH, van de Weijer T, Goossens GH, Hoeks J, van der Krieken S, Ryu D, et al. Calorie restriction-like effects of 30 days of resveratrol supplementation on energy metabolism and metabolic profile in obese humans. Cell Metab. 2011 Nov 2;14:612-22.

215. Yoshino J, Conte C, Fontana L, Mittendorfer B, Imai S, Schechtman KB, Gu C, Kunz I, Rossi Fanelli F, et al. Resveratrol supplementation does not

improve metabolic function in nonobese women with normal glucose tolerance. Cell Metab. 2012 Nov 7;16:658-64.

216. Alcain FJ, Villalba JM. Sirtuin activators. Expert Opin Ther Pat. 2009 Apr;19:403-14.

217. Kaeberlein M, Kirkland KT, Fields S, Kennedy BK. Sir2-independent life span extension by calorie restriction in yeast. PLoS Biol. 2004 Sep;2:E296.

218. Kaeberlein M, McDonagh T, Heltweg B, Hixon J, Westman EA, Caldwell SD, Napper A, Curtis R, DiStefano PS, et al. Substrate-specific activation of sirtuins by resveratrol. J Biol Chem. 2005 Apr 29;280:17038-45.

219. Pacholec M, Bleasdale JE, Chrunyk B, Cunningham D, Flynn D, Garofalo RS, Griffith D, Griffor M, Loulakis P, et al. SRT1720, SRT2183, SRT1460, and resveratrol are not direct activators of SIRT1. J Biol Chem. 2010 Mar 12;285:8340-51.

220. Leiro J, Arranz JA, Fraiz N, Sanmartin ML, Quezada E, Orallo F. Effect of cis-resveratrol on genes involved in nuclear factor kappa B signaling. Int Immunopharmacol. 2005 Feb;5:393-406.

221. Chun YJ, Kim MY, Guengerich FP. Resveratrol is a selective human cytochrome P450 1A1 inhibitor. Biochem Biophys Res Commun. 1999 Aug 19;262:20-4.

222. Schwarz D, Roots I. In vitro assessment of inhibition by natural polyphenols of metabolic activation of procarcinogens by human CYP1A1. Biochem Biophys Res Commun. 2003 Apr 11;303:902-7.

223. Hung LM, Chen JK, Huang SS, Lee RS, Su MJ. Cardioprotective effect of resveratrol, a natural antioxidant derived from grapes. Cardiovasc Res. 2000 Aug 18;47:549-55.

224. Kode A, Rajendrasozhan S, Caito S, Yang SR, Megson IL, Rahman I. Resveratrol induces glutathione synthesis by activation of Nrf2 and protects against cigarette smoke-mediated oxidative stress in human lung epithelial cells. Am J Physiol Lung Cell Mol Physiol. 2008 Mar;294:L478-88.

225. Kim S, Jin Y, Choi Y, Park T. Resveratrol exerts anti-obesity effects via mechanisms involving down-regulation of adipogenic and inflammatory processes in mice. Biochem Pharmacol. 2011 Jun 1;81:1343-51.

226. Tennen RI, Michishita-Kioi E, Chua KF. Finding a target for resveratrol. Cell. 2012 Feb 3;148:387-9.

227. Park LK, Friso S, Choi SW. Nutritional influences on epigenetics and age-related disease. Proc Nutr Soc. 2012 Feb;71:75-83.

228. Walle T, Hsieh F, DeLegge MH, Oatis JE, Jr., Walle UK. High absorption but very low bioavailability of oral resveratrol in humans. Drug Metab Dispos. 2004 Dec;32:1377-82.

229. Boocock DJ, Faust GE, Patel KR, Schinas AM, Brown VA, Ducharme MP, Booth TD, Crowell JA, Perloff M, et al. Phase I dose escalation pharmacokinetic study in healthy volunteers of resveratrol, a potential cancer chemopreventive agent. Cancer Epidemiol Biomarkers Prev. 2007 Jun;16:1246-52.

230. Health USNIo. A Clinical Study to Assess the Safety and Activity of SRT501 Alone or in Combination With Bortezomib in Patients With Multiple

Myeloma. 2012 March 2012 [cited 2013 May 15]; Available from: http://www.clinicaltrials.gov/show/NCT00920556

231. Beacon TM. GlaxoSmithKline Halts All Further Development Of Resveratrol Drug SRT501. 2010 November 30, 2010 [cited 2013 May 15]; Available from: http://www.myelomabeacon.com/news/2010/11/30/glaxosmithkline-halts-all-further-development-of-resveratrol-drug-srt501/

232. la Porte C, Voduc N, Zhang G, Seguin I, Tardiff D, Singhal N, Cameron DW. Steady-State pharmacokinetics and tolerability of trans-resveratrol 2000 mg twice daily with food, quercetin and alcohol (ethanol) in healthy human subjects. Clin Pharmacokinet. 2010 Jul;49:449-54.

233. Boocock DJ, Patel KR, Faust GE, Normolle DP, Marczylo TH, Crowell JA, Brenner DE, Booth TD, Gescher A, Steward WP. Quantitation of trans-resveratrol and detection of its metabolites in human plasma and urine by high performance liquid chromatography. J Chromatogr B Analyt Technol Biomed Life Sci. 2007 Apr 1;848:182-7.

234. Wenzel E, Soldo T, Erbersdobler H, Somoza V. Bioactivity and metabolism of trans-resveratrol orally administered to Wistar rats. Mol Nutr Food Res. 2005 May;49:482-94.

235. Marier JF, Vachon P, Gritsas A, Zhang J, Moreau JP, Ducharme MP. Metabolism and disposition of resveratrol in rats: extent of absorption, glucuronidation, and enterohepatic recirculation evidenced by a linked-rat model. J Pharmacol Exp Ther. 2002 Jul;302:369-73.

236. Abd El-Mohsen M, Bayele H, Kuhnle G, Gibson G, Debnam E, Kaila Srai S, Rice-Evans C, Spencer JP. Distribution of [3H]trans-resveratrol in rat tissues following oral administration. Br J Nutr. 2006 Jul;96:62-70.

237. Yu C, Shin YG, Chow A, Li Y, Kosmeder JW, Lee YS, Hirschelman WH, Pezzuto JM, Mehta RG, van Breemen RB. Human, rat, and mouse metabolism of resveratrol. Pharm Res. 2002 Dec;19:1907-14.

238. Wang LX, Heredia A, Song H, Zhang Z, Yu B, Davis C, Redfield R. Resveratrol glucuronides as the metabolites of resveratrol in humans: characterization, synthesis, and anti-HIV activity. J Pharm Sci. 2004 Oct;93:2448-57.

239. Goldberg DM, Yan J, Soleas GJ. Absorption of three wine-related polyphenols in three different matrices by healthy subjects. Clin Biochem. 2003 Feb;36:79-87.

240. Vitaglione P, Sforza S, Galaverna G, Ghidini C, Caporaso N, Vescovi PP, Fogliano V, Marchelli R. Bioavailability of trans-resveratrol from red wine in humans. Mol Nutr Food Res. 2005 May;49:495-504.

241. Kang W, Hong HJ, Guan J, Kim DG, Yang EJ, Koh G, Park D, Han CH, Lee YJ, Lee DH. Resveratrol improves insulin signaling in a tissue-specific manner under insulin-resistant conditions only: in vitro and in vivo experiments in rodents. Metabolism. 2012 Mar;61:424-33.

242. Bloomgarden ZT. Diabetes complications. Diabetes Care. 2004 Jun;27:1506-14.

243. Palumbo PJ. Gycemic control, mealtime glucose excursions, and diabetic complications in type 2 diabetes mellitus. Mayo Clin Proc. 2001 Jun;76:609-18.

244. Lekli I, Szabo G, Juhasz B, Das S, Das M, Varga E, Szendrei L, Gesztelyi R, Varadi J, et al. Protective mechanisms of resveratrol against ischemia-reperfusion-induced damage in hearts obtained from Zucker obese rats: the role of GLUT-4 and endothelin. Am J Physiol Heart Circ Physiol. 2008 Feb;294:H859-66.

245. Palsamy P, Subramanian S. Modulatory effects of resveratrol on attenuating the key enzymes activities of carbohydrate metabolism in streptozotocin-nicotinamide-induced diabetic rats. Chem Biol Interact. 2009 May 15;179:356-62.

246. Silan C. The effects of chronic resveratrol treatment on vascular responsiveness of streptozotocin-induced diabetic rats. Biol Pharm Bull. 2008 May;31:897-902.

247. Palsamy P, Subramanian S. Resveratrol protects diabetic kidney by attenuating hyperglycemia-mediated oxidative stress and renal inflammatory cytokines via Nrf2-Keap1 signaling. Biochim Biophys Acta. 2011 Jul;1812:719-31.

248. Palsamy P, Sivakumar S, Subramanian S. Resveratrol attenuates hyperglycemia-mediated oxidative stress, proinflammatory cytokines and protects hepatocytes ultrastructure in streptozotocin-nicotinamide-induced experimental diabetic rats. Chem Biol Interact. 2010 Jul 30;186:200-10.

249. Chi TC, Chen WP, Chi TL, Kuo TF, Lee SS, Cheng JT, Su MJ. Phosphatidylinositol-3-kinase is involved in the antihyperglycemic effect induced by resveratrol in streptozotocin-induced diabetic rats. Life Sci. 2007 Apr 10;80:1713-20.

250. Hansen JB, Arkhammar PO, Bodvarsdottir TB, Wahl P. Inhibition of insulin secretion as a new drug target in the treatment of metabolic disorders. Curr Med Chem. 2004 Jun;11:1595-615.

251. Sun C, Zhang F, Ge X, Yan T, Chen X, Shi X, Zhai Q. SIRT1 improves insulin sensitivity under insulin-resistant conditions by repressing PTP1B. Cell Metab. 2007 Oct;6:307-19.

252. Ramadori G, Gautron L, Fujikawa T, Vianna CR, Elmquist JK, Coppari R. Central administration of resveratrol improves diet-induced diabetes. Endocrinology. 2009 Dec;150:5326-33.

253. Rivera L, Moron R, Zarzuelo A, Galisteo M. Long-term resveratrol administration reduces metabolic disturbances and lowers blood pressure in obese Zucker rats. Biochem Pharmacol. 2009 Mar 15;77:1053-63.

254. Szkudelski T. Resveratrol inhibits insulin secretion from rat pancreatic islets. Eur J Pharmacol. 2006 Dec 15;552:176-81.

255. Szkudelski T. Resveratrol-induced inhibition of insulin secretion from rat pancreatic islets: evidence for pivotal role of metabolic disturbances. Am J Physiol Endocrinol Metab. 2007 Oct;293:E901-7.

256. Szkudelski T. The insulin-suppressive effect of resveratrol - an in vitro and in vivo phenomenon. Life Sci. 2008 Feb 13;82:430-5.

257. Lee JH, Song MY, Song EK, Kim EK, Moon WS, Han MK, Park JW, Kwon KB, Park BH. Overexpression of SIRT1 protects pancreatic beta-cells against cytokine toxicity by suppressing the nuclear factor-kappaB signaling pathway. Diabetes. 2009 Feb;58:344-51.

258. Robertson RP. Oxidative stress and impaired insulin secretion in type 2 diabetes. Curr Opin Pharmacol. 2006 Dec;6:615-9.

259. Lenzen S. Oxidative stress: the vulnerable beta-cell. Biochem Soc Trans. 2008 Jun;36:343-7.

260. Palsamy P, Subramanian S. Ameliorative potential of resveratrol on proinflammatory cytokines, hyperglycemia mediated oxidative stress, and pancreatic beta-cell dysfunction in streptozotocin-nicotinamide-induced diabetic rats. J Cell Physiol. 2010 Aug;224:423-32.

261. Kahn SE. The pathophysiologic defects of type 2 diabetes. Abnormal insulin action and impaired insulin secretion. Postgrad Med. 2000 May 15;107:11-5.

262. Goodpaster BH, Kelley DE, Wing RR, Meier A, Thaete FL. Effects of weight loss on regional fat distribution and insulin sensitivity in obesity. Diabetes. 1999 Apr;48:839-47.

263. Barger JL, Kayo T, Vann JM, Arias EB, Wang J, Hacker TA, Wang Y, Raederstorff D, Morrow JD, et al. A low dose of dietary resveratrol partially mimics caloric restriction and retards aging parameters in mice. PLoS One. 2008;3:e2264.

264. Szkudelska K, Szkudelski T. Resveratrol, obesity and diabetes. Eur J Pharmacol. 2010 Jun 10;635:1-8.

265. Szkudelska K, Nogowski L, Szkudelski T. Resveratrol, a naturally occurring diphenolic compound, affects lipogenesis, lipolysis and the antilipolytic action of insulin in isolated rat adipocytes. J Steroid Biochem Mol Biol. 2009 Jan;113:17-24.

266. Szkudelska K, Nogowski L, Szkudelski T. The inhibitory effect of resveratrol on leptin secretion from rat adipocytes. Eur J Clin Invest. 2009 Oct;39:899-905.

267. Kennedy A, Overman A, Lapoint K, Hopkins R, West T, Chuang CC, Martinez K, Bell D, McIntosh M. Conjugated linoleic acid-mediated inflammation and insulin resistance in human adipocytes are attenuated by resveratrol. J Lipid Res. 2009 Feb;50:225-32.

268. Lee DH, Steffes MW, Sjodin A, Jones RS, Needham LL, Jacobs DR, Jr. Low dose of some persistent organic pollutants predicts type 2 diabetes: a nested case-control study. Environ Health Perspect. 2010 Sep;118:1235-42.

269. Patel CJ, Bhattacharya J, Butte AJ. An Environment-Wide Association Study (EWAS) on type 2 diabetes mellitus. PLoS One. 2010;5:e10746.

270. Carpenter DO. Environmental contaminants as risk factors for developing diabetes. Rev Environ Health. 2008 Jan-Mar;23:59-74.

271. Codru N, Schymura MJ, Negoita S, Rej R, Carpenter DO. Diabetes in relation to serum levels of polychlorinated biphenyls and chlorinated pesticides in adult Native Americans. Environ Health Perspect. 2007 Oct;115:1442-7.

272. Wang SL, Tsai PC, Yang CY, Guo YL. Increased risk of diabetes and polychlorinated biphenyls and dioxins: a 24-year follow-up study of the Yucheng cohort. Diabetes Care. 2008 Aug;31:1574-9.

273. Dirinck E, Jorens PG, Covaci A, Geens T, Roosens L, Neels H, Mertens I, Van Gaal L. Obesity and persistent organic pollutants: possible obesogenic effect of organochlorine pesticides and polychlorinated biphenyls. Obesity (Silver Spring). 2011 Apr;19:709-14.

274. Walford RL, Mock D, MacCallum T, Laseter JL. Physiologic changes in humans subjected to severe, selective calorie restriction for two years in biosphere 2: health, aging, and toxicological perspectives. Toxicol Sci. 1999 Dec;52:61-5.

275. Lim JS, Son HK, Park SK, Jacobs DR, Jr., Lee DH. Inverse associations between long-term weight change and serum concentrations of persistent organic pollutants. Int J Obes (Lond). 2011 May;35:744-7.

276. Pelletier C, Doucet E, Imbeault P, Tremblay A. Associations between weight loss-induced changes in plasma organochlorine concentrations, serum T(3) concentration, and resting metabolic rate. Toxicol Sci. 2002 May;67:46-51.

277. Kim MJ, Pelloux V, Guyot E, Tordjman J, Bui LC, Chevallier A, Forest C, Benelli C, Clement K, Barouki R. Inflammatory pathway genes belong to major targets of persistent organic pollutants in adipose cells. Environ Health Perspect. 2012 Apr;120:508-14.

278. Hotamisligil GS, Peraldi P, Budavari A, Ellis R, White MF, Spiegelman BM. IRS-1-mediated inhibition of insulin receptor tyrosine kinase activity in TNF-alpha- and obesity-induced insulin resistance. Science. 1996 Feb 2;271:665-8.

279. Ventre J, Doebber T, Wu M, MacNaul K, Stevens K, Pasparakis M, Kollias G, Moller DE. Targeted disruption of the tumor necrosis factor-alpha gene: metabolic consequences in obese and nonobese mice. Diabetes. 1997 Sep;46:1526-31.

280. Peraldi P, Hotamisligil GS, Buurman WA, White MF, Spiegelman BM. Tumor necrosis factor (TNF)-alpha inhibits insulin signaling through stimulation of the p55 TNF receptor and activation of sphingomyelinase. J Biol Chem. 1996 May 31;271:13018-22.

281. Thong FS, Dugani CB, Klip A. Turning signals on and off: GLUT4 traffic in the insulin-signaling highway. Physiology (Bethesda). 2005 Aug;20:271-84.

282. Peraldi P, Spiegelman B. TNF-alpha and insulin resistance: summary and future prospects. Mol Cell Biochem. 1998 May;182:169-75.

283. Cawthorn WP, Sethi JK. TNF-alpha and adipocyte biology. FEBS Lett. 2008 Jan 9;582:117-31.

284. Torti FM, Torti SV, Larrick JW, Ringold GM. Modulation of adipocyte differentiation by tumor necrosis factor and transforming growth factor beta. J Cell Biol. 1989 Mar;108:1105-13.

285. Kienesberger PC, Lee D, Pulinilkunnil T, Brenner DS, Cai L, Magnes C, Koefeler HC, Streith IE, Rechberger GN, et al. Adipose triglyceride lipase

deficiency causes tissue-specific changes in insulin signaling. J Biol Chem. 2009 Oct 30;284:30218-29.

286. Kim SH, Henry EC, Kim DK, Kim YH, Shin KJ, Han MS, Lee TG, Kang JK, Gasiewicz TA, et al. Novel compound 2-methyl-2H-pyrazole-3-carboxylic acid (2-methyl-4-o-tolylazo-phenyl)-amide (CH-223191) prevents 2,3,7,8-TCDD-induced toxicity by antagonizing the aryl hydrocarbon receptor. Mol Pharmacol. 2006 Jun;69:1871-8.

287. Choi EY, Lee H, Dingle RW, Kim KB, Swanson HI. Development of novel CH223191-based antagonists of the aryl hydrocarbon receptor. Mol Pharmacol. 2012 Jan;81:3-11.

288. Cardoso FC, Sears W, LeBlanc SJ, Drackley JK. Technical note: comparison of 3 methods for analyzing areas under the curve for glucose and nonesterified fatty acids concentrations following epinephrine challenge in dairy cows. J Dairy Sci. 2011 Dec;94:6111-5.

289. McFarland VA, Clarke JU. Environmental occurrence, abundance, and potential toxicity of polychlorinated biphenyl congeners: considerations for a congener-specific analysis. Environ Health Perspect. 1989 May;81:225-39.

290. Everett CJ, Frithsen IL, Diaz VA, Koopman RJ, Simpson WM, Jr., Mainous AG, 3rd. Association of a polychlorinated dibenzo-p-dioxin, a polychlorinated biphenyl, and DDT with diabetes in the 1999-2002 National Health and Nutrition Examination Survey. Environ Res. 2007 Mar;103:413-8.

291. Hansen LG. Stepping backward to improve assessment of PCB congener toxicities. Environ Health Perspect. 1998 Feb;106 Suppl 1:171-89.

292. Harford KA, Reynolds CM, McGillicuddy FC, Roche HM. Fats, inflammation and insulin resistance: insights to the role of macrophage and T-cell accumulation in adipose tissue. Proc Nutr Soc. 2011 Nov;70:408-17.

293. DeFronzo RA. Pathogenesis of type 2 diabetes mellitus. Med Clin North Am. 2004 Jul;88:787-835, ix.

294. Chevrier J, Dewailly E, Ayotte P, Mauriege P, Despres JP, Tremblay A. Body weight loss increases plasma and adipose tissue concentrations of potentially toxic pollutants in obese individuals. Int J Obes Relat Metab Disord. 2000 Oct;24:1272-8.

295. Alsharif NZ, Lawson T, Stohs SJ. Oxidative stress induced by 2,3,7,8-tetrachlorodibenzo-p-dioxin is mediated by the aryl hydrocarbon (Ah) receptor complex. Toxicology. 1994 Sep 6;92:39-51.

296. Uemura H, Arisawa K, Hiyoshi M, Kitayama A, Takami H, Sawachika F, Dakeshita S, Nii K, Satoh H, et al. Prevalence of metabolic syndrome associated with body burden levels of dioxin and related compounds among Japan's general population. Environ Health Perspect. 2009 Apr;117:568-73.

297. Lee DH, Steffes MW, Sjodin A, Jones RS, Needham LL, Jacobs DR, Jr. Low dose organochlorine pesticides and polychlorinated biphenyls predict obesity, dyslipidemia, and insulin resistance among people free of diabetes. PLoS One. 2011;6:e15977.

298. Kern PA, Fishman RB, Song W, Brown AD, Fonseca V. The effect of 2,3,7,8-tetrachlorodibenzo-p-dioxin (TCDD) on oxidative enzymes in adipocytes and liver. Toxicology. 2002 Feb 28;171:117-25.

299. Ahn J, Lee H, Kim S, Ha T. Resveratrol inhibits TNF-alpha-induced changes of adipokines in 3T3-L1 adipocytes. Biochem Biophys Res Commun. 2007 Dec 28;364:972-7.

300. Zhu J, Yong W, Wu X, Yu Y, Lv J, Liu C, Mao X, Zhu Y, Xu K, Han X. Anti-inflammatory effect of resveratrol on TNF-alpha-induced MCP-1 expression in adipocytes. Biochem Biophys Res Commun. 2008 May 2;369:471-7.

301. Yen GC, Chen YC, Chang WT, Hsu CL. Effects of polyphenolic compounds on tumor necrosis factor-alpha (TNF-alpha)-induced changes of adipokines and oxidative stress in 3T3-L1 adipocytes. J Agric Food Chem. 2011 Jan 26;59:546-51.

302. Olholm J, Paulsen SK, Cullberg KB, Richelsen B, Pedersen SB. Anti-inflammatory effect of resveratrol on adipokine expression and secretion in human adipose tissue explants. Int J Obes (Lond). 2010 Oct;34:1546-53.

303. Kang L, Heng W, Yuan A, Baolin L, Fang H. Resveratrol modulates adipokine expression and improves insulin sensitivity in adipocytes: Relative to inhibition of inflammatory responses. Biochimie. 2010 Jul;92:789-96.

304. Rosenow A, Noben JP, Jocken J, Kallendrusch S, Fischer-Posovszky P, Mariman EC, Renes J. Resveratrol-induced changes of the human adipocyte secretion profile. J Proteome Res. 2012 Sep 7;11:4733-43.

305. He YG, Sun YJ, Xie YX, Zheng H, Zhang YD, Guo J, Xi JK. [Resveratrol attenuates oxidant-induced mitochondrial damage in embryonic rat cardiomyocytes via inactivating GSK-3beta]. Zhonghua Xin Xue Guan Bing Za Zhi. 2012 Oct;40:858-63.

306. Cheng AS, Cheng YH, Chiou CH, Chang TL. Resveratrol upregulates Nrf2 expression to attenuate methylglyoxal-induced insulin resistance in Hep G2 cells. J Agric Food Chem. 2012 Sep 12;60:9180-7.

307. Jeon BT, Jeong EA, Shin HJ, Lee Y, Lee DH, Kim HJ, Kang SS, Cho GJ, Choi WS, Roh GS. Resveratrol attenuates obesity-associated peripheral and central inflammation and improves memory deficit in mice fed a high-fat diet. Diabetes. 2012 Jun;61:1444-54.

308. Chen Q, Wang E, Ma L, Zhai P. Dietary resveratrol increases the expression of hepatic 7alpha-hydroxylase and ameliorates hypercholesterolemia in high-fat fed C57BL/6J mice. Lipids Health Dis. 2012;11:56.

309. Milne JC, Lambert PD, Schenk S, Carney DP, Smith JJ, Gagne DJ, Jin L, Boss O, Perni RB, et al. Small molecule activators of SIRT1 as therapeutics for the treatment of type 2 diabetes. Nature. 2007 Nov 29;450:712-6.

310. Casper RF, Quesne M, Rogers IM, Shirota T, Jolivet A, Milgrom E, Savouret JF. Resveratrol has antagonist activity on the aryl hydrocarbon receptor: implications for prevention of dioxin toxicity. Mol Pharmacol. 1999 Oct;56:784-90.

311. Beedanagari SR, Bebenek I, Bui P, Hankinson O. Resveratrol inhibits dioxin-induced expression of human CYP1A1 and CYP1B1 by inhibiting recruitment of the aryl hydrocarbon receptor complex and RNA polymerase II to the regulatory regions of the corresponding genes. Toxicol Sci. 2009 Jul;110:61-7.

312. Ishida T, Takeda T, Koga T, Yahata M, Ike A, Kuramoto C, Taketoh J, Hashiguchi I, Akamine A, et al. Attenuation of 2,3,7,8-tetrachlorodibenzo-p-dioxin toxicity by resveratrol: a comparative study with different routes of administration. Biol Pharm Bull. 2009 May;32:876-81.

313. Chen ZH, Hurh YJ, Na HK, Kim JH, Chun YJ, Kim DH, Kang KS, Cho MH, Surh YJ. Resveratrol inhibits TCDD-induced expression of CYP1A1 and CYP1B1 and catechol estrogen-mediated oxidative DNA damage in cultured human mammary epithelial cells. Carcinogenesis. 2004 Oct;25:2005-13.

314. Lu KT, Ko MC, Chen BY, Huang JC, Hsieh CW, Lee MC, Chiou RY, Wung BS, Peng CH, Yang YL. Neuroprotective effects of resveratrol on MPTP-induced neuron loss mediated by free radical scavenging. J Agric Food Chem. 2008 Aug 27;56:6910-3.

315. Singh NP, Singh US, Nagarkatti M, Nagarkatti PS. Resveratrol (3,5,4'-trihydroxystilbene) protects pregnant mother and fetus from the immunotoxic effects of 2,3,7,8-tetrachlorodibenzo-p-dioxin. Mol Nutr Food Res. 2011 Feb;55:209-19.

316. He X, Wang L, Szklarz G, Bi Y, Ma Q. Resveratrol inhibits paraquat-induced oxidative stress and fibrogenic response by activating the nuclear factor erythroid 2-related factor 2 pathway. J Pharmacol Exp Ther. 2012 Jul;342:81-90.

317. Johnson WD, Morrissey RL, Usborne AL, Kapetanovic I, Crowell JA, Muzzio M, McCormick DL. Subchronic oral toxicity and cardiovascular safety pharmacology studies of resveratrol, a naturally occurring polyphenol with cancer preventive activity. Food Chem Toxicol. 2011 Dec;49:3319-27.

318. Poulsen MM, Vestergaard PF, Clasen BF, Radko Y, Christensen LP, Stodkilde-Jorgensen H, Moller N, Jessen N, Pedersen SB, Jorgensen JO. High-dose resveratrol supplementation in obese men: an investigator-initiated, randomized, placebo-controlled clinical trial of substrate metabolism, insulin sensitivity, and body composition. Diabetes. 2013 Apr;62:1186-95.

319. Reagan-Shaw S, Nihal M, Ahmad N. Dose translation from animal to human studies revisited. FASEB J. 2008 Mar;22:659-61.

320. Detampel P, Beck M, Krahenbuhl S, Huwyler J. Drug interaction potential of resveratrol. Drug Metab Rev. 2012 Aug;44:253-65.

321. Arsenescu V, Arsenescu R, Parulkar M, Karounos M, Zhang X, Baker N, Cassis LA. Polychlorinated biphenyl 77 augments angiotensin II-induced atherosclerosis and abdominal aortic aneurysms in male apolipoprotein E deficient mice. Toxicol Appl Pharmacol. 2011 Nov 15;257:148-54.

322. Kopf PG, Walker MK. 2,3,7,8-tetrachlorodibenzo-p-dioxin increases reactive oxygen species production in human endothelial cells via induction of cytochrome P4501A1. Toxicol Appl Pharmacol. 2010 May 15;245:91-9.

323. Kopf PG, Scott JA, Agbor LN, Boberg JR, Elased KM, Huwe JK, Walker MK. Cytochrome P4501A1 is required for vascular dysfunction and hypertension induced by 2,3,7,8-tetrachlorodibenzo-p-dioxin. Toxicol Sci. 2010 Oct;117:537-46.

324. Rodbell M. Localization of Lipoprotein Lipase in Fat Cells of Rat Adipose Tissue. J Biol Chem. 1964 Mar;239:753-5.

325. Machado FS, Johndrow JE, Esper L, Dias A, Bafica A, Serhan CN, Aliberti J. Anti-inflammatory actions of lipoxin A4 and aspirin-triggered lipoxin are SOCS-2 dependent. Nat Med. 2006 Mar;12:330-4.

326. Bui P, Solaimani P, Wu X, Hankinson O. 2,3,7,8-Tetrachlorodibenzo-p-dioxin treatment alters eicosanoid levels in several organs of the mouse in an aryl hydrocarbon receptor-dependent fashion. Toxicol Appl Pharmacol. 2012 Mar 1;259:143-51.

327. Paschos GK, Ibrahim S, Song WL, Kunieda T, Grant G, Reyes TM, Bradfield CA, Vaughan CH, Eiden M, et al. Obesity in mice with adipocyte-specific deletion of clock component Arntl. Nat Med. 2012 Dec;18:1768-77.

328. Callero MA, Loaiza-Perez AI. The role of aryl hydrocarbon receptor and crosstalk with estrogen receptor in response of breast cancer cells to the novel antitumor agents benzothiazoles and aminoflavone. Int J Breast Cancer. 2011;2011:923250.

329. Gjernes MH, Schlenk D, Arukwe A. Estrogen receptor-hijacking by dioxin-like 3,3'4,4',5-pentachlorobiphenyl (PCB126) in salmon hepatocytes involves both receptor activation and receptor protein stability. Aquat Toxicol. 2012 Nov 15;124-125:197-208.

330. Labrecque MP, Takhar MK, Hollingshead BD, Prefontaine GG, Perdew GH, Beischlag TV. Distinct roles for aryl hydrocarbon receptor nuclear translocator and ah receptor in estrogen-mediated signaling in human cancer cell lines. PLoS One. 2012;7:e29545.

331. Rataj F, Moller FJ, Jahne M, Zierau O, Diel P, Vollmer G, Kretzschmar G. Regulation of uterine AHR battery gene expression by 17beta-Estradiol is predominantly mediated by estrogen receptor alpha. Arch Toxicol. 2012 Oct;86:1603-12.

332. Yan Z, Lu G, He J. Reciprocal inhibiting interactive mechanism between the estrogen receptor and aryl hydrocarbon receptor signaling pathways in goldfish (Carassius auratus) exposed to 17beta-estradiol and benzo[a]pyrene. Comp Biochem Physiol C Toxicol Pharmacol. 2012 Jun;156:17-23.

333. Simmons SL, Cummings JA, Clemens LG, Nunez AA. Exposure to PCB 77 affects the maternal behavior of rats. Physiol Behav. 2005 Jan 31;84:81-6.

334. Mortensen AS, Arukwe A. Activation of estrogen receptor signaling by the dioxin-like aryl hydrocarbon receptor agonist, 3,3',4,4',5-pentachlorobiphenyl (PCB126) in salmon in vitro system. Toxicol Appl Pharmacol. 2008 Mar 1;227:313-24.

335. Fleming CR, Billiard SM, Di Giulio RT. Hypoxia inhibits induction of aryl hydrocarbon receptor activity in topminnow hepatocarcinoma cells in an ARNT-dependent manner. Comp Biochem Physiol C Toxicol Pharmacol. 2009 Sep;150:383-9.

336. Terzuoli E, Puppo M, Rapisarda A, Uranchimeg B, Cao L, Burger AM, Ziche M, Melillo G. Aminoflavone, a ligand of the aryl hydrocarbon receptor, inhibits HIF-1alpha expression in an AhR-independent fashion. Cancer Res. 2010 Sep 1;70:6837-48.

337. Jiang C, Qu A, Matsubara T, Chanturiya T, Jou W, Gavrilova O, Shah YM, Gonzalez FJ. Disruption of hypoxia-inducible factor 1 in adipocytes improves insulin sensitivity and decreases adiposity in high-fat diet-fed mice. Diabetes. 2011 Oct;60:2484-95.

338. Ibrahim MM, Fjaere E, Lock EJ, Froyland L, Jessen N, Lund S, Vidal H, Ruzzin J. Metabolic impacts of high dietary exposure to persistent organic pollutants in mice. Toxicol Lett. 2012 Nov 23;215:8-15.

339. La Merrill M, Birnbaum LS. Childhood obesity and environmental chemicals. Mt Sinai J Med. 2011 Jan-Feb;78:22-48.

340. Barouki R, Gluckman PD, Grandjean P, Hanson M, Heindel JJ. Developmental origins of non-communicable disease: implications for research and public health. Environ Health. 2012;11:42.

341. Hue O, Marcotte J, Berrigan F, Simoneau M, Dore J, Marceau P, Marceau S, Tremblay A, Teasdale N. Increased plasma levels of toxic pollutants accompanying weight loss induced by hypocaloric diet or by bariatric surgery. Obes Surg. 2006 Sep;16:1145-54.

342. Imbeault P, Tremblay A, Simoneau JA, Joanisse DR. Weight loss-induced rise in plasma pollutant is associated with reduced skeletal muscle oxidative capacity. Am J Physiol Endocrinol Metab. 2002 Mar;282:E574-9.

343. Tremblay A, Chaput JP. Adaptive reduction in thermogenesis and resistance to lose fat in obese men. Br J Nutr. 2009 Aug;102:488-92.

344. Viluksela M, Unkila M, Pohjanvirta R, Tuomisto JT, Stahl BU, Rozman KK, Tuomisto J. Effects of 2,3,7,8-tetrachlorodibenzo-p-dioxin (TCDD) on liver

phosphoenolpyruvate carboxykinase (PEPCK) activity, glucose homeostasis and plasma amino acid concentrations in the most TCDD-susceptible and the most TCDD-resistant rat strains. Arch Toxicol. 1999 Aug;73:323-36.

345. Zhang W, Sargis RM, Volden PA, Carmean CM, Sun XJ, Brady MJ. PCB 126 and other dioxin-like PCBs specifically suppress hepatic PEPCK expression via the aryl hydrocarbon receptor. PLoS One. 2012;7:e37103.

346. Trumble SJ, Robinson EM, Noren SR, Usenko S, Davis J, Kanatous SB. Assessment of legacy and emerging persistent organic pollutants in Weddell seal tissue (Leptonychotes weddellii) near McMurdo Sound, Antarctica. Sci Total Environ. 2012 Nov 15;439:275-83.

347. Piaggi S, Novelli M, Martino L, Masini M, Raggi C, Orciuolo E, Masiello P, Casini A, De Tata V. Cell death and impairment of glucose-stimulated insulin secretion induced by 2,3,7,8-tetrachlorodibenzo-p-dioxin (TCDD) in the beta-cell line INS-1E. Toxicol Appl Pharmacol. 2007 May 1;220:333-40.

348. Petriello MC, Newsome B, Hennig B. Influence of nutrition in PCB-induced vascular inflammation. Environ Sci Pollut Res Int. 2013 Feb 17.

349. Redgrave TG, Wallace P, Jandacek RJ, Tso P. Treatment with a dietary fat substitute decreased Arochlor 1254 contamination in an obese diabetic male. J Nutr Biochem. 2005 Jun;16:383-4.

350. Arguin H, Sanchez M, Bray GA, Lovejoy JC, Peters JC, Jandacek RJ, Chaput JP, Tremblay A. Impact of adopting a vegan diet or an olestra supplementation on plasma organochlorine concentrations: results from two pilot studies. Br J Nutr. 2010 May;103:1433-41.

351. Newsome WH, Davies DJ, Sun WF. Residues of polychlorinated biphenyls (PCB) in fatty foods of the Canadian diet. Food Addit Contam. 1998 Jan;15:19-29.

352. Machado FS, Aliberti J. Impact of lipoxin-mediated regulation on immune response to infectious disease. Immunol Res. 2006;35:209-18.

353. Mortensen AS, Arukwe A. Interactions between estrogen- and Ah-receptor signalling pathways in primary culture of salmon hepatocytes exposed to nonylphenol and 3,3',4,4'-tetrachlorobiphenyl (congener 77). Comp Hepatol. 2007;6:2.

354. Wang L, Reiterer G, Toborek M, Hennig B. Changing ratios of omega-6 to omega-3 fatty acids can differentially modulate polychlorinated biphenyl toxicity in endothelial cells. Chem Biol Interact. 2008 Mar 10;172:27-38.

355. Jorgensen ME, Borch-Johnsen K, Bjerregaard P. A cross-sectional study of the association between persistent organic pollutants and glucose intolerance among Greenland Inuit. Diabetologia. 2008 Aug;51:1416-22.

356. Rignell-Hydbom A, Rylander L, Hagmar L. Exposure to persistent organochlorine pollutants and type 2 diabetes mellitus. Hum Exp Toxicol. 2007 May;26:447-52.

357. Rignell-Hydbom A, Lidfeldt J, Kiviranta H, Rantakokko P, Samsioe G, Agardh CD, Rylander L. Exposure to p,p'-DDE: a risk factor for type 2 diabetes. PLoS One. 2009;4:e7503.

358. Glauert HP, Tharappel JC, Banerjee S, Chan NL, Kania-Korwel I, Lehmler HJ, Lee EY, Robertson LW, Spear BT. Inhibition of the promotion of

hepatocarcinogenesis by 2,2',4,4',5,5'-hexachlorobiphenyl (PCB-153) by the deletion of the p50 subunit of NF-kappa B in mice. Toxicol Appl Pharmacol. 2008 Oct 15;232:302-8.

359. Gao J, He J, Zhai Y, Wada T, Xie W. The constitutive androstane receptor is an anti-obesity nuclear receptor that improves insulin sensitivity. J Biol Chem. 2009 Sep 18;284:25984-92.

360. He J, Gao J, Xu M, Ren S, Stefanovic-Racic M, O'Doherty RM, Xie W. PXR ablation alleviates diet-induced and genetic obesity and insulin resistance in mice. Diabetes. 2013 Jan 24.

361. Shi X, Wahlang B, Wei X, Yin X, Falkner KC, Prough RA, Kim SH, Mueller EG, McClain CJ, et al. Metabolomic analysis of the effects of polychlorinated biphenyls in nonalcoholic fatty liver disease. J Proteome Res. 2012 Jul 6;11:3805-15.

362. Flegal KM, Carroll MD, Ogden CL, Johnson CL. Prevalence and trends in obesity among US adults, 1999-2000. JAMA. 2002 Oct 9;288:1723-7.

363. Hedley AA, Ogden CL, Johnson CL, Carroll MD, Curtin LR, Flegal KM. Prevalence of overweight and obesity among US children, adolescents, and adults, 1999-2002. JAMA. 2004 Jun 16;291:2847-50.

364. Fantini F, Porta D, Fano V, De Felip E, Senofonte O, Abballe A, D'Ilio S, Ingelido AM, Mataloni F, et al. [Epidemiologic studies on the health status of the population living in the Sacco River Valley]. Epidemiol Prev. 2012 Sep-Oct;36:44-52.

365. Vasiliu O, Cameron L, Gardiner J, Deguire P, Karmaus W. Polybrominated biphenyls, polychlorinated biphenyls, body weight, and incidence of adult-onset diabetes mellitus. Epidemiology. 2006 Jul;17:352-9.

366. Fierens S, Mairesse H, Heilier JF, De Burbure C, Focant JF, Eppe G, De Pauw E, Bernard A. Dioxin/polychlorinated biphenyl body burden, diabetes and endometriosis: findings in a population-based study in Belgium. Biomarkers. 2003 Nov-Dec;8:529-34.

367. Lee DH, Jacobs DR, Jr., Porta M. Could low-level background exposure to persistent organic pollutants contribute to the social burden of type 2 diabetes? J Epidemiol Community Health. 2006 Dec;60:1006-8.

368. Lee DH, Lee IK, Jin SH, Steffes M, Jacobs DR, Jr. Association between serum concentrations of persistent organic pollutants and insulin resistance among nondiabetic adults: results from the National Health and Nutrition Examination Survey 1999-2002. Diabetes Care. 2007 Mar;30:622-8.

369. Swedenborg E, Pongratz I. AhR and ARNT modulate ER signaling. Toxicology. 2010 Feb 9;268:132-8.

370. Swedenborg E, Pongratz I, Gustafsson JA. Endocrine disruptors targeting ERbeta function. Int J Androl. 2010 Apr;33:288-97.

VITA

Name: Nicki Alyssa Baker

Educational History

August 2009 – PRESENT	University of Kentucky, Lexington, KY PhD candidate Graduate Center for Nutritional Sciences UK College of Medicine
May 2001	Michigan State University, East Lansing, MI Bachelor of Science Major: Civil Engineering

Research Experience

August 2009 – PRESENT	**University of Kentucky**, Lexington, KY Investigating the role of polychlorinated biphenyls in the development of type 2 diabetes and the use of resveratrol as a therapeutic intervention. *(Mentor: Lisa Cassis, PhD; Department of Molecular and Biomedical Pharmacology, University of Kentucky)*

Teaching Experience

Fall 2011 – Spring 2012	**Bluegrass Community and Technical College**
	Lexington, KY
	Adjunct faculty for Nutrition, Anatomy, and Physiology
Fall 2007 – Spring 2008	**Sullivan University**
	Louisville, KY
	Assistant instructor for Nutrition

Honors and Awards

2013 Third place poster presentation at Barnstable Brown Obesity and Diabetes Research Day, 2013.

2013 Reviewer of Scientific American Nutrition textbook, published by W.H. Freeman and Company, 2013.

2013 First-author manuscript selected for editorial article in January 2013 issue of *Environmental Health Perspectives* (PMID: 23099484).

2012 First-author manuscript selected by National Institutes of Environmental Health Sciences as Paper of the Month (PMID: 23099484).

2012 Karen Wetterhahn Memorial Award (issued by the Superfund Research Program, National Institutes of Environmental Health Sciences) for outstanding graduate student or post-doctoral fellow research and citizenship in environmental health sciences.

2006 Professional Engineer's License, State of Michigan, #6201052571.

Research Support

2010 – PRESENT Predoctoral financial support from Training Program in Oxidative Stress and Nutrition, National Institutes of Health T32 #3048107792.

Publications

Baker N, English V, Sunkara M, Morris A, Pearson K, and Cassis L. Resveratrol protects against polychlorinated biphenyl-mediated impairment of glucose homeostasis in adipocytes. Journal of Nutritional Biochemistry (Manuscript in review)

Baker N, Karounos M, English V, Fang J, Wei Y, Stromberg A, Sunkara M, Morris A, Swanson H, and Cassis L. Coplanar polychlorinated biphenyls impair glucose homeostasis in lean C57BL/6 mice and mitigate beneficial effects of weight loss on glucose homeostasis in obese mice. Environmental Health Perspectives. 2013; 121(1):105-10. PMID: 23099484

Arsenescu V, Arsenescu R, Parulkar M, Karounos M, Zhang X, **Baker N**, and Cassis L. Polychlorinated biphenyl 77 augments angiotensin II-induced atherosclerosis and abdominal aortic aneurysms in male apolipoprotein E deficient mice. Toxicology and Applied Pharmacology. 2011; 257(1):148-54. PMID: 21925196

Abstracts

Baker N, English V, Pearson K, Cassis L. Resveratrol improves PCB77-induced disruptions in glucose homeostasis in vitro and in vivo. Gill Heart Institute Cardiovascular Research Day, October 5, 2012, Lexington, KY.

Baker N, Karounos M, English V, Cassis L. Administration of PCB77 to C57BL/6 mice impairs glucose and insulin tolerance. Barnstable Brown Obesity and Diabetes Research Day, May 14, 2012, Lexington, KY.

Baker N, Karounos M, English V, Cassis L. Administration of PCB77 to C57BL/6 mice impairs glucose and insulin tolerance. Superfund Research Program Annual Meeting, October 24-26, 2011, Lexington, KY.

Baker N, Karounos M, English V, Cassis L. Administration of PCB77 to C57BL/6 mice impairs glucose and insulin tolerance. Gill Heart Institute Cardiovascular Research Day, October 21, 2011, Lexington, KY.

Baker N, Karounos M, English V, Cassis L. PCB77 promotes glucose intolerance in lean C57BL/6 mice and blunts beneficial effects of weight loss on glucose homeostasis in obese mice. Barnstable Brown Obesity and Diabetes Research Day, May 17, 2011, Lexington, KY.

Baker N, Karounos M, English V, Cassis L. PCB77 promotes glucose intolerance in lean C57BL/6 mice and blunts beneficial effects of weight loss on glucose homeostasis in obese mice. Superfund Research Program Annual Meeting, November 10-12, 2010, Portland, OR.

Baker N, Karounos M, English V, Cassis L. PCB77 promotes glucose intolerance in lean C57BL/6 mice and blunts beneficial effects of weight loss on glucose homeostasis in obese mice. Gill Heart Institute Cardiovascular Research Day, October 22, 2010, Lexington, KY.

Oral Presentations

Baker N. Karen Wetterhahn Scientific Presentation: Administration of PCB77 to C57BL/6 mice impairs glucose and insulin tolerance. Superfund Research Program Annual Meeting, October 21-24, 2012, Durham, NC.

Baker N. Resveratrol improves PCB77-induced disruptions in glucose homeostasis in vitro and in vivo. Gill Heart Institute Cardiovascular Research Day, October 5, 2012, Lexington, KY.

Baker N. The Role of Polychlorinated Biphenyls in the Development of Diabetes. Graduate Center for Nutritional Sciences Seminar Series, September 26, 2012, Lexington, KY.

Baker N. Administration of PCB77 to C57BL/6 mice impairs glucose and insulin tolerance. Barnstable Brown Obesity and Diabetes Research Day, May 14, 2012, Lexington, KY.

Baker N. The Role of Polychlorinated Biphenyls in the Development of Diabetes. Gill Heart Institute Cardiovascular Research Day, October 21, 2011, Lexington, KY.

Baker N. The Role of Polychlorinated Biphenyls in the Development of Diabetes. South Eastern Lipid Research Conference, October 6-8, 2011, Callaway Gardens, GA.

Baker N. The Role of Polychlorinated Biphenyls in the Development of Diabetes. Graduate Center for Nutritional Sciences Seminar Series, February 23, 2011, Lexington, KY.